

ANNALES
UNIVERSITATIS SCIENTIARUM
BUDAPESTINENSIS
DE ROLANDO EÖTVÖS NOMINATAE

SECTIO GEOLOGICA

TOMUS XIV.

1970

REDIGUNT

B. GÉCZY

J. KISS

L. STEGENA



BUDAPEST

1971

ANNALES

UNIVERSITATIS SCIENTIARUM
BUDAPESTINENSIS
DE ROLANDO EÖTVÖS NOMINATAE

SECTIO BIOLOGICA

inceptit anno MCMLVII

SECTIO CHIMICA

inceptit anno MCMLIX

SECTIO GEOGRAPHICA

inceptit anno MCMLXV

SECTIO GEOLOGICA

inceptit anno MCMLVII

SECTIO HISTORICA

inceptit anno MCMLVII

SECTIO IURIDICA

inceptit anno MCMLIX

SECTIO LINGUISTICA

inceptit anno MCMLXX

SECTIO MATHEMATICA

inceptit anno MCMLVIII

SECTIO PAEDAGOGICA ET PSYCHOLOGICA

inceptit anno MCMLXX

SECTIO PHILOLOGICA

inceptit anno MCMLVII

SECTIO PHILOLOGICA MODERNA

inceptit anno MCMLXX

SECTIO PHILOSOPHICA ET SOCIOLOGICA

inceptit anno MCMLXII

PROFESSOR LÁSZLÓ EGYED
1914–1970

László Egyed, Professor of Geophysics at Loránd Eötvös University, Budapest died suddenly on July 11, 1970. His untimely passing was a deep loss for many geophysicist around the world, to whom he was known, for several scientific groups and organizations whose work were coordinated or directed by him and in particular for us who have been privileged to be associated with him.

Born on 12th February, 1914 in Fogaras, Transsylvania, László Egyed entered in 1933 the University of Budapest. He studied mathematics and physics and received a Ph. D. in mathematics in 1938. From 1937 through 1941 he was employed by the same university as a lecturer in mathematics. At that time he mainly dealt with the theory of sets. At about the end of this period he became interested in geophysics and began to work for the Hungarian–American Oil Company. He continued this activity until 1948, making gravity and magnetic measurements at many places of Hungary. At 1947 he joined the University of Budapest again and became senior lecturer in geophysics. In 1951 he was appointed to a readership in geophysics and was placed in charge of organizing a new department, studying and teaching geophysics, which formed a part of the faculty of natural sciences. He became Head of the Department of Geophysics. Five years later he achieved the status of full professor and in 1966 he was appointed Dean of the faculty of natural sciences, positions which he held at the time of his death. In 1960 he was elected a corresponding member of the Hungarian Academy of Sciences and some months before his death he became an ordinary member.

In 1957 Professor L. Egyed was awarded the Kossuth prize, one of the highest awards of the Hungarian State.

Professor Egyed's career started with mathematics but he shortly turned to geophysics and from then onwards contributed ceaselessly to the renown of Hungarian geophysics. He carried out investigations concerning the reductions and interpretations of gravity and magnetic measurements, dealt with the structure of the Earth's

crust in Hungary and worked on various problems of pure geophysics. His most important and acknowledged scientific contribution, however, has been connected with the internal structure of the Earth. His dynamic theory of an expanding Earth has been very often referred to in the international literature. He accumulated evidences favoring the expansion and claimed that a radius increase of 0.65 ± 0.15 mm/year has taken place for the last 600 million years. He has shown that the expansion of the Earth is able to account for the formation of the crust and oceanic basins, the energies of tectonic forces and earthquakes, the origin of deep focus earthquakes, the continental drift and mountain building.

A considerable portion of geologists and geophysicist, working now in Hungary, attended his lectures and his high standard of teaching as well as his textbooks and lecture notes helped to ensure the rapid progress made in both applied and pure geophysics in this country.

Professor E g y e d travelled extensively in the last 15 years. He attended numerous international geophysical congresses and meetings in Europe, Asia and in the Americas and was invited by a number of universities and scientific institutions to give lectures on his investigations. He spent the 1967–1968 academic year in Japan as an UNESCO expert to the International Institute of Seismology and Earthquake Engineering.

Professor E g y e d's scientific organizational activity was also of great importance. He was instrumental in the organization of the Association of Hungarian Geophysicists and was the vice-president of the Association until his death. He was president, secretary or member of many professional groups including the international directory board of the Committee on Space Research (COSPAR), the European Seismological Commission, the Hungarian Committee of IQSY, the Hungarian Committee of IUGG, the Geophysical Committee of the Hungarian Academy of Sciences and many others. He was member of the editorial boards of some Hungarian and international periodicals, dealing with various aspects of geophysics.

Professor E g y e d possessed a rare combination of outstanding qualities including great professional ability, excellent talent for teaching and efficiency in organization. He is remembered with respect and affection by his many co-workers, friends and students.

ON THE LIASSIC AGE OF THE "BATHONIAN" OF VILLÁNY (BARANYA).

D. V. AGER

(University College Swansea) and

J. H. CALLOMON

(University College London)

(Received: 20 July 1970)

РЕЗЮМЕ

В районе гор Виллань южной Венгрии слои, считавшиеся до сих пор батскими (средняя юра) должны быть отнесены к нижнему плинбахскому ярусу (лейас, нижняя юра) на основании как аммонитов, так и брахиопод, найденных независимо друг от друга в естественном залегании отложений. Но несмотря на это, все же существуют некоторые верхнебатские отложения в виде мелких линзообразных гнезд. Они подстилаются резкой поверхностью размыва лейаса, а непосредственно над ними залегает келловейский слой с цефалоподами. Ирак, ранее описанные кажущиеся аномалии в аммонитовой фауне получают удовлетворительное объяснение.

Introduction

The old limestone quarries near the village of Villány have long been a profuse source of Jurassic ammonites, made famous through extensive descriptions in the monographs by Till (1910—11) and Lóczy (1915). Yet a detailed description of the section appears never to have been published. Lóczy gives the following summary. From below:

- (t_1) — TRIAS: Limestones of Muschelkalk-Dolomite type,
wholly unfossiliferous. Thick.
- (t_2) — Dolomitic marls with *Lingula* and bivalves 8—10 m
Slight angular unconformity, ? tectonic
— Sand or soft sandstone, unstratified, barren, poorly
exposed.
- (J_1) — JURASSIC: Upper Bathian and Bradfordian. Sand-
stone, grey, passing into sandy echinodermal
limestone or conglomerates. Many *Nautili* but
allegedly no ammonites.
- (J_2) — Cornbrash: sandy bituminous crinoidal limestone
also passing locally into conglomerates, much
more compact than the bed below. *Nautilus*,
belemnites, pectens, *Gryphaea*; *Zeilleria* and
Rhynchonella Alemanica Rollier (= *varians*
auctt.); no ammonites.

Thickness of J_1 and J_2 ,	12–16 m
	Sharp break.
(J_3) — Callovian, ammonite bed: marly ferruginous limestone, slightly oolitic, highly glauconitic, many corroded ammonites,	1.5–3 m
	Sharp break.
(J_4) — Upper Oxfordian: massive white limestones, with belemnites, bivalves and brachiopods. Thick.	

All the monographed ammonites were said to have come from the Callovian ammonite-bed, J_3 , and the majority are undoubtedly Callovian. Lóczy's attempts to establish a finer stratigraphical succession within the bed were apparently unsuccessful. The beds J_1 and J_2 were dated as Bathonian on the strength of the *Nautili* and brachiopods. The whole of the Lower and part of the Middle Jurassic were thus said to be absent in the Villány hills, in marked contrast to the succession in the Mecsek Mountains not far to the north and most of the rest of Hungary.

The description of the ammonites however raised some questions which remained unresolved. Thus:

(1) *Cosmoceras globosum* Till (1911, pl. iii (vii), figs. 2–4) is an unmistakable *Liparoceras*, close to *L. cheltiense* (Murchison) or *L. pseudostriatum* Trueman, from the Lower Pliensbachian. This was already noted by Späth (1931, p. 593). (The specimen is in the collections of the Natur-Museum Senckenberg, Frankfurt, reg. no. SMF XI 191a).

(2) *Stepheoceras extinctum* (Rollier) Lóczy (1915, pl. iv, fig. 10) is a typical *Polyplectites*, and although this genus is known to range up to the top of the Middle Bathonian, none has ever been found in the Callovian. Mr. Galácz and Prof. Géczy have pointed out to us that its matrix is typical red Ammonitico rosso limestone, and that it cannot thus be from Villány; perhaps it came from Mecsek, from where Böckh (1881) has also recorded it as Lóczy himself pointed out.

(3) A number of other specimens figured by Lóczy seemed to be Bathonian. A list was given by Arkell (1956, p. 191), drawn up at a time when he was monographing the Bathonian ammonites. Species of *Lytoceras* and *Phylloceras* are of course always debatable, but there is no doubt about the *Tulites* (in fact a *Bullatimorphites* according to Dr. Torrens and certainly not a *Macrocephalites*) and three species of *Prohecticoceras*.

(4) *Villania densilobata* Till (1909; 1911, pl. vii (xi), figs. 7–10, pl. viii (xii), figs. 1,2; holotype), if Callovian, is absolutely unique. No supporting material has since appeared (the specimen figured under this name by Lóczy is a normal perisphinctid and unrelated), and Arkell (1957, *Treatise*) was forced to create a whole new subfamily of Villaniinae for this single specimen, placing it in *Lytoceratidae* as the best that could be done.

(5) *Aspidoceras antiquum*, *amplexum* and *Rollieri* Lóczy were equally difficult to place and also remained without support. The first two species were based on a single fragment each; the last on two large well-preserved syntypes one of which has inner whorls and septal sutures strongly resembling *Lytoceras*.

Items (1) and (2) were clearly imports, and in view of the fact that the major portion of the material treated by Till and Lóczy came from old collections, or was bought from workmen, it was tempting to dismiss the other problematica as having crept into the the collections from outside also. On the other hand even so it was not easy to see where items (4) and (5) should be placed or could have come from; and the “*Aspidoceras*”, if in fact genuine, would assume a most important place as the oldest known member of the *Aspidoceras* lineage, common in younger beds and hitherto somewhat cryptogenic in origin (C all o m o n 1963, p. 39).

Stratigraphy

It was therefore an occasion of the greatest interest to be able to visit the classical localities as guests of the Jurassic Colloquium in 1969. Except for some talus, the quarries have changed little since the photographs reproduced by Lóczy (1915, p. 256–7) were taken. Parts had been specially cleaned and excavated to expose the beds. In the short time available only the following brief notes of the section could be made. From below:

- | | |
|--|------------------|
| 1. — Limestone, arenaceous, somewhat nodular, weathering yellow, the lowest beds exposed. Bivalves and belemnites on a bedding surface; also two large ammonites. | |
| 2. — Limestone, silty, brecciated, light grey-yellow, very fossiliferous with profuse bivalves and belemnites.
Several <i>Nautili</i> . | ca. 1 m |
| 3a. — Limestone, silty, or fine calcareous sandstone, grey, bituminous, in compact massive banks, fossils sparser: brachiopods
passing up into | 3–4 m |
| 3b. — Limestone, fine-grained, very hard, with chert concretions.
— — — Erosion-surface, planed very smooth, locally with hardground and epizoan encrustation | ca. 1 m |
| 4. — Limonitic marl or soft limestone, dark, slightly oolitic, in thin pockets resting on the erosion-surface below, containing laminated limonitic nodules with serpulid encrustations, present only locally. | 0 to ?
0.20 m |

5. — The Cephalopod Bed. Limestone, buff, micritic, brecciated and heavily subsolved, the cavities filled with dark glauconitic marlstone. Profuse ammonites at all angles throughout the bed, heavily corroded and encrusted with stromatolitic growths. ca. 0.40 m
 — — — Erosion-surface with hardground.
6. — Limestone, white, massive, tectonically somewhat brecciated and deformed. Thick, forming the south wall of the quarry.

Beds 1–3 clearly correspond to L ó c z y' s J_2 . The two ammonites seen *in situ* were not closely identifiable but most resemble large *Apodoceras* of the Jamesoni Zone, lower Pliensbachian. A part of these beds perhaps a metre thick was also seen immediately below the erosion plane at the base of the Cephalopod Bed (5) in a vineyard on the crest of Somsich-hegy, the westward continuation of Templom-hegy, and perhaps 1/2 km from the Villány quarry. The exposure here had also been specially prepared for the excursion, and during the excavations a magnificent large ammonite was revealed *in situ* 10 cms below the Cephalopod Bed (see figs. 1 and 2). It can be identified quite closely as

Apodoceras cf. *lobulatum* B u c k m a n 1921

and indicates Lower Pliensbachian, Jamesoni Zone, Taylori Subzone (see D e a n, D o n o v a n and H o w a r t h 1961, p. 462). Whether this level on Somsich-hegy correlates with the top of bed 3 in Villány quarry, or with a lower bed such as the ammonite-bearing bed 1 there, beds 2–3 having been cut out under the erosion-plane, remains to be established.

Bed 3a yielded the following brachiopoda in Villány quarry (D.V.A.):

Cincta numismalis (L a m a r c k)

Tetrahynchia of *T. argentinensis* (R a d o v a n o v i c)

Gibbirhynchia sp.

Spiriferina sp. aff. *rostrata* (S c h l o t h e i m)

These also indicate that the age of the bed is Lower Liassic, Pliensbachian (see further notes below).

Bed 4 yielded a well-preserved specimen of inner whorls of *Bullatimorphites* (coll. Colin P a r s o n s). The lithology matches the matrix of the specimens figured earlier by L ó c z y and suspected to be Bathonian; and the presence of such Bathonian elements in the museum collections thus receives a satisfactory explanation. All the specimens thus thought to be from bed 4 [see (3) in the Introduction above] indicate the lower parts of the Upper Bathonian, at least Retrocostatum and Aspidoides Zones (T o r r e n s 1969).

There is little to add to what has been written about the palaeontology of bed 5. The ammonites indicate the upper Anceps (= Jason) — Coronatum Zones of the Middle Callovian. There are some indications

also of the Athleta Zone (Upper Callovian), for the bed yielded (coll. J.H.C.) an early *Peltoceras* intermediate between the forms described as *Binatisphinctes fluctuosus* (P r a t t) from the uppermost Coronatum Zone of England and true *Peltoceras* s.s. from the Middle Athleta Zone. Forms like this are known from the English Lower Athleta Zone and can perhaps be placed in *P. (Metapeltoceras)*.



Fig. 1. Outcrop of the Lower-Middle Jurassic beds on the Somsich-hegy, Villány, looking north-westwards. In the foreground the hammer rests on the Callovian Cephalopod Bed. Immediately below, *in situ*, with a chisel leaning against it, a large *Apoderoceras* cf. *lobulatum* B u c k m a n of the Pliensbachian, Jamesoni Zone

The belemnites were described by Galácz and Vörös (1969). The sedimentology has been studied and well described by Radwansky and Szulcowski (1966). The bed seems to represent a good example of *heterogeneous condensation* — (As opposed to *homogeneous condensation* in which the concentration of fossils is due solely to the sparsity of sedimentation during the period of deposition, as in e.g. the classical Inferior Oolite of Dorset, England) — in which extensive preferential subsolution of the original matrix surrounding the ammonites has led to the total destruction of the primary stratification, reworking, partial corrosion and stromatolitic encrustation of the fossils so that they are now found in all attitudes and as a mixture of forms of different ages, as described by Hollmann (1964). The resemblance as a whole is

more to sub-Mediterranean facies (no red limestones, rich in glauconite or chamosite) than Tethyan types such as the Adneth facies.

Lastly, it should be noted that the thickness of bed 5 is quite constant at about 0.40 cm, not 1.5–3 m as stated by L ó c z y and quoted subsequently e.g. by A r k e l l (1956, p. 190).

Notes on the Liassic ammonites (J.H.C.)

The following is a summary of the fauna now known from Villány.

Family Eoderoceratidae Spath 1929

Genus *Apoderoceras* Buckman 1921

Type species *A. lobulatum* Buckman 1921

(1) *Apoderoceras* cf. *lobulatum* Buckman 1921

Apoderoceras lobulatum Buckman 1921, pl. 235

The specimen from Somsich-hegy collected on the excursion is somewhat worn by weathering on the outer whorl and slightly tectonically deformed. It agrees well with the holotype however in all essential respects. The species is rather smooth as *Apoderoceras* goes but develops a row of blunt ventrolateral tubercles on the outer whorls which are quadrate and depressed; and the inner whorls show rather irregular

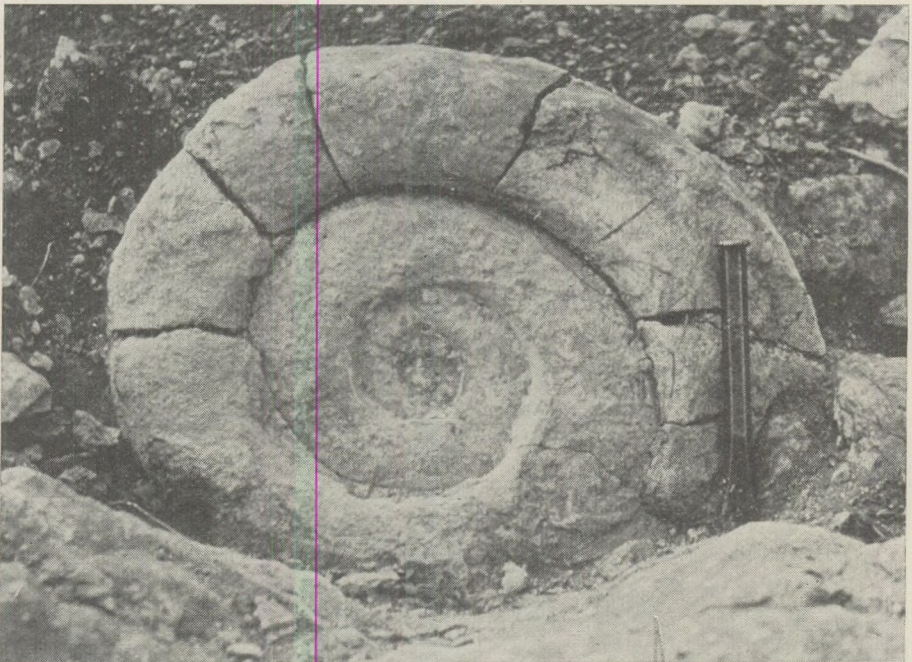


Fig. 2. Close-up view of the Liassic ammonite seen in the foreground of figure 1. The length of the chisel is 15 cms. — Both figures from colourslides by the author (J.H.C.)

striations too weak to be called ribbing proper. The poorly-preserved specimens seen in Villány quarry (bed 1) may also well belong to this species. In addition Mr. A. Galács showed me a further three fragmentary specimens in the collections of the University, Budapest, in similar preservation.

- (2) *Apoderoceras* cf. *aculeatum* (Simpson 1843).
 = *Aspidoceras antiquum* Lóczy 1915, p. 427, pl. xiv, fig. 1, 2
Deroceras aculeatum (Simpson) Buckman 1913, pl. 72A–C (a syntype)

Lóczy's specimen, holotype of *Asp. antiquum*, is too incomplete for closer identification, but agrees well with English material. It is in the collection of the Geological Institute, Budapest, reg. no. J117.

- (3) *Apoderoceras ferox* Buckman 1925
Apoderoceras ferox Buckman 1925, pl. 541

A fine large half-whorl in the University Collection, Budapest, agrees well with Buckman's figure.

No two of these tuberculate *Apoderoceras* are alike, and it remains for detailed monographic studies to show to what extent the many forms that have been described under different names, including *A. hastatum* (Young and Bird 1828), *A. hamiltoni* (Simpson 1843), *A. spicatum* (Simpson 1843), *A. submuticum* (Oppel 1853), *A. impavidum* (Buckman 1914), *A. tardarmatum* Buckman 1925 and *A. triornatum* Buckman 1928 are more than merely variants of a single species.

Genus **Epideroceras** Spath 1923

Type species *Amm. roberti* Hauer 1854

- (4) ? *Epideroceras* sp. juv.
 = *Aspidoceras amplexum* Lóczy 1915, p. 428, pl. xiv, fig. 3.

Closer identification of Lóczy's holotype of *Asp. amplexum* is doubly difficult. Besides the inadequacies of the fragmentary specimen itself, little is known about the detailed ontogenies of most of the eoderoceratids, and the fragment is here ascribed to *Epideroceras* because it is ribbed and mildly bituberculate, like the inner whorls of e.g. *Epideroceras exhaeredatum* Buckman 1923 (pl. 441). In the collection of the Geological Institute, Budapest, reg. no. J118.

- (5) ? *Epideroceras rollieri* (Lóczy 1915)
Aspidoceras rollieri Lóczy 1915, p. 430, pl. ix, fig 7, only.

Lóczy based the species on two syntypes. The larger of these is here designated lectotype. It is somewhat doubtfully placed in *Epideroceras* again for lack of a better alternative. The coiling is as in *Apoderoceras* but more involute, and it is ribbed on a round whorl-section rather than monotuberculate on a depressed quadrate whorl.

It is difficult to say whether the second syntype (pl. xiv, fig. 4) belongs to the same species. In the style of coiling, suture and ornament it resembles most a *Lytoceras* s.s.; but L ó c z y refers to a double row of tubercles on the inner whorls, recalling *Tetraspidoceras quadrarmatum* (D u m o r t i e r 1869, pl. x, fig. 1–3). In this species however the coiling on the outer whorls (ibid., pl. ix, fig. 1) appears to revert to the evolute, quadrate, bituberculate style of *Eoderoceras*, of which there is no sign in *Ep. rollieri*.

Genus *Villania* Till 1909

Type species *Villania densilobata* Till 1909

(6) *Villania densilobata* Till 1909

Villania densilobata Till 1909, p. 194.

Villania densilobata Till 1911, p. 45, pl. vii, fig. 6, 7; pl. viii, fig. 1, 2.

Till's holotype remains unique. His description and figures are good. On the outer whorl the specimen becomes hard to distinguish from *Apoderoceras* of the smooth *lobulatum* group, and even the sutures are strikingly similar (as they are to many other eoderoceratids, and *Lytoceras* itself). The temptation is hence to put *Villania* and *Apoderoceras* in synonymy. Unfortunately this would mean the fall of the well-known and well-characterised name *Apoderoceras* in favour of *Villania*, which is wholly lacking in precise details of origin and horizon. The inner whorls of *Villania* are however appreciably different from those of any described *Apoderoceras*, resembling again more closely *Epideroceras exhaeredatum* B u c k m a n (1923, pl. 441). "*Deroceras*" *retusum* (S i m p s o n) B u c k m a n (1913, pl. 82) and *validum* (S i m p s o n) B u c k m a n (1913, pl. 83) also seem close, but these are merely inner whorls of unidentified larger species. To avoid creating unnecessary confusion in the interpretation of well-established names, therefore, it seems safest to continue to keep *Villania* as a separate generic name until much more material is available.

The holotype is in the Natur-Museum Senckenberg, Frankfurt, reg. no. SMF XI 107, and not in the Geologische Bundesanstalt (formerly K. und k. geol. Reichsanstalt), Wien, as stated by Till.

[? (7) *Liparoceras* cf. *cheltiense* (M u r c h i s o n)

= *Cosmoceras globosum* Till 1911

See above, p. 6. The specimen is septate to 95 mm with a little bit of body-chamber. There are 3.0 secondary ventral ribs per external tubercle on the last half whorl. The matrix is a very fine dense ironshot oolite with limonitic crusts and veining suggesting a somewhat concretionary origin. It contains no other recognisable fossil fragments. The preservation is therefore quite unlike that of any other Liassic specimen from the immediate vicinity of Villány itself. Beds of similar age to those of Villány are however also described from the region around Siklós, at the other end of the Villány hills some 15 km to the west, by K a s z a p (1959, 1961).

Facies have changed appreciably in this short distance and are reported to include limonitic oolites. It seems not impossible therefore that Till's specimen, although not from Villány itself, might still have come from the region as a whole.]

Notes on the Liassic brachiopoda (D.V.A.)

Pliensbachian brachiopods were identified by the writer at Templom-hegy simultaneously with (but quite independently of) the discovery of Pliensbachian ammonites here. The finder had at the time no suspicion of the possibility of Liassic rocks being present. The brachiopod species collected on this occasion were as follows:

- Cincta numismalis* (L a m a r c k)
Tetrarhynchia cf. *T. argentinensis* (R a d o v a n o v i c)
Gibbirhynchia, sp.
Spiriferina sp. aff. *S. rostrata* (S c h l o t h e i m)

These all came from Bed 3a of Dr. Callomon's classification given above.

Subsequently in the Palaeontological Institute of the University at Budapest the writer saw further material collected from here. The bed terminology in these collections was different from those mentioned above, but there seems little doubt that the specimens came from the upper and lower parts respectively of the same Bed 3a mentioned above.

The specimens were identified as follows:

- Upper part *Cirpa fronto* (Q u e n s t e d t)
Gibbirhynchia aff. *G. muir-woodae* A g e r
Piarorhynchia juvenis (Q u e n s t e d t)
Lower part *Cirpa fronto* (Q u e n s t e d t)
Piarorhynchia cf. *P. juvenis* (Q u e n s t e d t)
Lobothyris sp.
Gibbirhynchia curviceps (Q u e n s t e d t)
? *Spiriferina* sp.

This assemblage undoubtedly indicates a Lower Pliensbachian age. It is very similar to the brachiopod fauna of the Jamesoni Zone in Britain.

Mr. A. V ö r ö s also drew the writer's attention to a specimen in the Palaeontological Institute from another locality, the neighbouring mountain of Harsányhegy. At this locality also, no Lower Jurassic rocks are recorded in the literature and the brachiopod in question again came from alleged "Bathonian". It is a much better preserved specimen than the others and it can be referred without doubt to *Spiriferina* aff. *S. rostrata* (S c h l o t h e i m). Again this suggests a Pliensbachian age and what is more, the brachiopod is embedded in a typical Pliensbachian oyster, *Gryphaea* aff. *G. cymbium* (S c h ä l f e). Similar oysters were seen in the brachiopod bed at Templom-hegy, but were impossible to extract and were much more difficult to determine.

One important point about these brachiopods is that they are characteristic of the Gresten facies of the Lias rather than the Adneth facies seen elsewhere in Hungary. Thus genera such as *Tetrarhynchia*, *Gibbirhynchia* and *Cincta* occur all round the outside of the Alps from southern Britain to Bulgaria and Turkey. Genera such as *Cirpa* are also found characteristically in this rather well-defined belt (Ager 1967, fig. 7) but also occur even more commonly in the more "alpine" zones. A very similar fauna has been collected by the author from the western part of the Balkan Mountains in Bulgaria and another has been described and figured from Yakacik in central Anatolia (Ager 1959).

The brachiopods are worth considering separately for stratigraphical purposes.

(1) *Cincta numismalis* (Lamarck).

This was divided by Buckman into no less than 20 nominal species on the basis of material from a single bed in a single quarry (Buckman 1907). None of these is more than a slight morphological variant and all constitute a side-line of zeilleriid terebratulids confined to the Lower Pliensbachian.

(2) *Tetrarhynchia* cf. *T. argotinensis* (Radovanovic).

Some poorly preserved specimens probably belong to this species which appears to be the eastern European equivalent (both morphologically and stratigraphically) of the well-known western European species *T. tetrahedra* (J. Sowerby) of the Pliensbachian.

(3) *Gibbirhynchia* sp.

This genus ranges from the bottom of the Pliensbachian to the basal Toarcian. *G. muir-woodae* is characteristic of the base of the Upper Pliensbachian and *G. curviceps* of the Lower Pliensbachian, especially the Jamesoni Zone (Ager 1962). The species are, however, very difficult to separate.

(4) *Cirpa fronto* (Quenstedt).

This is a very distinctive species of uppermost Sinemurian and Lower Pliensbachian age; again it is best known in the Jamesoni Zone (Ager 1958).

(5) *Piarorhynchia juvenis* (Quenstedt).

This is a long-ranging species of little stratigraphical value. It is known from the bottom of the Lower Sinemurian to the top of the Lower Pliensbachian (Ager 1962).

(6) *Lobothyris* sp.

This is a rather featureless terebratulid and hence a long-ranging nominal genus. It is especially common in the Pliensbachian, but is known as low as the Hettangian and as high as the Bajocian or even the Upper Jurassic.

(7) *Spiriferina* sp.

This is a particularly distinctive early Liassic genus and is extremely rare after the Pliensbachian. It is known in the basal Toarcian and has been recorded in the Bajocian, but the latter record cannot be confirmed. The genus is very much in need of systematic revision, which makes

specific identification difficult, but the smooth specimens seen seem to belong to the “extra-Tethyan” *S. rostrata* rather than to the “Tethyan” *S. alpina*.

The fauna as a whole is completely different from the rich brachiopod assemblages of similar age in the Bakony Mountains further north and is described by Dr. G. V i g h (1943) and currently being studied by Mr. A. V ö r ö s. This note is, therefore, in no sense a criticism of the magnificent work being done by Hungarian palaeontologists, since the fauna is otherwise unknown in their country.

It is also worthy of note that in this same region occur the famous Liassic coal measures of Pécs-Vasas. These are also characteristic of the Gresten facies.

So far as the later beds are concerned, the writer saw no example of the “*Rhynchonella*” *alemanica* recorded by L ó c z y, but this name and even more so its counterpart “*Rhynchonella varians*” have been used in a very broad way for many Jurassic rhynchonellids and have little significance. The Cephalopod Bed at the top of Somsich-hegy yielded specimens of a terebratulid comparable with *Loboidothyris zieteni* (D e L o r i o l) of the Callovian and later Jurassic.

Acknowledgements. It is a pleasure to thank the organizers of the Colloquium on the Mediterranean Jurassic, Budapest, for arranging the excursion to Villány and taking such care in the preparation of the sections and exposures. We thank also Professor B. G é c z y, Mr. A. G a l á c z and A. V ö r ö s for showing us the material in Budapest collections and many interesting discussions; Professor D o n o v a n and Dr. T o r r e n s for their opinions on systematic and stratigraphic matters; and Dr. K. W e r n e r, Frankfurt, for lending us types in the Senckenberg Museum and giving us much useful information.

CONCLUSIONS

Beds hitherto thought to be Bathonian (Middle Jurassic) at Villány, southern Hungary, are reassigned to the Lower Pliensbachian (Lias, Lower Jurassic) on the strength independently both of ammonites and brachiopods found *in situ*. Nevertheless some Upper Bathonian deposits are also still present in small lenticular pockets, lying between the sharp erosion surface of the Lias below and the Callovian Cephalopod Bed immediately above. Apparent anomalies in the ammonite-faunas previously described are thus given a satisfactory explanation.

REFERENCES

- A g e r, D. V. (1956–67): A monograph of the British Liassic Rhynchonellidae. *Monogr. Palaeont. Soc.*, pp. 172, 13 pls. Pt. I: 1956; Pt. II: 1958; Pt. III: 1962; Pt. IV: 1967.
– (1959): Lower Jurassic brachiopods from Turkey. *J. Paleont.* 33, 1018–28.

- (1967): Some Mesozoic brachiopods in the Tethys region. In: *Aspects of Tethyan Biogeography*, C. G. Adams and D. V. Ager, eds., Systematics Ass. Publ. No. 7, 135—51.
- Ar k e l l, W. J. (1956): *Jurassic Geology of the World*. Oliver and Boyd, Edinburgh and London.
- (1957): In *Treatise of Invertebrate Paleontology*, R. C. Moore ed., Geol. Soc. Amer. Part L, Mollusca 4, Cephalopoda, Ammonoidea.
- B ö c k h, J. (1881): Adatok a Mecsekhegység és Dombvidéke Jurakorbéli Lerakódásainak ismeretéhez. II. Pal. Rész. Értekezések a Természett. Kőréből (Budapest), xi, no. 9, 1—107, pls. i—x.
- B u c k m a n, S. S. (1907): Brachiopod morphology: *Cincta*, *Eudesia* and the development of ribs. *Quart. J. geol. Soc. Lond.* 63, 338—43.
- (1909—30): *Yorkshire Type Ammonites* (vols. 1, 2) and *Type Ammonites* (vols. 3—7). London.
- C a l l o m o n, J. H. (1963): Sexual dimorphism in Jurassic ammonites. *Trans. Leics. Lit. Phil. Soc.* 57, 21—56, pl. 1.
- D e a n, W. T., D o n o v a n, D. T., and H o w a r t h, M. K. (1961): The Liassic ammonite zones and subzones of the North-West European Province. *Bull. Brit. Mus. (Nat. Hist.)*, geol., 4, 437—505, pls. 63—75.
- D u m o r t i e r, E. (1869): Études paléontologiques sur les dépôts jurassiques du Bassin du Rhône. 3^e Partie: Lias Moyen. Paris.
- G a l á c z, A. and V ö r ö s, A. (1969): Belemnite fauna of the ammonite-rich Callovian bed at Villány, south Hungary. *Ann. Univ. Scient. Budapestinensis*, sect. geol. 12, 117—39, pls. 1—4.
- H o l l m a n n, R. (1964): Substitutions-Fragmente. *N. Jb. Geol. Palaeont., Abh.*, 119, 22—82, pls. 7—10.
- K a s z a p, A. (1959): Dogger rétegek a Villányi-hegységben. *Földtani Közlemény* 89, 262—9, pls. 8—16.
- (1961): Die Bath-Kallov-Schichten in dem Villányer Gebirge. *Ann. Inst. Geol. Publ. Hungarici* 49, 659—64.
- L ó c z y, L. von. (1915): Monographie der Villányer Callovien-Ammoniten. *Geol. Hungarica* 1, 255—507, pls. i—xiv.
- O p p e l, A. (1853): Der mittlere Lias Schwabens neu bearbeitet. *Württemberg. naturwiss. Jahresh.* 10, 39—136, pls. i—iv.
- R a d w a n s k y, A. and S z u l e z e w s k i, M. (1966): Jurassic stromatolites of the Villány mountains (southern Hungary). *Ann. Univ. Sci. Budapestinensis*, sect. geol., 9, 87—107, pls. 1—6.
- S i m p s o n, M. (1843): *A monograph of the ammonites of the Yorkshire Lias*. London.
- S p a t h, L. F. (1931): Revision of the Jurassic Cephalopod Fauna of Káchh. (Cutch). *Palaeont. Indica*, N. S. 9, Mem. 2, Pt. V, 551—658, pls. 103—124.
- T i l l, A. (1909): Neues Material zur Ammonitenfauna des Kelloway von Villány (Ungarn). *Verh. k. k. geol. Reichsanst.* (Wien), 1909 (8), 191—5.
- (1910—11): Die Ammonitenfauna des Kelloway von Villány (Ungarn). *Beitr. Paläont. Österr.—Ungarns* 23, 251—72, pls. xvi—xix (1—4), 24, 1—49, pls. i—viii (5—12).
- T o r r e n s, H. S. (1969): The stratigraphical distribution of Bathonian ammonites in Central England. *Geol. Mag.* 106, 63—76.
- V i g h, G. (1943): A Gerecse hegység északnyugati részének földtani és őslénytani viszonyai. *Földtani Közlemény*, 73, 301—612.
- Y o u n g, G. M. and B i r d, J. (1828): *A geological Survey of the Yorkshire coast*. 2nd Ed. Whitby.

MINERALOGICAL AND GEOCHEMICAL STUDY OF ZIRCONS IN THE GRANITOIDS OF HUNGARY

by

L. BOGNÁR

Chair of Mineralogy, Eötvös University, Budapest)

(Received: 2 June 1970)

Introduction

Escaping even the process of weathering, zircon is an important accessory component of igneous rocks. It can be used well for tracing the origin of sedimentary rocks.

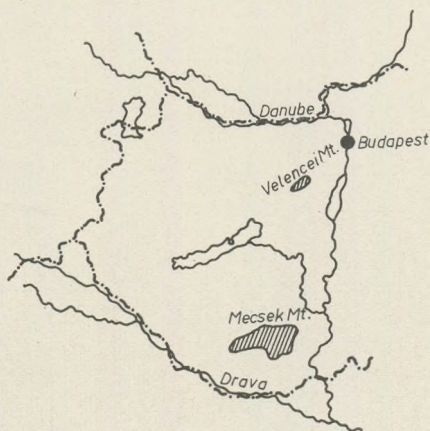


Fig. 1. Sketch of the geographic situation of the Velence and Mecsek Mountains.

Thanks to investigations by Poldervaart (1950), it is well-known, that the morphological characteristics of magmatogenic zircons are diagnostic for the individual rock types. Elongation of zircon crystals can be used for drawing conclusions as to the origin of calc-alkaline granitization. The value of elongation of zircons in orthogranites is a characteristic feature. If the maximum of its distribution is 2.5 or more, then the enclosing granitoid must be of primary origin; whereas at values lower than 2.5 the respective granitoid must have been brought about by remelting, magmatization. The statistical analy-

sis of zircon of granitic origin in mineralogical studies was introduced by Larsen and Poldervaart (1957), an excellent method for the comparison of granitoids of different type and genesis. The present writer in his analogical investigations of zircons in Hungarian granitoids, has relied upon the above results and has supplemented them with his trace element analyses of zircon.

His investigations were aimed at finding out any divergency or identity between the granitoids of the Mecsek Mountains (South Hungary) and the Velence Mountains [some 60–70 km SW of Budapest (Fig. 1)].

Morphological-statistical analysis

200 doubly terminated zircon grains were selected for statistics. Under the polarization microscope their lengths along the c-axis and their breadth along the a-axis were measured. Afterwards the expansion ratio was calculated for each particular grain. All these results were represented graphically using the so-called Reduced Major Axis (RMA) introduced by Larsen and Poldervaart (1957), a method most suitable for comparative studies.

For the construction of the RMA the following data are necessary:

N = number of crystals measured (if this value is at least 200, the sample can be easily evaluated statistically),

\bar{x} = mean length

\bar{y} = mean breadth,

Sx = standard deviation (scatter) of length,

Sy = standard deviation (scatter) of breadth.

The above data can be calculated as follows:

$$\bar{x} = \frac{\sum(x)}{N}$$

$$\bar{y} = \frac{\sum(y)}{N}$$

$$Sx = \sqrt{\frac{\sum(x - \bar{x})^2}{N}}$$

$$Sy = \sqrt{\frac{\sum(y - \bar{y})^2}{N}}$$

$$\text{Hence: } a = \frac{Sy}{Sx}, \text{ where}$$

a is the tangent of the angle at which the fitted line (RMA) is drawn through the point (\bar{x}, \bar{y}) .

On the basis of the data available one can draw the straight line having a tangent \bar{a} through points \bar{x} and \bar{y} .

Correlation coefficient:

$$r = \frac{\sum_1^{200} (x - \bar{x})(y - \bar{y})}{\sqrt{\sum_1^{200} (x - \bar{x})^2 \sum_1^{200} (y - \bar{y})^2}}$$

is a measure of how well this fitted line, RMA, is able to represent the dot diagram; in other words, it is a measure of closeness of the relationship between length x and breadth y .

If $r = \pm 1$, correlation is perfect; if $r = 0$, correlation is absent.

Another characteristic of RMA,

$$Dd = 100 \sqrt{\frac{2(1-r)(Sx^2 + Sy^2)}{\bar{x}^2 + \bar{y}^2}},$$

is the coefficient of relative dispersion, expressing (per cent) the relative scatter of points about the RMA.

A measure of the reliability of the fitted line (RMA), the standard error of slope:

$$\sigma_a = a \sqrt{\frac{1-r^2}{N-2}}.$$

The smaller the value of the standard error, the more reliable the estimate.

The above data are of significance, when the results of measurement of a number of comparable samples are available.

Possibilities for studying zircons in thin sections have been rather limited, for the examined rocks contain very low amounts of zircon. Therefore monomineral concentrates of zircon have been used.

The zircon grains in the granitoid rocks of the Velence Mountains are predominantly light-yellow, those recovered from similar rocks from the Mecsek Mountains being darker, honey-coloured in a cloudy pattern — phenomenon due, in most of the cases, to continued growth.

The use of large populations of monomineral zircons and their careful optical examination have enabled the author to summarize their general characteristics as follows:

a) The Velence Mountains zircons are characterized by the appearance of simple crystal faces: it is the (100) prism and the (111) dipyrmaid that are most abundant, the (001) basal plane being scarcer (Plate I, Fig. 1). In spite of the distinct forms, the shape of the grains is no always perfect, as continued growth, eventually zoned (Plate I, Fig. 1), is frequent. Some of the grains are fractured (Plate I, Fig. 2). Inclusions, in many cases distinctly parallel to the *c*-axis, occur rather frequently (Plate I, Fig. 2, 4; Plate II, Fig. 5).

b) Like the Velence Mountains zircons, zircon grains in granitoid rocks from the Mecsek Mountains are also characterized by simple faces such as the (100) prism, the (111) dipyrmaid and the (001) basal plane (Plate II, Fig. 7, 8).

Characteristically enough, in the various rock types of the quarry at Erdősmecke, Mecsek Mountains, both transparent grains and zircons of cloudy colouring can be shown to be present in great quantities. Continued growth is frequent, but the abundance of zoned zircon grains is yet more characteristic (Plate II, Fig. 7, 8). Another common phenomenon is the fact that many grains have their nuclei darker, rounded, in contrast with their light and, usually, zoned rim (Plate II, Fig. 8). The Mecsek Mountains zircons often contain inclusions which in nucleated grains occur mainly in these, darker, nuclei.

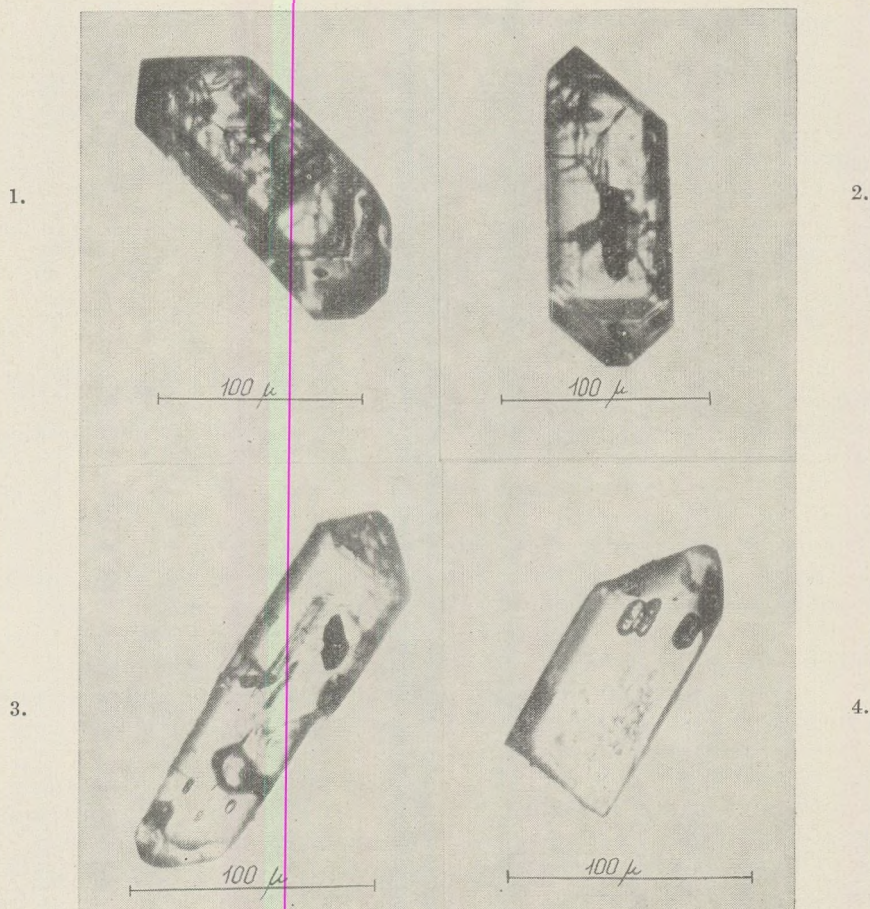


Plate I.

1. Idiomorphic zircon crystal with a basal plane at one end (Velence Mountains, Székesfehérvár).
2. Idiomorphic zircon crystal with an opaque inclusion (Velence Mountains, Székesfehérvár).
3. Zircon crystal with oriented inclusions, showing continued growth at one end (Velence Mountains, Pákozd).
4. Broken zircon crystal with oriented inclusions (Velence Mountains, Szűzvár).

Using the method of Larsen and Poldervaart (1957), the present writer has constructed the frequency curve of elongation (Fig. 2, 3) and the RMA (Fig. 4, 5) of each sample. The morpho-statistical data necessary for the construction of the RMAs are shown in Table 1.

The RMAs, the frequency curves of elongation and the data given in the tabulation show the following characteristics:

a) The average grain sizes of zircon crystals from Erdősmecke, Mecsek Mountains, are practically the same. The difference of four samples



Plate II.

5. Two idiomorphic zircon crystals with oriented inclusions (Mecsek Mountains, Véménd, South Hungary).
6. Fractured zircon crystal with plenty of inclusions (Mecsek Mountains, Erdősmecke, South Hungary).
7. Dark zircon crystal with zoned continued growth (Mecsek Mountains, Erdősmecke, South Hungary).
8. Two idiomorphic zircon crystals. In the smaller grain the darker rounded nucleus, showing a zoned continued growth, can be readily observed (Mecsek Mountains, Erdősmecke, South Hungary).

in mean length is as low as 5μ , the difference in mean breadth being also 6μ only, a fact indicating that all the Erdősmecke samples are characterized by the same elongation. As evident from a comparison of grain sizes, the zircons of the Véménd granite are longer, thus their elongation is also longer, than the former. Two of the elongation frequency curves obtained for the Mecsek zircon grains show two distinct peaks each.

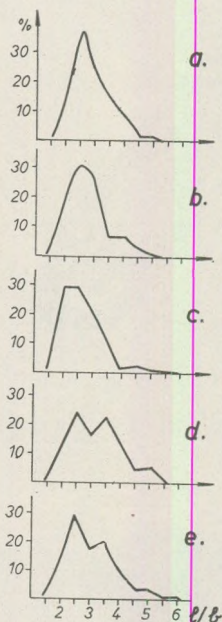


Fig. 2. Elongation frequency curves of zircon samples from the Mecsek Mountains.

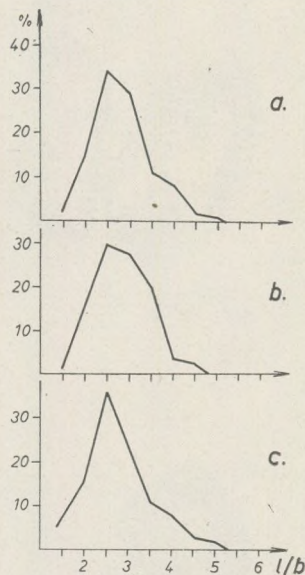


Fig. 3. Elongation frequency curves of zircon samples from the Mecsek Mountains.

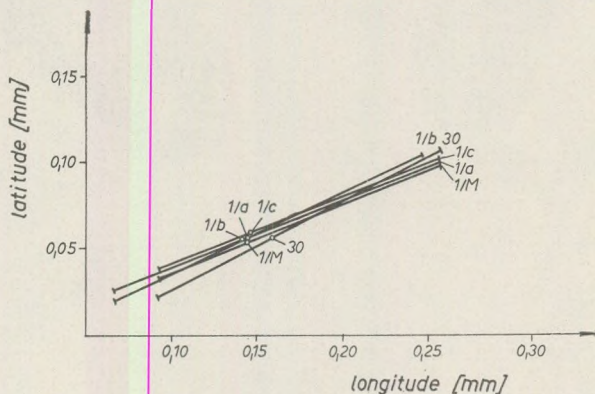


Fig. 4. Reduced major axes (RMA) of zircons from Mecsek Mountains granitoids.

b) The mean sizes of the Velence Mountains zircon grains show a wider variability range than it is the case with their Mecsek counterparts. It should be taken into consideration here that it is the zircons of microgranites (Székesfehérvár) that have the lowest grain size.

Despite differences in size, mean elongations show a surprising agreement. If the elongation ratio is cut down to the first decimal – a measure

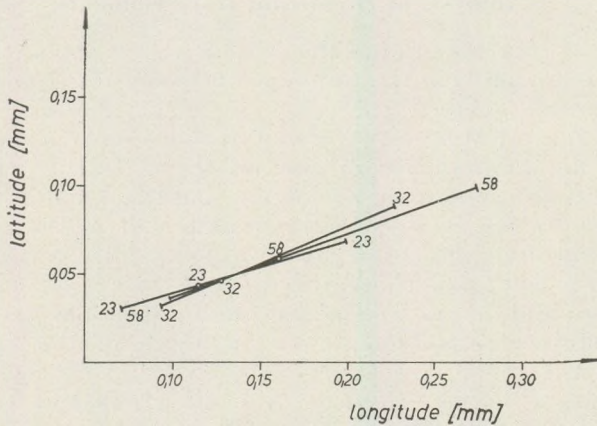


Fig. 5. Reduced major axes (RMA) of zircons from Velence Mountains granitoids.

Table 1

Morphological-statistical data of zircon grains

Sample	N	\bar{x}	\bar{y}	\bar{x}/\bar{y}	Sx	Sy	a	r	Dd	σ_a
Mecsek Mountains:										
Erdősmecke	200	144.6	52.5	2.75	33.65	14.08	0.4185	0.6657	19.38	0.0222
1/m (molybdenitic granite)										
Erdősmecke 1/a	200	144.5	55.4	2.60	33.30	13.17	0.3955	0.7086	17.66	0.0198
Erdősmecke 1/b	200	141.8	54.4	2.60	34.20	15.70	0.4591	0.7466	17.65	0.0217
Erdősmecke 1/c	200	146.7	58.6	2.50	36.70	14.35	0.3910	0.6990	19.35	0.0199
Véménd	200	159.2	55.8	2.81	28.54	14.06	0.4926	0.9145	7.80	0.0141
Velence Mountains:										
Székesfehérvár (23.)	200	113.9	42.4	2.69	37.87	12.16	0.3211	0.5909	29.61	0.0184
Pákozd (32.)	200	127.8	46.7	2.73	30.13	12.87	0.4271	0.7776	16.06	0.0191
Szűzvár (58)	200	160.0	59.0	2.71	35.89	12.92	0.3600	0.7453	15.96	0.0171

N = number of grains

Sx = standard deviation of length

Dd = coefficient of relative dispersion

 \bar{x} = mean length, in μ

Sy = standard deviation of breadth

 σ_a = standard error of slope \bar{y} = mean breadth, in μ

a = slope of fitted line (RMA)

r = correlation coefficient

 \bar{x}/\bar{y} = mean elongation

advisable from many points of view — a complete identity will result. As evident from the figures of the RMA, the points \bar{x} and \bar{y} of the three fitted lines lie nearly in one straight line.

It is remarkable that the small-grained zircons of microgranites are least correlated, an observation confirmed by their coefficient of relative dispersion ($Dd = 29.6\%$).

Analysis of zircons for trace elements

During his complex studies the present writer attempted to use several methods for proving the difference between the granitoid rocks of the two mountain ranges.

At the Chair of Mineralogy of Eötvös University a method for the quantitative determination of Zr was developed. In the granitoids there is a close relationship between Zr content and the amount of zircons, for the Zr content of the rock is concentrated practically in the zircon mineral. The Zr content of zircons is 50% or so; consequently, twice the amount of Zr is equal to the zircon content of the rock.

Zr content and the trace elements content of zircons were determined by X-ray fluorescence techniques (with a device of the type Siemens-Kristalloflex-4).

On the basis of the papers of Norton (1956), Birks (1965) and Zussmann (1967) a semi-quantitative method for analysing zircons for trace elements has been developed. Taking into consideration the techniques developed by Birks and Brooks (1950), Norton (1956) and Abdel-Gawad (1966), the staff of the above Chair has also developed a method for the quantitative assessment of Zr and Hf.

In their measurements they applied a scintillation counter discriminated for the line of $ZrK\beta_{1,3}^{II}$ ($\lambda = 0.702 \text{ \AA}$) and they measured its II-nd order at the 40.73° value of the 2θ angle, using analyser crystal LiF. In determining Hf they used, unlike earlier students, the line $HfL\beta_2 = \lambda = 1.326 \text{ \AA}$ as analysing line and they measured the intensity at the value 38.47° of the 2θ angle with crystal analyser LiF.

Discrimination data of scintillation counter:

a) voltage of detector at $ZrK\beta_{1,3}^{II}$	557.0 V
basal line	11.6 V
channel width	6.3 V
b) voltage of detector at $Hf\beta_2^I$	601.5 V
basal line	10.8 V
channel width	7.8 V

The results have led the present writer to conclude that measuring with the above analysing lines allows one to calculate the Zr/Hf ratio with the highest accuracy, as at the given points of measuring, 40.73° and 38.47° , the Zr : Hf ratio is likely to be 12.5 : 1 provided that Zr/Hf is ~ 50 .

The advantage of these two lines has been confirmed by the lack of interference with the line of any other element at the above value of angle in case of zircons.

As inner standard in quantitative analyses, ZrO_2 and HfO_2 of spepure quality have been used.

X-ray fluorescence results have confirmed the assumption, based upon observations of thin sections, that the granitoids of the Mecsek Mountains contain about thrice the amount of zircons contained in their Velence Mountains counterparts.

Out of the potential trace elements first of all Y, Hf, Th, U and Pb and Fe have been detected in zircon concentrates.

The detected trace elements are shown in Table 2:

Trace elements

Table 2

Sample	Element g/t						
	Fe	Y	Hf	U	Th	Pb	Others
Velence Mountains:							
Székesfehérvár	900	2000	1900	400	400	1200	—
Pákozd	400	1800	250	100	100	8000*	Ce, La
Szűzvár	1200	900	200	400	400	1000	—
Mecsek Mountains:							
Erdősmecske-a	2500	900	650	500	500	500	—
Erdősmecske-b	2500	1000	600	1000	1000	?	—
Véménd	1000	950	800	—	—	—	—

* Because of impurity due to galena

As shown in the references cited, the two most frequent trace elements of zircon are Hf and Y. Both the distribution and quantity of these two elements are important for the qualification of zircons. Hafnium (Hf) is always indicative of the original environment in which zircons crystallized, whereas yttrium (Y), often enriched like Hf, is mostly associated with inclusions in xenotime (Plate I, Fig. 3, 4).

The analyses have shown that the yttrium content of the Velence Mountains zircon is a little higher than that of the Mecsek Mountains zircons.

Actinid elements could not be detected in all zircon grains. Despite this fact, the Mecsek Mountains zircons are supposed to have higher U and Th contents. As regards their relative amounts, the regularity notified by A h r e n s (1964) could not be observed, a regularity according to which the U content of granitoids would be higher than their Th. In the analysed samples the Th/U ratio was 1 : 1 or so.

It is in connection with radioactive elements that zircons can be shown to contain lead, though the strikingly high Pb content of the zircons from Pákozd, Velence Mountains, is due to impurities because of the admixture of galena.

The amount of iron (Fe) is likely to affect the colour of zircons, hence the darker stain of the Mecsek Mountains zircons.

In the Pákozd sample, beside the above elements, Ce and La were also detected, both in an amount of 10 g/t or so.

The determination of the Zr/Hf ratio was made possible, despite the low amount of zircon concentrate, by the analysing lines applied. The values of Zr/Hf obtained for the Velence Mountains rocks vary between 14 and 16, those obtained for the Mecsek Mountains rocks, between 15 and 58.

The Zr/Hf values were compared with the results of Chess ex and Delaloye (1965), according to which the mean Zr/Hf ratio of zircons in calcalkaline granitoid rocks would range from 25 to 45. The figure obtained for Hungarian granitoids is in good agreement with these. Inasmuch as the results of Veniale et al. (1968) (who found the Zr/Hf ratio in the individual zones within one crystal to show divergences ranging from 10 to 40) are confirmed by further investigations, the ratio of zoned crystals to the crystals of simple structure will be proved to affect decisively the behaviour of the Zr/Hf ratio.

Conclusions

Zircons in the granitoids of the Mecsek Mountains represent "structurally normal" zircon and thus they show a good agreement with one another.

Morphological examination of the grains has shown them to be built up of combinations of simplest crystal faces and thus has indicated that the zircons of the Hungarian granitoids must have crystallized at a comparatively high temperature, prior to the rest of rock-forming minerals.

As evidenced by the low size of zircon grains (mean length 110 to 160 μ) and by the large regional distribution of their, more or less equal, elongation values, their crystallization must have taken place under the same physico-chemical conditions. In a freely cooling melt, zircons will crystallize within a comparatively short span of time. Hence the identity of sizes and the one-peak curve shown by elongation frequencies.

The elongation frequency curves of Velence Mountains zircons are also characterized by one frequency peak, whereas the two-peak curves of the Mecsek Mountains samples (Poldervert, 1950) are suggestive of magmatic re-melting.

The presence of zoned zircon crystals proves that the physico-chemical environment must have changed within a comparatively short phase of crystallization. That the zoned crystals in the Mecsek Mountains zircons are essentially more frequent is a testimony to magmatic origin, too. In the Mecsek Mountains zircons such grains having darker, rounded nuclei, contrasting with a light, honey-coloured rim, sharp-edged and well-crystallized, can often be encountered. Two hypotheses may account for the origin of these:

a) The nucleus is constituted by a magmatically remolten zircon grain of an older rock and the intact crystal rim may have crystallized from its partly molten portion combined with the new material of the secondary magma.

b) The nucleus is constituted by a similarly early, rounded, elastic zircon grain and the intact rim was formed during assimilation, with incorporation of the assimilating magma itself.

Accordingly, the zircon crystals consisting of a rounded nucleus and an intact rim must be manifestations of remelting. However, it is only

an analysis for trace elements by electron micro probe that would be able to decide the validity of either of the two hypotheses. Should in this case the percentages of trace elements in the rim and the nucleus prove to be essentially different, this would be an evidence in favour of the assimilation of sedimentary zircon.

Inclusions occur frequently in zircons. As far as their substance is concerned, a considerable part is supposedly xenotime: a hypothesis supported by the quantity of Y detected by trace analyses, by the identity of xenotime structure with that of zircon and by the frequently oriented arrangement of the inclusions. A substantial part of the opaque minerals is magnetite.

In both the Mecsek and Velence Mountains, zircon inclusions are connected with biotite. Zircon content in the Velence Mountains averages 50 to 70 grams per ton, in the Mecsek Mountains it attains about thrice this figure — 200 grams per ton or so. However, zircon content is not proportional to the biotite content of the rocks.

On account of its early crystallization zircon is very poor in trace elements. Beside the elements Fe, Y, Hf, U, Th and Pb it is alone in the Pákozd sample that Ce and La could be detected in a quantity of 10 grams per ton or so. Except for the Véménd sample, U and Th could be identified in all zircons, both in equal quantity. This is in part contradictory to A h r e n s' statement, according to which the quantity of U in granitoids would be higher than that of Th. The divergence of the present writer's measured quantities from the references is unessential and corresponds to the average observed in connection with granitoid rocks in general.

According to the first determination of Hf and of the Zr/Hf ratio ever made in Hungarian rocks, the Zr/Hf ratio in Velence Mountains zircons is lower than in the Mecsek Mountains samples. A comparison of the analyses with published data has shown this difference to be unessential, especially with regard to the different methods involved and to the relative divergences of the published data themselves.

On the basis of the mineralogical and geochemical characteristics of the investigated zircons let us conclude that the conditions of segregation of the Mecsek Mountains granitoids must have been much more diversified than those of the Velence Mountains rocks. This supports the hypothesis that most of the Mecsek Mountains rocks were brought about by magmatic metasomatism. Zircon testing of Velence Mountains rocks has shown these to be of juvenile, primary magmatic origin.

REFERENCES

- A b d e l - G a w a d, A. M. (1966): X-ray spectrographic determination of hafnium-zirconium ratio in zirconium minerals. *Am. Min.* 51. p. 464.
- A h r e n s, L. H. (1965): Some observations on the uranium and thorium distributions on accessory zircon from granitic rocks. *Geoch. Cosmoch. Acta* vol. 29. p. 711 — 716.
- B i r k s, L. S. (1965): X-ray spectrochemical analysis. Interscience Publishers, Inc. New York.

- Birks, L. S. — Brooks, E. J. (1950): Hafnium-Zirconium and Tantalum-Columbium Systems. Quantitative Analysis by X-ray Fluorescence. *Anal. Chem.* 22. p. 1017—1020.
- Buttler, J. R. — Thompson, A. J. (1965): Zirconium-hafnium ratios in some igneous rocks. *Geoch. Cosmoch. Acta* vol. 29. p. 167—175.
- Chessex, R. — Delaloye, M. (1965): Données sur les teneurs en hafnium et en yttrium des zircons. *Sch. Min. Petr. Mitt.* vol. 45. p. 295—315.
- Dennen, W. H. — Shields, R. (1956): Yttria in zircon. *Am. Min.* p. 655.
- Fleischer, M. (1955): Hafnium Content and Hafnium-Zirconium Ratio in Minerals and Rocks. *Geol. Surv. Bull.* vol. 1021 a.
- Koszttyerin, A. V. — Sevaljevskij, I. D. — Ribalova, E. K. — Tolok, K. P. (1963): Szootnosenyije Zr/Hf v cirkonah nyekotorih izverzsennih porod szevernovo Kazahsztana. *Geokhimiya*. No. 10. p. 966—968.
- Larsen, E. S. — Waring, C. L. — Berman, J. (1953): Zoned Zircon from Oklahoma. *Am. Min.* p. 1118—1125.
- Larsen, L. H. — Poldervaart, A. (1957): Measurement and distribution of zircons in some granitic rocks of magmatic origin. *Min. Mag.* 1957. vol. 31. No. 238. p. 544.
- Levinson, A. A. — Borup, R. A. (1959): High Hafnium Zircon from Norway. *Am. Min.* vol. 45. p. 562—565.
- Ljahovics, B. B. — Sevaljevskij, I. D. (1962): Geokhimiya szootnosenyij cirkonija i gafnija v akcesszornom cirkone granitoidov. *Geokhimiya* No. 5. p. 440—452.
- Mertie, J. B. (1958): Zirconium and Hafnium in the South Eastern Atlantic States. *Geol. Surv. Bull.* 1082—A.
- Norton, D. A. (1956): X-ray fluorescence as applied to cyrtolite. *Am. Min.* 49. p. 492.
- Poldervaart, A. (1950): Statistical Studies of Zircon as a Criterion in Granitisation. *Nature*, vol. 165. p. 574.
- Poldervaart, A. (1956): Zircon in rocks. 2. Igneous rocks. *Am. Journ. of Sc.* vol. 254. No. 9. p. 521—554.
- Poldervaart, A. — Eckelman, F. D. (1956): Growth Phenomena in Zircon of Autochthonous granites. *Bull. of Geol. Soc. of Am.* vol. 66. p. 947—948.
- Szádeczky-Kardoss, E. (1959): On the mechanism of the magmatism in the Carpathians. A kárpáti közbenső tömeg magmás mechanizmusáról. *Geokém. Konf. Kiadv.* Budapest.
- Veniale, F. — Pigorini, B. — Soggetti, F. (1968): Petrological Significance of the Accessory Zircon in the Granites from Baveno. M. Orfano an Alzo (North Italy). XXIII. Intern. Geol. Congress. vol. 13. p. 243—268. Prague.

THE PLIENSBACHIAN OF KERICSER HILL, BAKONY MOUNTAINS, HUNGARY

by
B. GÉCZY

(Department of Paleontology, Eötvös University, Budapest)

(Received: 6 June, 1970)

РЕЗЮМЕ

На основании качественно-количественной оценки аммонитовой фауны холма Керичер на территории гор Баконь можно предположить, что рассматриваемый участок в плинсбахском веке соответствовал краевой зоне бассейна, расположенного между подводными уступами (seamounts), где осадконакопление происходило в сочетании с процессами реседиментации окружающих районов. В результате разрывных тектонических нарушений рассматриваемый участок, который в позднетриасовую эпоху образовывал еще выдержанное подводное плато, был в раннем лейасе разобран на уступы и впадины. Благодаря подводным оползням типа слэмпинг с участков были снесены сначала уже уплотненные, а затем также и еще неуплотненные, приблизительно одновозрастные осадки, которые впоследствии отлагались в выдержанно пелагических условиях краевой части осадочного бассейна лептогеосинклинального типа. Местное увеличение мощности плинсбахских отложений обусловлено привнесением аллохтонного биогенного материала (брахиоподы, криноидеи и мелкие аммониты, обитавшие на уступах). Исчезновение аллохтонных элементов в конце плинсбаха связано с уравниваемостью палеоэкологических условий на относительно большой территории.

Наряду со средиземноморским характером лейасовых отложений гор Баконь и с кажущимися ненарушенными условиями их залегания, интенсивность разрывных нарушений также соответствует условиям, существующим в Южных Альпах (БЕРНУЛЛИ, 1964; ОБУЭН, 1965). Следовательно, центральная масса Альп ограничивается площадями аналогичной структуры не только с юга, но также и с востока.

In the Bakony Mountains the Middle Lias is generally represented by red ammonitic limestones — the so-called ammonitico rosso facies wide-spread in the Mediterranean region. As shown by the fauna of six standard sections developed and geologically characterized by K o n d a, the thickness of the Pliensbachian totals as low as 4.55 m. The section on the Kericsér shows certain differences in thickness, lithology and faunal character from the rest of those standard sections. Hence the need for its investigation in fuller detail.

The Kericsér is a small hill on the northern slope of Mt. Papod, at 2 km SSE of Lókút village, near the town of Zire, northern Bakony Mountains.

The Liassic beds were developed by the staff of the Hungarian Geological Institute, under the direction of K o n d a. He recognized the

occurrence of hiatus in this sequence of Hierlatz facies beginning with the Upper Sinemurian, and he hinted at the allochthonous mode of emplacement of the limestone blocks of dachsteinkalk type (1970). In 1967 K o n d a entrusted the present writer with elaborating the fauna. The author feels indebted to him for this greatly appreciated confidence of his.

I. STRATIGRAPHY

Excavations have shown the Kericser section to comprise 36 beds. The thickness of the beds varied between 12 and 55 cm, averaging at 28 cm. Lithologically, the sequence can be split up into three units.

1. The lower red limestones

The slightly rough surface of the Lower Liassic oolitic and pseudo-ölitic limestones of dachsteinkalk type is overlain, with a marked change in lithology, by poorly stratified red limestones attaining a total of 214 cm in thickness (Beds 29 to 36). As for their texture, these limestones are not uniform. The dark- and light-red, locally yellowish-pink or greyish-white limestone lenses or mottles, the nodules or coatings constituted by ferromanganese oxide, and the clayey incrustations, greenish, grey or black in colour, are manifestations of a varied composition and genesis. Also, the material of the lower red limestones is a mixture. This is particularly

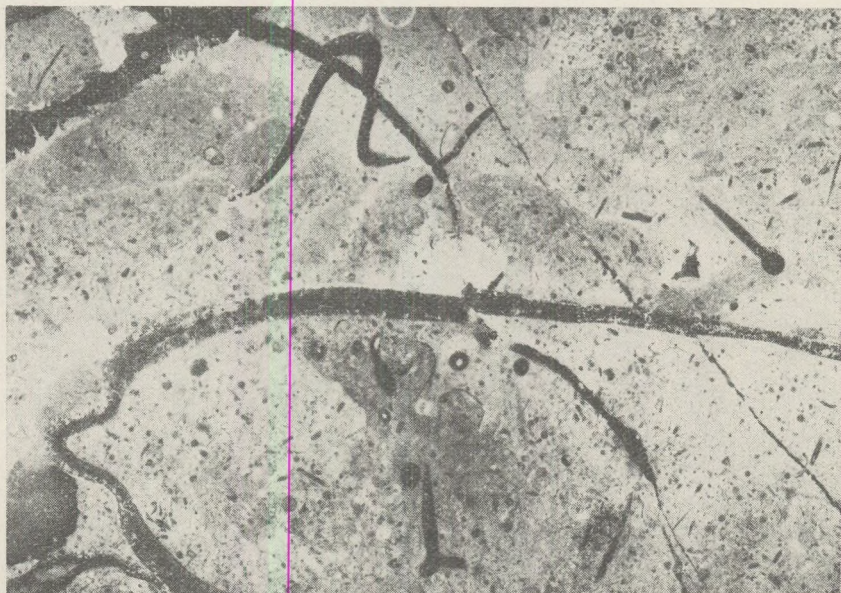


Fig. 1. The lower red limestone (Bed 36) with benthonic foraminifers, spicules of silicospongia and detritus of lamellibranchs, ammonites and crinoids (magnification: 11 x)

emphasized by the exotic boulders of Lower Liassic limestones. Both the big size and angularity of these boulders contradict any explanation suggesting surf action or currents as possible agents responsible for their introduction into this environment. The absence of any comminuted detrital material is also a testimony against the action of currents whatever. The introduction of the exotic boulders into the basin characterized by red silts may have been due to synsedimentary slumping and, indirectly, to synsedimentary tectonic deformations.

The fine-grained red calcareous silts correspond to the type of sediment referred to as microfossiliferous calcilutite by F a b r i c i u s (1966) and/or to W ä h n e r ' s (1886) variegated cephalopodal limestones and A u b o u i n ' s (1965) calcareous ammonitico rosso, the only difference consisting in the more subordinate occurrence of subsolution phenomena and in the indistinctness of strata contacts.

The lower red limestones contain sporadic representatives of foraminifera, multiaxial spicules of sponges, lamellibranchs, small gastropods, ammonites, nautiloids, belemnitoids, brachiopods and crinoids. One coral calix has also been encountered. The sponge spicules show an upward decrease, the foraminifera and crinoids an upward increase, in number.

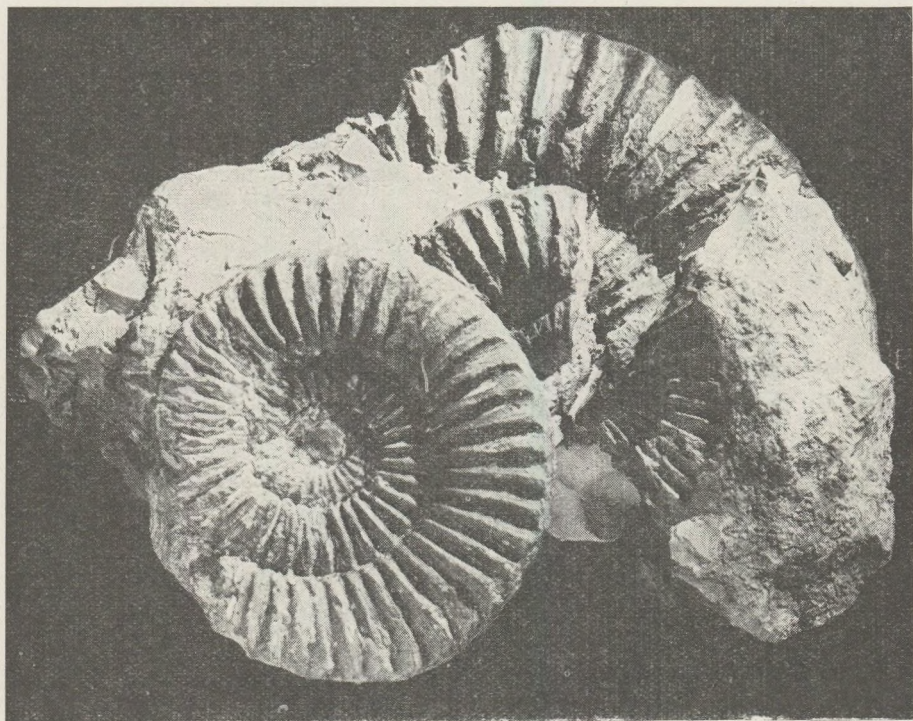


Fig. 2. Parallel arrangement of the specimens of *Arnioceras ceratitoides* (Q u e n s t e d t, 1849) (Bed 35)

The fauna is in different state of preservation. Most of the ammonites are shelled specimens, the rest being represented by internal moulds. The shells or moulds are often coated by ferromanganese oxide. The shells of certain specimens have not been infilled by calcareous silt. In these cases calcite crystals have precipitated on the inner wall of the shell. Surprisingly enough, both silt-filled and empty shells can be collected from one and the same bed. Accordingly, it is quite possible that the ammonites were originally buried under different conditions of sedimentation in different areas and later introduced into the basin by slumping together with the sediment still partly unconsolidated. A valuable example of a similar phenomenon was quoted by Hudson and Jenkins (1969). No complete specimen having an intact peristome has been found, it is true, but heavily fragmented, incomplete specimens are rare too — a phenomenon contradicting the suggestion of any permanent reworking of the material.

In the lower red limestones the ammonites are usually distributed at random. A regular arrangement is exhibited merely by the specimens of *Arnioceras ceratitoides* of Bed 35. Admitting the possibility of redeposition from elsewhere and mixing, it is quite possible here too, that the parallel arrangement of the ammonites reflects the conditions of the first burial rather than those of the final one. The same may hold true of the oriented ammonites of Bed 33, a fact suggesting that the calcareous mud bottom may have been consolidated to some extent before the ammonites were parallelly arranged.

The ammonites are of medium to great size, except for the groups characterized, as a rule, by small size (*Gemellaroceras*, *Polymorphites*). Faunal density is low: an average of 64.5 specimens per 1 m³. Compared with the allochthonous elements, the autochthonous ones seem to have been more reduced in number.

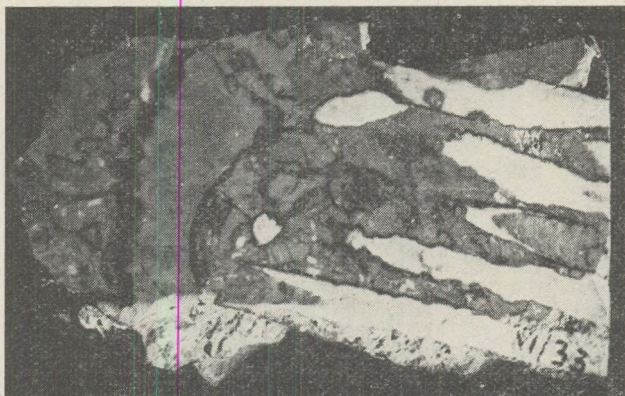


Fig. 3. Oriented belemnite rostra in the lower red limestone (Bed 33)

The representatives of *Phylloceras* and *Lytoceras* here are scarcer than in the calcareous ammonitico rosso (34.9%). It can be supposed that the red limestones may have been deposited in a comparatively deeper part of the neritic zone.

The oldest ammonites are indicative of the Lower-Middle Sinemurian boundary — the Obtusum Zone, or possibly of a yet deeper horizon — the upper part of the Turneri Zone. There is no doubt that at the Kericser locality, or at least in its vicinity, the deposition of the red limestones began as early as the beginning of Upper Sinemurian time. The latest representatives of the ammonites in the red limestones, *Tropidoceras* and *Acanthopleuroceras* cf. *valdani*, are characteristic of the lower and middle subzones of the Middle Carixian. Consequently, the deposition of these limestones must have lasted up to the top of the Middle Carixian. Traces of sedimentation in the intermediate time units are indicated by a few specimens of *Angulaticeras* and *Palaeoechioceras* ? sp. (Oxynotum Zone); of *Gleviceras victoris*, *Echioceras* ? sp., *Eoderoceras* cf. *armatum*, *Cruciloboceras densinodum* (Raricostatum Zone) as well as of *Radstockiceras* cf. *buvignieri*, *Polymorphites* sp. (Jamesoni Zone). Rather reduced in thickness, the limestones cover a wide stratigraphic range. No ammonitic horizons could be distinguished within them. Even the basal bed contains a great amount of stratigraphically young, Middle Carixian, forms; but on the other hand, older ammonites, indicating the Raricostatum Zone (*Eoderoceras* sp. aff. *miles*) or the Jamesoni Zone (*Platypleuroceras rotundum*), have been found in the uppermost bed, too. Both *Tropidoceras* cf. *masseanum*, a subzonal index in the Ibex Zone, and *Oxynoticeras* sp. indicative of the Upper Sinemurian, can be found together in one and the same hand specimen of rock. In case of mixed faunas the fauna is, as

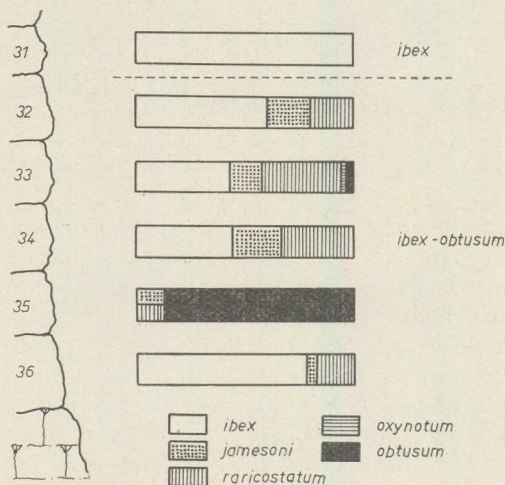


Fig. 4. Percentage distribution of the ammonite species characteristic of the different zones of the lower red limestones

a rule, dated by the occurrence of the latest index fossil. A more difficult problem is faced in a condensed fauna, which is undoubtedly the case with the Kericser section, given its very reduced thickness.

Limiting the age of the limestones under consideration to the Ibex Zone seems to be exaggerated, though there can be no doubt that during the time interval of this Zone a considerable change took place. As usual with areas of specific sedimentation, to specify this change would require the knowledge of the regional conditions of sedimentation. Until this knowledge is acquired, the fauna of the red limestones will be considered condensed and mixed.

2. The middle white limestones

With the organodetrital elements getting enriched and the waning of the red ferrioxide and ferrihydroxide stain, the lower red limestones grade into white, locally light-pink, limestones. These limestones, called middle white limestones, total 566 cm in thickness (Beds 7–28). They



Fig. 5. Grading of the lower red limestones into the middle white limestone (Bed 30). Ammonites filled up partly by calcareous silt (magnification: 6 x)

are constituted by the tests of contemporaneous organisms, fine-grained calcilutite, and tiny calcite crystals. Both organic detritus and calcareous silts are practically synchronous, while the calcite crystals are products of post-sedimentary filling up of the one-time cavities of the shells and, particularly so, of the free spaces between them. Subordinately, the white limestones also contain some older, angular limestone detritus. The original sedimentary material — the organic detritus and the fine calcareous silt — shows an irregular distribution within the bed. Strata contacts are vague. In the white limestone sequence there is no trace of any lasting break in sedimentation during which the lower bed could have been completely consolidated. As for sedimentation, it can be traced to have remained essentially unchanged throughout the 21 beds, indicating,

beside the total absence of terrigenous materials, the comparatively subordinate nature of calcareous ooze deposition. Empty shells and the free interspaces between them are due to the lack of matrix. Since the red limestones do not show any substantial difference in lithology with regard to the calcilutite lenses of the white limestones, the calcareous oozes seem to have been deposited more or less independently of the accumulation of biogenic elements. In other words, the difference with respect to the lower red limestones consists only in the great amount of allochthonous elements.

On the basis of their lithological character the white limestones would belong to the "organodetrital limestone" ("Organotrümmer-Kalkarenit") group of *Fabricius*' (1966) classification. In the territory of the Northern Alps this rock type is more or less connected with the Rhaeto-Liassic shoals, but it cannot be regarded to be of reef origin because of the absence of any reef bottom. According to *Fabricius*, the relatively calcilutite-rich crinoidal limestones were deposited in a non-agitated shallow-water sea environment, possibly in its comparatively deeper tracts. According to the classification developed by *Prestat* (1967), the bioclastic limestones would represent a near-reef facies (faciès pararéefal) deposited below the zone of erosion, in an environment characterized by transporting and reworking in situ, at any rate: in agitated waters. As suggested by *Dollfus* (1963), the echinoderm breccias and calcarenites would be controlled by marginal faults, their materials having been drifted by currents from a morphologically higher region.



Fig. 6. The middle white limestone (Bed 22). Small ammonites filled up by fine calcareous silt (bottom) and by calcite (top) (magnification: 6.5 x)

In the Northern Alps the analogical facies was given the name "hierlatz" first by S u e s s (1852), later by G e y e r (1886). The similarity of the limestones at Kericsér locality to the Alpine facies was recognized by L a c z k ó as early as 1898.

The middle white limestones, for the most part, are constituted by ammonites and brachiopods and ossicles of Crinoidea. Lamellibranchs (especially, thin-shelled pectinids) and gastropods (especially, *Discohelix*) as well as Nautiloidea, *Atractites* and Belemnites are just accessory elements.

After the death of the animal most of the ammonite shells remained empty or just the lower part of shell was infilled by calcareous ooze. The empty shells may be filled by post-sedimentary calcite crystals. In case of forms of narrow whorl cross-section, such as *Protogrammoceras* or *Fuciniceras*, the shell may be completely filled up, whereas in wide-whorled forms the original cavity is partly preserved (e.g. *Coeloceras*). A part of the inner cavity may be preserved even in case of specimens enclosed in calcareous silt lenses. The shells of the the ammonites have been mostly preserved, specimens represented by internal moulds being rare. A small fraction of the ammonites are in an excellent preservation state, the rest being differently incomplete. Shells may break down within

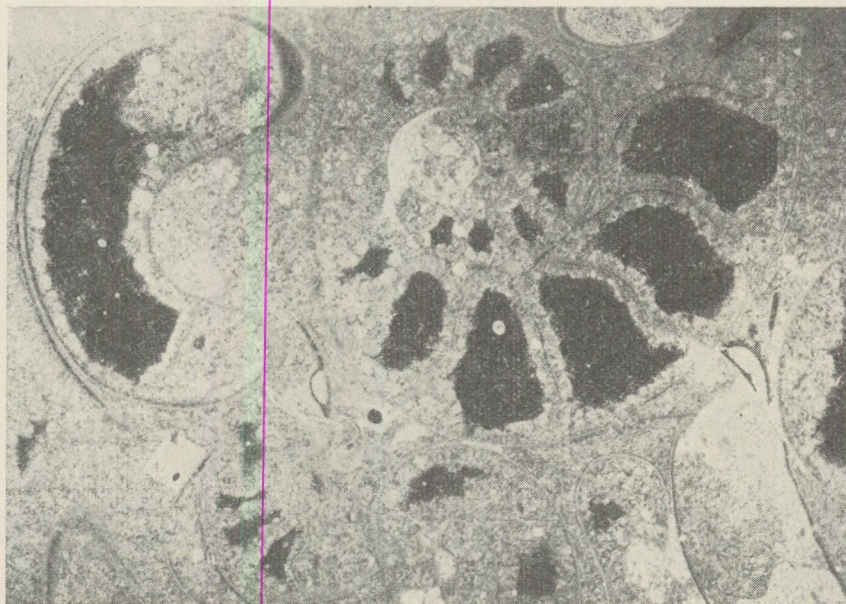


Fig. 7. The middle white limestone (Bed 10). Small ammonites filled up by calcite crystals (magnification: 8 x)

the sediment. Generally, however, the shells were crushed before being finally buried. Their comminution is so advanced, or the interstitial matrix so poor, that the shells may be squeezed into, or upon, one another. The heavy comminution of the ammonite shells suggests a reworking, the orientation of the empty shells and calcareous silt lenses being indicative of transport. It seems probable, however, that heavy water movement was periodical. The excellently preserved fragile specimens of the fauna such as the long *Cidaris radiolae*, high-spined gastropods, the representatives of *Coeloceras* preserving even their tubercles, provide testimony to a comparatively more quiet phase of sedimentation.

The majority of the ammonites have been buried at random. Some lie parallel to stratification. Records of a burial parallel to the bedding plane can be recognized even on hand specimens of rock, if the red or pink calcareous silt fills up the lower part of shell, leaving the upper space empty, like a "libella". As a rule, the ammonites enclosed in calcareous silts show a more regular orientation, unlike the freely accumulated mass of tests more liable to mobilization. From the point of view of burial, the fauna of the calcareous silt lenses is "more autochthonous" than that of the elastic limestones, even though this statement does not hold true for the way of living of the animals. As for orientation, there is no shade of it in the middle white limestone bed.

The ammonites of the middle white limestones are small. Larger specimens, usually fragmentary, are rare (first of all, a few specimens of *Phylloceras* and *Lytoceras*). Some of the small specimens belong to species which must have been small even originally. According to Bremer (1965), the size of *Coeloceras* hardly exceeds 6–7 cm, being, in fact, substantially below this value in most of the cases. The small *Coeloceras* of Kericser are surely of "normal" size. *Phylloceras disciforme*, *Lytoceras hierlatzicum*, *Holcolytoceras nodostrictum*, *Holcolytoceras quadrijugum* and *Protogrammoceras pseudofieldingii* also belong to small-sized species. As concerns the rest of the small specimens, the question arises whether the small size is due to an early death, or to adaptation to a special habitat which would give rise to a dwarfed fauna, or possibly to mechanical sorting produced by post-sedimentary transporting. The question may be answered by a quantitative analysis of the inner structure of shell: specimens lacking a body chamber suggest post-sedimentary sorting, specimens with relatively closely spaced septa are suggestive of dwarfing. Most of the ammonites of the limestones under consideration are, however, heavily recrystallized. Thus, neither the suture line, nor the length of the body chamber, nor the spacing of the septa can be directly examined. As evidenced by the type of microfacies sampled from Bed 10, the septum can be analysed in thin section. The recrystallized tests, however, are too friable, the number of complete specimens being too low to enable one to undertake any biostatistical analysis of dwarfing upon its merits. Sporadic occurrence of large specimens would not preclude the possibility of dwarfing, since these may have come from a foreign habitat and got admixed to the small specimens. It is rather the abundance of small-sized

species, particularly so of *Coeloceras*, that speaks against the presence of a dwarfed fauna. The preservation of these is very much like that of the rest of the fauna, so that it would be rather difficult to explain their presence by a different habitat. Accordingly, there is no need to suppose any such external factor which would have negatively affected the growth of the entire fauna. Considering the fact that the thicker shells of the adults are more resistive to mechanical stresses than it is the case with the youthful specimens, it is improbable that the small specimens would be inner whorls, crushed posthumously and thus preserved, of adult shells. The fauna of the middle white limestones seems to consist of "normal" specimens of small-sized species and of youthful specimens of "normal" species. This hypothesis is still to be verified by quantitative analyses.

The middle white limestones (inclusive of the transitional Beds 29 and 30) are extremely abundant in ammonites: 192 specimens per cubic metre have been collected. In reality, however, the ammonite content of the rock is the multiple of this figure! The separation of ammonite shells superimposed upon, or deposited in, one another — a prerequisite for exact counting — is unfeasible. Also the presence of fragments renders counting difficult. The given value does not express in absolute figure the faunal abundance of the limestones under consideration. It is merely a means of comparison with the faunal contents of the under- and overlying strata. The marked fluctuation of faunal abundance in the different beds, expressed in converted values with regard to an average bed thickness of 10 cm, is due to the uneven distribution of organic detritus and calcareous silt lenses.

From the point of view of its way of living, the fauna can be divided into two main groups. Foraminifers, sponges, lamellibranchs, gastropods, brachiopods, and echinoderms form bottom-dwelling communities, while Cephalopoda and "Paleotrix" belong to the pelagic habitat situated above sea bottom. Of the group of benthonic organisms the foraminifers, lamellibranchs, gastropods, and sea urchins conduct a mobile way of living on sea bottom, whilst siliceous sponges, brachiopods and crinoids are sessile. However, considering that the spicules of siliceous sponges and the crinoid ossicles are isolated and that the light shells of Brachiopoda, very liable to transporting, are unanchored from sea bottom after the death of the animal, there is no evidence which would prove that the place of burial of sessile benthos, predominant in the Kericsér fauna, would correspond to its habitat. On the contrary, an unconsolidated bottom, consisting of a detritus of organic tests, is unsuitable for sessile benthonic life. Hence the total absence of organisms grown on sea bottom (calcareous algae, *Serpula*, *Ostrea*, *Bryozoa*). The exposed profile provides direct information only about the place of burial of the benthonic and pelagic organisms. Thus the original habitat, which in the case of sessile benthonic organisms must have been a hard bottom, remains obscure. Judging by the abundance and preservation of the fauna, the rocky sea bottom, more or less free of sedimentation and often exposed to submarine erosion, seems to have lain near-by. The young ammonites may have dwelt close to this hard

bottom. As suggested by Eichler-Ristedt (1966), present-day *Nautilus* attaches its ovules to the bottom and lives, while young, in shallow waters. Hence the absence of youthful ammonites in the ammonitico rosso facies corresponding to a basin environment.

The limestones are surprisingly poor in *Phylloceras* and *Lytoceras*: 10.5%. The change of this percentage, accompanied by a boom of benthonic organisms, suggests the shallowing of the sea, at least as regards the surrounding, morphologically higher, areas. Sedimentation becomes more regular: from Bed 31 on, the ammonites indicative of a mixed or condensed fauna are absent. That the lower part of the white limestones belongs to the Ibex Zone is evidenced by the presence of *Holcolytoceras nodostrictum* (Bed 27) and *Beaniceras* sp. aff. *costatum*, respectively. The single specimen of *Androgynoceras* sp. aff. *sparsicosta* found in Bed 20 suggests the presence of the lower part of the Davoei Zone (Maculatum Subzone). On the basis of the occurrence of *Prodactylioceras* cf. *davoei*, Bed 11 still undoubtedly belongs to the Davoei Zone. Judging by the identity of fauna and facies, no change in environment took place at the Carixian-Domerian boundary (Bed 10). Beside the lack of *Prodactylioceras* and *Coeloceras*, the Lower Domerian is indicated by those representatives of *Protogrammoceras* (*P.* sp. aff. *isseli*: Bed 7) and *Fuciniceras* (*F.* cf. *portisi*: Bed 8) which in the territory of Aveyron occur in the Stokesi Zone. In Aveyron, *Protogrammoceras isseli* is the index fossil of the top of the Stokesi Zone. Since the white limestones do not contain any species indicative of a higher, Margaritatus, zone, the deposition of these limestones must have lasted from the top of the Ibex Zone up to that of the Stokesi Zone.

3. The upper red limestones

The upper red limestones overlie the white ones with a marked change in facies. Their thickness totals 227 cm (Beds 1–6). The limestone is red, well-stratified, with brown, grey and yellow mottles, locally with manganese nodules. Like the lower red limestones, this facies also belongs to the type of the calcareous ammonitico rosso.

The lower beds of the upper red limestones contain brachiopods, crinoids, foraminifers and siliceous sponges, whereas their upper part is characterized by cross-sections of *Bositra* (?) shells ("Paleotrix").

The limestone contains few and normal-sized ammonites. These are poorly preserved specimens, mostly shelled and often coated by limonite. In many cases, the shell is preserved only on one side, the other having been lost to subsolution. The majority of the collected specimens are fragments, which is also due to subsolution processes. The quantity of ammonites per one cubic metre is 12,7 specimens.

In Bed 4 of the red limestones, rounded ossicles of Crinoidea are frequent. Initially, these were impregnated by iron-rich solutions which have prevented the skeleton from being completely comminuted. Already affected by attrition, the outer parts of crinoid ossicles were later bleached

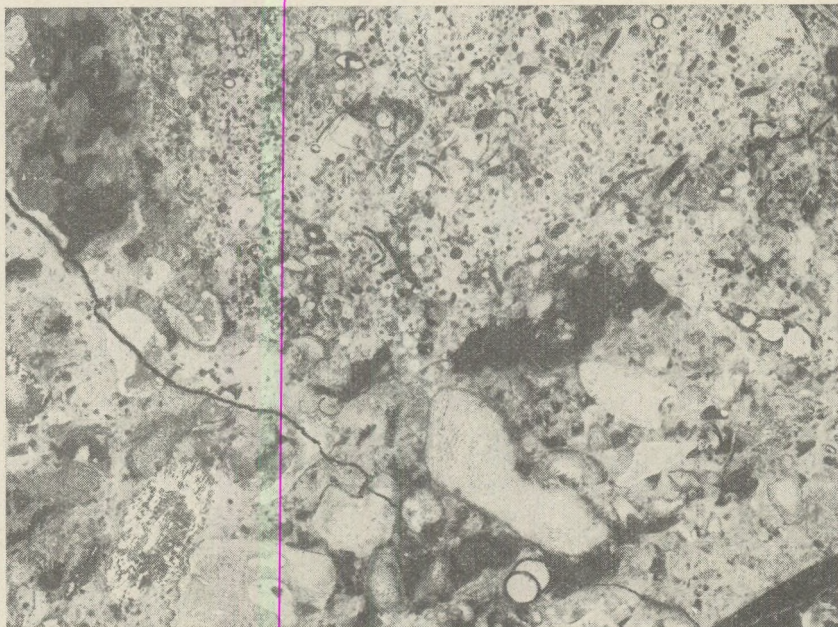


Fig. 8. The upper red limestones. Crinoid ossicles (first impregnated by iron oxide and then rounded off) and benthonic foraminifers (Bed 4) (magnification: 11 x)

by subsolution processes. All these phenomena indicate, beside reworking and redeposition, an enrichment of the Fe content and, undoubtedly, a break in sedimentation. The unconsolidated bioclastics underneath seem to have been responsible for the fact that no ferromanganese-coated hardground could develop at the contact of the white and red limestones.

In the fauna of the upper red limestones the representatives of *Phylloceras* and *Lytoceras* have a larger share (31%). The increase of the abundance of "Paleotrix" and the decline of benthonic organisms indicate either the cessation of earlier resedimentation processes (the neighbouring, higher, seamount-benches may have subsided so deep that the exuberance of benthos was cut short, or the direction of transporting was changed) or the onset of a new phase of subsidence.

As regards their faunal character (frequency; percentage of *Phylloceras* + *Lytoceras*), the lower beds of the red limestones correspond to the Upper Domerian (Spinatum Zone) of the vicinity. Accordingly, despite the fact that *Emaciatoceras*, a fauna rather frequent in other areas, could not be found at Kericsér locality, the basal Beds 6 and 5 (having a total thickness of 64 cm), which do not yet contain any "Paleotrix", are considered to be the final member of the Pliensbachian.



Fig. 9. The upper red limestone (Bed 2). *Bositra* (= "Paleotrix") cross-sections, foraminifers and ostracods (magnification: 12 x)

On the basis of the presence of *Hildaïtes* cf. *serpentinum* the upper part of the red limestones, Bed 3, must belong to the Falceifer (Serpentinum) Zone of the Lower Toarcian Substage. As for the Tenuicostatium Zone, its presence cannot be evidenced by fauna here either. The *Hildoceras* specimens of Beds 1 and 2 testify to the presence of the lower part of the Bifrons Zone.

II. PALEONTOLOGY

Irrespective of the new species, a total of 86 ammonite species and subspecies have been identified out of the Kericser fauna. The greater number of forms determined with a question mark can be explained by the adverse conditions of preservation. According to the classification developed by Arkell (1957), the fauna belongs to 12 families.

1. Phylloceratidae

Irrespective of ammonite-free Bed 6 and of Bed 26 poor in fauna, the family is represented, though subordinately, in all beds. The following species have been determined:

Phylloceras hantkeni (Schloenbach in Prinz, 1904)

Phylloceras sp. aff. *hantkeni* (Schloenbach in Prinz, 1904)

- Phylloceras zetes* (d'Orbigny, 1849)
Phylloceras meneghini Gemmellaro, 1874
Phylloceras bonarelli Bettoni, 1900
Phylloceras hebertinum (Reynès, 1868)
Phylloceras disciforme (Reynès, 1868)
Phylloceras sp.
Partschiceras cf. *anonymum* (Haas, 1913)
Partschiceras sp.
Calliphylloceras alontinum (Gemmellaro, 1884)
Calliphylloceras seroplicatum (Hauer, 1854)
Calliphylloceras emeryi (Bettoni, 1900)
Calliphylloceras cf. *bicolorae* (Meneghini, 1867–1881)
Calliphylloceras cf. geyeri (Bonarelli, 1895)
Calliphylloceras sp.

Known to occur in almost all beds, the family is most abundant in Beds 32 and 36. *Phylloceras* and *Calliphylloceras* can be traced throughout the profile. *Calliphylloceras emeryi* is particularly frequent. The representatives of *Partschiceras* are rather characteristic of the lower part of the profile: available in the lowermost Bed 36, they are particularly abundant in Beds 32 and 33. Single specimens occur in Beds 25–14, too. Because of its long stratigraphic range, the family is of subordinate importance.

2. Juraphyllitidae

Except for the top of the profile, the representatives of Juraphyllitidae are rather frequent:

- Juraphyllites libertus* (Gemmellaro, 1884)
Juraphyllites sp. aff. *libertus* (Gemmellaro, 1884)
Juraphyllites planispira (Reynès, 1868) n. subsp.
Juraphyllites cf. *nardii* (Meneghini, 1853)
Juraphyllites cf. *lunensis* (De Stefani, 1886)
Juraphyllites sp.
Harpophylloceras eximius (Hauer, 1854)
Meneghiniceras cf. *bicolorae* (Bonarelli, 1895)
Galaticeras aegoceroïdes (Gemmellaro, 1884)
Galaticeras (n. subgen.) n. sp.
Galaticeras sp.

Numerically, the family is most abundant in Beds 36, 35, 16 and 5. Of *Juraphyllites*, the species *J. libertus* is most abundant; its specimens, and the ones identified with a question mark because of their poor preservation, can be traced across almost the entire profile — from Bed 33 up to Bed 7 inclusive. The first, uncertain, representatives of *Harpophylloceras* appear in Bed 31 and still occur in Bed 7, too. *Meneghiniceras* is confined to the lower red limestones (Beds 34–30) *Galaticeras*, to the lower beds of these limestones (Beds 36–33).

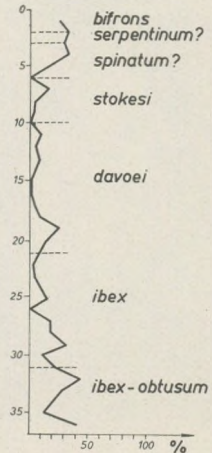


Fig. 10. Percentage distribution of *Phylloceras* by beds

3. Ectocentritidae

The family is very rare at Kericser locality:

Holcolytoceras quadrijugum (Rosenberg, 1909)

Holcolytoceras nodostrictus (Q u e n s t e d t, 1885)

Holcolytoceras sp.

Peltolytoceras ? sp.

Holcolytoceras nodostrictus was found in Beds 27 and 34, *H. quadrijugum* in Beds 20 and 21. *Peltolytoceras* belongs to Bed 35. *Holcolytoceras* is characteristic of the Ibex Zone, while *Peltolytoceras* belongs to the Sinemurian.

4. Lytoceratidae

On the Kericser the following *Lytoceras* species have been found:

Lytoceras ovimontanum (Geyer, 1893)

Lytoceras cf. *baconicum* V a d á s z, 1910

Lytoceras cf. *czjzekii* (Hauer, 1853)

Lytoceras cf. *fuggeri* Geyer, 1893

Lytoceras cf. *fimbriatum* (Sowerby, 1817)

Lytoceras cf. *haasi* G é c z y, 1967

Lytoceras sp. aff. *celticum* (Geyer, 1886)

Lytoceras cf. *fimbriatoides* Gemmellaro, 1884

Lytoceras hierlatzicum Geyer, 1886, n. subsp.

Lytoceras sp.

Audaxlytoceras apertum (Geyer, 1893)

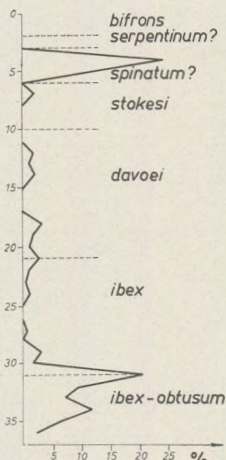


Fig. 11. Percentage distribution of *Lytoceras* by beds

The genus *Audaxlytoceras* — which Arkell (1957, p. 199) referred, with some reserve, to the family Nannolytoceratidae — has been discussed here with the family Lytoceratidae. A few representatives of Lytoceratidae can be encountered in most beds, but they do not become predominant in any of them. It is in the lower red limestones, Beds 31, 32 and 34, that they can be collected in comparatively great number. In percentage terms, Bed 4 too is *Lytoceras*-bearing, but this occurrence cannot be evaluated upon its merits because of the extremely low number of specimens.

5. Schlotheimiidae

The family is represented by a single specimen of

Angulaticeras sp.

found in Bed 33.

6. Arietitidae

Of this family three genera are known:

Arnioceras ceratitoides (Quenstedt, 1849)

Arnioceras sp.

Arnioceras ? sp.

Asteroceras ? sp.

Cymbites ? sp.

All representatives of *Arnioceras* and the big specimen, which because of its poor preservation has been referred, just with a question mark, to the genus *Asteroceras*, were found in Bed 35. Owing to its poor preservation state, *Asteroceras* cannot be evaluated chronologically. *Arnioceras ceratitoides* is characteristic of the middle part of the Sinemurian (conf. Wissner, 1958, p. 64).

7. Oxynoticeratidae

The specimens belonging to the family derive from Bed 34. These are as follows:

Gleviceras victoris (Dumortier, 1867) n. subsp.

Gleviceras sp.

Radstockiceras cf. *buvignieri* (d'Orbigny, 1844)

According to Bremer (1965, p. 149), *Gleviceras victoris* is frequent in the Raricostatum Zone, while *Radstockiceras buvignieri* is indicative of the Jamesoni Zone.

8. Echioceratidae

In the lower member of the lower red limestones 10 poorly preserved ammonite specimens were found, which have been referred conditionally to the following three genera of the family:

Palaeoechioceras ? sp.

Paltechioceras ? sp.

Echioceras ? sp.

Palaeoechioceras ? was found in Beds 33 and 34, *Paltechioceras* ? in Bed 36, *Echioceras* ? in Bed 33. As shown by Dean, Donovan and Howarth (1961, p. 458), *Palaeoechioceras* occurs in the upper part of the Oxynotum Zone. *Paltechioceras* and *Echioceras* are indicative of the Raricostatum Zone.

9. Eoderoceratidae

On the Kericser the family is rather richly represented:

Microderoceras cf. *birchi* (Sowerby, 1820)

Microderoceras n. sp. aff. *heberti* (Oppel, 1856)

Microderoceras n. sp.

- Eoderoceras* cf. *armatum* (Sowerby, 1815)
Eoderoceras sp. aff. *armatum* (Sowerby, 1815)
Eoderoceras n. sp. aff. *sellae* (Gemmellaro, 1884)
Cruciloboceras gemmellaroii (Levi, 1896)
Cruciloboceras densinodum (Quenstedt, 1849)
Cruciloboceras cf. *muticum* (d'Orbigny, 1884)
Cruciloboceras sp.
Cruciloboceras ? *uhligi* (Rosenberg, 1909)
Coeloceras sp. aff. *pettos* (Quenstedt, 1843)
Coeloceras sp. aff. *pettos planula* (Quenstedt, 1885)
Coeloceras sp.
Coeloceras ? *incertum* Fucini, 1905
Coeloceras ? *incertum* Fucini, 1905 n. subsp.
Coeloceras ? cf. *simulans subplanatum* Fucini, 1905
Coeloceras ? *fallax* Fucini, 1905
Coeloceras ? cf. *obesum* Fucini, 1905
Coeloceras ? n. sp. aff. *obesum* Fucini, 1905
Coeloceras ? sp. aff. *intermedium* Fucini, 1905
Coeloceras ? n. sp.
Coeloceras ? sp.
Productylioceras cf. *davoei* (Sowerby, 1822)
Productylioceras cf. *enodis* (Quenstedt, 1885)
Productylioceras cf. *italicum* (Meneghini in Fucini, 1900)
Productylioceras cf. *aegrum* (Fucini, 1905)
Productylioceras sp.

Microderoceras is known to occur sporadically in the lower red limestones (Beds 33–34). According to Dean, Donovan and Howarth, *Microderoceras birchi* is a subzonal index in the upper member of the *Caenisites turneri* Zone. According to Wissner (1958, p. 82), it is characteristic of the Obtusum Zone. Bremer (1965, p. 152) has shown *M. birchi* s. l. to reach as high as up to the Oxynotum Zone. A few specimens of *Eoderoceras* were found in Beds 36, 33 and 32. According to Dean, Donovan and Howarth (1961, p. 459, 461),

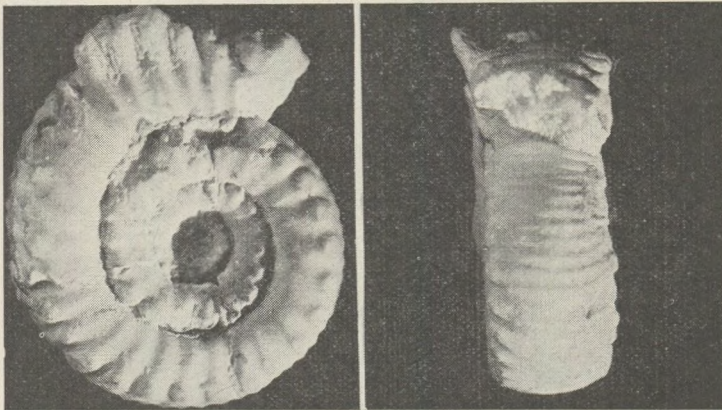


Fig. 12 a, b. *Coeloceras* ? n. sp. aff. *obesum* Fucini, 1905 (Bed 25)

Eoderoceras armatum and *E. miles* characterize the Raricostatum Zone (*E. miles* does so the upper part of the zone: Macdonelli and Aplanatum Subzones). *Cruciloboceras* has somewhat greater vertical range — its representatives are most frequent in the basal bed (Bed 36) of the red limestones, while the last specimens can be collected from Bed 30. In the territory of Central Württemberg the species *Cruciloboceras densinodum* forms, as shown by S ö l l (1956, p. 371), the lowermost subzone of the Raricostatum Zone. The representatives of *Coeloceras* occur sporadically in the upper beds of the lower red limestones (Bed 31). In Bed 27 they show a sudden increase in number, to become abundant (34 specimens) in Bed 25. Still rather frequent in Beds 21 — 19, they show a rapid decrease in the higher member of the middle white limestones, to disappear totally in Bed 9.

Those forms of a new genus, which have *Coeloceras*-shaped inner whorls and a *Reynesoceras*-like, simple-ribbed body chamber, have been conditionally referred to *Coeloceras*.

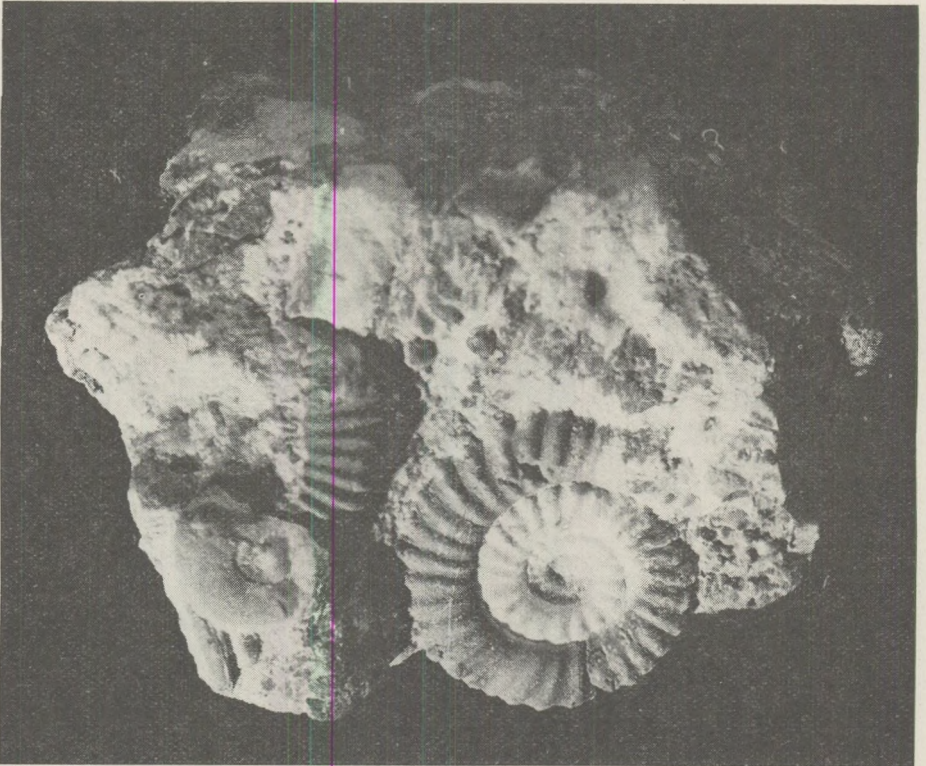


Fig. 13. *Coeloceras* ? *incertum* F u c i n i, 1905 n. ssp. The red calcareous silt fills up only the lower part of the body chamber (Bed 26)

The acme of *Productylioceras* follows that of *Coeloceras*: the first representatives of the former appear in Bed 19, they are most abundant in 12, and they have their last representatives in Bed 11. According to Dean, Donovan and Howarth (1961), *P. davoei* occurs in the top of the zone named after it (Capricornum and Figulinum Subzones). In the Mediterranean regions both genera are represented by several species of clear systematic position. *Productylioceras* can be readily used as indices of the Davoei Zone, while the life range of *Coeloceras* is longer than in the territory of Southwest Europe (conf. Spath, 1928, p. 257).

10. Polymorphitidae

Rather poor in population, the family is represented by a rich variety of species:

Polymorphites sp.

Platypleuroceras rotundum (Quenstedt, 1885)

Platypleuroceras ? sp.

Gemmellaroceras alloplocum (Gemmellaro, 1884)

Gemmellaroceras sp.

Acanthopleuroceras cf. *valdani* (d'Orbigny, 1844)

Acanthopleuroceras sp.

Tropidoceras subariefforme (Futterer, 1893)

Tropidoceras cf. *ariefforme* (Oppel, 1853)

Tropidoceras cf. *masseanum* (d'Orbigny, 1842)

Tropidoceras cf. *masseanum mediterraneum* (Gemmellaro, 1884)

Tropidoceras cf. *flandrini* (Dumortier, 1869)

Tropidoceras cf. *galatense* (Gemmellaro, 1884)

Tropidoceras cf. *ellipticum* (Sowerby, 1815)

Tropidoceras cf. *actaeon* (d'Orbigny, 1843)

Tropidoceras cf. *calliplocum* (Gemmellaro, 1884)

Tropidoceras sp. aff. *lineatum* (Spath, 1923)

Tropidoceras n. sp. aff. *ariefforme* (Oppel, 1853)

Tropidoceras sp.

It is strictly confined to the lower part of the lower red limestones (Beds 36–32). Single specimens of *Polymorphites* were encountered in Beds 33 and 34. According to Arkell (1957, p. 248), this genus characterizes the Jamesoni Zone. Also characteristic of the Jamesoni Zone, *Platypleuroceras* can be found in Beds 33 and 32. *Gemmellaroceras*, embracing, as shown by Arkell (1957, p. 249), the Raricostatum and Jamesoni Zones, is represented by a single specimen in both Bed 35 and Bed 33. Two specimens of *Acanthopleuroceras* are known from Bed 33. As shown by Dean, Donovan and Howarth (1961, p. 465), *A. valdani* is the index fossil of the middle subzone of the Ibex Zone. *Tropidoceras* is the richest genus of the family. Particularly frequent in Bed 36, its representatives can also be found in Beds 34 and 33. *Tropidoceras* is characteristic of the lower part of the Ibex Zone (Futterer, 1893, p. 328), *T. masseanum* itself being the index fossil of the lower subzone of the Ibex Zone (Dean, Donovan, Howarth, 1961 p. 464).

11. Liparoceratidae

The following representatives of the family have been collected:

- Liparoceras* sp. aff. *substriatum* Spath, 1938
Liparoceras sp.
Liparoceras (*Becheiceras*) sp.
Liparoceras (*Becheiceras*) ? sp.
Beaniceras sp. aff. *costatum transiens* Spath, 1938
Androgynoceras sp. aff. *sparsicosta* (Trueman, 1919)
Androgynoceras sp.

The first representatives of *Liparoceras* appear as low as the lower, mixed part of the lower red limestones (Bed 34) and reach up to Bed 22. *Liparoceras* sp. aff. *substriatum* was found in Bed 32. According to Spath (1938, p. 56), the type of *substriatum* belongs to the Ibex Zone. A subgenus of *Liparoceras* (*Becheiceras*) can be traced from Bed 21 up to Bed 12. A single specimen of the genus *Beaniceras* is known from Bed 22. According to Spath, *Beaniceras* characterizes the upper part of the Ibex Zone (Centaurus Subzone) (1938, p. 98). Whereas the representatives of *Liparoceras* and *Beaniceras* are just accessory elements of the Kericsér fauna, in Beds 11 and 12 a comparatively large number of small ammonites, referred conditionally to the genus *Androgynoceras*, can be collected. In Bed 12 *Androgynoceras* ? n. sp. is represented by 45 specimens, in Bed 11 *Androgynoceras* ? sp. is by 7 specimens. The first *Androgynoceras* appeared in Bed 23, the form related to *A. sparsicosta* did so in Bed 20. According to Spath (1938, p. 35), *sparsicosta* is characteristic of the lower part (Maculatum Subzone) of the Davoei Zone.

12. Hildoceratidae

The family Hildoceratidae is the predominant group of the Kericsér fauna:

- Arietoceras* sp.
Protogrammoceras pseudofieldingii (Fucini, 1904)
Protogrammoceras isseli (Fucini, 1900) n. subsp.
Protogrammoceras sp. aff. *isseli* (Fucini, 1900) in Monestier, 1934
Protogrammoceras ? sp. aff. *instabile* (Monestier, 1934)
Protogrammoceras ? *inconditum* (Monestier, 1934)
Protogrammoceras sp. aff. *naxense* (Gemmellaro, 1885) in Monestier, 1934
Protogrammoceras sp.
Fucinoceras inclytum (Fucini, 1900)
Fucinoceras lavinianum (Fucini, 1900)
Fucinoceras cf. *lavinianum brevispiratum* (Fucini, 1900)
Fucinoceras cf. *capellinii* (Fucini, 1900) in Monestier, 1934
Fucinoceras cf. *portisi* (Fucini, 1900)
Fucinoceras portisi zitteliana (Fucini, 1900)
Fucinoceras cf. *ambiguum* (Fucini, 1900)
Fucinoceras n. sp. aff. gr. *schoepeni* Bettoni, 1900 non Gemmellaro, 1885
Fucinoceras n. sp.
Fucinoceras ? sp.
Polyplectus sp.

Polyplectus cf. *pluricostatus* (H a a s, 1913)
Maconiceras sp.
Hildaïtes sp.
Hildaïtes cf. *serpentinum* (R e i n e c k e, 1812)
Hildaïtes ? sp.
Orthildaïtes orthus B u c k m a n, 1923
Hildoceras sp.

Most frequent representatives of the family are *Protogrammoceras* and *Fuciniceras*: in Bed 3 their share exceeds 90%. In case of youthful specimens it has been rather difficult to distinguish between the two



Fig. 14. *Orthildaïtes* cf. *orthus* B u c k m a n from the upper red limestones

genera. D u b a r and M o u t e r d e (1961, p. 239) have every right to emphasize the marked variability of the two groups during ontogenesis. Therefore it seems to be justified to include the specimens still lacking generic features in a separate group (= *Fuciniceras* ? sp.) and to delay any more precise identification until further research may unravel the puzzle of their relation to the adults of *Protogrammoceras* or *Fuciniceras* species. Sporadically, *Protogrammoceras* can also be encountered in the lowermost beds (Bed 36), being frequent in the lower, rather than the

upper, part of the profile. According to a revision by Mattei (1967), the form described as *Protogrammoceras isseli* by Monestier is a subzonal index of the upper part of the Stokesi Zone. According to Monestier, 1934, *Protogrammoceras* ? *inconditum* and *P.* ? *instabile*

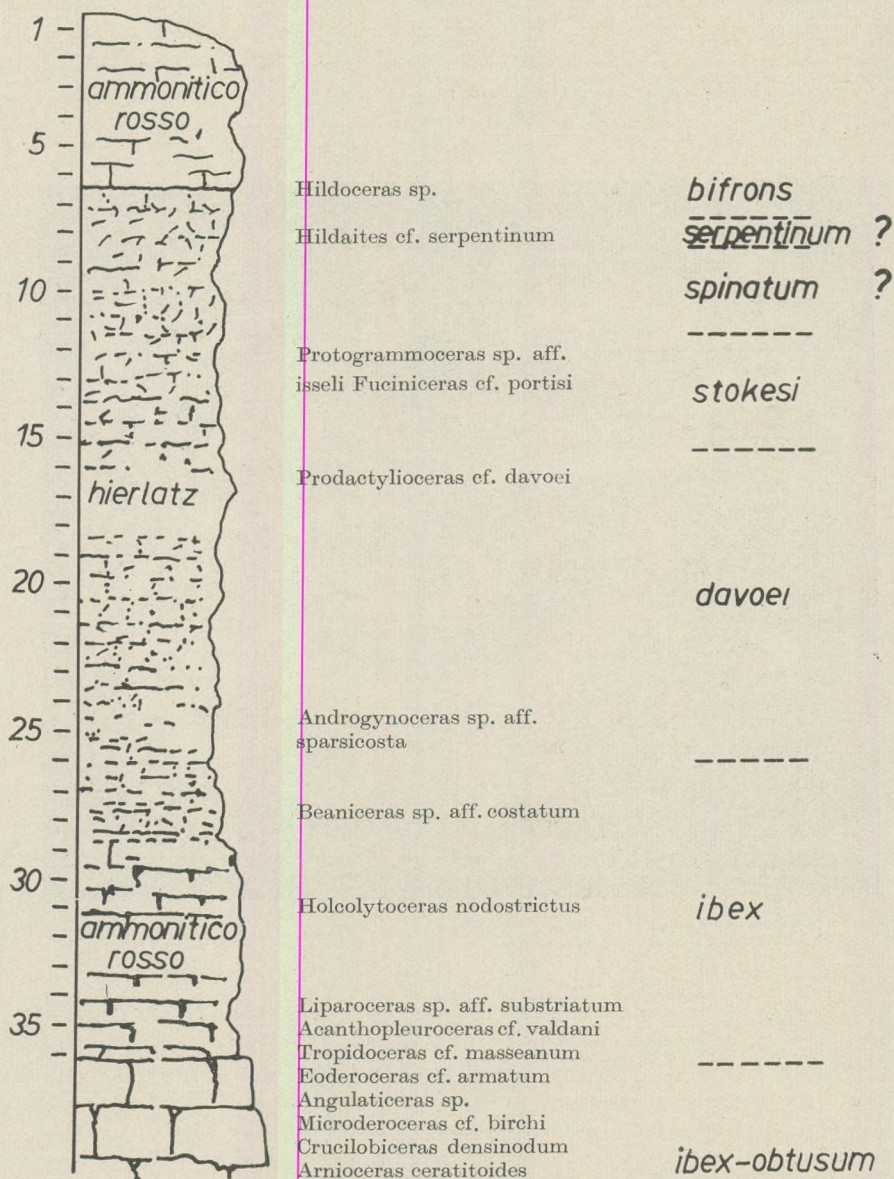


Fig. 15. Occurrence of chronologically characteristic species in the Kericser profile

are also characteristic of the lowermost Domerian. The first representatives of *Fuciniceras* can be collected in Bed 34. In the upper beds of the profile, with the decline of *Protogrammoceras*, they become gradually more frequent. According to Mouterde, 1967, *Fuciniceras portisi* is characteristic of the lowermost Domerian. Arkell (1957) considers *Protogrammoceras* and *Fuciniceras* to belong to the Upper Pliensbachian Substage and, conditionally, to the Lower Toarcian. In the West Mediterranean region, the territory of the High Atlas, Dubar showed them convincingly to occur in association with *Tropidoceras* and *Eoderoceras* in the Lower Pliensbachian. At Kericser locality both genera are undoubtedly frequent in the Ibex Zone already, and, considering the mixed and condensed nature of the lower red limestones, their extension into even deeper-seated strata does not seem improbable at all. The representatives of *Hildaites* and *Orthildaites* are indicative of the Lower Toarcian Serpentinum Zone, whereas *Hildoceras* testifies to the presence of the Bifrons Zone.

Conclusions

On the basis of the quantitative and qualitative analyses of ammonites from the Kericser, it can be admitted that in Pliensbachian time this area lay in the marginal zone of an inter-seamount basin, where sedimentation was affected by the resedimentation processes of the surrounding territory. A still continuous submarine platform in Late Triassic time, it was disintegrated into seamounts and inter-seamounts during the Early Lias. Disintegration was due to dilatational tectonic movements. The penecontemporaneous sediments of the seamounts — first the already consolidated sediments and then also the still unconsolidated ones — were removed by slumping and deposited under continuous pelagic conditions in the marginal zone of the leptogeosynclinal sedimentary basin. The locally increased thickness of the Pliensbachian is due to the accumulation of allochthonous biogenic materials (seamount-dwelling brachiopods, crinoids and small ammonites). The disappearance of allochthonous elements in the uppermost Pliensbachian indicates that the environmental conditions must have been well-balanced over a considerably large area. Beside the Mediterranean nature of the Bakony Mountains Liassic sediments and the apparent lack of deformations, the rate of tectonic movements also corresponds to the conditions existing in the Southern Alps (Bernouilli, 1964, Aubouin, 1965). Accordingly, it is not only in the south, but in the east as well that the central mass of the Alps is bordered by areas of analogical structure.

REFERENCES

- Aubouin, J. (1965): Reflexions sur le faciès "ammonitico rosso". Bull. Soc. Géol. France, 7 ser. 6, Paris.
Arkell, J. W. (1957): Mesozoic Ammonoidea in: Moore, C.: Treatise on invertebrate Paleont. Kansas.

- Bernouilli, D. (1964): Zur Geologie des Monte Generoso, Beiträge Geol. Kart. Schweiz N.F. 118. Bern.
- Bremer, H. (1965): Zur Ammonitenfauna und Stratigraphie des unteren Lias (Sinemurium bis Carixium) in der Umgebung von Ankara. Neues Jb. Geol. Paläont. Abh. 122, Stuttgart.
- Dean, W. T., Donovan, D. T., Howarth, M. K. (1961): The Liassic ammonite zones and subzones of the North-West European province. Bull. Brit. Mus. Nat. Hist. Geol. 4/10, London.
- Dollfus, S. (1965): Über den Helvetischen Dogger zwischen Linth und Rhein. Ecl. Geol. Helv. 58. Basel.
- Dubar, G. (1954): Succession des faunes d'Ammonites de types italiens au Lias moyen et inférieur dans le Haut Atlas marocain. Compt. Rend. XIX. Congr. Geol. Int. Alger, 1952. 13. fasc. 15, Alger.
- Dubar, G. (1961): Les Hildoceratidae du Domérien des Pyrénées et l'apparition de cette famille au Pliensbachien inférieur en Afrique du Nord. Coll. Lias. Mém. Bur. Rech. Géol. Min. 4, Paris.
- Eichler, R., Ristedt, H. (1966): Untersuchungen zur Frühontogenie von *Nautilus pompilius*. Paläont. Zeitschr. 40, Stuttgart.
- Fabricius, H. (1966): Beckensedimentation und Riffbildung an der Wende Trias-Jura in den bayerisch-tiroler Kalkalpen. Coll. Int. Sed. Petr. 9. Brill.
- Hudson, J. D., Jenkyns, H. C. (1969): Conglomerates in the Adnet Limestones of Adnet (Austria) and the origin of the "Scheck". Neues Jahrb. Geol. Paläont. Abh. Mh. Stuttgart.
- Konda, J. (1970): Lithologische und Fazies-Untersuchung der Jura-Ablagerungen des Bakony-Gebirges. Ann. Inst. Geol. Publ. Hung. 50, Budapest.
- Mattei, J. (1967): Analyse des termes fossilifères domériens dans les Causses du Sud du Massif Central français. In: Coll. Jurassique, II. Luxembourg.
- Mouterde, R. (1965): Sur quelques Ammonites du Lias Rif, remarques paléontologiques, Not. Serv. Géol. Maroc. Rabat.
- Mouterde, R. (1967): Le Lias du Portugal. Co. im. Serv. Geol. Portugal 52, Lisboa.
- Prestat, B. (1967): Étude micropaléontologique du passage Bathonien-Callovien dans le centre sud-ouest du Bassin de Paris. in: Coll. Jurass. II. Luxembourg.
- Söll, H. (1956): Stratigraphie und Ammonitenfauna des mittleren und Oberen Lias (Lotharingien) in Mittel Württemberg. Geol. Jahrbuch 72, Hannover.
- Spath, L. F. (1928): The Ammonite from the Belemnite Marls, Quart. Journ. Geol. Soc. 84, London.
- Spath, L. F. (1938): Catalogue of the Ammonites of the Liassic Family Liparoceratidae. London.
- Wissner, U. (1958): Ammonitenfauna und stratigraphie der Lias-Fleckenmergel Sinemurian bis Domerian in den Bayerischen Alpen. Diss. Univ. Tübingen.

KOHLENGEOLOGISCHE UNTERSUCHUNG DER LAGERSTÄTTE HIDAS IM MECSEK-GEIRGE

von
DR. Á. GROSSZ

(Lehrstuhl für Angewandte und Ingenieurgeologie Eötvös Universität, Budapest)
(Eingegangen am 4. 7. 1970)

РЕЗЮМЕ

Вскрытие и разработка среднемиоценовых (тортонских) лигнитов месторождения Хидаш в северо-восточной части гор Мечек были начаты 110 лет тому назад. Однако, состоящая из семи пластов лигнитонная толща до сих пор не была подвергнута углегеологическим исследованиям. Результаты, полученные различными исследовательскими методами, сводятся к следующему.

Тортонские лигнитовые пласты являются гетеропической фацией толщи типа „лейта“, представленной пресноводными и солоноватоводными осадками, образовавшимися в прибрежно-мелководных условиях. Внутри толщи можно выделить три подразделения как по горизонтали, так и по вертикали. Тектоническое строение лигнитового бассейна характеризуется частым чередованием антиклиналей и синклиналей, осевые линии которых простираются с СВ на ЮЗ. С юга на север увеличивается мощность лигнитонной толщи (с 30–45 м до 90–110 м).

По результатам палинологических исследований (106 элементов флоры) лигнитонная толща характеризуется среднемиоценовым спектром флоры гор Мечек. В отличие от результатов проведенных до сих пор исследований — в основном ксилотомических —, очевидно, что наряду с представителями сосновых листопадающие деревья также сыграли значительную роль в формировании угля. Об этом свидетельствуют результаты углепетрографических исследований. Изучением образцов под микроскопом было выделено десять типов лигнитов, на основании качественно-количественного распределения которых можно было сделать как научные, так и практические выводы.

Проведенные углехимические исследования дополнили результаты углепетрографических исследований новыми данными и подтвердили их. При этом были установлены углехимические параметры лигнитов месторождения Хидаш. На этом основании было установлено, что из-за небольшой степени углефикации лигниты месторождения Хидаш пригодны для использования в химической промышленности. В качестве топлива лигниты могут быть экономично использованы после гидратации, так как до зольности 20% они имеют калорийность свыше 4000 ккал/кг.

Судя по результатам исследований рассеянных элементов распределение этих элементов не позволяет выделять какие либо болотные зоны, причем нельзя установить никакую другую закономерность. Наблюдаемое обособление элементов обусловлено исключительно биофильным характером отдельных элементов. В противоположность прежним выводам автора настоящей работы (1966–67 гг.), барий (Ba) не обнаруживает коррелятивной связи с относительно более повышенным содержанием стронция (Sr). Это тем более любопытно, так как в 1968 г. Дь. Буда установил корреляцию между этими двумя элементами в полевых шпатах гранитов кристаллического фундамента южного предполя бассейна Хидаш, то есть в минералах, из которых по всей вероятности происходят рассматриваемые элементы. Вместе с тем, автор работы установил, что содержание SrO в мергелистых прослоях

лигнитоносной толщи и в золе самих лигнитов составляет 1,53%. Концентрация стронция уменьшается с 2,3% в южной части бассейна до 0,78% в северной части.

В заключение можно сделать вывод о том, что интенсивные колебательные движения бассейна привели к частому чередованию болотных зон в нижней и верхней частях лигнитоносной толщи, в то время как соседняя часть образовалась в условиях сплошного, выдержанного болота, охватывавшего большую часть рассматриваемой территории. На основании результатов исследований можно с большой надежностью выявить как область сноса, так и направление транспорта.

Einleitung

Die kohlengeologische Untersuchung der im NO-Teil des Mecsek-Gebirges bei Hidas bekannten Braunkohlenserie tortonischen Alters wurde im Rahmen eines komplexen Forschungsprogrammes: der geologischen Erforschung der mittelmiozänen Braunkohlenlagerstätten von Ungarn vorgenommen.

Die folgende Aufgabe ist noch zu lösen: auf Grund detaillierter Bergbau- und Tiefbohrangaben, sowie anhand der Ergebnisse von Laboruntersuchungen muss der geologische Bau der Braunkohlenserie geklärt werden. Zu erkunden sind noch die ehemalige Vegetation und das Klima, das zur Bildungszeit der Kohlenflöze herrschte. Ferner müssen auch noch die Bildungsbedingungen, die Moor- und Sumpfverhältnisse, die zu erwartende Qualitätsverteilung der Kohle und die Frage deren Brikettierfähigkeit anhand der qualitativen und quantitativen Verteilung der Kohlegesteinstypen geklärt werden. Eine weitere Aufgabe ist die Feststellung der Qualität, der chemischen Zusammensetzung und Nutzbarkeit der Braunkohle anhand verschiedener kohlenchemischer Parameter. Ausserdem ist auch noch die Verteilung von Spurenelementen in der Kohlenserie zu ermitteln und die eventuell bestehenden Gesetzmässigkeiten dieser Verteilung sind nachzuweisen.

Die komplexe geologische Untersuchung der Kohlenserie von Hidas ist bis heutzutage nicht vorgenommen worden, trotz der Tatsache, dass die geologische Forschung und Erkundung, sowie die Inangriffnahme der Braunkohlenförderung auf eine 110-jährige Vergangenheit zurückblicken kann (1860). Gleich nach jenem Datum im Jahre 1861 erarbeitete der österreichische Geologe K. F. Peters ein Gutachten und in seinem 1862 erschienenen Aufsatz beschrieb er die stratigraphischen Verhältnisse des Gebietes.

Dem ersten Aufsatz folgten die Arbeiten von J. K o k á n (1874), I. L ó r e n t h e y (1894), F. H a u e r (1870) und F. H o f f m a n n — J. B ö c k h (1888, bzw. 1907) über die Lagerstätte Hidas bzw. das Mecseker Gebiet.

Die nächste Forschungsperiode und mitsamt auch die geologische Erkennung der Umgebung von Hidas wird durch die Tätigkeit von E. V a d á s z (1935) gekennzeichnet. Ausser ihm befasste sich noch L. S t r a u s z (1926) mit den jungterziären Ablagerungen des Mecsek-Gebirges.

In der intensiven Entwicklung der geologischen Erkundungsarbeiten und der Kohlenförderung spielte S. V i t á l i s die Rolle des Anregers,

der im Jahre 1944 — trotz des niedrigen Erkundungsgrades — die Braunkohlevorräte von Hidas auf 100 Millionen Tonnen schätzte. S. Vitáliš hat die geologische Reambulierung des Braunkohlenbeckens durchgeführt. Dank diesen Arbeiten wurde die Kohlenlagerstätte eingehend erkundet und die Kohlenförderung erheblich beschleunigt.

Die montangeologischen Beobachtungen von Gy. Wein (1949), die geologischen Aufnahmen von J. Noszky (1950) und die monographische Bearbeitung der Fossilien durch I. Cs. Meznierics (1950) leisteten grosse Beiträge zur geologischen Erkennung der Lagerstätte Hidas. Im Bereiche der Stratigraphie, Fazilogie und Tektonik waren G. Hámor (1961), M. Földi (1964), sowie L. Gyovai (1962) — der die Erkundungsarbeiten leitete — tätig.

Geologische Verhältnisse der Kohlenserie von Hidas

Das Braunkohlenbecken von Hidas ist sowohl im S als auch im N durch grössere Strukturelemente begrenzt. Seine südliche Endung hat das Becken einer annähernd O—W streichenden Aufschiebung zu verdanken, wo das kristalline (im SW-Teil) bzw. das mittelliasische Grundgebirge auf die miozänen Formationen geschoben ist. An der N- und NW-Seite wird die Braunkohlenserie durch den Querbruch von Nagymányok bzw. durch die infolge einer Aufschuppung nördlicher Vergenz zu Tage getretenen und verhältnismässig hochragenden mitteltriadischen Scholle begrenzt (siehe Abb. 1).

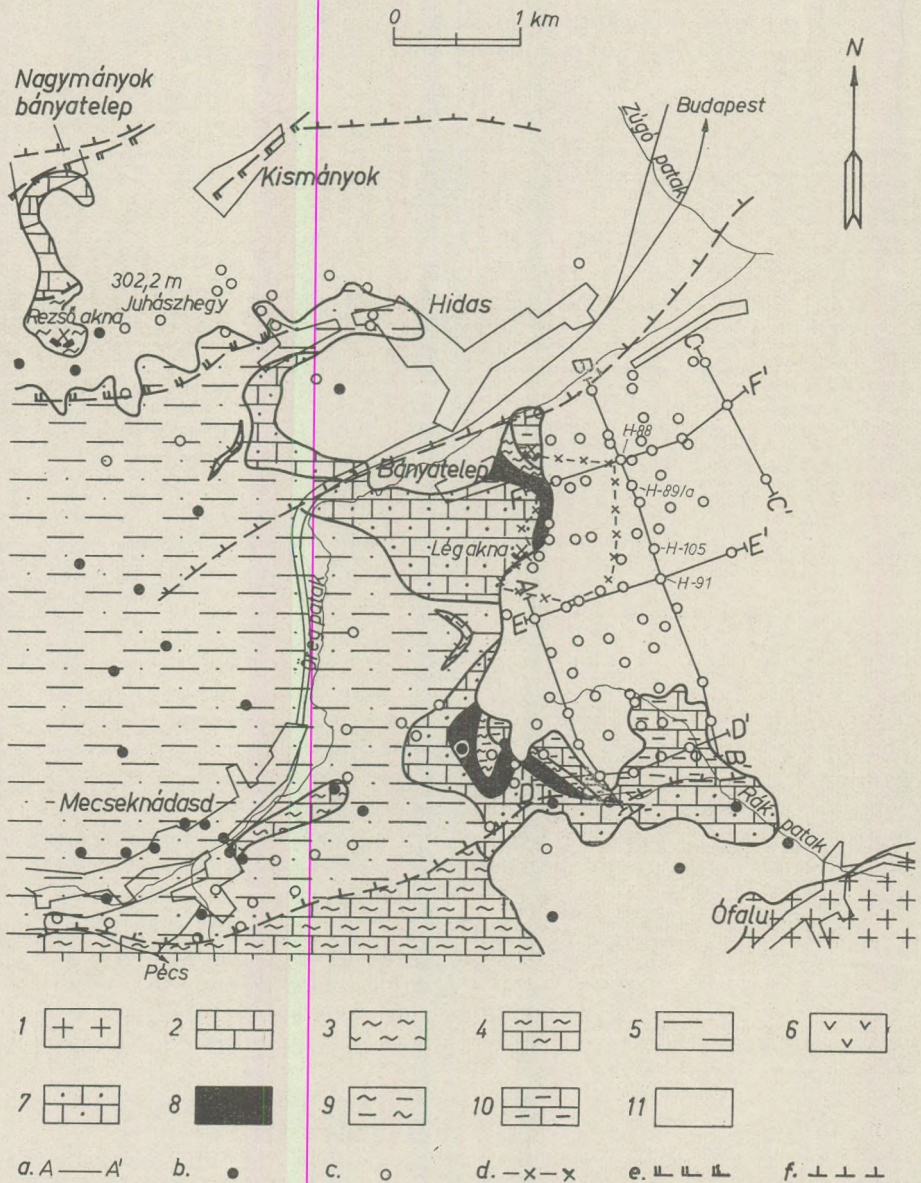
Gegen W ergibt sich in einer submeridionalen Richtung eine natürliche Grenze für die Kohlenserie, infolge ihres Auskeilens. Wegen des NO gerichteten Einfallens der Kohlenflöze und des Nebengesteins ist die Verbreitung der Kohlenserie ost- bis nordostwärts offen, d. h. noch nicht abgegrenzt. Die östlichst gelegene Tiefbohrung (H-53) im Gebiet hat die Kohlenserie in einer Tiefe von 590 m unter der Tagesoberfläche, in einer Gesamtmächtigkeit von ca. 80 m angestossen. Während die Kohlenserie bis zu 2 km Entfernung von der westlichen Oberflächen-Auskeilungslinie nicht abgegrenzt ist, findet man längs der submeridionalen Streichrichtung in 3,2 bis 3,3 km Entfernung ihre deutliche Abgrenzung (siehe Abb. 1).

Auf einer Fläche von ca. 6 km² wurden insgesamt 82 Bohrungen niedergebracht, davon durchteuften 79 die Braunkohlenserie.

Die Braunkohlenserie von Hidas stellt eine geologisch umrahmte, gegen O und NO offene Ausbildung dar. Die Kohlenserie ist mitsamt ihrem Hangenden (bis zum unteren Pannon) in miteinander parallele Antiklinalen und Synklinalen von SW-NO—Achsenrichtung gefaltet. Die Achsen dieser tektonischen Richtungen fallen nordostwärts ein, demzufolge ist die Kohlenserie allmählich immer tiefer gesunken.

Eine heteropische Fazies der mittelmiozänen (tortonischen) Leithakalkformationen, die Braunkohlenserie von Hidas schliesst sieben Flöze in sich ein. Ihr geologischer Bau und ihre räumliche Gliederung können auf folgende Weise zusammengefasst werden. In der Kohlenserie lässt sich sowohl horizontal, als auch vertikal eine dreifache Gliederung

UNBEDECKTES GEOLOGISCHES PROFIL AUS DER UMGEBUNG VON HIDAS (SÜDUNGARN)



Legende: 1. kristallines Grundgebirge; 2. mitteltriadischer (Anis) Kalkstein; 3. unterliassischer Handgemergel und Kohlenserie; 4. mittelliassischer Mergel; Kalkmergel; 5. helvetischer Sand-, Schotter- und Tonmergelkomplex; 6. Rhyolith (Dazit)-Tuff; 7. tortonischer Konglomerat- und Lithothamnienkalk-Komplex von Leithafazies; 8. tortonischer Tonmergel mit Turritellen und Corbulen; 9. sarmatischer Kalkstein, Kalkmergel; 10. pannonischer Sand, Schotter und Mergel;
a: Spurenlinien geologischer Profile; *b*: geologische Kartierungsbohrung; *c*: Tiefschürfböhrung auf Kohle; *d*: bergtechnische Grenze der Grube; *e*: Aufschübung; *f*: Verwerfung.

erkennen. Von unten nach oben, in vertikaler Richtung, gehen die Süßwasserfazies allmählich in Sedimente von immer höherem Salzgehalt und schliesslich in echte Meeresablagerungen über. In horizontaler Richtung kann auf Grund der von dem Verlauf der litoral-sublitoralen Zone und von der Verbreitung des Beckengebietes abhängigen Absonderung eine dreifache Gliederung in unterschiedlichen Fazies nachgewiesen werden.

Die vertikale Gliederung widerspiegelt folgende Faziesunterschiede (M. Földi 1966).

a) Unteres Glied. Es reicht bis zum Hangenden des aus mehreren Bänken bestehenden Flözes VII. In diesem Gliede sind die Gesteinszwischenlagerungen vorwiegend durch gelb-gestreifte, zumeist feinsandige Tonmergel mit *Brotia escheri inornata* Wenz., *Planorbis alienius* Rolle, *Planorbis* sp., *Unio* sp. vertreten. *Rissoa hidasensis* Mezn. kann in dieser Formation nur vereinzelt angetroffen werden.

b) Mittleres Glied, das zugleich auch die grösste Mächtigkeit besitzt. Das Bergmittelschliessende Glied reicht vom Flöz VI bis zu Flöz II. Hier sind die ausgesprochen Süßwasser-Formen in den Hintergrund gedrängt. Die Gesteinszwischenlagerungen werden hauptsächlich durch *Rissoa hidasensis* Mezn. — eine schon für leicht salziges Wasser charakteristische Form — gekennzeichnet.

c) Oberes Glied. Es ist das Hangende des Flözes II, und seine Mächtigkeit erreicht nur 1,5–2 m. Dies ist schon eine ausgesprochen neritische Fazies mit Brackwasser-Übergängen. Das ausschliesslich oberhalb dieser Schichten befindliche Flöz I berechtigt die Zugehörigkeit dieser Formationen zur Kohlenserie. Das beweisen die in grosser Zahl vorkommenden Exemplare von *Ostrea* sp., *Anomia* sp., *Cardium* sp., *Cardita* sp. sowie die spärlicheren Vertreter von *Aloidis* (*Varicorbula*) *gibba* Olivi, *A. carinata* Dujl. usw.

In horizontaler Richtung kann die Kohlenserie auf folgende Weise gegliedert werden:

- südliche Rand- oder litorale Zone;
- mittlere oder Übergangszone;
- nördliches oder Beckenfazies-Gebiet;

1. In der südlichen litoralen Zone ist die Kohlenserie am kleinsten (35 bis 40 m mächtig). Im südlichsten Teil dieser Randzone sind die Kohlenflöze dünn, auskeilend, in Linsen zersplittert. Daneben wurden die Flöze auch der Erosion unterworfen und z. T. abgetragen. Die Kohlenserie besteht vor allem aus oligohalinen Schichten mit *Rissoa hidasensis* Mezn. und nur stellenweise treten Brackwassereinlagerungen von etwas höherem Salzgehalt auf.

In den nördlichen Teilen der Randzone ist die Kohlenserie schon mächtiger, obwohl die Flöze immer noch in Auskeilen begriffen sind und auch der Effekt der Erosion nachgewiesen werden kann.

2. An der südlichen Seite der mittleren oder Übergangszone ist die Mächtigkeit der Kohlenserie noch 30 bis 45 m, an der Nordseite erreicht

sie aber schon 50 bis 75 m und in der Regel können alle sieben Flöze angetroffen werden. Das an der Basis gelegene Flöz VII besteht aus 5 bis 7 Bänken, die voneinander durch dünne Zwischenlagerungen mit *Brotia-Planorbis* oder eventuell mit *Rissoa* getrennt sind. In den Zwischenlagerungen können auch mehrere, ein paar cm dicke Rhyolithuffbänder nachgewiesen werden. Die Mächtigkeit des Flözes, zusammen mit den Einlagerungen, beträgt 4 bis 8 m. Darüber lagern 3 bis 6 m mächtige *Brotia-Planorbis*-Mergel und dann folgt das 1–2 m mächtige, aus 2–3 Bänken bestehende Flöz VI. Obzwar hie und da sowohl das Flöz VI als auch das darüber lagernde Flöz V ausbleiben bzw. auskeilen, können die beiden auf dem Gebiet der betreffenden Zone gewöhnlich angetroffen werden. Dasselbe gilt auch für die Flöze III und II. Das Flöz IV ist das mächtigste (3–5 m), zusammenhängende Kohlenlager des Gebietes und es besteht bloss aus zwei Bänken. Die vertikale Gliederung ist in dieser Zone schon nachweisbar.

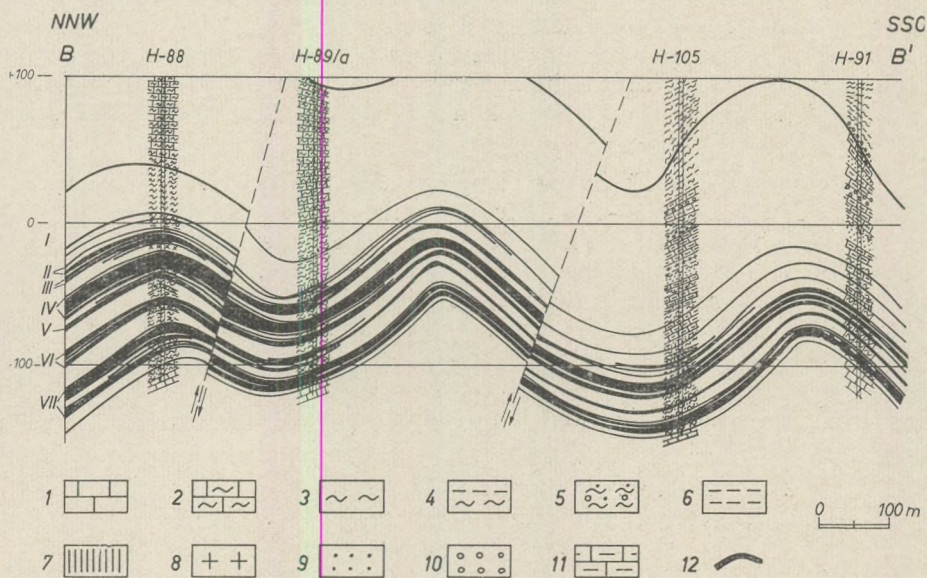


Abb. 2. Geologisches Profil B—B' durch die Lagerstätte Hidas (mit doppelter Übererhöhung des vertikalen Massstabes)

3. Im Raume der Beckenfazies im N ist die Kohlenserie den Formationen der Übergangszone ähnlich aufgebaut. Der Unterschied zwischen den beiden besteht vor allem in der Mächtigkeit der Flöze. Hier schwankt die Mächtigkeit der Kohlenserie zwischen 75 m und 90–105 m. Das Flöz VII, welches sogar eine Mächtigkeit von 10 bis 18 m erreicht, besteht aus 6 bis 10 Bänken. Die Fazies der dazwischen geschalteten Gesteine stimmt mit der vorigen überein. Auch in diesem Teilgebiet ist das

Flöz IV am mächtigsten (15 bis 20 m), aber gegen N verzweigt es immer mehr. Im S ist es jedoch noch vollkommen ungegliedert und 8 m mächtig.

Die Flöze III und II sind im Südteil des Beckenfaziesgebietes bekannt. Weiter nach N folgt über dem Flöz IV unmittelbar das Flöz I; die Flöze II und III bleiben aus. Diese Tatsache ist darauf zurückzuführen, dass die Torton-Transgression den NO-Teil früher als den Südteil des betreffenden Gebietes erreicht haben muss. Die Braunkohlenserie wird also vom S nach N zu mächtiger. Während im S die Mächtigkeit noch 30–45 m ist, beläuft sie sich im N auf 90–105 m.

Die im weiteren zu besprechenden Teiluntersuchungen wurden an den Proben der hiermit veranschaulichten Bohrungen (siehe Abb. 2) und Grubenprofile (siehe Abb. 3) durchgeführt.

Die Zahl der analysierten Kohlenproben betrug 115, die der Gesteinszwischenlagerungen ca. 200.

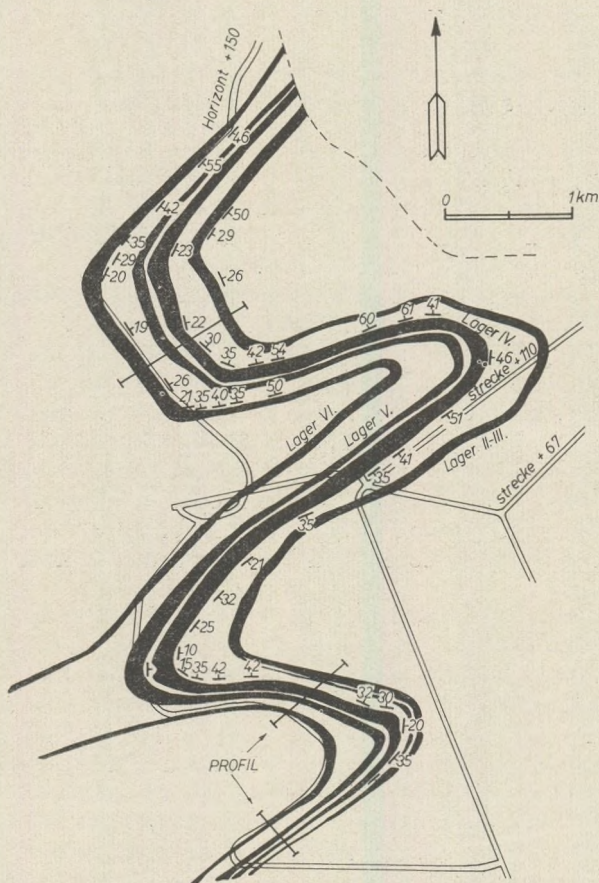


Abb. 3. Grundriss des Bergwerkes von Hidas am Niveau +150 (entworfen von L. Tamáshidy)

Palynologische Untersuchungen

An den Floratüberresten der Miozänablagerungen des Mecsek-Gebirges hat E. Nagy (1965) eingehende palynologische Untersuchungen durchgeführt. Dabei bestimmte sie das Pollenspektrum der Flora der einzelnen Miozänstufen, woraus sie Schlüsse über die Zusammensetzung der Vegetation und über die klimatischen Verhältnisse zog.

Vor der Besprechung der palynologischen Untersuchungen müssen wir noch die von Á. Haraszty (1957) durchgeführten xylotomischen Untersuchungen erwähnen, welche die Zugehörigkeit fossiler Pflanzen zur Familie *Taxodiaceae* nachgewiesen haben. Dieser Verfasser hat folgende drei Typen unterschieden:

1. den Typ *Taxodioxyylon gypsaceum* Kräusel, welcher der Art *Sequoia sempervirens* entspricht;
2. den Typ *Taxodioxyylon taxodi* Gothan, welcher der Art *Taxodium distichum* entspricht und
3. den Typ *Glyptostroboxylon tenerum* Conventz, welcher der Art *Glyptostrobus pensilis* entspricht.

Taxodioxyylon gypsaceum (*Sequoia*) ist ein immergrüner Nadelbaum der trockenen, sanften Bergabhänge, die beiden anderen Arten sind laubabwerfende Nadelbäume, welche die Moor- und Sumpflandschaften bevorzugen. Nach Á. Haraszty wären also die Braunkohlenflöze von Hidas aus einem ehemaligen Sumpfland, unter bald wärmeren, bald vollkommen ausgeglichenen Klimaverhältnissen entstanden. In den stärker versumpften Gebieten müssen *Taxodium* und *Glyptostrobus*, an den sanften Bergabhängen aber *Sequoia* vorgeherrscht haben.

Die palynologischen Untersuchungen wurden an einer Gesamtzahl von 59 Kohlen- und Gesteinsproben durchgeführt. Darunter waren 35 Proben Kohle und tonige Kohle, 24 Proben kamen aus dem unmittelbaren Deckgebirge oder aus den Gesteinszwischenlagerungen. Die untersuchten Proben stammen aus 4 Tiefbohrungen (H-88, H-89, H-91, H-105) und aus 3 Grubenprofilen (siehe Abb. 2–3) und umfassen die ganze Kohlenserie. Die Sporen und Pollen wurden von E. Nagy bestimmt.

Aus den 59 Proben wurden 106 Formen der Flora bestimmt. Von diesen 106 Formen gehören 15 zu den Nacktsamern (darunter Coniferen), 67 zu den Bedecktsamern (darunter laubabwerfende Bäume). Mit dem grössten Formenreichtum zeichnet sich *Tricolporopollenites* aus: 20 Arten. Ein ähnlicher Formenreichtum konnte bei keiner anderen Gruppe beobachtet werden und die einzelnen Gattungen waren höchstens durch 2 oder 3 Arten vertreten (z. B. *Pinus*, *Ilexpollenites*, *Myricipites* usw.).

Allgemein verbreitet und stellenweise massenhaft vertreten ist das Pollen der *Taxodiaceae*, dessen Anteil in manchen Proben 35 bis 40, ja sogar 50% erreicht. Die oben erwähnten 3 Gattungen der Familie *Taxodiaceae* können palynologisch nicht abge sondert werden, da diese in meisten Fällen ein sich aufspaltendes, uncharakteristisches Pollen mit

kleiner *Lingula* besitzen. Auf Grund der xylotomischen Untersuchungen müssen wir ohne Zweifel mit dem Vorhandensein aller drei Gattungen rechnen.

Ausser *Taxodiaceae* sind die Pollen von *Pinus silvestris*, *Pinus haploxyton*, *Myricipites* und *Carya* in verhältnismässig grosser Menge vorhanden. Die Vertreter von *Pinus* machen insgesamt 20 bis 30%, *Myricipites* ca. 10% aus, während der Anteil der Vertreter von *Carya* stellenweise 18 bis 20%, in manchen Fällen aber auch 25% beträgt. Von den 106 Pollenformen gibt es lediglich 30–40 solche, die nur vereinzelt angetroffen werden können.

Von den 67 bedecktsamigen Pollenarten gehören 58 zu den Zweiblattkeimern und bloss 9 zu den Einblattkeimern. Darunter zeichnen sich die Pollen der Laubgewächse nebst ihrem Artenreichtum auch mit ihrem hohem Prozent aus, der jenem der Nadelbäume nahekommt. Unter den Zweiblattkeimern zeichnen sich folgende mit dem höchsten Pollenreichtum aus: *Ulmus*, *Zelkova*, *Betula*, *Quercus* und *Myricipites*. Relativ häufig ist unter den weichstengeligen Zweiblattkeimern das Pollen der *Nymphaceae* und *Ericaceae*. Ausser diesen ist auch noch das Pollen der weichstengeligen Zweiblattkeimer *Rubiaceae*, *Artemisia*, *Chonopodiaceae* und *Urticoides* nachweisbar.

Vom Pollenspektrum leuchtet es hervor, dass die Laubbäume an Arten reich und stellenweise auch sehr häufig waren, obwohl ihr Anteil denjenigen der Nadelbäume nicht erreicht. Diese Tatsache bringt einen scheinbaren Widerspruch gegenüber den kohlenpetrographischen Ergebnissen, nach denen der Xylith von Laubbaum-Struktur nur in untergeordneter Menge vorhanden ist, zum Ausdruck. Der kohlenpetrographisch nachgewiesene geringe Anteil der Laubbäume im Vergleich mit der palynologisch bestimmten Menge kann auf mehrere Ursachen zurückgeführt werden.

a) Der Anteil der Laubbäume ist von vorherein geringer in der Braunkohle, da Xylit nur von Coniferen und von laubabwerfenden Kernbäumen zurückgelassen werden kann. Demzufolge bleibt Laubbaum-Xylith nur ausnahmsweise erhalten. So ist die Menge des kohlenpetrographisch nachweisbaren Xylits von Laubbaum-Ursprung kleiner als sie in der ursprünglichen Vegetation gewesen sein konnte.

Bei den Laubbäumen, die nicht zur Kategorie des Kernholzes gehören, können wir lediglich mit der Erhaltung ihrer Rindensubstanz rechnen, dessen Anhäufung und Inkohlung nicht zur Entstehung von Xylit, sondern zum Periblinit führt.

Die Braunkohle von Hidas enthält Periblinit und Xylit-Periblinit in grösserer Menge als Xylit. Da es kohlenpetrographisch nicht unterschieden werden kann, ob der Periblinit von einem Laubbaum oder einem Nadelbaum stammt, ist es zu vermuten, dass in der periblinitischen Kohle das Prozent der Laubbaum-(Rinden) Substanz höher als im Xylit selbst ist.

b) Der schlechtere Erhaltungszustand des Xylits von Hidas dürfte vielleicht für den kleineren Anteil des Laubbaum-Xylits verantwortlich

sein. Demzufolge lässt sich Xylit in den meisten Fällen lediglich auf Grund des Melanoresinitis und Xanthoresinitis nachweisen (siehe das Kapitel „Kohlenpetrographische Untersuchungen“). Die Möglichkeit solch einer Bestimmung bei Laubbäumen ist – dem Xylit der Nadelbäume gegenüber – äusserst beschränkt.

c) Da die beste Möglichkeit zum Nachweis des Laubbaum-Xylits durch die Erkenntnis der charakteristischen Zellstruktur gesichert wird, ist diese Möglichkeit im Falle von Hidas wegen des schlechteren Erhaltungszustandes des Xylits beschränkt. Die schlechte Erhaltung des Xylits ist einem ungewöhnlich grossen biologischen Effekt – das sich noch vor dem Inkohlungsprozess geäussert haben muss –, sowie der Gelierung des Xylits zuzuschreiben. Nach *Kirchheimer* (1957) sind die Pollen der Laubbäume schlechter erhalten als diejenigen der Nadelbäume. Die Gelierung sowie das stellenweise massenhafte Auftreten von das Holz angreifenden Pilzen – welche für die Vorbereitung der biologischen Verwitterung verantwortlich sind – haben wir auch im Xylit nachgewiesen.

Unter Berücksichtigung der obigen Ausführungen beweisen die palynologischen Ergebnisse, dass in der Genese der Braunkohle von Hidas neben den Nadelbäumen auch die Laubbäume eine grössere Rolle spielten, als diese anhand der xylotomischen und kohlenpetrographischen Ergebnisse zu vermuten war. Ausser den palynologischen Untersuchungsangaben dient der grössere Anteil des Periblinits im Vergleich mit dem Xylit als ein negativer Beweis.

Anhand des Pollenspektrums kann es festgestellt werden, dass die ehemalige Vegetation der Braunkohlenserie keinen wesentlichen Unterschied von dem durch *E. Nagy* (1965) hinsichtlich des Mecsek-Gebirges nachgewiesenen mittelmiozänen Florenbild aufweist. Auf Grund der Pflanzenzusammensetzung war das Klima zum Teil ausgeglichen warm, vorwiegend subtropisch und lediglich zum kleineren Teil dürfte es als tropisch betrachtet werden. Hierauf deutet das Pollenspektrum, das vor allem aus den Vertretern von Moor- und Sumpfwäldern sowie von subtropischen Mischwäldern (die vom Bergfuss bis auf die Berge hinauf reichten) besteht und in dem nur sehr spärliche tropische Elemente vorzufinden sind.

Kohlenpetrographische Untersuchungen

Den kohlenpetrographischen Untersuchungen wurden 110 Kohlenproben aus Gruben und Tiefbohrungen unterzogen. Die Bestimmungen erfolgten mit dem von *Szádeczky* und *Soós* (1964) erarbeiteten Schnellverfahren.

Mit dieser Methode wurden folgende Kohlegesteinstypen nachgewiesen:

1. *Xylit*. Es konnten drei Abarten dieses Typs unterschieden werden: gewöhnlicher Xylit, Resinoxylit (harziges Holz) und Telinitstreifen der

Periblinite. Der Xylit stammt überwiegend von Nadelgewächsen; Xylit von Laubbaum-Ursprung ist nur in verschwindend geringer Menge vorhanden.

Der gewöhnliche Xylit ist in ein paar mm bis dm dicken Streifen oder selten in Form von feinen Trümmern, vor allem aber in Form von Vitritdetritus, zu finden. Ist der Xylit durch dickere Streifen vertreten, so stellt er eine selbständige Gesteinsart dar, aber in detritischer Form (50 μ bis 1–2 cm) ist er lediglich eine Streifenkomponente. In den Flözen III und IV von Hidas kann Xylit sogar in einer Dicke von 10 bis 20 cm häufig angetroffen werden, mit einem makroskopisch erkennbaren Holzgewebe: Holzstämme, feinere Details und Asttrümmer. Bei teilweisem oder völligem Fehlen der Zellwandstruktur wird die Erkenntnis des ehemaligen Gefüges durch den Melanoresinit erleichtert, der nach dem Längsparenchym und Markstrahlzellen (Flobaphenit) angeordnet ist (siehe Bilder I/1 und I/2).

Da der grössere Teil des Xylits von Hidas entweder überhaupt kein Gefüge oder kaum etwas aufweist, muss seine Bestimmung unter dem Mikroskop hauptsächlich auf der von der originalen Struktur zeugenden Anordnung des Resinits beruhen. Der Grossteil der Xylite von Hidas führt keinen Xanthoresinit und stellt, mit den xylotomischen Untersuchungsergebnissen von Á. H a r a s z t y übereinstimmend, vorwiegend die Derivaten von *Taxodiales* dar.

Der schlechte Strukturehaltungszustand des Xylits von Hidas steht offenbar mit der vor der Inkohlung stattgefundenen intensiven biologischen Verwitterung in Zusammenhang. Die Richtigkeit dieser Annahme bestätigt das stellenweise massenhafte Auftreten der holzangreifenden Pilze (siehe Bild I/1). Zur Zerstörung der Zellstruktur des ehemaligen Baumes führt die Gelierung, sowie das Vorhandensein von Gelhuminit oder Collinit, der in der huminitischen Grundmasse der Kohle oft, aber seltener auch im Xylit selbst nachgewiesen werden kann (siehe Bild I/1).

Von einer Abstammung von Laubgewächsen zeugendem Xylit haben wir nur in einigen Fällen angetroffen. Auf Grund der palynologischen Untersuchungen müssen wir jedoch den Laubgewächsen zweifellos grössere Bedeutung in der Kohlenbildung beimessen.

2. *Resinoxylit*. Zwischen den Xyliten nur in 1 bis 2% vorhanden. Am häufigsten ist Resinoxylit an die Anhäufungen von Harzkörnchen gebunden, aber manchmal können auch selbständige Harzkörper beobachtet werden. Während die kleineren Harzkörnchen hauptsächlich in den Markstrahlzellen zu finden sind, treten die grösseren (vor allem die Harzkörper) unregelmässig, zerstreut auf.

3. *Telinitstreifen*. Das sind Komponenten des Periblinits, in ihnen kann — zwar nicht ganz deutlich — auch Melanoresinit nachgewiesen werden. Zu den Xyliten rechnet man sie darum, weil das ehemalige Holzgewebe manchmal auch durch parallele Streifung angedeutet wird. Die Dicke der Streifen schwankt von 0,1 bis 2–3 mm. Die Häufigkeit dieser Streifen ist proportionell mit der Menge der Periblinite.

4. *Periblinnit*. Kohlenkomponente, welche die grösste Inhomogenität aufweist. Die typischsten Komponenten des Periblinnits von Hidas sind – in Reihenfolge ihrer abnehmenden Häufigkeit – folgende:

- a) *ausgezogene (ausgedehnte) Bastfasern*;
- b) *Telinittstreifen (die beim Xylit erwähnt wurden)*;
- c) *dunklere Flobaphenitkörper und -streifen*;
- d) *verschiedene Bituminittetzen (Harzkörnchen, Harzkörper)*;
- e) *Paragewebe-Streifen*;
- f) *Oxydationsränder und -Flecken*;
- g) *Fusinit (endogener und exogener Fusinit)*.

Hier seien noch die verschiedenen Pilzderivaten erwähnt: Pilzfäden (Hyphen), Pilz- und Teleutosporen, sowie Sklerozium. Diese können am öftesten im Periblinnit, aber zuweilen auch im Xylit angetroffen werden. Hie und da treten sie massenhaft, zusammen mit den Bastfasern auf. Am häufigsten sind die Sporen der ehemaligen annähernd kreisförmigen, holzangreifenden Pilze und dann folgen die ein- bis dreizelligen Teleutosporen.

5. *Blätterkohle* und blätterkohleführender Brennschiefer. Auf Grund des Aschengehaltes handelt es sich vor allem um Brennschiefer, obwohl auch Blätterkohle (siehe Bild II/5) von kleinem Aschengehalt (10 bis 20%) vorhanden ist. Eine charakteristische Komponente der Blätterkohle bzw. des blätterkohleführenden Brennschiefers ist der gewöhnlich in grosser Menge vorhandene sägezahnrandige Kutinit: ein Abkömmling der Kutikula. Daneben lassen sich auch mit Kutinit umrandete, vitritisierte Ast-Reste und andere Pflanzenderivaten beobachten (siehe Bild II/6).

Der Kutinitstreifen ist manchmal ungewöhnlich dick: 10 bis 15 μ , stellenweise erreicht seine Dicke sogar 30 bis 35 μ (siehe Bild II/7). Der dickere Kutinit zeugt von Überresten xerophiler Pflanzen. Neben den erwähnten Komponenten tritt im Brennschiefer auch noch Collinit zusammen mit Detritovitritinit auf (T e i c h m ü l l e r 1968). Im Falle von verhältnismässig kleinerem Aschengehalt ist Collinit hauptsächlich zusammen mit Periblinnit, als ein Übergang zwischen dem Periblinnit und der Blätterkohle zu finden. In der Blätterkohle ist Periblinnit bloss untergeordnet, und in reiner Blätterkohle fehlt er schon vollkommen.

Wurzelkohle und vitritdetritische Kohle, collinitführender Ton. Während die Wurzelkohle ziemlich leicht von der huminit-detritischen (vitritdetritischen) Kohle unterschieden werden kann, stösst die Erkenntnis der Komponente Collinit unter dem Mikroskop – unseren Erfahrungen nach – auf beträchtliche Schwierigkeiten, was vor allem durch die subjektive Beurteilung des Gelierungsgrades bedingt ist.

6. *Die vitritdetritische Kohle* besteht in der Regel aus voneinander deutlich unterschiedbaren hell- bis dunkelbraunen, stellenweise oxynitisierten Huminittrümmern (siehe Bild II/8). Bezüglich der bisweilen beobachtbaren linsenförmigen Huminitkörper kann es nachgewiesen werden, dass es sich um die Derivaten von Flobaphen (Melanoresinit)

handelt. Ausser den vorher erwähnten Komponenten enthält die vitrit-detrithische Kohle auch noch Stengel- und Ast-Teile, Kutinit, Bituminitrümmer verschiedener Herkunft, sowie Gelhuminit und verschiedene Mengen von Oxynit und Pyrit.

7. In der *Wurzelkohle* und dem wurzelkohleführenden Brennschiefer gibt es überhaupt keinen Huminit oder nur eine äusserst geringe Menge. In Dünnschliffen beobachtet, besteht dieser Gesteinstyp aus parallelen oder verzweigten, oxydierten Vitritfäden und -Bündeln, von denen sich weitere Wurzelhaar-Derivaten abzweigen. Darunter sind die dickeren vitritischen Komponenten weniger oxydiert, als die dünneren. Die oxydierten Vitritkörper sind stellenweise mit einem Para-Kranz umrandet. Auch in diesem Gesteinstyp können noch Gehluminit, Huminit- und Bituminitrümmer, ferner vitritisierte Ast-Teile, sowie Oxynit und Pyrit angetroffen werden.

8. Der *collinitführende Ton* besteht ausser dem überwiegenden Ton vor allem aus Gelhuminit, Wurzelvitrit, aber die Menge von Wurzelvitrit, vitritisierten Stengel- bzw. Ast-Teilen und Pyrit ist kleiner als im vorigen Gesteinstyp.

Die angeführten Kohlegesteinstypen kommen nicht immer in reiner Form vor, ihre Übergänge ineinander sind häufig. Nach unseren Untersuchungen können in den Kohlenflözen von Hidas folgende Gesteinstypen angetroffen werden (ihre quantitative Verteilung ist auch mit angeführt):

1. *Xylit (Resinoxylit)*: 15% (davon 2% *Resinoxylit*),
2. *Xylit-Periblinnit*: 30%,
3. *Periblinnit*: 19%,
4. *Periblinnit-Blätterkohle*: 9%,
5. *Blätterkohle bzw. tonige Blätterkohle*: 4%,
6. *tonige, vitritdetrithische Kohle*: 2%,
7. *vitritdetrithischer Brennschiefer*: 9%,
8. *blätter- und wurzelkohleführender Brennschiefer*: 3%,
9. *blätter- und wurzelkohleführender Ton*: 5%,
10. *collinitführender Ton*: 4%.

Der mittelmiozänen Kohle von Borsod-Nógrád gegenüber enthält die Braunkohle von Hidas auch vitritdetrithische (huminitdetrithische) Kohle, die in offenen Mooren (Flach- oder Tiefmoor) abgelagert wurde. In den beiden Gebieten fehlt jedoch die für die tieferen, geschlossenen Sumpfe charakteristische Pollen- und Algenkohle.

Der Anführung der Kohlegesteinstypen von Hidas ist zu entnehmen, dass etwa $\frac{2}{3}$ (64%) der untersuchten Gesteinsproben aus Xylit und Periblinnit (15 + 19%) bzw. aus ihrer Mischung (30%) besteht. Das ist ein Zeichen dafür, dass das Kohlenbecken von Hidas zumeist ein Moorwald war, der höchstens bis zur äusseren Zone des Flachmoores reichte und nur an manchen Stellen die innere Zone des Flachmoors erreichte. Es fehlen die charakteristischen Bildungen der geschlossenen Sumpfe (Algen- und Pollenkohle) und in verhältnismässig kleiner Menge

sind die Kohlenbildungen der durch schwache und mittelmässige Strömungen charakterisierten Flachmoore – und zwar die vitritdetritische Kohle bzw. die collinitführende, tonige Kohle – vorzufinden.

Im Laufe der Bestimmung und Benennung der Kohlegestinstypen wird auch die Klärung von Nomenklaturfragen erforderlich. Wir sind der Meinung, dass unsere gegenwärtigen Untersuchungen – verglichen mit den Ergebnissen analoger Untersuchungen im Gebiete von Borsod und Nógrád – diese viel diskutierte und widerspruchsvolle Frage der Nomenklatur näher zur endgültigen Lösung bringen können.

Anhand des Materials der mittelmiozänen Braunkohle von Borsod – Nógrád haben E. Szádeczky-Kardoss und E. Soós (1964) einen natürlichen Grenzwert im Aschengehalt zwischen Kohle und Brennschiefer nachgewiesen. Diese Grenze liegt bei einem Aschengehalt von 20% und nicht bei 30%, wie sie früher angenommen wurde (Vadász, 1952). Ihre Feststellung motivierten die Verfasser damit, dass der Aschengehalt von Xylit und Periblinit in der Regel unterhalb 20% ist.

Neben den Feststellungen von Szádeczky – Soós sind die Nomenklaturen-Vorschläge von A. Juhász (1967) bezüglich des Ost-Borsoder Gebietes beachtenswert. Gegenüber der Klassifikation von Szádeczky – Soós (Kohle, Brennschiefer und kohlenführender Ton: mit Aschengehalten von 20%, 20–50% und über 50%) schlägt A. Juhász eine detailliertere Gliederung für die Braunkohle mit einem Aschengehalt von 20 bis 50% vor. Die von ihm vorgeschlagenen Benennungen sind folgende:

(Braun)kohle	Aschengehalt:	< 20%
Tonige Kohle	Aschengehalt:	20 bis 35%
Brennschiefer	Aschengehalt:	35 bis 40%
Kohlenführender Ton	Aschengehalt:	> 50%

Die Anwendung des Begriffes Braunkohle bis zu 20-prozentigem Aschengehalt begründet A. Juhász damit, dass der Aschengehalt von Xylit und Periblinit am öftesten unterhalb 20% und vor allem zwischen 15 und 20% liegt und dass eine Kohle mit einem Aschengehalt von <10% im betreffenden Gebiet nur äusserst selten vorkommt. Die Benennung „tonige Kohle“ bei 20 bis 35% Aschengehalt wird dadurch berechtigt, dass, gemäss den Analysen, der strukturlose Periblinit, die Kutikulenkohle und die vorwiegend aus Bastgewebe bestehende Kohle am öftesten einen Aschengehalt von ca. 30% haben.

Die kohlenpetrographische Untersuchung der Braunkohle von Hidas hat die Richtigkeit der von A. Juhász vorgeschlagenen Begriffe im grossen und ganzen bestätigt. Eine auch kohlenpetrographisch bestätigte Absonderung (Grenze) kann zweifellos bei 20-prozentigem Aschengehalt nachgewiesen werden. Kohle mit einem Aschengehalt von <10% kommt auch in der Lagerstätte Hidas selten vor, daher ist es berechtigt, den Begriff der (reinen) Kohle bis zu einem Aschengehalt von 20% zu erweitern, gegenüber der früheren (1952) Stellungnahme von Vadász (10%). Es ist jedoch wohl begründet, die aus einer Mischung von Xylit

und Periblinnit bestehenden Kohlengesteinstypen, sowie Blätterkohle und Periblinnit-Blätterkohle mit einem gewöhnlichen Aschengehalt von 20 bis 30% *nicht Brennschiefer, sondern tonige Kohle zu nennen*. Da der Aschengehalt dieser Kohlengesteine sich nicht über 30% beläuft, ist es richtiger, die von A. J u h á s z vorgeschlagene Nomenklatur in solcher modifizierten Form anzunehmen, *daß die Grenze zwischen toniger Kohle und Brennschiefer nicht bei 35%, sondern bei 30% gezogen wird*.

Solch eine Modifizierung wird durch den Vergleich der quantitativen Verteilung der Kohlengesteinstypen und der Kohlenproben je nach dem Aschengehalt bekräftigt. Auch aus der Aufzählung der Kohlengesteinstypen leuchtet es hervor, dass Xylit und Periblinnit sowie ihr Mischgestein, ferner Blätterkohle, Periblinnit-Blätterkohle und (die äusserst geringe) vitritdetritische Kohle etwa $3/4$ (77%) der untersuchten Proben ausmachen. Die Analysen des Aschengehaltes haben dabei beinahe den gleichen Wert (80%) ergeben. Werden die auf den Xylit und Periblinnit bezüglichen Daten einzeln in Betracht genommen, so ergibt sich, dass sie sowohl kohlenpetrographisch wie auch betr. des Aschengehaltes gleichwertige Angaben aufweisen. Die erwähnten anderen Kohlengesteinstypen können jedoch bei weitem nicht für Brennschiefer gehalten werden, sondern sie dürften eher als tonige Kohle angesehen werden. Neben der mit den Kohlengesteinstypen übereinstimmenden Menge der Kohle von unter 30%-igem Aschengehalt wäre es auch aus feuerungstechnischen Gründen unbegründet, die Kohlentypen mit 20- bis 30-prozentigem Aschengehalt zu den Brennschiefern zu rechnen.

Die untersuchten 110 Proben verteilen sich nach ihrem in lufttrockenem Zustand berechneten Aschengehalt auf folgende Weise:

Tabelle 1

Aschengehalt in %		
Benennung	Aschengehalt %	Verteilung der Proben
Kohle	20%	55%
Tonige Kohle	20 – 30%	22%
Brennschiefer	30 – 50%	15%
Kohlenführender Ton	50%	8%

Der Vergleich der Verteilung des Aschengehaltes mit den kohlenpetrographischen Untersuchungsangaben unterstützt eindeutig die Richtigkeit der von A. J u h á s z vorgeschlagenen und von uns etwas modifizierten Nomenklatur.

Gegenüber den palynologischen Ergebnissen haben die kohlenpetrographischen Untersuchungen wenig Xylit von Laubbaum-Ursprung nachgewiesen. Das ist vor allem auf die vor der Inkohlung stattgefundene und weit verbreitete biologische Verwitterung und die ebenfalls häufige Gelierung – Prozesse, die auch die schlechte Erhaltung der Struktur des Xylits von Hidas zur Folge hatten – zurückzuführen.

Die nachgewiesene Veränderung in der Struktur des Xylits gestattet uns jedoch nicht nur eine unterschiedliche Beurteilung der Beteiligung der laubabwerfenden Bäume, der Nadelbäume und deren kohlenpetrographischen Derivaten am Kohlenbildungsvorgang, sondern ermöglicht uns auch die Klärung einer vom praktischen Gesichtspunkt wichtigen Frage, und zwar der Möglichkeit zur Brikettierung ohne Anwendung von speziellen Bindemitteln.

Abweichend von der von K e g e l (1948) vertretenen früheren Auffassung – nach welcher das Vorhandensein von Xylit schädlich für die Brikettierung sei – haben in jüngster Zeit R a m m l e r und B i l k e n r o t h (1954) nachgewiesen, dass der strukturengebundene Xylit günstig für die Brikettierung ist und mit zunehmendem Xylitgehalt auch die Festigkeit des Briketts ansteigt. Dementsprechend können wir feststellen, dass die ohne Auswahl genommene Durchschnittskohle von Hidas mit sehr kleinem, strukturengebundenen Xylitgehalt ohne Bindemittel entweder überhaupt nicht oder nur schlecht brikettiert werden kann. Das ist auf folgende Ursachen zurückzuführen:

1. *Der Xylitgehalt der Braunkohle von Hidas ist gewöhnlich gering (15)%.*
2. *In diesem geringen Xylitgehalt ist der Anteil des Xylits von höherem Zellulosegehalt mit gut erhaltener Struktur sehr klein.*
3. *Die häufige Gelierung der Braunkohle von Hidas verringert die Brikettierbarkeit und verdirbt stark die mechanischen Beschaffenheiten des Briketts.*

Kohlenchemische Untersuchungen

Die 110 Kohlenproben wurden auch chemischen Analysen unterzogen. Die Untersuchungen umfassten gewöhnliche Schnellanalysen und Serienanalysen auf die einzelnen Elemente. Die chemischen Analysen wurden im Laboratorium des Lehrstuhls für Angewandte und Ingenieurgeologie der Eötvös Universität durchgeführt. In der Regel wurden dieselben Proben analysiert, die für die kohlenpetrographischen Untersuchungen ausgewählt wurden.

Die Ergebnisse können wie folgt zusammengefasst werden. Wie ersichtlich von der auf dem Aschengehalt fussenden Gliederung, hatten 4 Proben einen Aschengehalt von < 10% (3,68%). Die Zahl der Proben mit einem Aschengehalt zwischen 10 und 25% beträgt 57 (51,4%). Davon hatten 24 Proben (22%) 10- bis 15-prozentigen Aschengehalt. Der Aschengehalt von 15 bis 20% ist also noch häufiger als jener von 10 bis 15%. Nur 5 Proben erreichen einen Aschengehalt zwischen 30 und 35% (3,5%). Diese letztere Angabe ist ein weiterer Grund für die Grenzziehung tonige Kohle–Brennschiefer nicht bei 35-prozentigem, sondern bei 30-prozentigem Aschengehalt.

Der grubenfeuchte Wassergehalt der Braunkohle von Hidas schwankt zwischen 30 und 50%, die häufigsten Werte sind 40 bis 45%. Die hygrosko-

pische Feuchtigkeit ist gewöhnlich 10 bis 13% und auch das — in einer einzelnen Probe beobachtete — Maximum war nur 14%. Die in diesen Proben gemessene minimale Feuchtigkeit ist ca. 5%, der häufigste Wert vertritt jedoch 10%. Im Falle der reinen Kohle ergibt sich also ein engerer, bei den Brennschiefern und der tonigen Kohle ein breiterer Wertebereich für den hygroskopischen Feuchtigkeitsgehalt.

Die Menge der brennbaren Substanz schwankt zwischen verhältnismässig engen Grenzen und verändert sich fast ausschliesslich in Abhängigkeit des Aschengehaltes. In der Kohle mit einem bis 20-prozentigem Aschengehalt ist der Anteil der brennbaren Substanz — unter Berücksichtigung des beinahe standarden Wertes der hygroskopischen Feuchtigkeit — von 60–70 bis 78%. Mit weiterer Zunahme des Aschengehaltes verringert sich die Menge der brennbaren Substanz auf lineare Weise.

Die Veränderung der hygroskopische Feuchtigkeit enthaltenden Kohle und des fixen C in Abhängigkeit des Aschengehaltes weist die folgende Korrelationsbeziehung auf (siehe Diagramm 1). Bei einer hygroskopischen Feuchtigkeit von 10 bis 13% nimmt der Heizwert bei 20-prozentigem Aschengehalt relativ plötzlich um etwa 200 bis 300 kcal/kg ab. Demzufolge wird sein Wert nunmehr kleiner als 4000 kcal/kg.

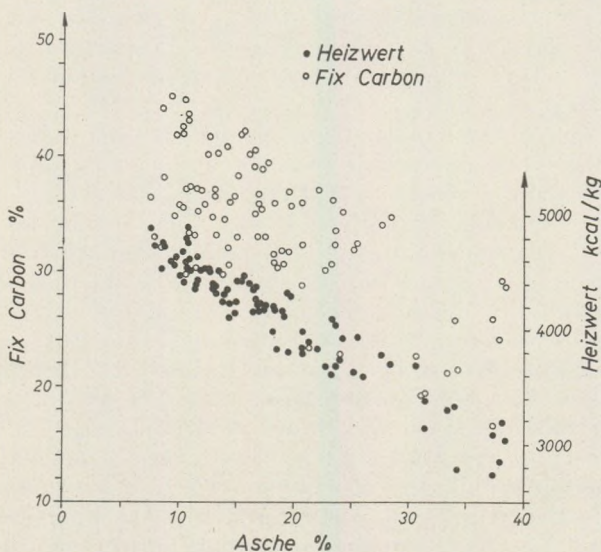


Diagramm 1. Verteilung des fixen C und des Heizwertes in Abhängigkeit vom Aschengehalt

Nach seinem, bei 20-prozentigem Aschengehalt beobachtbaren, verhältnismässig kleinen, plötzlichen Absinken — zeigt der Heizwert wiederum eine lineare Abnahme. Bei einem Aschengehalt von 30% liegt dieser Wert ca. um 3500 kcal/kg. Über dem 30-prozentigen Aschengehalt ist der

Heizwert — trotz seiner ausgeprägten Tendenz zur Abnahme — äusserst veränderlich.

Die Menge des fixen C liegt bei einem Aschengehalt von 30% gewöhnlich über 30% und dann nimmt diese Grösse — ebenfalls ziemlich rasch — auf 20 bis 25% ab. Bei der Kohle von 20-prozentigem Aschengehalt liegt der Wert des fixen C um 40 bis 45%; mit zunehmendem Aschengehalt sinkt er auf lineare Weise und bei 25-prozentigem Aschengehalt wird er schon kleiner als 40%; dann bei 30% Asche fällt er plötzlich um weitere 10–15%.

Ähnlich ist die Situation, wenn man das fixe C und den Heizwert mit Bezugnahme auf wasserlose Asche prüft. Der Unterschied besteht nur darin, dass der vorherige Sprung in der Veränderung des Heizwertes bei 22- bis 23-prozentigem Aschengehalt auftritt.

Vom Gesagten stellt es sich heraus, dass gewisse Sprünge sowohl bei 20- als auch bei 30-prozentigem Aschengehalt beobachtet werden können. Der bei 30-prozentigem Aschengehalt beobachtbare Heizwert von über 3500 kcal/kg beweist, dass es unberechtigt ist, auf die Kohle von über 20% Aschengehalt aus feuerungstechnischen Gründen zu verzichten bzw. sie als Brennschiefer zu qualifizieren.

Die weiteren Untersuchungsergebnisse beweisen, dass innerhalb der Menge des brennfähigen Stoffes — bis zu 20-prozentigem Aschengehalt — das fixe C bei den Volatilen in grösserer Proportion auftritt, aber dass dieses Verhältnis über dem 20-prozentigen Aschengehalt schon umgekehrt wird.

Die Menge der Volatile liegt in der Hidaser Kohle von maximum 20-prozentigem Aschengehalt zwischen 30 und 40%. Da die Veränderung des Anteiles der Volatile den Inkohlungsgrad widerspiegelt (und sich als dessen Funktion verändern kann), auf Grund des engen Wertbereiches des Volatilengehaltes gibt es keinen wesentlichen Unterschied im Inkohlungsgrad zwischen den untersuchten Kohlentypen. Alle sind von niedrigem Inkohlungsgrad und entsprechen dem Begriff des Lignits.

Dasselbe beweisen die Veränderungen des für eine aschen- und feuchtigkeitslose Kohle berechneten H und des Bitumen-Extraktes in Abhängigkeit des Volatilengehaltes (siehe Diagramm 2). Daraus ist es ersichtlich, dass der Wert von H sich zwischen 4 und 7,2% verändert und sein Durchschnitt bei 4,4–5,4 Gewichts% liegt. Die Menge des extrahierten Bitumens verändert sich zwischen 1,8 und 5,2% und ihr häufigster Durchschnittswert liegt zwischen 2 und 4%. Der kleine H- und Bitumengehalt zeugt von dem beinahe einheitlichen Inkohlungsgrad der Braunkohle von Hidas, von ihrer petrochemischen Homogenität, d.h. davon, dass diese Kohle (oder eher Lignit) ungeeignet zur Verarbeitung in der chemischen Industrie ist.

Die Menge des Gesamtschwefels in der Kohle mit hygroskopischem Feuchtigkeitsgehalt schwankt zwischen 4 und 7% und beträgt im Durchschnitt 5%. Die Menge des „Bombenschwefels“ schwankt jedoch zwischen 2,5 und 5,5%. Die Maxima des Anteils der beiden treten in der Kohle von geringem Aschengehalt (10–15%) auf. Mit Zunahme des Aschenge-

haltes nimmt die Menge der beiden Schwefelarten — mit linearer Veränderung — bis zu 30-prozentigem Aschengehalt ab. Im Brennschiefer — dessen Aschengehalt noch höher ist — kann keine Tendenz oder Gesetzmässigkeit in dieser Veränderung wahrgenommen werden.

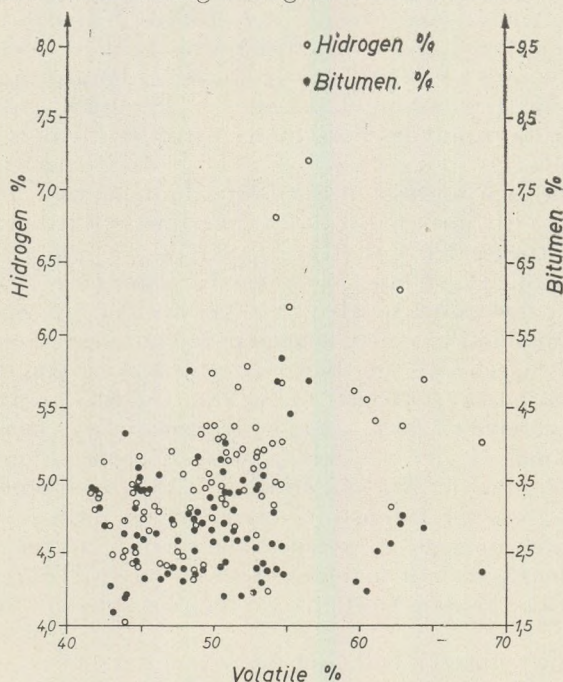


Diagramm 2. Veränderung des H- und Bitumengehaltes in Abhängigkeit von den Volatilen

Die Ergebnisse der chemischen Analysen zusammenfassend können wir feststellen, dass wir neben der Erkennung des chemischen Charakters der Kohle von Hidas auch die kohlenpetrographischen Untersuchungsergebnisse unterstützen konnten. Es ist klar, dass die Kohle einen niedrigen Inkohlungsgrad besitzt und zu Zwecken der chemischen Industrie ungeeignet ist. Am wirtschaftlichsten wäre ihre Anwendung zur Feuerung nach völligem Austrocknen.

Untersuchungen auf Spurenelemente

Mit der Verteilung von Spurenelementen hat sich Verfasser in einem seiner früheren Aufsätze befasst (Á. Grossz 1967). Es ist jedoch erforderlich, auf diese Frage nach dem Abschliessen der Untersuchungen nochmals einzugehen, da die auf Teilergebnissen beruhenden Feststellungen in mehreren Beziehungen eine wesentliche Veränderung benötigen.

Zu dieser Frage wurden ca. 400 Analysendaten von 118 Gesteins- und Aschenproben benützt. Die qualitativen bis semiquantitativen Be-

stimmungen wurden grösstenteils mit Quarzspektrographen gemacht und auch mit flammenfotometrischen Untersuchungen ergänzt. Die Aufnahmen wurden von I. Kubovics gemacht. Ergänzende bzw. Kontrollenuntersuchungen wurden ausserdem am Lehrstuhl für Anorganische und Analytische Chemie der Eötvös Universität (E. Zapp), im Geochemischen Laboratorium der Ungarischen Geologischen Anstalt (M. Földvári-Vogl), im Komlóer Laboratorium des Landesunternehmens für Erkundung und Bohrung (S. Juhász), sowie im Chemischen Laboratorium des Forschungsinstitutes für Bergbau (I. Száva) vorgenommen.

Die Analysen umfassten die Bestimmungen von 35 Spurelementen. Davon waren 10 unterhalb der Grenze der spektrographischen Nachweisbarkeit vorhanden: Cd, Hg, Tl, Sb, Bi, Te, Th, U, Ta und W. Nur in einigen Proben und mit schwacher Linienintensität konnten folgende Elemente nachgewiesen werden: Ni, Ag, Zn, Ga, Ge, Sn, Pb, As, Be, Y, La, Ce, V, Mo und P. Vonden letzteren sind mit stärkerer Linienintensität in der Kohlenasche als im Bergmittel vertreten, oder ausschliesslich in der Kohlenasche konzentriert: Ni, Ag, Zn, Ga, Sn, As, Be, V und Mo.

In variierender, doch kleiner Konzentration sind sowohl in der Asche als auch in den Gesteinsproben folgende Elemente zu finden: Co, Cu, Li, Sr, Ba, Ti, Zr, Cr, Mn und B. Davon sind gewöhnlich nur Co und Ba mit grösserer Intensität vertreten. Die nachweisbare Konzentration von Cu ist dagegen in jedem Falle im Bergmittel grösser als in der Asche. Ist der Cu-Gehalt in letzterer 10 bis 60 g/to, so reicht seine Grösse im Bergmittel (in den Gesteinszwischenlagerungen) von 60–100 g/to bis 600 g/to.

Gegenüber unserer früheren Annahme (Á. Grossz, 1967) kann keine generalisierbare Gesetzmässigkeit in der räumlichen Verteilung der Spurenelemente wahrgenommen werden. Was diesbezüglich überhaupt zu beobachten ist, kann auf den biophilen Charakter der Elemente zurückgeführt werden. Dies kommt dadurch zum Ausdruck, dass einige Elemente sich ausschliesslich in der Kohlenasche, andere hingegen in den Gesteinszwischenlagerungen konzentrieren. Zugleich ist es auffallend, dass das Kupfer immer an diese letzteren gebunden ist.

In einem früheren Aufsatz (Á. Grossz, 1967) haben wir bereits auf die ungewöhnlich hohe Konzentration von Sr und Ba aufmerksam gemacht. Auf Grund der untersuchten 40 Proben (13 Aschen- und 27 Gesteinsproben) haben wir nachgewiesen, dass der durchschnittliche SrO-Gehalt der 13 Aschenproben 0,76%, während jener der ohne Auswahl genommenen Gesteinsproben 0,9% war. Der Durchschnitt des SrO-Gehaltes der ausschliesslich kalkig-mergeligen Gesteine erreichte jedoch 0,9%. Dabei – anhand von verhältnismässig wenigen Angaben – haben wir eine eindeutige Korrelationsbeziehung zwischen Ba und Sr vermutet. Auf Grund der vollständigeren Untersuchungsangaben lässt sich folgendes feststellen.

Obwohl in den kalkigen Aschen- und Gesteinsproben die Menge von Sr – welches hie und da isomorphe Verdrängung durch Ca aufweist –

veränderlich ist, kann Ba am häufigsten in einer Konzentration von 0,04 bis 0,06% oder in seltenen Fällen von 0,1% nachgewiesen werden. Auf dieser Grundlage können wir feststellen, dass Ba in keiner Korrelationsbeziehung mit Sr steht.

Nach den Analysen der 118 Aschen- und Gesteinsproben der Braunkohlenserie erreicht der SrO-Gehalt der Proben im Durchschnitt 1,43%. 77 Aschenproben enthalten 1,5% SrO, 41 Gesteinsproben 1,3% SrO. Lässt man die Sr kaum enthaltenden klastischen, tuffogenen Bildungen von den Berechnungen aus und analysiert man ausschliesslich die kalkig-mergeligen Gesteine auf SrO, so ergibt sich für 32 Gesteinsproben ein Durchschnittswert von 1,6%.

Wenn wir die Untersuchungsangaben für die einzelnen Bohrprofile zusammenfassen, so kommen wir zur Schlussfolgerung, dass keine regelmässige Veränderung in der Konzentration von Sr nachweisbar ist. Sowohl in den Proben der – vom Liegenden bis zum Hangenden bemusternten – Bohrungen, als auch in jenen der Grubenprofile lassen sich äusserst variierende Sr-Konzentrationswerte beobachten. Eine ausgeprägte Regelmässigkeit ist jedoch in horizontaler Richtung zu beobachten. Die 22 Gesteins- und Aschenproben der am nördlichsten gelegenen Bohrung (H-88) enthalten 0,77% bzw. 0,78%, die 27 Proben der am südlichsten gelegenen Bohrung (H-91) 1,2% bzw. 2,3% SrO.

Die nordwärts abnehmende Konzentration des Sr-Gehaltes der Braunkohlenserie ist ein Beweis dafür, dass das Sr aus den durch einen höheren Sr-Gehalt bezeichneten Graniten des kristallinen Grundgebirges im Vorlande des Braunkohlenbeckens von Hidas herzuleiten ist. Diese Feststellung ist besonders durch die Untersuchungen von G. y. B u d a bekräftigt, der in den Feldspäten des Granits einen Sr-Gehalt von 400 bis 600 g/to nachgewiesen hat.

Als eine wesentliche Abweichung von unseren vorhergehenden Untersuchungsergebnissen kann festgestellt werden, dass auf Grund von 109 Proben die Durchschnittskonzentration von SrO 1,53% ist. Aus diesem Grunde kann der untersuchten Kohlenserie auch wirtschaftsgeologisch eine grössere Bedeutung beigemessen werden.

Entstehungsbedingungen und Moor-Sumpf-Verhältnisse

Auf Grund der eingehenden Untersuchung der Braunkohlenflöze können die Moor-Sumpf-Verhältnisse der einzelnen Flöze und die Umstände der Entstehung der Braunkohlenserie geklärt werden. Aus einer Summierung der Untersuchungsergebnisse leuchtet es hervor, dass in der Anfangsphase der Entstehung der Kohlenserie (vor allem des Flözes VII und in kleinerem Masse des Flözes VI) der noch mobile Beckenuntergrund Oszillationsbewegungen erlitten hat, die sogar innerhalb kleinerer Räume veränderliche Intensität aufwies. Das ist vermutlich auf die Regression zurückzuführen, welche auf die neritischen Ablagerungen des Kohlenliegenden folgte. Infolge der unterschiedlichen Oszillationen des mobilen Beckenuntergrundes scheint die Kohle in den beiden Flözen

in äusserst unregelmässig variierender Ausbildung, in verschiedenen Moor- und Sumpfbzonen entstanden zu sein. Das Auftreten von verschiedenen Moorwald-, Flachmoor- und stellenweise auch Tiefmoor-Fazies konnte sogar auf einer Horizontaldistanz von 100 bis 200 m nachgewiesen werden.

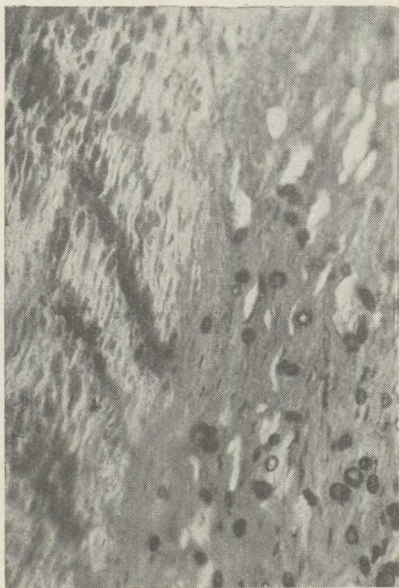
Die sich auf kleinerer Distanz äussernde Intensität der Oszillationen verschwindet im mittleren Abschnitt der Kohlenserie, und zwar in den Ausbildungen des Flözes V und noch ausgeprägter im Flöz IV. In diesen Flözen herrschten nämlich in der Regel identische Moor-Sumpf-Verhältnisse in einem grösseren Raum. Davon zeugt die Tatsache, dass diese Flöze in grosser räumlicher Verbreitung einheitlich ein gemischtes Xylit-Periblinnit-Kohlengestein bzw. Xylit und Periblinnit enthalten. Dabei sind sie auch hinsichtlich ihrer kohlenchemischen Beschaffenheiten beinahe homogen und weisen die geringste Veränderlichkeit auf.

Für den Oberteil der Kohlenserie (Flöze III, II und am anschaulichsten für das Flöz I) ist – den unteren Flözen ähnlich – eine häufige Veränderung der Moor-Sumpf-Verhältnisse charakteristisch, d. h. sogar innerhalb kleinerer Gebiete können äusserst unterschiedliche Fazies, Kohlengesteinstypen beobachtet werden.

Während also die Entstehungsverhältnisse der beiden mittleren Flöze (IV und V) der Kohlenserie durch die Gleichheit der Moor-Sumpf-Verhältnisse auf grösserer Distanz und dementsprechend auch durch horizontal identische Kohlengesteinstypen gekennzeichnet sind, können die Fazies der beiden unteren, sowie der oberen Flöze – infolge der sich auf kleineren Distanzen äussernden, lokalen Oszillation – durch den häufigen Wechsel der Moor-Sumpf-Verhältnisse charakterisiert werden. Die lokalen Oszillationen in der Basis der Kohlenserie können als Resultat der auch für die Entstehung von Torfmooren verantwortlichen Regression aufgefasst werden. Dabei ist die Transgression, die sich nach dem Abschluss der Vermoorung einsetzte, als Vorzeichen der beginnenden Absenkung des Beckenuntergrundes zu betrachten.

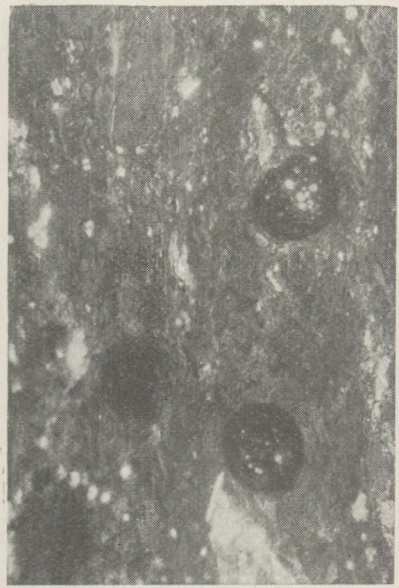
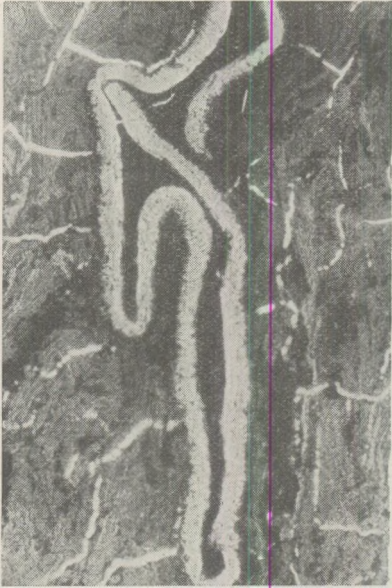
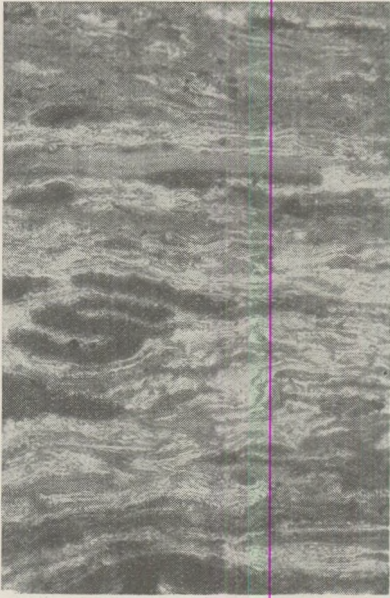
Die Entstehung der verschiedenen Flöze und die Erkenntnis der dafür verantwortlichen Ursachen und Faktoren lassen sich mit den Ergebnissen der Faziesuntersuchungen der Gesteinszwischenlagerungen gut abstimmen.

Ebenfalls anhand der Ergebnisse der Faziesuntersuchungen der Moor-Sumpf-Verhältnisse sowie der Gesteinszwischenlagerungen können die betreffenden Transportrichtungen und Abtragungsgebiete bestimmt und angegeben werden. So war der südliche, südwestliche – und in gewissen Fällen auch der westliche – Teil des Kohlenbeckens von Hidas ein erhobenes Festland, das zugleich als Abtragungsgebiet diente. Dementsprechend erfolgte der Transport der Sedimente vom S-SW bzw. vom W gegen NO-N zu. Das wird auch durch die bei den Spurenelement-Untersuchungen für die Sr-Konzentration erhaltenen Angaben bestätigt.



Tafel I

1. Melanoresinite verschiedenen Oxydationsgrades im Xylit. 125 X
2. Melanoresinitführender Xylit mit Überresten von Markstrahlzellen. 32 X
3. Resinoxylit mit Pilzsporen. 125 X
4. Resinitspindel und Körnchen im gelierten Xylit. 80 X



Tafel II

5. Blätterkohle. 125 X

6. Oxydationsflecken und Kutinit im blätterkohlenführenden Brennschiefer. 200 X

7. Dickrandiger Kutinit und Oxydationsflecken in der gelierten Huminit-Grundmasse. 125 X

8. Vitritdetritische Kohle mit Sklerozium. 80 X

LITERATUR

- Babics, A. (1958): A barnaköszén kutatásának és bányászatának története a Mecsek-hegységben és környékén (Die Geschichte der Erkundung und Förderung der Braunkohle im Mecsek-Gebirge und Umgebung). Dunántúli Tud. Gyűjt. Pécs. Ser. Hist. 10.
- Böckh, J. (1876): Pécs városa környékének földtani és vízi viszonyai (Geologische und hydrologische Verhältnisse der Stadt Fünfkirchen und Umgebung). M. Áll. Földt. Int. Évkönyve. 4. 129–287.
- Böckh, J. – Hofmann, K. (1872–1876): 1 : 28 000-es földtani térképek (Geologische Karten im Maßstab 1 : 28 000). M. Áll. Földt. Int. Térképtára.
- Buda, Gy. (1968): A Mecsek- és Velencei-hegység gránitoid kőzetek földpátjainak vizsgálata (Untersuchung der Feldspäte der Granitoid-Gesteine des Mecsek- und Velence-Gebirges). Egyetemi doktori értekezés, Budapest.
- Burkov, V. V. – Podporina, E. K. (1926): Stroncij. Izd. Ak. Nauk. SSSR, Moskva.
- Földi, M. (1966): A hidasi terület földtani felépítése (Geologischer Bau der Lagerstätte Hidas). M. Áll. Földt. Int. Évi Jel. 1964. 93–111.
- Földi, M. (1967): A hidasi fúrások malakológiai feldolgozása (Malakologische Bearbeitung der Bohrungen von Hidas). M. Áll. Földt. Int. Évi Jel. 1964.
- Grossz, Á. (1966): A hidasi barnaköszén összlet nyomelemeinek eloszlása (Verteilung der Spuren elemente in der Braunkohlenserie von Hidas). Földt. Közl. 96. 4. 436–440.
- Grossz, Á. (1967): Strontium concentration and distribution of trace elements in the Lignite of Hidas. Acta Geol. Ac. Sci. Hung. 11. 1–3. 253–259.
- Grossz, Á. (1967): Geochemische Verteilung der seltenen Elemente im Braunkohlenkomplex von Hidas. Annales, Univ. Sec. Sect. Geol. Budapest. 10. 59–65.
- Gyovai, L. (1962): A hidasi terület összefoglaló földtani jelentése (Zusammenfassender Bericht über die Geologie der Lagerstätte Hidas). Kézirat. Budapest, Közp. Földt. Hiv. Adattára.
- Hámor, G. (1964): A K-i Mecsek miocén képződményeinek vizsgálata (Untersuchung der Miozänablagerungen des östlichen Mecsek-Gebirges). M. Áll. Földt. Int. Évi Jel. 1961. 109–117.
- Hantken, M. (1878): A Magyar Korona Országainak szentelepei és szénbányászata (Die Kohlenlagerstätten und Kohlenförderung der Länder der Ungarischen Krone). Budapest. 90–139.
- Haraszthy, Á. (1957): Die mikroskopischen Untersuchungen der Xylite von Hidas. Annales Univ. Sci. Sect. Biol. Budapest. 71–87.
- Hofmann, K. (1907): Adatok a pécsi hegység geológiájához (Beitrag zur Geologie des Fünfkirchner Gebirges). Földt. Közl. 37. 111–116.
- Juhász, A. (1967): Vegyes és szerves eredésű üledékes kőzetek nevezéktanának kérdései (Fragen der Nomenklatur von Sedimentgesteinen gemischter und organischer Herkunft). Földtani Kutatás. Budapest. 10. 4. 6–15.
- Kegel, K. (1948): Brikettierung der Braunkohle, Berg- und Aufbereitungstechnik. Band 4. Aufbereitung und Brikettierung, Teil 1. W. Knapp. Halle. 3. 358.
- Kirchheimer, Fr. (1957): Die Laubgewächse der Braunkohlenzeit. Halle/Saale.
- Kokán, J. (1874): Hidasi kövületek (Die Fossilien von Hidas). Földt. Közl. 4. 250.
- Meznerics, Cs. I. (1950): A hidasi tortónai fauna (Die tortonische Fauna von Hidas). M. Áll. Földt. Int. Évk. 39.
- Nagy, L-né (1962): Reconstructions of vegetation from the eastern Mecsek mountains on the strength of palynological investigations. Acta Botanica. Budapest. 8. 319–328.
- Noszky, J. (1953): A Mecsek hegység ÉK-i szegélyének földtani vázlata (Geologische Skizze des Nordostrandes des Mecsek-Gebirges). M. Áll. Földt. Int. Évi Jel. 1950. 145–151.
- Peters, K. F. (1862): Die Miozän-Localität Hidas bei Fünfkirchen in Ungarn. Sitzb. 6. 44. 581–617.
- Rammer, E. – Bilkenroth, G. (1954): Über die Zusammenhänge zwischen Brikett- und Koksigenschaften bei der Braunkohlenhochtemperaturverkokung. Freiberg. Forschungshefte. A. 24. Brikettierung Technische Braustoffverwertung. 32–46.

- Strausz, L. (1926): A Mecsek hegység mediterrán rétegei (Die mediterranen Schichten des Mecsek-Gebirges). Budapest. Mat. és Term. Tud. Ért. 43. 177–180.
- Strausz, L. (1942): Adatok Baranya geológiájához (Beitrag zur Geologie von Baranya). Földt. Közl. 72. 181–192.
- Szádeczky, K. E. (1952): Szénkőzetan (Kohlenpetrographie). Budapest.
- Szádeczky, K. E. – Földvári-Vogl, M. (1955): Geokémiai vizsgálatok magyarországi kőszenek hamuin (Geochemische Untersuchungen an ungarischer Kohlenasche). Földt. Közl. 85. 7–43.
- Szádeczky, K. E. – Soós, L. (1964): Barnakőszenek szénkőzetani gyorselemzése és a lépöves rendszer (Kohlenpetrographische Schnellanalyse von Braunkohlen und das Moorzonensystem). Budapest. Akadémiai Kiadó.
- Vadász, E. (1912): Földtani vázlat a Mecsek hegység K-i részéről (Geologische Skizze des Ostteiles des Mecsek-Gebirges). Földt. Int. Évi Jel. 1910. 69–73.
- Vadász, E. (1936): A Mecsek hegység (Das Mecsek-Gebirge). Budapest. Magyar Tájak Földtani Leírása I.
- Vadász, E. (1952): Kőszénföldtan (Kohlengeologie). Budapest.
- Vitális, I. (1939): Magyarország szénelőfordulásai (Die Kohlenlagerstätten Ungarns). Sopron.
- Vitális, S. (1946): Magyarország kőszén- és tőzegkészlete (Die Kohlen- und Torfvorräte Ungarns). Magyar Technika. 1. 6. 210–214.
- Vitális, S. (1947): Jelentés a hidasi lignitterületről (Bericht über das Lignitgebiet von Hidas). Kézirat. ELTE Alk. Földt. Tanszék Adattára.
- Wein, Gy. (1949): A hidasi lignitterület (Das Lignitgebiet von Hidas). Kézirat. M. Áll. Földt. Int. Adattára.
- Wein, Gy. (1966): Magyarázó Magyarország 200 000-es földtani térképsorozatához (Erläuterungen zur geologischen Karte Ungarns, Maßstab 1 : 200 000). Budapest. L. 34. XIII. Pécs.

CONSTITUTION MINÉRALOGIQUE ET GENÈSE DU GISEMENT URANIFÈRE DE LA MONTAGNE MECSEK (II.)

par
J. KISS

(Institut de Minéralogie, Faculté des Sciences, Université L. Eötvös, Budapest)

(Reçu: le 15. 6. 1961)

Introduction

La présente communication est la continuation de l'étude publiée en 1965 (Ann. Univ. Sci. Bp. Eötvös, IX, 1965, pp. 139–188) sur la constitution minéralogique du gisement uranifère de la Montagne Mecsek. Dans le présent ouvrage on présente les résultats des examens géochimiques, sédimentologiques et litologiques concernant le dit gisement, effectués entre 1957 et 1961. Les explorations postérieures de grande envergure, ont, en effet, apporté des preuves à la genèse présumée, en la complétant par de nombreux détails. P. e., l'enrichissement d'uranium par des solutions venant de l'aire de dénudation semble avoir joué un rôle plus grave.

Sommaire

1 — *L'enrichissement en uranium dans le complexe de minérai uranifère permien de la Montagne Mecsek représente, à côté des detritus d'oxydes d'uranium, un type sédimentaire oxydé et silicaté, lié principalement aux micas épigéniques (chromifères et potassiques).*

2 — *La mode d'apparition des minéraux d'uranium, les formations épigéniques-descendantes, et la présence décisive des micas chromifères et potassiques justifient de considérer la formation uranifère psammitique de la Montagne Mecsek comme un type indépendant de minérai d'uranium sédimentaire. Peu de gisements semblables sont connues dans la littérature mondiale.*

3 — *L'uranium est accompagné, d'un façon remarquable, par des éléments vanadium et germanium. En vertu de ce fait, le gisement uranifère de la Montagne de Mecsek doit être considéré un gisement combiné des éléments U—V—Ge. Étant donné que leurs concentrations sont considérables (330 à 950 ppm pour le vanadium et 1 à 10 ppm pour le germanium), ils pourront être exploités dans l'avenir.*

4 — *On ignore la forme minéralogique du vanadium et du germanium.*

5 — *L'absence d'une zone d'oxydation du gisement et la présence sporadi-*

dique des minéraux secondaires d'uranium sont dues aux solutions hydrocarbonatées du Ca et du Mg, et à la quantité réduite des ions $(PO_4)^{3-}$; $(AsO_4)^{3-}$; $(VO_4)^{3-}$, etc.

6 — La genèse du gisement uranifère est double: il s'est formé de l'uranium libéré par la décomposition physico-chimique d'une formation à Bi—Co—Ni d'une part, et des roches granitoïdes et d'autres roches métamorphiques et magmatogènes de l'autre, en précipitant dans le milieu réductif de la sédimentation de l'eau stagnante, marécageuse d'un delta.

1. Position stratigraphique du complexe uranifère

D'après Böckh (1876), le Permien de la Montagne Mecsek se compose d'une série bipartite, qui représente le Permien inférieur et celui supérieur. Vadász (1909) préfère la subdivision tripartite; les deux parties inférieures correspondraient au Permien inférieur et moyen, tandis que le cycle regressif, à partir des conglomérats du Mont Jakabhegy, est attribué au Permien supérieur.

Le membre inférieur du Permien consiste, d'après V a d á s z, entre Cserkút et Boda, en grès vert grisâtre, localement rouge brunâtre, à grains gros, meuble, aux intercalations des schistes argillacés rouges, des schistes à plantes fossilisées, et des grès de type arkose. Dans la zone Cserkút—Kővágószőlős—Töttös les troncs d'arbre silicifiés sont fréquents à trouver. Il s'agit, selon les études de Heer et d'après la révision faite par Tuzson, des Araucarites; ils indiquent le Permien supérieur.

Le membre Permien inférieur passe insensiblement aux conglomérats composés de galets de gneiss, phyllite, granit, et de porphyre quartzifère. Ceux-là se rejoignent vers le Nord et le Sud, au membre inférieur, qui fut identifié par Böckh et Vadász avec le «verrucano» alpin. Là-dessus se trouvent les grès et conglomérats du Mont Jakabhegy, dont le complexe supérieur, argileux et gypsifère, passe graduellement au complexe du Trias inférieur, daté par la faune y trouvée.

B a r a b á s (1956), se fondant sur les données fournies par les sondages et les affleurements artificiels, en tenant compte de la subdivision tripartite établie par V a d á s z, y distingue des détails plus fins.

Voici la caractéristique lithologique de la séquence permienne (basée sur les données fournies par B a r a b á s (1956):

a) Permien inférieur

Argile schisteuse, grès fin, siltite, marne argileuse rouge, rouge — brunâtre, marne dolomitique et porphyre quartzifère. La puissance totale varie de 300 à 600 m. Dans les argiles schisteuses et dans les siltites il y a des noeuds carbonatés, bandes de dolomie microstratifiée, jouant, par endroits, le rôle du ciment.

b) Permien moyen

La série précédente est suivie, d'abord, par un banc gréseux, très différent du point de vue sédimentologique et lithologique: grès gris

clair et gris verd tre, aux stries de gr s rouge. La-dessus repose un banc de conglom rat gris. L' paisseur de chacun de ces deux bancs varie de 0,5   3,0 m. Ils constituent le d but ou la base d'une s rie de 500   700 m de puissance.

S rie bigarr e

Cette s rie consiste en gr s d tritique rose, gr s gris verd tre, gr s fin intercal , conglom rats rose ou gris, surmont s par des argiles schisteuses, gr s gris et verts, gr s grossiers et gr s verts, qui alternent   plusieurs reprises. Si l'on consid re la succession chronologique, la s rie bigarr e se compose des vari t s lithologiques suivantes: au-dessus du siltite on trouve des gr s fins dont les grains rev tent souvent une teinte verd tre, ce qui repr sente le passage vers la s rie verte. Plus haut, on rencontre des gr s fins aux plagioclases acides (avec la pr dominance de l'oligoclase), qui passe aux gr s brun tres,   grains moyens et grossiers. La partie sup rieure se compose des gr s   teinte verd tre, passant aux gr s vert, vert gris tre, susjacents. Les gr s inf rieurs sont caract ris s par la rar faction successive des feldspaths acides (oligoclase), qui sont graduellement remplac es par d'orthose et microcline, accompagn s par des fragmens de porphyre quartzif re et de quartzite. Les gr s vert, vert gris tre, sont pratiquement d pourvus d'uranium. Ils renferment des bancs rouges,   orthose, de type arkose. Encore plus haut, on trouve un complexe gris, un peu verd tre, caract ris  par la pr sence des feldspaths blancs, l g rement s ricitifi s et carbonatis s (orthose, oligoclase). Dans celui-ci les troncs d'arbre silicifi s et dolomit s, les stries et les lentilles de houille, et des empreintes de foug res ne sont pas rares.

Le complexe sus-mentionn  passe, sans aucun changement observable du faci s, aux gr s vert, gris verd tre du complexe uranif re, qui comprend des intercalations minces (de quelques cm   quelques m) du gr s rouge («gr s rouges intercal s»). Au sommet de ce complexe reposent des d p ts chimiques, d'origine aquatique, d'aspect p litique, par leur nature dolomitique-ank ritique. Dans ce complexe p litique-carbonat  on trouve des concr tions de forme caract ristique, ainsi que des spores et pollens indiquant le Permien sup rieur: *Nuskoisporites dulhunty* R. Pot. et Klaus, *Florinites* sp., *Loeckisporites virkkiae* R. Pot. et Klaus, *Pityosporites delasouci* R. Pot. et Klaus (D e   k, 1960). Les s diments de ce faci s sont d pos s, semble-t-il, dans un secteur stagnant pauvre en oxyg ne, du bassin s dimentaire, o  n' taient apport s que des suspensions et le d bris organique,   poids sp cifique peu  lev . Dans ce complexe par endroits se trouvent des stries de houille, empreintes de feuilles carbonis es, et troncs d'arbres. L'enrichissement en lentilles d'uranium dans le complexe uranif re se laisse subdiviser en trois parties:

-  ) *Le faisceau inf rieur est d'un d veloppement tr s capricieux et d'une teneur en uranium peu  lev e;*

- β) Le faisceau moyen ou principal, une minéralisation à plusieurs lentilles. Dans le champ du Nord-ouest il est plus homogène, et il s'y compose des lentilles à concentration plus élevée; dans le champ du Sud, il est constitué par des lentilles tectoniquement dissectées tant au sens vertical qu'horizontal.*
- γ) Faisceau supérieur, capricieux comme celui inférieur, mais à un enrichissement localement beaucoup plus considérable.*

Les roches encaissantes des lentilles, au dedans du complexe uranifère, possèdent une teneur en uranium à un ou deux ordres de grandeur plus élevées, si l'on compare avec les concentrations observées dans la série grise sous-jacente ou dans le grès rouge du toit (grès intercalé, grès du Mont Jakabhegy).

c) *Permien supérieur*

Au-dessus du Permien moyen, dont le membre terminal est le complexe gréseux, vert, uranifère, reposent les conglomérats et grès rouges du Mont Jakabhegy, subdivisés par Barabás (1956) en deux membres; dont l'un montre une stratification arquée, et l'autre — une stratification diagonale. La partie supérieure de celui-ci, gypsifère et par endroits cuprifère, passe insensiblement au Trias inférieur marin.

La subdivision tripartite de la séquence permienne de la Montagne Mecsek (Permien inférieur, moyen et supérieur) est basée uniquement sur les différences lithologiques; donc elle n'est pas complètement justifiée. Aussi Vadasz (1909) lui-même indique des incertitudes y relatives. Le problème se pose, si elle soit nécessaire et soutenable?

Tableau 1

Le Permien de la montagne Mecsek

Étage	D'après E. Vadasz, 1957	D'après A. Barabás — J. Kiss, 1958
Thuringien	Complexe d'évaporites à développement local (gypse, anhydrite). Grès rouge à stratification diagonale et arquée	Grès à stratification diagonale, à peu de feldspaths
Saxonien	Complexe pséphitique à grains grossiers et plus fins	a) Grès rouge fluviatile, à une quantité moyenne de feldspaths b) Conglomérat gros, fluviatile c) Grès (arkose) lacustre d) Grès gris-vert, lagunaire, à grès rouge intercalé
Autunien	Grès jaune-gris-vert, conglomérat à grains fins, à lentilles de houille, plantes carbonisées, à troncs d'arbres silicifiés. Grès rouge clair meuble, argile sableuse rouge, Porphyre quartzifère	Marne dolomitique marine, siltite, schiste argileux, lava, dyke et pyroclastite de porphyre quartzifère

Avec la prise en considération les données paléobotaniques et lithologiques, le Permien de la Montagne Mecsek se laisse subdiviser en deux étages (inférieur et supérieur), sans aucune modification importante de la subdivision tripartite proposée par *Vadász* et adoptée par *Barabás*.

a) Le membre inférieur représente le Permien inférieur; b) le membre moyen à plantes fossilisées correspondrait au Permien supérieur, tandis que le «membre supérieur», (les grès et conglomérats du Mont Jakabhegy, qui débutent par des dépôts continentaux et passent concordamment aux sédiments marins), peut être identifié avec le Trias inférieur.

Voilà la subdivision proposée:

Trias inférieur

- A) Trias inférieur fossilifère (à *Pseudomonotis* sp.)
- B) Complexe gypsifère
- C) Grès rouge du Mont Jakabhegy, fluviatile, de type delta;
- D) Conglomérat grossier

Permien supérieur

- A) Grès rouge intercalé, complexe uranifère, à lentilles de houille, troncs d'arbre, empreintes de fougères, troncs d'arbre dolomités, pollens indiquant le Zechstein;
- B) Paquet des grès gris, gris-verdâtre, à troncs d'arbre silicifiés, et d'autres empreintes de plantes (groupe d'*Araucarites*);
- C) Groupe des grès bariolés (sédimentation inquiète), dont la puissance atteint 150 à 200 m au champ du Nord, et 200 à 300 m dans le champ du Sud.
Conglomérat (0,5 – 3,0 m)

Permien inférieur

Grès fin, siltite, argile schisteuse, marne argileuse rouge et brune, dont l'épaisseur varie entre 300 et 500 m.

Paléozoïque plus ancien

Granit et roches métamorphisées.

* * *

La séquence permienne peut être interprétée donc comme le produit d'un cycle de transgression bi-rythmique, dont la phase première (Permien inférieur) a déposé le complexe à siltites, caractérisé par des silicopélites, jusqu'à l'apparition du banc conglomératique (0,5 – 3,0 m).

Avec ce conglomérat débute une sédimentation nouvelle, une transgression inachevée dont les roches variées, pséphitiques-psammitiques, indiquant des oscillations du fond, représentent les dépôts du cycle sédimentaire du Permien supérieur.

Avec le conglomérat grossier du Mont Jakabhegy débute un nouveau cycle sédimentaire, qui dépose des sédiments psammitiques d'origine

fluviatile et deltaïque aux évaporites dues aux inondations marines temporaires. Il passe insensiblement à la séquence transgressive du Trias inférieur de la Montagne Mecsek.

On a déjà aperçu que le complexe uranifère se trouve dans la partie supérieur du membre moyen (d'après V a d á s z), donc selon la subdivision proposée par l'auteur, dans la partie supérieur du Permien supérieur.

Le membre moyen du Permien (= Permien supérieur) lui-même est aussi tripartite, si l'on considère les caractéristiques lithologiques. En dépit de certaines recurrences dues aux accidents tectoniques et aux événements répétés de sédimentation, la subdivision en trois parties est significative. La partie inférieure est pauvre en feldspaths, même pratiquement dépourvue de feldspaths; dans la partie moyenne on observe l'apparition des plagioclases intermédiaires-basiques (andésine, labrador); dans la partie supérieure c'est l'oligoclase et l'orthose qui s'enrichissent, à côté des galets de porphyre quartzifère.

Les feldspaths du grès gris, gris-verdâtre sont en général de couleur blanc. Les plagioclases intermédiaires-basiques s'enrichissent de nouveau. La couche inférieure du complexe uranifère (grès vert) est du type arkose, caractérisée par la présence des plagioclases acides (oligoclase) et de l'orthose. Vers les faisceaux principal et supérieur l'oligoclase va à perdre son importance, cédant son rôle à l'orthose et ses variétés (orthose-microcline pertithique), tandis que le faisceau supérieur est caractérisé par des grès du type arkose, constitué principalement de l'orthose. Entre certaines lentilles du faisceau principal, dans le champ du Sud et celui du Nord, dans le complexe du grès vert s'est développé un banc pséphitique à orthose, de plusieurs centimètres en épaisseur; celui-ci, qui ressemble au granite porphyroïde, peut renfermer les orthoses des noeuds pegmatitiques également (arkose basal).

Le débris du quartz métamorphisé ou magmatogène montre une répartition caractéristique en sens vertical. Les zones plus basses sont caractérisées par le débris d'origine métamorphique; dans la « roche-mère » du faisceau principal les quartz métamorphiques et magmatiques sont présents ensemble; puis dans le faisceau supérieur c'est le quartz magmatique qui devient prépondérant.

Les faciès lithologiques esquissés plus haut, la distribution des feldspaths et les divers quartz, reflètent très bien l'évolution de ce membre permien, en fonction de la composition pétrographique de l'aire de dénudation: *la partie inférieure de la série (grès gris) est le produit des roches métamorphisées, tandis que le complexe du grès vert (uranifère) est le produit mixte de la décomposition des roches métamorphisées et granitoïdes. Cette différence se manifeste dans la distribution des éléments des roches pséphitiques-psammitiques, ainsi que dans la nature des minéraux d'uranium. Le membre inférieur de la série est riche en substances organiques, et pauvre en uranium. Les membres moyen et supérieur, psammitiques sont caractérisées, outre la teneur élevée en substances organiques, par la concentration considérable de Cr, U et V. La partie supérieure de la série est pauvre en sub-*

stances organiques ou bien totalement anorganique, et elle revête un coloris plus expressément rouge, produit par la présence remarquable des ions Fe^{3+} . (Fig. 2.)

2. Les caractéristiques sédimentologiques du complexe uranifère et des corps minéralisés

Les échantillons soigneusement récoltés ont été étudiés d'une façon multilatérale, au but d'éclaircir les conditions géochimiques et de dépôt.

Tout d'abord on a établi la granulométrie, qui a beaucoup contribué à la connaissance de l'aire de dénudation et de la direction de l'apport des matériaux.

Les roches psammitiques se composent, en prédominance, des grains à un diamètre inférieure de 0,5 mm. Par endroits on y trouve des remplissages «à sac» plus grossiers, intercalés, qui se laissent distinguer très bien, même à l'œil nu.

Leur interprétation s'appuie sur deux phénomènes indépendants:

a) Sur le fond tranquille, moins agité et ondulé du bassin les courants d'eau véhéments ont apporté et déposé des particules plus grossières.

b) De pareils remplissages grossiers peuvent se produire sur le fond très accentué du littoral fortement attaqué par les ondes, qui sont brisées au-dessus de ces dépressions ou sacs, passent aux mouvements turbulents, en centrifugant les particules plus fines, n'y laissant que celles plus grossières. Cette explication-ci peut être exclue, pour la plupart des cas, par le caractère fluvial des sédiments. Il serait peu vraisemblable de supposer une explication par fracturation tectonique.

L'échantillonnage a été fait, dans tous les deux champs minéralisés, aux intervalles égaux, en y ajoutant des échantillons supplémentaires pris à tous les changements lithologiques observables à l'œil nu. Le matériau des lentilles de minéral a été examiné séparément.

On a fait les examens suivants sur les roches uranifères et encaissantes:

- a) granulométrie des particules clastiques, par tamisage et par la pipette de Köhn;
- b) établissement de la teneur en carbonates par la méthode de Scheibler;
- c) dosage chimique quantitative des éléments U, V et Cr;
- d) dosage spectrographique semi-quantitative des éléments de trace;
- e) détermination du rapport U^{4+}/U^{6+} à partir des données d'analyse.

La composition granulométrique a été déterminée, après l'ameublissement de la roche, par la pipette de Köhn; pour les roches minéralisées, par tamisage. L'ameublissement consistait dans un traitement par la solution concentrée de $MgSO_4 \cdot 7 H_2O$, produisant, sauf quelques cas, la désintégration totale de l'échantillon. Cette méthode s'est prouvée plus efficace que le procédé de congélation ou celui de l'ultrason. Les grès à ciment siliceux ont été traités par acide hydrochlorique. La quantité dissolue du ciment a été ajoutée à la fraction la plus fine. Bien entendu, il est impossible d'aboutir à une désintégration parfaite. Donc on a véri-

fié, sous microscope, le pourcentage des grains agrégés. Si cela ne dépassait pas le 1%, on a modifié les pourcentages des fractions granulométriques par l'indice de correction établi par méthode statistique, en faveur des fractions plus fines. Dans le cas contraire, on a répété le traitement par acide pour arriver à un degré acceptable de désaggrégation, ce qui permet l'application de la correction mentionnée.

Les valeurs granulométriques sont représentées en histogrammes, pour le profil entier du complexe uranifère, à partir du mur jusqu'au toit. On a étudié la distribution verticale des fractions individuelles. Tout cela était confronté avec les variations dans la teneur moyenne en uranium de la roche.

De l'évaluation de la distribution granulométrique, on peut tirer les conclusions générales comme suit:

α) Complexe uranifère du champ du Nord, sauf les lentilles de minéral (Fig. 1a).

a) Le faisceau supérieur s'est développé, avec peu d'exceptions, dans des roches psammitiques caractérisées par la distribution à trois maximums des sédiments fluviatiles proche au delta, avec une éventuelle modification causée par des phénomènes de torrent.

b) Les roches encaissantes du faisceau principal consistent en grès à deux maximums granulométriques. Une distribution à trois maximums ne se trouve qu'aux niveaux supérieurs et inférieurs du faisceau principal.

c) Les psammites du faisceau inférieur à trois maximums ressemblent à la roche-encaissantes des lentilles supérieures, reflétant une sédimentation inquiète.

Le faisceau principal du champ du Nord revêt expressément un caractère fluviatile. Les lentilles, à concentrations en uranium moins élevées des faisceaux supérieur et inférieur semblent plutôt d'être déposées dans des deltas. La question se pose: le milieu fluviatile est-il un facteur indispensable pour l'accumulation sédimentaire de l'uranium, ou bien il ne s'agit que d'une connexion par hasard de la situation géomorphologique et de la sédimentation?

Le rapport entre la distribution granulométrique et la teneur en uranium des roches encaissantes est frappant (Fig. 1a). Presque tous les échantillons à deux maximums ont une teneur en uranium plus élevée, tandis que dans les échantillons à trois maximums, l'uranium tend à décroître.

En comparant la distribution verticale des fractions granulométriques avec la variation de la teneur en uranium on constate pour les fractions de 0,5 mm et 0,1–0,05 mm un rapport inverse. Pour la fraction plus fine de 0,05 mm, par contre, un rapport direct est établi.

Ces liens sont difficiles à interpréter. Néanmoins on essaie de les éclaircir comme suit.

a) Le rapport inverse observé pour les fractions relativement plus grossières (0,5–0,05 mm) peut être dû, en partie, à la «substitution de grains»:

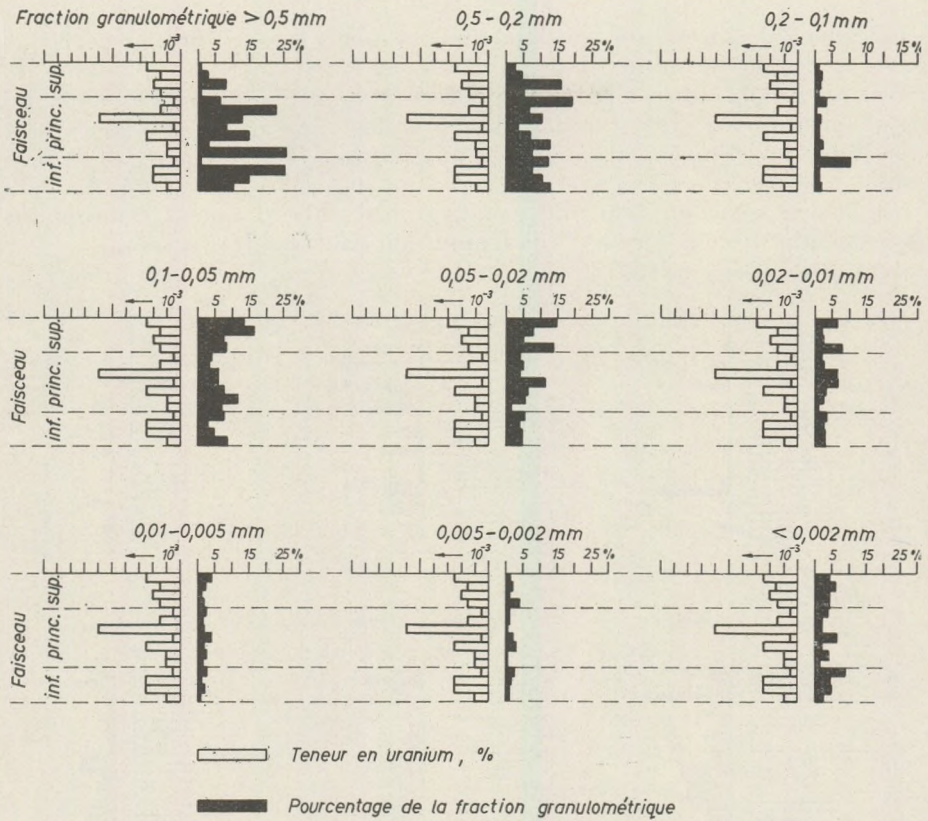


Fig. 1a. Le rapport entre les fractions granulométriques du complexe uranifère et la teneur en uranium (sauf les lentilles de minérai) (Champ du N).

une partie des grains plus fins est remplacée par l'uranium dissolue par l'acide. En général ces échantillons ne renferment de débris de minérai d'uranium qu'en quantité subordonnée.

b) Le rapport direct établi pour les fractions plus fines de 0,05 mm est facile à interpréter: on y trouve souvent de la suie d'uranium friable dont le diamètre moyen varie de 0,05 mm jusqu'à <0,002 mm.

Le champ du Nord consiste donc, d'après la distribution granulométrique de la roche encaissante, en dépôts fluviatiles proches au delta.

β) Complexe uranifère du champ du Sud (Fig. 2a)

La roche encaissante du champ du Sud appartient, avec l'exception d'un seul échantillon provenant du faisceau inférieur, au type à trois ou plusieurs maximums, ce qui caractérise les sédiments de delta. Le rapport entre la distribution quantitative des constituants pétrographiques et la teneur en uranium diffère de celui établi pour le champ du Nord. L'échantillon pris de la lentille inférieure, à deux maximums, pratiquement ne

En comparaison avec la distribution granulom trique en coupe verticale, la teneur en uranium se comporte inversement que dans le champ du Nord.

La teneur en uranium varie presque parall lement avec le pourcentage des fractions   un diam tre plus grand de 0,5 – 0,2 mm. Dans les fractions plus fines,   0,2 mm et p litiques, on observe la situation oppos e: un rapport inverse (Fig. 2a).

Les diff rences dans la teneur en uranium et dans la distribution granulom trique s'explique par l'assomption que l'uranium soit apport  au champ du Sud en pr dominance dans solution, et le d bris uranif re n'y jouait qu'un r le subordonn .

Il faut mentionner, que dans ce champ minier on observe des manifestations tr s remarquables de dissolution et de migration  pig niques. C'est pourquoi,   l' tat actuel, on ne peut pas tracer la limite entre les pr cipitations de la «solution primaire» et celle  pig nique. Les observations disponibles   pr sent t moignent en faveur d'une quantit  a priori  lev e des solutions uranif res arriv es dans les d pressions   eau stagnante, du delta mar cageux divis  par des c nes d'alluvion.

Le mat riau des lentilles de min rai est compos  des constituants plus grossiers, tr s bien observables   l'oeil nu. La forme «dentiforme» ou «en sac» peut  tre attribu e aux conditions trait es plus haut. D'apr s les observations de l'auteur, en g n ral il y a un chapeau argileux   illite dans la partie sup rieure des lentilles ou des sacs de min rai, tandis qu'il manque au-dessus des «sacs» non-uranif res. L'explication plausible s'impose que tous les sacs   grains grossiers avaient  t  uranif res, mais l'uranium ne s'est pas conserv  que dans ceux prot g s par un chapeau imperm able,  tant dissolu dans les autres.

On constate une grande diff rence dans la composition granulom trique des lentilles de min rai entre les champs du Nord et du Sud, respectivement.

Le mat riau des lentilles du Nord est tr s faiblement sorti,   2–3 ou m me plusieurs maximums. Le gr s du toit «st rile» est d'origine fluviatile,   deux maximums. Les lentilles montrent une composition granulom trique plus diff renci e. C'est le type le plus uranif re de la Montagne Mecsek. Le rapport entre la teneur en uranium et les variations de la composition granulom trique n'a pas besoin des explications suppl mentaires.

Les lentilles du champ du Sud sont moins riches en uranium,   une distribution granulom trique plus uniforme;   c t  de la distribution pr pond rante   deux maximums on trouve aussi des  chantillons   un seul maximum. Ces traits lithologiques-s dimentologiques correspondent bien   la conclusion tir e que l'uranium du champ du Sud d rive des solutions uranif res. Les formations uranif res et st riles des champs du Nord et du Sud se sont d pos es, d'apr s les r sultats de l'examen de leurs constituants m caniques, par un transport de NW vers le SE. Le territoire du champ du Nord repr sente, semble-t-il, la partie sup rieur du delta d'une rivi re, pr s d'une baie. Vers le SE, le courant se divisait en plu-

sieurs bras, en formant des crues marécageuses. Alors, dans le champ du Nord, le courant était capable de tenir en mouvement des fragments de minéral à un diamètre de 0,5–à 1,0 mm; par contre, au SE, le courant de moins en moins rapide ne transportait plus que des grains de minéral à quelques mm en diamètre, et la plus grande partie d'uranium était transportée en solution.

3. La teneur en carbonate du complexe uranifère

Dans la communication sur la description et la genèse des minéraux (75) l'auteur a traité, du point de vue minéralogique, les minéraux carbonatés du complexe psammitique, sans entrer dans l'étude du rôle sédimentologique des carbonates et de leur rapport avec la teneur en uranium. (Fig. 3.)

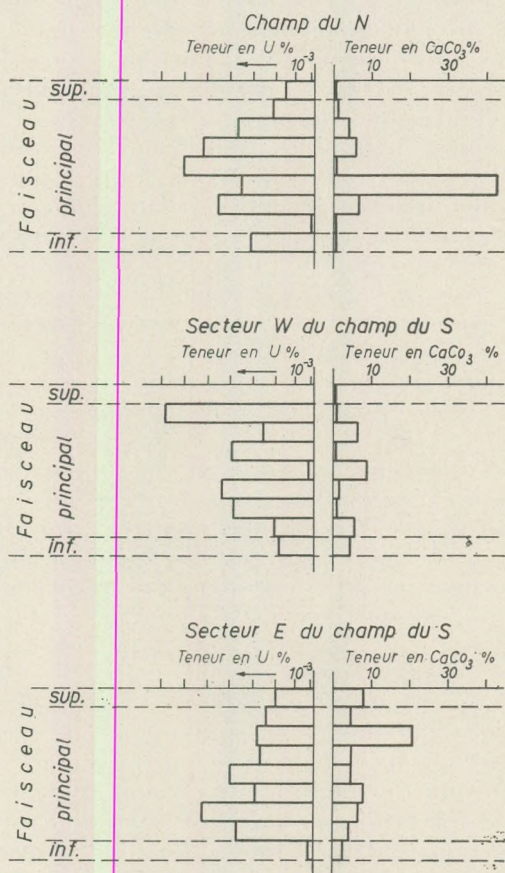


Fig. 3. Distribution en coupe verticale de l'ensemble des carbonates dans les lentilles de minéral par rapport à la teneur en uranium.

La distribution de la somme des carbonates, d termin e par le proc d  de Scheibler, ne r v le aucune r gularit  pour la coupe verticale du complexe uranif re du Nord. Dans le niveau sup rieur du faisceau sup rieur les constituants carbonat s, calcul s sous forme de calcite, sont repr sent s par 1,5%; dans la couche inf rieur du m me faisceau, la valeur correspondant est 0,5–3,5%; du milieu jusqu'au lentilles du faisceau inf rieur: 0,5   8,5%, et dans les lentilles inf rieures: 0   2,0%.

La teneur en carbonates ne montre aucun rapport d finitif avec les concentrations d'uranium et de vanadium, sauf en quelques cas sporadiques, qui peuvent  tre des enrichissements locaux (p. e. l'apparition de la liebigite).

Quant   la distribution des carbonates, de l'uranium et du vanadium dans le complexe uranif re du champ du Sud (Fig. 4) on observe les contours d'une certaine r gularit : la somme des carbonates augmente graduellement,   partir des moyennes peu  lev es (1   9%) trouv es pour le faisceau sup rieur vers le faisceau inf rieur.

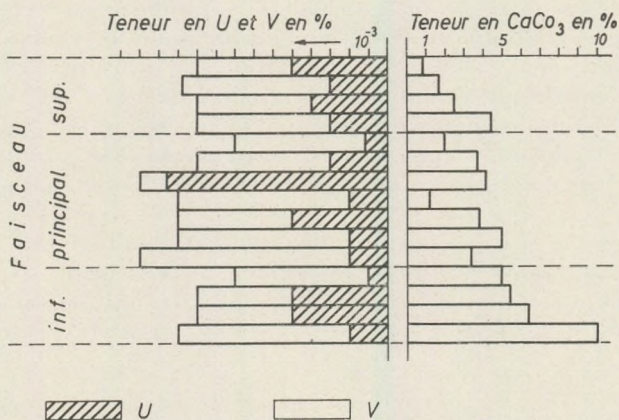


Fig. 4. La teneur en carbonates du complexe uranif re par rapport   l'uranium et au vanadium (Champ du S).

Il existe un rapport entre la somme des carbonates et la teneur en uranium,   partir de la partie inf rieure du faisceau sup rieur jusqu'au niveau sup rieur du faisceau inf rieur. On ne peut pas  tablir un parall lisme semblable avec le vanadium.

Le comportement des carbonates du champ du Sud, tr s oppos    celui observ  dans le champ du Nord, peut  tre d    trois facteurs:

- le r le du bassin s dimentaire assurant un d p t plus tranquille,
- la concentration plus  lev e en substances organiques du milieu,
- l'oxydation progressive des substances organiques et la concentration plus  lev e des ions Ca^{++} , Mg^{++} , Na^+ et K^+ qui lient le CO_2 ;

d) *les roches moins bien sorties et plus poreuses sont mieux infiltrées par des solutions à hydrocarbonates du Ca, du Mg et de l'U.*

La quantité des minéraux carbonatés uranifères est subordonnée. En vertu de ce fait, le rapport entre la somme des carbonates et la teneur en uranium est lié principalement aux phénomènes de dissolution épigénique, dont le rôle sera traité plus bas.

Les roches encaissantes du complexe uranifère sont, en moyenne, moins carbonatées, que les corps minéralisés mêmes. Se fondant sur les valeurs moyennes des analyses, on peut établir la répartition suivante des carbonates (en somme) par rapport à la teneur en uranium, pour les roches encaissantes et pour les lentilles de minéral, dans les deux champs miniers.

Les roches «stériles» du champ du Nord renferment la moitié de carbonates environ, comparées aux lentilles de minéral. La même proportion est valide pour le champ du Sud également, avec la différence que la somme de carbonates dépasse deux fois celle observée dans le champ du Nord.

Le pourcentage des carbonates des lentilles mêmes de minéral, pour tous les deux champs, ne montre aucun parallélisme avec la teneur en uranium, qui soit comparable à celui établi pour les roches stériles du complexe uranifère du champ du Sud, en dépit de la présence de la liebigite dans les lentilles de minéral du champ du Nord. Les deux constituants semblent être complètement indépendents l'un de l'autre dans le cas des concentrations élevées; si tous les deux sont présents en quantité mineure, p.e. dans le champs du Sud, on peut soupçonner l'existence d'un certain rapport entre eux.

La différence caractéristique dans le pourcentage des carbonates entre les deux champs est due à la sédimentation a priori.

En conséquence de la sédimentation plus tranquille, dans le champ du Sud la migration épigénique des solutions uranifères a été plus uniforme et a affecté de plus larges territoires.

4. La répartition des éléments U, Cr et V dans le complexe uranifère (grès vert)

(Le rôle géochimique du vanadium, du chrome et des hydromicas dans l'enrichissement épigénique de l'uranium.)

Les gisements uranifères de la Montagne Mecsek possèdent quelques traits particuliers en ce qui concerne leur aspect sédimentologique et l'association géochimique un peu aberrante des éléments. Les grès vert clair, vert grisâtre, qui représentent le complexe de grès productif, est développé sur un épaisseur plus considérable dans le champ du Nord que dans celui du Sud. Dans tous les deux, il est divisé, vers le faisceau supérieur, par le grès rouge intercalé, qui en représente un faciès substituant. Le complexe est plus homogène dans le champ du Nord, et se laisse plus aisément subdiviser dans le champ du Nord, en unités répétées, bien in-

dividualis es. Un trait commun — outre la coloration vert-grisverd tre — consiste dans le ciment   hydromicas et carbonates (dolomie, ank rite), associ    l'enrichissement d'uranium. Les gr s gris, gris-verd tre du membre inf rieur du complexe uranif re sont riches en substances organiques et pauvres en  l ments radioactifs. Le complexe moyen, dit vert, est caract ris ,   c t  de l'abondance des substances organiques, par la concentration relativement  lev e des  l ments U, V et Cr. Dans les roches encaissantes du faisceau sup rieur (au voisinage du gr s rouge intercal ) on a constat  l'accumulation relative des ions Fe^{3+} , Mg^{2+} et Ca^{2+} , et la pr sence remarquable des feldspaths. Les gr s verts (complexe productif), dont l'uranium, le vanadium et le chrome constituent des composants caract ristiques, ont  t  soumis aux  tudes approfondies, qui ont apport  des r sultats consid rables du point de vue scientifique et pratique,  galement. Pour cette raison ils seront expos s un peu plus largement.

L'association du chrome avec l'uranium refl te une liaison g ochimique inattendue,  tant donn  qu'il s'agit de deux  l ments de comportement g ochimique tr s diff rent, qui s'enrichissent dans des g ophases bien  loign es l'une de l'autre.

Le chrome, sid rophile, s'accumule plut t dans la phase introductoire de la cristallisation du magma et dans les m t orites de fer. Dans la pr sence du soufre, il rev t un caract re calcophile; mais son abondance  lev e dans la cro te terrestre sugg re  galement des affinit s lithophiles.

Dans la phase principale de la cristallisation, dans les roches basiques et dans les ultrabasites, il se pr sente sous forme de chromite et de picotite. En outre il appar it, dans quelques roches (bombes d'olivine, m tamorphites basiques) en rempla ant l'aluminium, p.e. dans les min raux suivants: Cr- pidote, Cr-diopside, uwarowite, fuchsite, mariposite etc.

Le chrome lithophile se manifeste sous deux formes: Cr^{3+} et Cr^{6+} , en fonction du potentiel oxydo-r ductif.

Les concentrations moyennes  tablies pour les g ophases diverses sont comme suit:

m�t�orite de fer, ultrabasites:	2000 — 3400 ppm
phase des sulfures:	1200 � 2400 ppm
roches gabbro�dales:	340 � 410 ppm
granit:	2 — 6,8 ppm
gr�s vert de Mecsek, en moyenne:	10 � 1600 ppm
hydromica potassique («illite»):	450 ppm
mica chromif�re, en moyenne:	4,05%

Donc le chromium est li , en premier lieu, au magma ultrabasique. Alors, on ne conna t pas de telles roches parmi les formations primaires de la Montagne Mecsek, sauf quelques gangues et dykes («schliers»)   lamprophyre des granits. Les mesures g omagn tiques faits par V. S c h e f f e r ont r v l  quelques anomalies particuli res (outre celles dues aux trachydol rites   P csv rad) qui peuvent  tre attribu es aux roches basiques des r gions pal zo iques et ant -pal zo iques. Ces roches-ci pouvaient af-

fleurer au Permien, ensemble avec les roches granitoïdes et métamorphiques (gneisses, amphibolites, serpentines). Elles peuvent être responsables aussi pour la teneur stable en chrome des houilles de Komló (E. Szádeczky-Kardoss, M. Földvári-Vogl).

C'est le debris de désintégration des roches sus-mentionnées, qui a alimenté, en fonction du relief d'érosion, le bassin sédimentaire permien, au temps du dépôt du complexe uranifère. D'abord le detritus et les produits de dissolution du manteau métamorphisé et des roches basiques, puis les produits de la décomposition mécanique et chimique des roches granitoïdes, fournissaient le matériau pour une sédimentation continue, sans limites internes décélables, psephitique-psammitique.

Jusqu'à présent, on n'a pas réussi de démontrer la présence des minéraux chromifères allotigènes parmi les constituants mécaniques du complexe uranifère (chromite, picotite etc.). On peut donc supposer que le chrome enrichie dans le Permien de la Montagne Mecsek devienne de la dissolution des constituants fémiques et des silicates chromifères des roches métamorphiques, basiques, associés au manteau granitique.

C'est au cours de la décomposition chimique, que le chrome est entré en solution, et il semble d'avoir migré dans un milieu hydrocarbonaté. Le chrome se laisse assez aisément exsoudre des minéraux silicatés. P.e. le mica chromifère épigénique du champ du Sud de la montagne Mecsek a fourni les données suivantes:

Quantité mesurée: 1 g de mica chromifère pulvérisé

Solvant: 100 ml 2 n HCl

Durée: 168 heures

Dissolu: 0,3204 g, dont les pourcentages élémentaires:

Cr	9,9%
Fe	7,4%
Mg	4,0%
K	18,8%

Les pourcentages relatifs au matériau originaire figurent dans le Tableau 2.

Tableau 2
Les pourcentages relatifs au matériau originaire

Éléments	Mica chromifère originaire	Dissolu
Cr	7,24%	3,17%
Fe	2,27%	2,37*
Mg	1,62	0,13
K	6,21	6,03

* = + Ni + V

Il ressort des analyses, que le fer octaédrique est entré complètement en solution, tandis que la moitié environ du chrome du mica chromifère y restait.

Un rôle semblable est joué par le vanadium. Il est lié en partie au mica chromifère, en partie à l'hydromica potassique («illite»). Les concentrations moyennes correspondantes sont 610 ppm et 210 ppm. Néanmoins, une partie considérable du vanadium est associée à l'uranium: sous forme inconnue dans le péchblende, accompagné par de la mottramite $[\text{Pb}(\text{Cu}, \text{Zn})(\text{VO}_4)(\text{OH})]$ subordonnée.

Les minéraux à U_3O_8 des filons hydrothermaux à U-Ni-Co Bi renferment jusqu'à 500 ppm de vanadium (selon les données publiées). On peut supposer que le vanadium ainsi que le chrome, qui s'enrichit remarquablement dans la phase de la première-cristallisation du magma, dérivent des roches basiques hypothétiques. Quand même, une partie de la teneur en vanadium des gîtes d'uranium dans la Montagne Mecsek est indépendant de la péchblende et des hydromicas chromifères et potassiques sus-mentionnés; sa forme minéralogique est à présent inconnue. On peut admettre, également, l'enrichissement en vanadium, des substances organiques, de la houille etc. P.e., d'après E. Sz á d e c z k y-K a r d o s s et M. F ö l d v á r i - V o g l le vanadium constitue un des éléments de trace constants des huiles de Komló.

Les analyses faites sur les roches encaissantes des champs N et S (écartées les lentilles de minérai) indiquent des rapports remarquables entre les éléments U, Cr et V. (Anal.: E. Uppor)

Les valeurs de la teneur en uranium, chrome et vanadium montrent une répartition capricieuse dans le champ du Nord, mais elles apparaissent parallèlement, avec peu d'exceptions. Le chrome est le moins irrégulier, en s'augmentant faiblement vers le faisceau inférieur. (Dans le tableau ne figurent que les concentrations en chrome obtenues par analyse chimique quantitative, laissant à côté les données microchimiques.)

<i>Faisceau supérieur:</i>	10 à 50 ppm de Cr
<i>Faisceau principal:</i>	10 à 50 ppm de Cr
<i>Faisceau inférieur:</i>	10 à 60 ppm de Cr

Voici la distribution du vanadium:

<i>Faisceau supérieur:</i>	250 à 600 ppm de V
<i>Faisceau principal:</i>	80 à 1000 ppm de V
<i>Faisceau inférieur:</i>	20 à 400 ppm de V

Donc le vanadium montre une croissance monotone du haut en bas, avec très peu d'exceptions. Il ne suit pas simplement les variations de la teneur en uranium. La teneur en vanadium montre des maximums locaux au niveau situé immédiatement au-dessous des maximums locaux en uranium. La cause de ce phénomène est à présent inconnue.

L'uranium est présent dans les roches des faisceaux supérieur et inférieur en concentrations basses, mais uniformes, tandis qu'il varie capricieusement dans le faisceau principal.

La répartition de tous les trois éléments est beaucoup plus homogène dans le champ du Sud. Il y a un parallélisme évident entre les faibles teneurs en chrome et les hautes teneurs en uranium, et parfois entre les hautes teneurs en chrome et les faibles teneurs en uranium.

Dans ce champ-ci, le chromium montre un maximum particulier pour chacun des faisceaux:

<i>Faisceau supérieur:</i>	200 ppm Cr
<i>Faisceau principal:</i>	1400 ppm Cr
<i>Faisceau inférieur:</i>	400 ppm Cr

Outre ces maximums, on trouve des concentrations beaucoup moins élevées, entre 15 et 20 ppm.

La distribution du vanadium est caractérisée par les données suivantes:

<i>Faisceau supérieur:</i>	100 à 450 ppm V
<i>Faisceau principal:</i>	100 à 600 ppm V
<i>Faisceau inférieur:</i>	100 à 350 ppm V

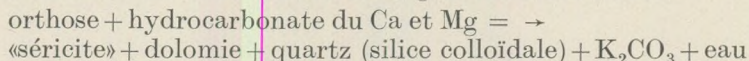
Le champ du Sud a une concentration moyenne moins élevée, distribuée d'une façon plus uniforme:

<i>Moyenne du champ du Nord:</i>	100 à 650 ppm V
<i>Moyenne du champ du Sud:</i>	100 à 460 ppm V

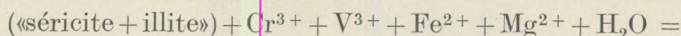
L'uranium varie parallèlement au vanadium, à trois maximums (un pour chaque faisceau), moins bien développées, en comparaison au champ du Nord.

Le ciment carbonaté (dolomitique-ankéritique) à hydromicas des variétés psammitiques du complexe uranifère est largement répandu, en particulier dans le grès vert à mica chromifère.

La formation sédimentaire des hydromicas sous conditions hydrothermales, est un processus bien connu: il suppose une quantité convenable des ions alcalins et des ions à pH changeant (p.e. hydrocarbonates des terres alcalines); la pression et la température normales lui conviennent. La décomposition de l'orthose du grès arkosique peut être attribuée principalement à l'influence des solutions aux hydrocarbonates du calcium et du magnésium, apportant aussi de l'uranium, du chrome et d'autres métaux lourds. La décomposition de l'orthose et des plagioclases dépend de la saturation des solutions hydrocarbonatées et de la porosité des roches, suivant la formule généralement connue:



Dans le complexe uranifère de la Montagne Mecsek, la décomposition des feldspaths (orthose, plagioclases) n'a jamais atteint les conditions de la formation de kaolinite, ce qui affectait d'une manière décisive le développement de l'échange des éléments au cours de la diagénèse, p.e. la formation du mica chromifère:



=K[(Fe, Mg) (OH)₂] [Cr, V, Al][(AlSi₄O₁₀)] (SiO₄) (OH)₂ = mica chromif re ou (dans le cas si l'un ou l'autre des m taux lourds  num r s avait jou  un r le subordonn ): hydromica potassique.

Le chrome commence   jouer un r le actif dans l'accumulation de l'uranium, quand il est entr  dans la structure de l'hydromica en produisant une nouvelle modification. Ce r le dure jusqu'  la saturation totale pour uranium (sous les conditions donn es). L'installation du chrome, du vanadium et des autres m taux lourds dans la structure du mica augmente sans doute sa surface adsorptive (?), ce qui facilite l'adh sion des ions U⁴⁺ sur les  cailles de mica.

Le mica potassique et les hydromicas potassiques, peu connus en d tail, ont pi g , non seulement l'uranium, mais aussi le chrome, le vanadium etc. L'adsorption beaucoup moins forte des hydromicas, en comparaison avec le mica chromif re, peut fournir une explication   l'observation qu'ils renferment, en moyenne, moins d'uranium, que le mica chromif re:

<i>Mica chromif�re:</i>	300 ppm U
<i>Mica potassique (illite-s�ricite):</i>	60 ppm U

L'uranium adsorb  sur les micas  pig niques se pr sente  galement sous formes de diss minations fines et enclaves, comme p chblende. Les noeuds de p chblende etc., associ s   soddyite et coffinite, sont toujours li s au micas chromif res ou potassiques.

De tout cela il ressort que les micas chromif res et les autres hydromicas potassiques ont jou  le r le d'une «barri re» cristallochimique-g ochimique, en filtrant et pr cipitant une partie de l'uranium contenu dans la solution. L'uranium s'est pr cipit , ensemble avec la silice, sous forme de silicates (soddyite et coffinite), et dans un milieu   un potentiel oxydo-r ductif plus  lev , directement sous forme d'oxyde. A notre avis, dans le cas d'absence du ciment   micas chromif res et hydromicas potassiques et des substances organiques (houille) la majorit  de l'uranium transport  dans les solutions a priori et descendantes aurait eu migr  plus loin.

Le r le ult rieure des micas chromif res et des hydromicas potassiques consiste dans le fait que le ciment a diminu  le volume des pores, en produisant une zone imperm able   tous les deux flancs de l'anticlinal de la r gion. La stagnation des solutions qui en a r sult , la produit la pr cipitation des min raux d'uranium  pig niques, c'est- -dire   une accumulation secondaire d'uranium.

La distribution de l'uranium et du vanadium dans les lentilles de min rai. La parall lisation des lentilles

On a pr lev  plusieurs  chantillons   lithologie et radioactivit   gales des lentilles du champ du Nord et du Sud. La site d' chantillonnage a  t  choisie, apr s des observations   l'oeil nu, sur la base d'une valeur de rayonnement (moins la radiation du fond)  gale   ou plus  lev e de 150 gammas. On a envisag  de conna tre les variations de la constitution

élémentaire et minéralogique des lentilles situées parallèlement avec la direction du complexe uranifère.

En illustrant les données analytiques conformément à leur position dans la coupe (Fig. 5), on trouve que — comme dans le cas des roches encaissantes également — la croissance de la teneur en uranium précède, presque toujours, celle du vanadium. Par exemple:

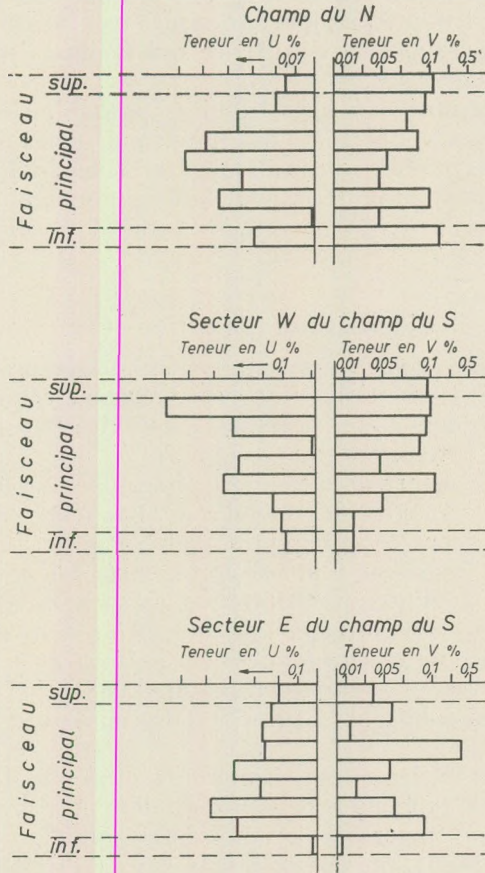


Fig. 5. Distribution verticale de l'uranium et du vanadium dans les lentilles de minéral

- Lentille (a): uranium croissant,*
Lentille (b): vanadium croissant, uranium décroissant,
Lentille (c): uranium croissant, vanadium décroissant,
Lentille (d): vanadium croissant, etc.

Quant à la répartition observé dans le champ du Nord, la concentration d'uranium va augmentant, à partir du faisceau supérieur jusqu'au maximum au milieu du faisceau principal, puis — après une décroissance

transitoire — il croit de nouveau dans les lentilles inf rieures, pour d velopper un deuxi me maximum d'enrichissement dans les lentilles les plus basses.

Au secteur est du champ du Sud on observe une distribution d'uranium enti rement diff rente. Les concentrations, malgr  les mineurs enrichissements locaux, sont consid rablement moins  lev es en comparaison avec le champ du Nord. La teneur en uranium va augmentant d'une fa on monotone des lentilles du faisceau sup rieur jusqu'au maximum observ  dans les lentilles inf rieures du faisceau principal, suivi par une forte d croissance vers les lentilles du faisceau inf rieur. Aux secteurs ouest et est du champ du Sud la distribution d'uranium correspond   celle esquiss e traitant le rapport entre l'uranium et le vanadium, c'est-  dire la croissance de la teneur en uranium s'observe dans des lentilles de plus en plus basses au fur et   mesure que l'on va de l'Ouest vers l'Est, suivant le sch ma (Tableau 3).

Tableau 3

Les changements de la teneur d'uranium dans les lentilles

Lentille	Secteur Ouest	Secteur Est
a)	conc. d'U �lev�e	conc. d'U peu �lev�e
b)	conc. d'U d�croissante	croissante
c)	croissante	d�croissante
d)	d�croissante	croissante
e)	croissante	d�croissante
f)	croissante	croissante
g)	d�croissante	d�croissante
h)	d�croissante	plus fortement d�croissante

FAISCEAU
Sup rieur
Inf rieur

La distribution de l'uranium dans tous les deux champs est due aux conditions de s dimentation en fonction de la g omorphologie et les diff rences temporelles de l'apport du mat riau.

Pendant le d p t des fragments m canoclastiques de min rai dans le champ du Nord, une partie de l'uranium contenu dans les solutions s'est pr cipit e; au secteur Ouest du champ du Sud n'arrivaient que peu de fragments uranif res et les solutions moins concentr es en uranium. Tandis que l'apport et le d p t des fragments de min rai d'uranium s'est accompli essentiellement dans le champ du Nord, l'uranium en solution est migr e plus loin vers le Sud, en atteignant un maximum au secteur Ouest, la concentration des solutions  tant moins  lev e dans la partie est, pour des raisons   pr sent inconnues.

Le processus  valu  et la g n se con ue sur la base des  tudes faites jusqu'  pr sent (1960) peut  tre modifi , bien entendu, par les  tudes en laboratoire   venir. D'abord, l'auteur pense   l' claircissement de l'influence de la position du g te sur les processus  pig niques: p.e. l'enrichissement en uranium dans la partie plus basse du secteur est du champ du Sud peut  tre expliqu  par descendance  galement.

La teneur en vanadium des lentilles de minérai reflète deux distributions différentes. Le rapport du vanadium à l'uranium est antagoniste dans les lentilles supérieures et les lentilles supérieures du faisceau principal de tous les deux champs, mais il devient parallèle à partir du milieu du faisceau principal jusqu'au faisceau inférieur. L'antagonisme constaté pour la partie supérieure du complexe uranifère peut être dû au potentiel oxydo-réductif plus élevé. Le vanadium est particulièrement concentré aux endroits riches en substances organiques, à un effet réductif marqué. Les valeurs moyennes de la teneur en vanadium, obtenues pour les lentilles de minérai, indiquent pratiquement le même rapport qui est établi pour les roches encaissantes: la teneur plus élevée en uranium du champ du Nord est accompagnée par des concentrations plus élevées de vanadium:

Moyenne du champ du Nord: 950 ppm V

Moyenne du champ du Sud: 330 ppm V

L'enrichissement du vanadium dans les roches encaissantes est 14 fois environ, pour le champ du Nord, et 30 à 35 fois pour le champ du Sud, comparé aux concentrations des lentilles de minérai.

Quant à la variation des teneurs en uranium et vanadium au dedans des lentilles mêmes, on a pu déceler les connections suivantes.

Champ du Sud:

α) Uranium

- a) Faisceau supérieur: croissance du haut en bas,*
- b) Faisceau principal: décroissance vers la base,*
- c) Lentilles basales du faisceau principal: croissance,*

β) Vanadium:

- | | | |
|------------------|------------------|-----------------|
| 1. a) = 100 ppm | 2. a) = 350 ppm | 3. a) = 470 ppm |
| b) = 500 ppm | b) = 180 ppm | b) = 500 ppm |
| 4. a) = 1100 ppm | 5. a) = 1400 ppm | 6. a) = 150 ppm |
| b) = 720 ppm | b) = 520 ppm | b) = 600 ppm |
| | 7. a) = 220 ppm | |
| | b) = 220 ppm | |

- a) Faisceau supérieur: croissance du haut en bas,*
- b) Faisceau principal: croissance conséquente du haut en bas,*
- c) Lentilles basales du faisceau principal (au dessus de la lentille du faisceau inférieur) et l'uranium, et le vanadium augmentent.*

Pour le champ du Nord, on n'a pas fait de pareils examens.

Dans le champ du Nord, on a séparé le matériau des lentilles de minérai riches en uranium et contenant de la liebigite en deux fractions, afin de déterminer la nature du minérai de vanadium à poids spécifique relativement bas. Il ressort que tous les deux fractions contiennent de la péchblende (U_3O_8), et une partie du vanadium est présent sous forme de mottramite [$Pb(Cu, Zn)VO_4(OH)$]. Les données de tous les deux fractions

relatives aux  l ments V, Ni, Co et Cu figurent dans le tableau 4. (Analyste V. T o l n a y, Institut G ologique de Hongrie.)

Les fractions relatives aux  l ments V, Ni, Co. et Cu.

Tableau 4

D�nomination	Fraction	V ₂ O ₅ %	NiO %	CoO %	CuO %
1. Min�ra� riche en uranium	a) lourde	2,25	0,02	—	0,01
	b) l�g�re	3,83	0,08	traces	0,01
2. Min�ra� � pyrite, riche en uranium	a) lourde	0,22	0,15	trace forte	0,07
	b) l�g�re	1,75	—	—	0,01

Alors le vanadium s' richit dans la fraction l g re (  30% environ).

Dans la fraction lourde du min ra    pyrite, riche en uranium, on a d montr  la pr sence de quelques fragments de calcopyrite, de nick line et de cobaltine.

Les examens trait s plus haut sont support s par l'analyse chimique compl te (analyste V. T o l n a y, Institut G ologique de Hongrie)

SiO ₂ :	46,51%
TiO ₂ :	0,17
Al ₂ O ₃ :	2,10
Fe ₂ O ₃ :	9,59
FeO:	— *
Cr ₂ O ₃ :	0,07
V ₂ O ₅ :	9,93
NiO:	0,01
CoO:	0,01
CaO:	0,01
As ₂ O ₃ :	0,83
PbO:	0,70
MnO:	0,02
MgO:	0,15
K ₂ O:	3,19
Na ₂ O:	0,07
— H ₂ O:	2,22
+ H ₂ O:	3,18
CO ₂ :	trace
P ₂ O ₅ :	0,11
S:	5,68
U ₃ O ₈ :	16,16**
ThO ₂ :	0,27
	<hr/>
	102,65%
— 0	2,84%
	<hr/>
	99,81%

* Ind terminable

** Analyse faite par le laboratoire   P cs

En conséquence des considérations théoriques, on a essayé de tracer le germanium, dont la présence était établie par les études de E. Szádeczky-Kardoss et M. Földvári-Vogl.

Il ressort que les parties riches en uranium sont, en même temps, enrichies en germanium. Afin d'obtenir des données supplémentaires, M. Földvári-Vogl a fait des analyses spectrales demi-quantitatives. Dans la fraction lourde du minéral, séparé par bromoforme, le germanium peut atteindre une concentration jusqu'à 100 ppm, tandis que dans la fraction légère la valeur correspondante est 1 ppm environ. Dans les lentilles riches on a trouvé en général 1 à 10, occasionnellement 100 ppm de germanium (Ge).

Les lentilles 218 (champ du Nord) et 342 (champ du Sud) se sont prouvées particulièrement riches en germanium.

En vertu du caractère équivoque du germanium, il joue un double rôle dans les minerais d'uranium. D'après E. Szádeczky-Kardoss le germanium est un élément (oxi)calcophile et non pas sidérophile, parce qu'il montre un parallélisme avec la distribution de la rhabdite (FeP) dans le fer météoritique. Urey-Craig, Onishik, El Waldani etc. ont soutenu l'opinion exposée par Goldschmidt, parce que la moyenne du Ge dans les chondrites est $9,4 \cdot 10^{-4}\%$ environ; leur fraction magnétique contient $29,0 \cdot 10^{-4}\%$ Ge, c'est-à-dire sept fois de plus que la fraction silicatée.

Parmi les minéraux silicatés, l'augite est plus pauvre en germanium, que l'amphibole ou l'olivine. L'hématite est trois fois plus riche en germanium que l'ilménite et la magnétite.

En ce qui concerne les roches sédimentaires, les calcaires et les dolomies ne renferment point du germanium; les grès en contiennent de 0 à $5 \cdot 10^{-6}\%$, les argiles et les schistes argileuses de 1,5 à $1,6 \cdot 10^{-6}\%$. Quant aux minéraux d'argile, il est plus abondant dans la kaolinite que dans l'illite; dans la montmorillonite il varie de 0,5 à $12,0 \cdot 10^{-6}\%$ et dans la goethite il est présent à $16 \cdot 10^{-6}\%$ environ. Dans les sédiments marins actuels ce sont les minéraux argileux et les détritiques mécaniques qui renferment la plus grande quantité de germanium.

Dans les sulfures, le germanium peut remplacer des ions, p.e. dans la sphalérite Ge^{2+} peut substituer le Zn^{+2} ($= 0,89 \text{ \AA}$), et dans la cérussite le Pb^{2+} . Dans le cas d'une soudure covalent, Ge° ($= 1,22 \text{ \AA}$) peut remplacer Zn° ($= 1,33 \text{ \AA}$). Récemment Cl. Frondel et I. Ito (1957) supposent que le germanium est présent sous forme d'une solution ferme dans l'énergite, tennantite, rennietite etc. de Tsumeb. Dans les arsénates des phases hypergènes il peut substituer l'arsenic, $\text{Ge}^{4+} = 0,44 \text{ \AA}$, $\text{As}^{5+} = 0,47 \text{ \AA}$, de la même façon que dans le cas de SiO_4 , dont le $\text{Si}^{4+} = 0,39 \text{ \AA}$.

La fraction lourde (obtenue par séparation en bromoforme) se compose de péchblende, de pyrite et de quelques fragments de sphalérite. Le germanium, 100 ppm environ, y contenu est lié probablement à ces sulfures (particulièrement à la sphalérite), mais les quantités très infimes ne permettent pas la preuve définitive. Une autre apparition du germanium, c'est dans le mica chromifère, où il substitue, semble-t-il, le silicium.

cium. L'enrichissement et le r le du germanium dans le min raux uranif re de la Montagne de Mecsek est donc loin d' tre suffisamment  clairci.

Dans le mat riau r colt  des lentilles de min raux, Mme M. F ldv ri-Vogl a d termin  la pr sence d'une s rie d' l ments, par une m thode demi-quantitative d'analyse spectrale, dont les r sultats sont reproduits dans les tableaux 5 et 6.

La r partition des donn es spectrales dans la coupe des  chantillons de min raux indique de remarquables connexions.

Au champ du Nord (Fig. 6) le nickel montre un peu de d croissance dans les lentilles sup rieures et dans un cas dans les lentilles inf rieures du faisceau principal; en outre il montre une r partition homog ne, tout en enrichissant un petit peu dans le faisceau inf rieur. Le cobalt est repr sent  par les concentrations peu  lev es dans les faisceaux sup rieur et inf rieur, il montre un comportement oppos    celui du nickel, sauf dans les lentilles du faisceau principal, ou on observe un parall lisme

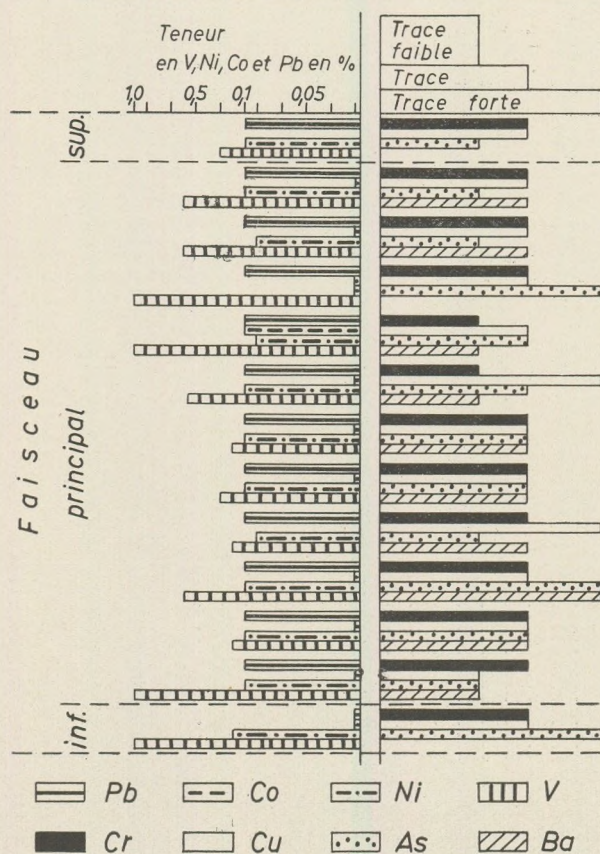


Fig. 6. Distribution verticale des  l ments mineurs et de trace dans le complexe uranif re (Champ du N) (dosage semiquantitatif).

Tableau 5

Champ du Sud

No	Site de prélèvement	V%	Ni%	Co%	Pb%	As	Cu	Cr	Ba	Sr
1	115/a 2 m	~0,1	0,1	0,01	0,1	tr. fb.	tr.	—	tr.	—
2	118/a 11,3 m	0,1-0,3	0,01	tr.	0,1	tr. fb.	tr.	—	tr.	—
3	137 10 m	0,3	0,1	0,01	0,1	tr. fb.	tr.	tr.	tr.	tr. fb.
4	202 5 m	0,3	<0,1	0,01	~0,1	tr. fb.	tr.	tr.	tr.	?
5	203 15 m	~1,0	0,1	0,01	~0,1	tr.	tr.	tr. f.	tr.	tr.
6	204 14 m	~0,5	<0,1	0,01	~0,1	tr. fb.	tr.	tr. fb.	tr. f.	tr.
7	206 2 m	0,3	0,01	0,01	~1,0	tr. f.	tr.	tr. fb.	tr. fb.	tr. fb.
8	207 2 m	0,1-0,3	0,1	0,01	>0,1	—	tr. fb.	tr.	tr. f.	tr.
9	210 II, 2 E.	0,1	~0,1	tr.	>0,1	—	tr. fb.	?	tr.	?
10	210 III-a 2 W, 9 m	~0,1	~0,1	0,01	<0,1	tr. f.	tr. fb.	tr.	tr.	tr.
11	210 III-a 2 W, 6 m	>0,3	~0,1	tr.	~0,1	tr.	tr. fb.	tr. f.	tr. f.	tr.
12	210 IV 18-19 m	~0,1	<0,1	tr.	~0,1	tr. fb.	tr.	—	tr.	tr.
13	215-W, 18 m	>0,1	~0,1	~0,1	<0,1	tr. fb.	tr. fb.	tr. fb.	tr.	tr.
14	219-lentille	~0,3	~0,1	~0,01	<0,1	tr. fb.	tr. fb.	tr.	tr.	tr.
15	233-E, 13 m	~0,1	~0,1	—	~0,1	tr. fb.	tr. fb.	tr.	tr.	tr.
16	236-W, 5 m	~0,1	~0,1	—	~0,1	tr. fb.	tr. fb.	tr.	tr.	tr.
17	240/a 4 m	~0,1	~0,1	—	~0,1	tr. fb.	tr. fb.	tr.	tr.	tr.
18	241-lentille	~0,1	~0,1	0,01	~0,1	tr. f.	tr. fb.	tr.	tr.	tr. fb.
19	241/a-W, 5 m	0,1-0,3	0,01	tr.	<0,1	—	tr.	—	tr.	—
20	242/a-W, 4 m	>0,1	0,01	>0,01	>0,1	tr.	tr.	tr. fb.	tr.	tr. fb.
21	242/b-W, 32 m	>0,1	0,01	>0,01	>0,1	tr.	tr.	tr.	tr.	tr. fb.
22	245	0,1	0,01	>0,01	0,01	tr. fb.	tr.	—	tr.	?
23	305-E, 3 m	~0,1	~0,1	tr. fb.	~0,1	tr. fb.	tr.	tr.	tr.	tr. fb.
24	306 8 m-E.	~0,1	~0,1	—	~0,1	tr. fb.	tr. fb.	tr.	tr. f.	tr.
25	307-W 5 m	>0,3	~0,1	—	~0,1	tr. fb.	tr. fb.	tr. fb.	tr. f.	tr.
26	315 38 m	~0,1	~0,1	<0,1	~0,1	tr. fb.	tr. fb.	tr. fb.	tr.	tr. fb.
27	340/a 5-6 m	>0,3	~0,1	tr.	~0,1	tr. fb.	tr. fb.	tr.	tr.	tr.
28	340/b-W 3-4 m	>0,3	~0,1	~0,1	<0,1	tr. fb.	tr. fb.	tr.	tr.	tr.
29	341-1 8 m	1,0	0,1	<0,01	<0,1	—	tr.	tr. f.	tr. f.	tr.
30	341/a-E, 18 m	~0,3	~0,1	tr. fb.	~0,1	tr.	tr. fb.	tr. f.	tr. f.	tr.
31	342/-1, 5 m	0,5-1,0	<0,1	tr. fb.	~0,1	tr. fb.	tr. fb.	tr. f.	tr. f.	tr.
32	346-E, 6 m	0,5-1,0	0,1	~0,01	0,1	tr. fb.	tr.	tr.	tr. f.	tr.

Tableau 6

Champ du Nord

N ^o	Site de prélèvement	V%	Ni%	Co%	Pb%	As	Cu	Cr	Ba	Sr
33	303-W 7-8 m	0,3	0,1	tr. fb.	0,1	tr. fb.	tr. fb.	tr.	-	-
34	312-E	0,3-1,0	0,1	0,01	0,1	tr. fb.	tr. fb.	tr.	tr.	tr. fb.
35	318/a	0,3-1,0	0,1	0,01	0,1	tr. fb.	tr. fb.	tr. fb.	tr.	tr. fb.
36	218/b-1 m	0,3	0,1	tr. fb.	0,1	tr. fb.	tr. fb.	tr.	tr.	tr.
37	218/b	0,3	0,01	-	0,1	tr.	tr. f.	tr. f.	tr.	tr. fb.
38	319/b-W-38 m	1,0	0,1	0,1	0,1	tr.	tr. fb.	tr. fb.	tr. fb.	tr. fb.
39	319/c-E-6 m	1,0-0,3	0,1	0,01	0,1	tr.	tr. f.	tr. fb.	tr. fb.	tr. fb.
40	319-5-15 m	0,3	0,1	0,01	0,1	tr.	tr.	tr.	tr.	tr. fb.
41	319-5-15 m	0,3	0,1	0,01	0,1	tr.	tr.	tr.	tr.	tr.
42	218/a	0,3	0,1	0,01	0,1	tr.	tr.	tr.	tr.	tr.
43	218/b-W-1 m	0,3	0,1	tr. fb.	0,1	tr. fb.	tr.	tr.	tr.	tr.
44	218/b-W-1 m	1,0-0,3	0,1	0,01	0,1	tr. f.	tr.	tr.	tr. f.	tr.
45	225-3 m	0,3	0,1	0,01	0,1	tr.	tr.	tr.	tr.	tr.
46	329(-W 42 m	1,0	0,1	0,01	0,1	tr. fb.	tr. fb.	tr.	tr. fb.	tr. fb.
47	252-W 4,5 m	1,0	0,1	tr. fb.	0,1	tr. f.	tr.	tr.	-	-

Remarque: tr. f. = trace forte; tr. = trace,
tr. fb. = trace faible.

marqué entre eux. Tout cela peut être interprété en invoquant le fait qu'il est plus sensible à l'effet de l'oxydation et de la dissolution. Le parallélisme révélé entre le cobalt et le vanadium est, à l'avis de l'auteur, indirect et inévitable. Il est généralement connu, que Co^{2+} se transforme aisément en Co^{3+} (Co^{2+} peut substituer, en vertu de son rayon ionique, le Fe^{2+}). Les valeurs pH entre 6 et 8 constatées dans le complexe uranifère de la Montagne Meesek assure la coexistence des ions V^{3+} et V^{4+} ; à côté des ions Co^{2+} et Co^{3+} le fer est présent sous encore la forme de Fe^{2+} . Tandis que l'ion Co^{2+} peut complètement substituer le Fe^{2+} , les ions Co^{3+} (rayon ionique 0,65 Å) peut remplacer V^{3+} et V^{4+} , dont l'un est 0,65 Å, et l'autre 0,61 Å. Les rapports exposés plus haut sont supportés également par les valeurs basses de l'Eh. Dans la partie minéralogique, l'auteur a indiqué la transformation $\text{U}^{4+} \rightarrow \text{U}^{6+}$, en fonction de l'Eh, qui est indicatif de l'intervalle ferreux. La prédominance des ions $\text{U}^{4+}/\text{U}^{6+}$ semble indiquer la circonstance que dans le milieu de la sédimentation renaient un pH non dépassant 6 à 8 et un Eh inférieur de +0,4 (autre-

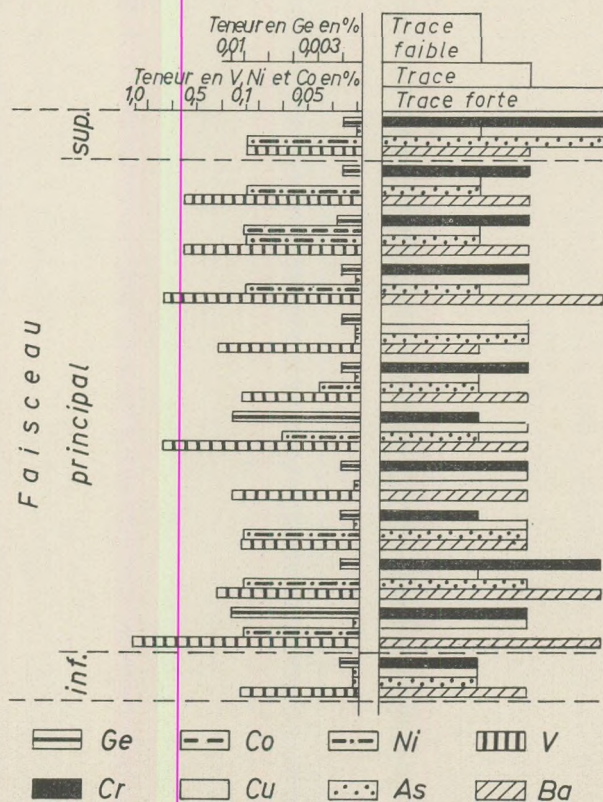


Fig. 7. Distributions verticale des éléments mineurs et de trace dans le complexe uranifère (Secteur W du champ du S) (dosage semiquantitatif).

fois, U^{4+} aurait  t  compl ttement transform  en U^{6+} et lessiv ); ainsi les ions Co^{2+} , Co^{3+} , V^{4+} , V^{3+} , U^{4+} , Ni^{2+} et Fe^{2+} ont pu subsister c te   c te et s'enrichir syng n tiquement.

Le chromium et le cuivre sont des  l ments de trace constants, dont la r partition suit celle du plomb. Les traces fortes de l'arsenic sont toujours pr sentes dans les  chantillons dans lesquels l'abondance de Ni, Co et V est plus  lev e. Il est possible que les fragments de min raux allotig nes jouissent un r le plus grave.

Le germanium est repr sent  par des concentrations de 1   10 ppm, distribu e uniform ment.

Le nickel montre deux minimums dans le secteur ouest du champ du Sud (Fig. 7), en atteignant ses maximums dans le faisceau sup rieur et dans les lentilles sup rieures et inf rieures du faisceau principal. Dans le faisceau inf rieur, en opposition   la situation observ  dans le champ du Nord, le pourcentage du Ni d cro t brutalement. La teneur en cobalt varie au sens inverse avec celle du nickel dans le faisceau sup rieur, tandis que dans les autres lentilles ils semblent montrer un certain parall lisme. La corr lation du cobalt et du vanadium est bien marqu e dans ce champ-ci, tandis que la r partition du germanium est beaucoup plus capricieuse que dans le champ du Nord.

En ce qui concerne le rapport constat  dans le champ du Nord entre les  l ments As, Ni et Co, il n'est pas retrouv  ici, d    l'absence des fragments de min rai allotig nes du Ni et du Co.

Le champ du Sud est plus riche en chromium et en barium. Par contre, le teneur en cuivre est tr s mod r e.

En consid rant la variation des teneurs des oligo- l ments au dedans des lentilles, vers le profondeur, dans le champ du Sud, on obtient les donn es suivantes:

α) Nickel

1. Lentille 240/a = 0,1%	2. Lentille 241 = 0,1%
Lentille 340/a = 0,1%	Lentille 341 = 0,1%
3. Lentille 206 = 0,01%	4. Lentille 207 = 0,1%
Lentille 306 = 0,1%	Lentille 307 = 0,1%
5. Lentille 241/a = 0,01%	6. Lentille 242/a = 0,01%
Lentille 341/a = 0,1%	Lentille 342/a = 0,01%
7. Lentille 219 = 0,1%	
Lentille 319 = 0,1%	

Le nickel est en g n ral stagnant, dans quelques cas il augmente vers le profondeur.

β) Cobalt

1. Lentille 240/a = 0,01%	2. Lentille 241 = 0,01% environ
Lentille 340/a = trace	Lentille 341 = ?
3. Lentille 206 = 0,01%	4. Lentille 207 = 0,01%
Lentille 306 = —	Lentille 307 = —
5. Lentille 241/a = trace	6. Lentille 242/a = 0,01%
Lentille 341/a = (trace)	Lentille 342/a = —
7. Lentille 219 = 0,1%	
Lentille 319 = —	

Donc le cobalt décroît vers la profondeur au dedans de la même lentille, jusqu'à disparaître.

 γ) Plomb

1. Lentille 240/a = 0,1%	2. Lentille 241 = 0,1%
Lentille 340/a = 0,1% env.	Lentille 341 = 0,1% env.
3. Lentille 206 = 1,0% env.	4. Lentille 207 = 0,1%
Lentille 306 = 0,1%	Lentille 307 = 0,1% env.
5. Lentille 241/a = 0,1% env.	6. Lentille 242 = 0,1%
Lentille 341/a = 0,1% env.	Lentille 342 = 0,1%
7. Lentille 219 = 0,1%	
Lentille 319 = ?	

La concentration du plomb est homogène dans le faisceau supérieur et dans les lentilles supérieures et moyennes du faisceau principal; elle s'abaisse un peu dans les lentilles inférieures.

L'enrichissement local en galène, démontré dans la partie minéralogique, pose le problème suivant: le plomb n'est que tout entier le produit de démantèlement d'une minéralisation hydrothermale antérieure, ou bien une partie du plomb peut être d'origine radioactive? La distinction et séparation des isotopes du plomb, le dosage de l'isotope radio-génique, pourrait contribuer à deux problèmes graves:

a) l'isotope Pb contenu dans les détritiques de minéral mécanique, pourrait dater la formation du gisement d'uranium lié à la géophase magmatique, primaire;

b) la galène épigénique pourrait donner une approximation concernant la formation du complexe uranifère sédimentaire (?!).

Parallèlement avec la décroissance des concentrations des éléments majeurs dans les lentilles du secteur est du champ du Sud (U, V), on observe l'appauvrissement en éléments mineurs, dont la distribution montre «un équilibre chaotiquement bouleversé» (Fig. 8).

L'oligo-élément le plus constant, c'est le germanium, dont la concentration moyenne est 10 ppm environ; il y en a d'autres, p.e. le barium

(trace forte) et le cuivre (trace). Les Ni, Co, As et le V sont distribu s en sens oppos  en dehors d'une m me lentille.

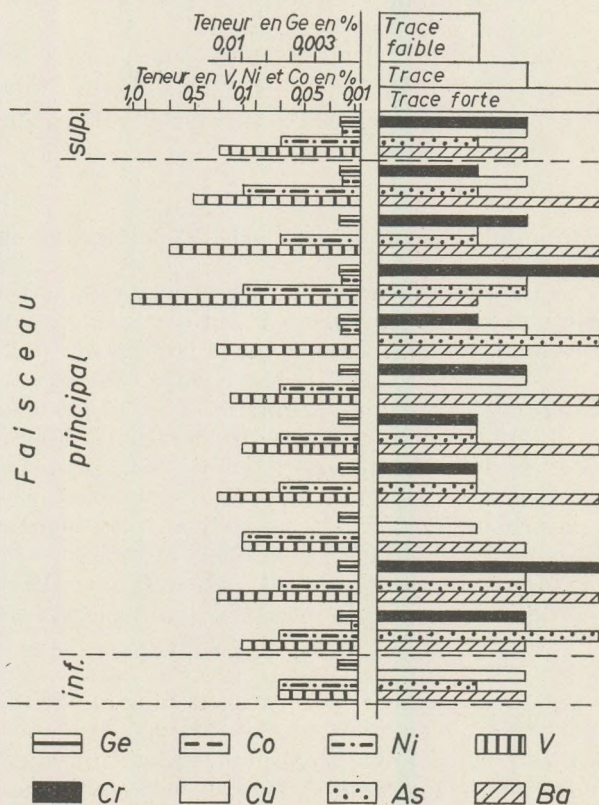


Fig. 8. Distribution verticale des  l ments mineurs et de trace dans le complexe uranif re (Secteur E du champ du S).

La r partition des oligo- l ments est interpr t e comme une preuve des processus d'accumulation des  l ments. Le transport et l'apport des m taux lourdes,   partir de l'aire de d nudation au Nord, se poursuivaient vers le Sud de plus en plus sous une forme ionique; puis la migration  pig n e a produit et stabilis  la r partition actuelle.

5. Parall lisation des lentilles de min rai

Tous les deux champs uranif res sont d' ge permien; pourtant l' ge montre un certain d calage du Nord vers le Sud. C'est particuli rement  vident au champ du Sud, ou — de l'Ouest vers l'Est — la puissance du complexe uranif re d cro t et l'uranium est de plus en plus concentr  dans

des lentilles plus pauvres. La parallélisation des lentilles de minéral se laisse faire en s'appuyant sur leur position relative au mur et au toit, ce qui ne signifie pas nécessairement la formation au même lieu de ces lentilles.

L'auteur envisage de décèler les traits communs minéralogiques, sédimentologiques et géochimiques, qui permettront à faire le groupement et l'identification correspondant à la position stratigraphique assez aisément, même sur le terrain.

6. La variation du rapport U^{4+}/U^{6+} dans les lentilles de minéral

La proportion des deux formes U^{4+} et U^{6+} , et sa répartition actuelle, reflète le développement du complexe uranifère, en fonction du degré d'oxydation. (Les analyses sont faites dans le laboratoire de l'Institut de Recherche des Métaux; analyste S. Duna y; Tableaux 7-8).

Si l'on considère ces proportions en fonction de la position stratigraphique des lentilles de minéral, on constate une tendance d'agrandissement des concentrations de U^{4+} . La proportion de faisceau principal est probablement due au degré d'oxydation plus élevé. Vers le secteur est du champ du Sud, la proportion U^{4+}/U^{6+} varie considérablement; la valeur 2,8 est le maximum observé dans les faisceaux principaux du complexe uranifère dans le Montagne de Mecsek. Il peut être interprété par la position tectonique de cette partie du gisement. jetée par des failles parallèles entre elles dans une position plus basse, elle a échappé à l'oxydation plus intensive.

La répartition des valeurs U^{4+}/U^{6+} dans la minéralisation de la Montagne Mecsek est attribuée aux caractéristiques géochimiques de la sédimentation, modifiés par des phénomènes épigéniques de migration:

a) L'enrichissement en uranium (sauf le détritit mécanique) a été contrôlé par les valeurs O_{Fe} , pH du milieu de dépôt et par d'autres facteurs locaux (concentration des substances organiques, présence des éléments capables de réduction p.e. Fe, V etc.);

b) Le degré d'oxydation, $O_{Fe} \frac{Fe_2O_3}{FeO}$ (d'après l'interprétation par

E. Szádeczky-Kardoss) montre des valeurs entre 3,0 et 3,8. Selon A. Barabás, cela favorise l'accumulation des ions $(UO_2)^{2+}$. La degré d'oxydation était, certes, moins élevé au cours de la sédimentation même, les valeurs actuelles ne jouent qu'un rôle stabilisant (?) de l'uranium.

Les variations du rapport U^{4+}/U^{6+} suivant la position stratigraphique du minéral sont illustrées dans le tableau 9.

Ces valeurs très différentes sont étroitement liées à la migration ultérieure de l'uranium et des éléments associés. C'est l'apparition des minéraux secondaires d'uranium (p.e. uranopilite, zippéite) sur les parois des galeries minières qui a tiré l'attention à la migration.

Tableau 7

Champ du Nord

Site de l'�chantillon	U ⁴⁺ /U ⁶⁺ %	Site de l'�chantillon	U ⁴⁺ /U ⁶⁺ %	Site de l'�chantillon	U ⁴⁺ /U ⁶⁺ %
Lentille 218 - 1	2,2	Lentille 225 - 3 m	—	Lentille 318	2,6
Lentille 218 - a	1,7	Lentille 252 - 4,5 m	1,2	Lentille 319 - 50 E 6 m	1,1
Lentille 218/1 m	1,7	Lentille 303 W - 7 - 8 m	0,9	Lentille 319 E - 6 m	0,9
Lentille 218 - b	3,0	Lentille 318/1 3 m	0,9	Lentille 319 - b W 38 m	0,7

Tableau 8

Champ du Sud

Site de l'�chantillon	U ⁴⁺ /U ⁶⁺ %	Site de l'�chantillon	U ⁴⁺ /U ⁶⁺ %	Site de l'�chantillon	U ⁴⁺ /U ⁶⁺ %
115 - a E/2 m	0,7	219 v.	0,9	340 - a 5 - 6 m	0,8
118 - a W/f 113 m	4,4	235 E v. 13 m	4,7	340 - b W 3 - 4 m	0,8
118 - a W/f 3. 3 m	0,5	236 W 5 m	0,5	341 1 8 m	0,5
118	7,0	240 - a 1 4 m	3,6	341 - a E 18 m	0,2
137 g. 10 m W	0,9	241	1,0	342 I. 5 m	0,6
202 E 5 m	2,8	241 - a W 3 m	6,1	346 E	0,2
203 4 15 m	0,9	242 - a W 4 m	4,2	315 38 m	1,3
204 E 14 m	1,7	242 - b W 32 m	4,2		
206 W 2 m	3,4	245	7,0		
207 W 2 m	6,2	305 E 3 m	0,8		
210 II. E v.	0,9	306 E 8 m	0,4		
210 III - a W 9 m	0,5	307 W 5 m	0,9		
210 III - a W 6 m	0,5	307 W 1 m	0,4		
210 IV. 0. 18 - 19 m	0,7	319 2 25 m	4,6		

La variation du rapport U^{4+}/U^{6+} dans les lentilles

Tableau 9

Champ du Nord		Champ du Sud			
		Secteur Ouest		Secteur Est	
Lentille	$\frac{U^{4+}}{U^{6+}}$	Lentille	$\frac{U^{4+}}{U^{6+}}$	Lentille	$\frac{U^{4+}}{U^{6+}}$
3/a	0,9	3/a	0,2	1	2,8
3/b	0,8	2/b	4,2	2	1,7
3/a	1,7	2/a	4,2	3	0,9
3/b	0,9-1,1	2/a	6,1	4	3,4
3/c	0,7	2	1,0	5	6,2-4,7
2/a	3,0	2/c	7,0	6	?
2/b	2,2				0,5-1,3
2/c	1,2				0,5

Les analyses des échantillons d'eau

Tableau 10

Analyse mg/l	1.	2.	3.	4.	5.	6.	7.	8.	9.	10.
Mg ⁺⁺	88,0	43,2	97,0	52,1	38,2	54,7	99,6	74,1	42,8	29,6-102,4
Ca ⁺⁺	29,6	39,7	33,2	73,2	62,4	40,0	31,4	32,6	71,2	12,0-101,4
K + Na ⁺	7,7	27,0	10,6	24,1	24,1	6,2	17,9	8,9	46,7	0,7-23,0
(SO ₄)	27,5	59,0	9,7	115,9	80,2	75,0	44,4	72,1	97,8	9,0-48,7
(HCO ₃) ⁻	500,2	360,2	579,5	361,2	324,6		570,4	373,9	402,6	195,8-577,6
Cl ⁻	9,7	16,0	13,2	20,0	11,0	21,3	9,4	13,4	9,3	3,2-48,6
Résidu sec	467,2	440,0	469,2	539,0	462,0	.	478,8	395,6	479,2	195,2-870,8
pH	7,7	7,5-7,8	76,5	7,2 7,9	7,25 7,95	7,8	7,4	7,5	7,4	6,8-8,0

1. Eau saillante de la galerie 3 du champ du Nord; 2. Eau courante de la galerie II du champ du Nord; 3. Eau du forage 1001; 4. Puits 1; 5. Eau courante du champ du Sud; 6. Eau courante à la surface du champ du Sud I; 7. Galerie III, 10 m; 8. Puits I, galerie transverse; 9. Champ du Sud, I, 69 m; 10. Eau superficielle

On a essayé de tracer les variations de la teneur en uranium des eaux apparaissant dans les galeries par la méthode des réactions «en goutte». Il ressort que les eaux du champ du Nord contiennent moins d'uranium. Le pH est 6 à 7 pour les eaux des galeries supérieures et entre 7 et 8 dans les galeries inférieures. On a réussi de démontrer la présence des ions Ca^{++} , Mg^{++} , SO_4^{--} et Cl^- . Les résultats des analyses des échantillons d'eau figurent dans le tableau 10.

Sur la bases des analyses, les eaux circulant dans les galeries renferment des hydrocarbonates de Ca et Mg, des sulfates de Ca et des métaux alcalins, avec peu de Cl. Au cours de l'évaporation lente de l'eau, c'est une incrustation jaune, uranifère, associée au gypse et aux carbonates des métaux alcalins et alcalo-terreux, qui fait son apparition. La constitution minéralogique de cette précipitation uranifère n'est éclaircie qu'en partie; il est présente en sulfates, mais avec la prédominance des carbonates de Ca, Mg et U (schwartzite, andersonite). Ces minéraux, pourtant, sont retrouvés sur le parois des galeries assez rarement.

Les eaux hydrocarbonatés, à Ca et Mg, qui circulent dans les galeries, représentent un solvant excellent des minéraux d'uranium, en particulier de ceux qui renferment des ions U^{6+} . Les variations de la concentration de l'uranium dans les eaux peuvent être interprétées par le rôle corrosif des eaux circulantes. Plusieurs dépressions «en entonnoir» se forment; par conséquent, la teneur en uranium des eaux actuelles peut être plusieurs fois plus élevée de celle des eaux descendantes le long des pores et des accidents structuraux.

En calculant avec une teneur en uranium égale à $10^{-4}\%$, et en supposant la migration (pour tous les deux champs) de $50-50 \text{ m}^3$ d'eau, on peut compter avec la dissolution de 180 kg d'uranium an 10 ans. A partir du Tertiaire, ça signifie 1,1 million tonnes d'uranium; à partir du Crétacé, une quantité double.

Le fait évident des analyses, notamment que les eaux des mines contiennent quelques fois une concentration plus élevée d'un ordre de magnitude, souligne l'importance pratique, et scientifique de ce problème. Si l'on suppose que le complexe permien de la Montagne Mecsek soit émergé définitivement au début du Tertiaire, même en comptant avec le minimum de migration d'uranium, les réserves d'uranium connues à présent ne peuvent représenter qu'une fraction de l'accumulation originelle (en particulier si l'accumulation primaire, sédimentaire occupait un territoire plus large).

La dissolution et la migration de l'uranium pose le problème, quels sont les secteurs aux deux flancs de l'anticlinal, où les solutions uranifères se sont arrêtées, en produisant un enrichissement tertiaire d'uranium?

Les études faites jusqu'à l'heure actuelle ont révélé, que ce n'est qu'une partie de l'uranium dissolue qui s'est éloignée définitivement; la majorité s'est arrêtée in situ, en fonction de l'Eh local et du ciment à hydromica (chromifère et potassique) du grès. Donc on peut compter sur une accumulation tertiaire considérable le long du linéament sud de la

montagne d'une part, et au secteur situé NO-NE du champ uranifère du Nord.

7. La répartition des minéraux dans le gisement d'uranium

La source d'uranium et l'aire de dénudation

Au cours de ses études, l'auteur mettait à point à plusieurs reprises les difficultés posées par la distinction et séparation des minéraux uranifères précipités de la solution a priori de ceux épigéniques. Pourtant, ayant esquissé les conditions géologiques et sédimentologiques, et ayant précisé la répartition et la mode d'apparition des minéraux d'uranium, on a pu reconnaître quelques caractéristiques qui peuvent servir de base pour la distinction envisagée. On peut établir la séquence temporelle suivante de l'accumulation d'uranium:

- a) *détritus mécanique*;
- b) *incrustation «en taches» (oxydes d'uranium)*;
- c) *dissémination fine des oxydes d'uranium, à microstratification*;
- d) *poussière ou bien suie d'uranium (toujours oxydes) remplissant des diaclases et fissures; («stockwerk» des fissures de quelques mm, disposées en toile d'araignée)*;
- e) *formation des minéraux uranifères secondaires.*

Les minéraux mentionnés sous point a) consistent en uraninite et péchblende, ils sont allotigènes, dont la quantité diminue sensiblement du Nord vers le Sud. (Quatre fois moins dans le champ du Sud en comparaison avec celui du Nord.)

Les minéraux uranifères cités sous point b) et c) sont supposées d'être précipités à priori de solution. Les incrustations, noeuds et taches de péchblende (plus rarement de soddyite et de coffinite) sont très bien contourés entre les grains de quartz et de feldspaths, entourés, de leur tour, par une auréole noir grisâtre, due à la dissolution postérieure. Les micas chromifères et potassiques d'origine épigénique, sont plus fréquents à trouver dans la «croûte» même que dans l'auréole. Il est donc possible que l'enrichissement en uranium a été facilité par un nucléus d'adsorption plus actif. L'auréole de dissolution postérieure est absente de la plupart des lentilles en dépit de cela, que dans le ciment englobant la croûte des fragments de quartz et d'autres minéraux les micas sus-mentionnés sont présents, bien qu'ils soient subordonnés.

Il faut mentionner que les micas épigéniques sont présents à un pourcentage d'un ordre de magnitude moins élevée que dans la suie d'uranium. (parapéchblende) A la base de tout ce qui vient d'être dit, les minéraux uranifères de l'incrustation sont qualifiés comme constituants diagénétiques.

Les incrustations minces (de quelques centimètres en épaisseur) à observer le long des plans de faille de dimensions très diverses, représentent le passage vers l'enrichissement épigénique de l'uranium. Ces incrustations portent bien souvent des traces de déplacement. Ces failles donnent lieu aux accumulations locales d'uranium. Les précipitations de suie d'uranium (parapéchblende) finement dispersées, disposées pa-

rall lement avec la stratification du gr s uranif re, sont consid r es syng n tiques. Elles sont   trouver plut t dans les lentilles inf rieures du faisceau principal.

Les min raux des fissures et des plans moins ouverts, compos s dans leur majorit  par suie d'uranium, d rivent des solutions descendantes, y compris les min raux secondaires d'uranium.

La suie d'uranium (parap chblende) est plus r pandue dans le champ du Sud que dans le champ du Nord. La diffusion tr s accentu e des rayons X n'est pas due exclusivement   la r partition dispers e de la suie d'uranium (parap chblende), mais elle peut  tre li e  galement   la dispersion fine des micas chromif res et potassiques associ s.

La suie d'uranium (parap chblende) ne se trouve jamais associ e   la pyrite, tandis que les grains syng n tiques du p chblende sont souvent entour s par de pyrite, ou bien ils se sont form s autour des noeuds de pyrite ou de bact riopyrite.

Les min raux secondaires d'uranium, caract ristiques de la zone d'oxydation, jouent un r le subordonn  quant   leur vari t  et pourcentage. Une zone d'oxydation proprement dite ne s'est pas d velopp e ici, ce qui peut  tre d ,   l'avis de l'auteur,   deux raisons.

1. *Il y avait peu d'ions complexes (phosphates, ars nates) qui auraient pu r agir avec les ions d'uranile entrant en solution.*

2. *La pr dominance de la solution hydrocarbonat e de Ca et Mg, migrant en sens descendant, qui entraine avec soi les ions d'uranium dissolus.*

Les min raux comme la liebigite, l'uranopilite, la zippeite et des min raux secondaires, douteux, d'uranium se sont form s aux endroits o  la migration de la solution  tait lente ou z ro. Il n'y a jamais de filtration d'eau   une  chelle consid rable aux endroits o  on rencontre des min raux secondaires d'uranium; ce sont, en g n ral, les secteurs plus secs du champ uranif re.

Les min raux uranif res de la Montagne Mecsek et leurs associ s permettent de concevoir un paragen se. L'uranitite-p chblende, la cobaltine, la nick line, le Bi et Ag dont la pr sence a  t  constat  par l'analyse spectrale, constituent une association d' l ments et min raux qui caract rise les min raux primaires de la formation de Bi-Co-Ni. D'apr s les donn es de la litt rature y relative, ce type de gisement est en g n ral situ  dans le manteau englobant un pluton granitique, impliquant de nombreux filons   «stockwerk». Il montre une zonalit  en profondeur: zone sup rieure   Ni-Co-Bi-As avec d'argent natif, zone inf rieure,   min raux uranif res. (Erzgebirge, Schneeberg, Jachimov, Chingolowe, Cornwall, Lac du Grand Ours, etc.).

Les sulfures de Pb, Zn, et Cu sont subordonn s. Le p chblende se trouve dans l'int rieur du filon, associ    dolomie,   ank rite et, par endroits,   pyrite.

Une partie du min rai d'uranium de la montagne Mecsek peut  tre le produit de demant lement d'une telle formation   Bi-Co-Ni (voir Fig. 2.), dont les phases sont   trouver dans le mat riau des faisceaux inf rieur, principal et sup rieur.

a) *Les lentilles inférieures, d'un développement capricieux et riche en uranium peuvent représenter le gisement sommital du gisement de Bi-Co-Ni. Cette assumption est appuyée par l'abondance relative des sulfures de Pb, Zn, Cu, et de l'argent, dans les lentilles en question.*

b) *Les lentilles riches en uranium du faisceau principal correspondent à la zone d'optimum, à filons, du gisement de Bi, Co, Ni. La quantité décroissante et des éléments Co et Ni et leurs minéraux vers les lentilles supérieures témoigne en faveur de cette hypothèse. Les éléments Bi et Ag sont présents dans ces lentilles dans l'ordre de 0,01%; leur forme minéralogique est ignorée.*

c) *Le faisceau supérieur ressemble à celui inférieur autant qu'il montre des concentrations très capricieusement variées d'uranium, qui sont pourtant par endroits assez élevées. Il peut renfermer le matériau de la partie disséminée dans le granit et dans les pegmatites et filons de Bi, Co, Ni. Les sulfures allotigènes en sont complètement absentes. La teneur en thorium, dont on dispose malheureusement très peu de données, suggèrent une croissance du bas en haut, vers les lentilles supérieures; cette tendance doit être prouvée par des analyses ultérieures.*

L'apport du matériel du NO vers le SE supposé par l'auteur et évoqué déjà à plusieurs reprises est indiqué par la décroissance du détritit uraniumifère dans cette direction, le développement plus homogène du champ du Nord, le démembrement autant horizontal que vertical du champ du Sud, sa puissance réduite, l'orientation correspondante générale des troncs d'arbres silicifiés dans le champs du Nord, en contraste avec leur disposition sans orientation préférée dans la région du Sud. D'après les études faciologiques plus récentes faites par Á. G r o s s z (1916) il y a également une autre direction, celle O-ONO, venant, à l'avis de l'auteur de la présente communication, de l'aire de dénudation de Fazekasboda, Mórágý et Ófalu. Il faut donc supposer la présence d'un gisement primaire de la formation à Bi, Co et Ni, au NO du champ du Nord, dans le manteau antécambrien, métamorphisé du pluton granitique, qui peut avoir eu un enrichissement original disséminé d'uranium (antérieur du métamorphisme et de la formation des filons hydrothermaux).

L'auteur a construit une carte de la structure en profondeur de la région, se fondant sur les affleurements, les données de sondages et des mesures géophysiques. (Voir Fig. 1.)

Les données géophysiques dérivent des mesures géomagnétiques faits par V. S c h e f f e r comme suit:

a) *il y a un maximum magnétique d'origine inconnue au-dessous de la ville de Szekszárd, entre Bogyiszló et Mócsány;*

b) *un autre maximum marqué est constaté entre Csibrák et Magócs, dans le territoire des roches métamorphes épi- et mésozonales;*

c) *le troisième maximum, prolongé dans la direction de Pécsvárad-Komló-Dombóvár, correspond aux trachidolérites connues en affleurement et dans des sondages aussi;*

d) *le quatrième et le cinquième maximum, dont l'origine est encore ignoré, sont situés entre Szigetvár et Kaposvár, et dans la direction de Tengőd-Mágocs respectivement.*

CARTE GÉOLOGIQUE DE LA SURFACE ET DE LA STRUCTURE PROFONDE DE LA RÉGION

„DÉLDUNÁNTÚL”

d'après les mesures géophysiques, les sondages profonds et les observations sur terrain

par J. Kiss 1958

0 25 km



- | | | | | | |
|----|----|----|----|-----|-----|
| 1. | 3. | 5. | 7. | 9. | 11. |
| 2. | 4. | 6. | 8. | 10. | 12. |

1. Affleurement de rhyolite; 2. Affleurement des roches secondaires; 3. Grès et conglomérat permien; 4. Formations primaires marines, peu métamorphisées (Carbonifère); 5. Granite de Mecsek; 6. Granite de Velence; 7. Schistes cristallins de l'épizone et de la mésozone; 8. Maximum magnétique (trachydolérite!); 9. Maximum magnétique d'origine inconnue; 10. Sondage; symbole de la roche atteinte: rhyolite, granite, porphyre quartzifère; 11. Direction du démantèlement; 12. Limite des formations à la surface, en sous-sol.

Fig. 1.

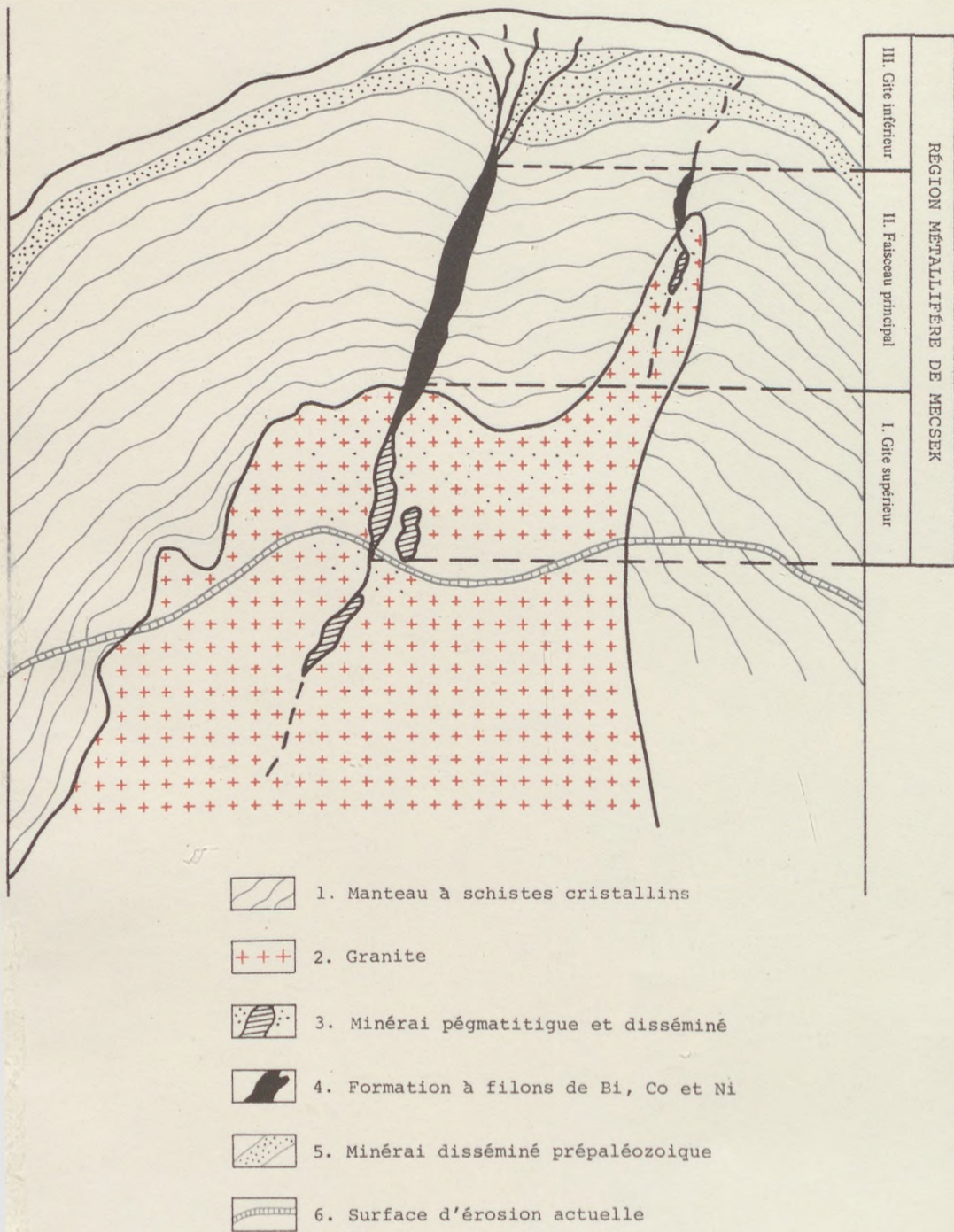


Fig. 2. Rapport entre les phases d'érosion de la formation à Bi-Co-Ni hypothétique

A Tengőd, un forage à creusé de rhyolite. On peut supposer l'existence d'une bande ou zone individualisée de rhyolite située dans la direction de Tengőd—Sárszentmiklós—Kulcs, orientée parallèlement avec le plan d'imbrication.

Les maximums de Bogyiszló, de Mocsány et de Szigetvár sont dus, semble-t-il, aux roches éruptives ou métamorphes anciennes, liées au manteau métamorphisé (amphibolites, schistes chloritiques, serpentines etc.).

Le maximum magnétique du carré Szigetvár—Bakonya—Kaposvár—Dombóvár est causé par le granit, ce qui est prouvé par les affleurements de granit à Nyugatszenterzsébet et de porphyre quartzifère à Dinnyeberek, ainsi que par le granit mis à découvert par le sondage de Korpád.

Les granits et granodiorites de la Mecsek du midi (de Mórógy à Erdősmecke) comprend un territoire de 650 km². Les variétés pétrographiques y connues sont des aplites, les dykes de lamprophyre, des pegmatites d'orthose, des faciès marginaux à syénite et à essexite, à bostonite. (D'après B. M a u r i t z). Les granits de Korpád (vers le N-NO du champ uranifère), s'étendent sur une surface de 600 km² également. Ils sont des granits à biotite, à veins de quartz, contenant peu de constituants colorés. On peut supposer que ces deux types de granit dérivent de deux intrusions différentes, celui de Mórógy étant plus récent que le granit de Korpád. Mais il n'est pas exclu qu'il s'agisse des produits de différenciation dans l'espace de la même intrusion.

Sur la carte on peut discerner deux zones ou bandes antécambriennes et paléozoïques du socle cristallin, qui se rejoignent au-dessous d'Igal, à peu près parallèlement avec le lac Balaton, le long le plan d'imbrication. La bande sud, attribuée à l'Antécambrien, est constituée par des roches épi- et mésozonales (phyllite, schiste cristallin, gneiss, amphibolite, schistes à actinolite, etc). Il y a de roches d'injection et des migmatites au contact de cette bande avec le granit. (Sondage de Pécs 7).

Au Nord du plan d'imbrication (dans la ligne des villages d'Igal, de Karád et de Buzsák) on trouve des formations marines d'âge carbonifère (prouvé faunistiquement par L. M a j z o n), qui ressemblent, du point de vue lithologique, aux calcaires bitumineux et schistes argileux d'âge viséen connus à Szabadbattyán. Le granit des Monts de Velence, le porphyre quartzifère de Polgárdi (d'après A. V e n d l c'est une aplitite), le granit de Ságvár, et des porphyres quartzifères rencontrés à plusieurs endroits au Nord du lac Balaton en affleurement et dans les sondages, indiquent qu'il s'agit, ici aussi, d'un pluton granitique d'une étendue considérable (c'est le pluton des Monts de Velence).

Déjà J. B ö c k h, L. L ó c z y Sen. et E. V a d á s z ont tiré l'attention aux différences faciologiques et sédimentologiques qui existent entre le Permien de la montagne Mecsek et celui situé au Nord du lac Balaton. Ce fait généralement reconnu peut être interprété par la supposition que le Permien pséphitique-psammitique du lac Balaton est le produit du demantèlement du pluton granitique de Pátka—Ságvár et des roches carbonifères à peine métamorphisées y associées.

Cette hypothèse nous donne la réponse à la question concernant la possibilité d'un enrichissement d'uranium dans le Permien situé au Nord du lac Balaton. En tenant compte des données disponibles des Monts de Velence, la réponse est négative. Bien entendu, on a besoin encore d'une multitude d'examen afin de pouvoir tirer là-dessus une conclusion définitive.

Les matériaux du complexe permien de la Montagne Mecsek dérivent des roches épi-meso-zonales et du granit. A l'avis de l'auteur, la source principal c'était le granit du Nord (celui de Korpád) et le manteau entourant, tandis que le granit du Sud (celui de Mórágý) a joué un rôle beaucoup moins grave.

C'est au maximum le grès et le conglomérat du Mont Jakabhegy, les roches clastiques du Mésozoïque (Rhaétien-Lias) et les roches pséphitiques-psammitiques du Miocène à la formation desquels le granit du Sud a pu contribuer.

La teneur en uranium du granit de Mecsek est beaucoup plus élevée que celle des roches granitoïdes des Monts de Velence. (Portant il y a quelques variétés de granit de Velence dont l'activité est proche à celle du granit de la Montagne de Mecsek.) Le rayonnement procède, d'après A. Földvári, des auréoles pléochroïques à biotite («halos radioactifs») qui renferment des éléments radioactifs, en fonction directe du pourcentage de la biotite. On a constaté des valeurs semblables de rayonnement pour les lamprophyres. S'appuyant sur ce fait, M. Földvári-Vogl a postulé un rôle enrichissant en uranium et thorium pour les portions de magma basiques. Dans la Montagne Mecsek, l'activité des roches alcalines dépasse considérablement celle du granit; la répartition de la radioactivité dans les dykes est diamétralement opposée à celle qui vient d'être signalée: les dykes d'aplite, donc plutôt acides, sont plus riches en substances radioactives. A. Földvári suppose un rapport $U > Th$ pour les roches granitoïdes de Mecsek et un rapport inverse pour les roches alcalines plus riches en zircon. (Il faut noter ici, que la teneur en potassium de la roche peut influencer essentiellement les résultats des mesures instrumentaux.)

En résumant les résultats de la séparation gravimétrique et magnétique, A. Földvári constate que la substance radioactive est liée dans la plupart aux minéraux lourds, vert clair, sans biotite. A l'avis de l'auteur de la présente communication cela est en contradiction avec sa thèse imposée en rôle géochimique nouveau, notamment que ce soit la biotite qui accumule les éléments radioactifs la plus intensivement.

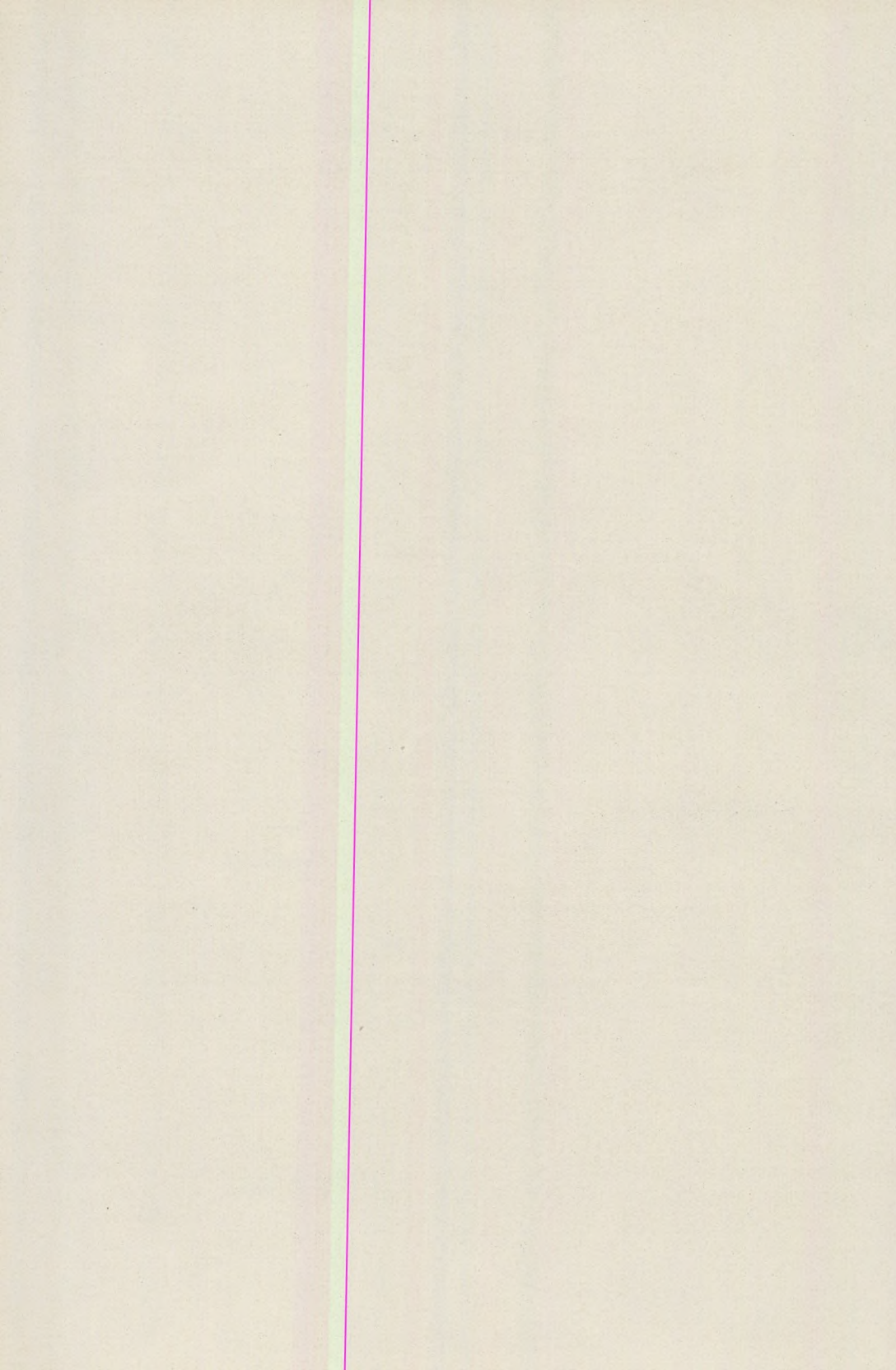
En adoptant 1 ppm pour valeur moyenne de la teneur en U et Th des roches granitoïdes de Mórágý, et en supposant la décomposition du granite sur un territoire de 650 km² et sur une puissance de 2 000 m, à un rapport de $3 : 2 = U : Th$, il résulte que 22 000 tonnes d'uranium pourraient se déposer dans le complexe sédimentaire. Donc, c'est à peu près 1/20^{ème} de la quantité contenue, selon les estimations moyennes, dans le complexe permien. Ces calculs justifient, semble-t-il, l'opinion de l'auteur exprimée plus haut, notamment que l'enrichissement en uranium dans le Montagne Mecsek dérive d'une minéralisation primaire situé au NO, et, en partie mineure, seulement, du granit de Mórágý. (SE).

LITTÉRATURE

- Aubel Van R. (1927): Sur la gèneses des gîtes uranifères de Kasolo. — *Compte Rend. Ac. Sci. Paris.*
- Aubel Van R. (1927): Sur la gèneses des gîtes uranifères de Kasolo. — *Compte Rend. Ac. Sci. Paris.*
- Aubel Van R. (1935): Sur l'uraninite cristallin de Kasolo., Chinkolobwe (Katanga). — *Ann. Soc. Géol. Belge XVIII.*
- Barabás A. (1956): A mecseki perm-időszaki képződmények (disszertáció). Kézirat. (Les formations permiennes de la montagne Mecsek. — Diss., manuscrit, en hongrois).
- Barabás A. — Kiss J. (1958): La gèneses et le caractère pétrographique sédimentaire de l'enrichissement de minerais d'uranium dans la Montagne Mecsek. — *Deuxième Conf. Int. des Nations Unies etc. Genève—Suisse.*
- Berman, R. M. (1957): The rôle of lead and excess oxygen in uraninite. — *The Amer. Min. Vol. 42. No. 11—12.*
- Bichau, W. J. (1951): Beaverlodge—Athabaska geology search for new pitchblende fields. — *Canad. Min. Journ. Vol. 72. No. 6.*
- Bizard, C. (1955): Présence de pitchblende dans le Permo-trias métamorphique des Alpes françaises. — *Compte Rend. Ac. Sci. Paris, 240.*
- Böckh J. (1872): A Bakony déli részének földtani viszonyai. (La géologie du Bakony du Sud. — En hongrois.) — *Földt. Int. Évk. 2.*
- Böckh J. (1876): Pécs városa környezetének földtani és vízi viszonyai. (Géologie et hydrogéologie des environs de Pécs. — En hongrois.) — *Földt. Int. Évk. 4.*
- Brooker, E. J. — Nuffield, E. W. (1952): Studies of radioactive Compounds: IV. Pitchblende from Lake Athabaska Canada. — *Am. Min. Vol. 37. No. 5—6.*
- Cerveira, A. (1953): Über die Metallogenie des Urans in Portugal. (Abstract: Zentralblatt für Min. Teil. II/2.)
- Chervet, J. — Branche, G. (1955): Contribution à l'étude des minerais secondaires d'uranium français. — *Sciences de la terre. Tome III. Nos. 1—2. Nancy.*
- Coffin, R. C. (1921): Radium, uranium and vanadium deposits in south-western Colorado. — *Col. Geol. Surv. Bull. 16. (cit)*
- Dines, A. G. (1930): Uranium in Cornwall. — *Min. Magazin Vol. XLII. No. 4.*
- Domarev, V. S. (1956): Geologiya uranovih mestorozhdenii kapitalističeskih stran. — *Gosgeolizdat. Moscou.*
- Douglas, G. V. (1930): Observation on the geology and mines of the Belgian Congo. — *Min. Magazin Vol. 42.*
- Evans, H. T. — Frondel, Cliff (1950): Studium of uranium minerals II. Liebigite and uranothalite. — *The Amer. Min. Vol. 35. No. 3—4.*
- Fischer, R. P. (1937): Sedimentary deposits of copper, vanadium, uranium and silver in south-west United States. — *Econ. Geol. Vol. XXXII. no. 7.*
- Fischer, R. P. (1950): Uranium bearing sandstone deposits of the Colorado Plateau. — *Econ. Geol. Vol. 45.*
- Földvári A. (1948): A magyarországi radioaktív kutatás földtani és közettani vonatkozásai. (Les aspects géologiques et pétrographiques des explorations radio-métriques en Hongrie.) (En hongrois.) — *MÁFI Évi Jel. 10. B.*
- Földvári A. (1952): A szabadbattyáni ólomércs és kővületes karbonelőfordulás. (Le minerais de plomb et le Carbonifère à fossiles à Szabadbattyán.) (En hongrois.) — *MTA Múz. Oszt. Közl. 5.*
- Frondel, Cliff. — Jun Ito (1957): Geochemistry of germanium in the oxidized zone of the Tsumeb mine, South-west Africa. — *Amer. Min. Vol. 42. No. 11—12.*
- Frondel, Cliff (1957): X-ray powder data for uranium and thorium minerals. — *Geol. Surv. Bull. 1036—G.*
- Frondel, Cliff (1957): Mineralogy of uranium. — *Amer. Min. Vol. 42.*
- German, D. H. (1952): Studies of radioactive compounds: V. Soddyite. — *Amer. Min. Vol. 37.*
- Grossz, Á. (1961): A mecseki perm É-i szárnyának földtani vizsgálata. (Disszertáció.) Kézirat. (Étude géologique du flanc septentrional du Permien de la montagne Mecsek. En hongrois, diss.)

- Gruener, J. V. etc. (1951): Uranium mineralization in Todilto limestone near Grants McKinley County New Mexico. — Bull. Geol. Soc. Amer. Vol. 62. No. 12.
- Jantsky, B. (1957): A Velencei hegység földtana. (Géologie de la Montagne de Velence. En hongrois). — Geol. Hung. Ser. Geol. Tom. 10. Res.: fr.
- Jantsky, B. (1950): A mecseki kristályos alaphegység földtani viszonyai. (Les conditions géologiques du socle cristallin du Mecsek. En hongrois). — MÁFI Évi Jel. R.: fr.
- Jantsky, B. (1952): A Velencei hegység hidrotermális ércesedése. (La minéralisation hydrothermale des Monts de Velence. En hongrois). — MTA Műsz. Tud. Oszt. Közl.
- Katz, J. — Rabinovich, E.: The chemistry of uranium.
- Kerr, P. F. — Hamilton, P. K. (1958): Chrome mica clay Temple Mountain, Utah. — Amer. Min. Vol. 43. No. 1—2.
- Kerr, P. F. (1950): Mineralogical studies of uraninite and uranium bearing deposits. — Intern. Techn. Rep. USAEC-RMO.
- King, A. G. (1957): Pyrite — uraninite polycrystal. — Amer. Min. Vol. 42. No. 9—10.
- Kiss, J. (1958): La genèse du chrome uranifère et son rôle paragenétique dans l'ensemble permien du Mecsek. — Deuxième Conf. Int. des Nations Unies etc. Genève — Suisse.
- Kiss, J. (1955): Recherches sur les bauxites de la Hongrie. — Acta Geol. Tom. III. Fasc. 1—3.
- Kiss, J. (1951): A szabadbattyáni Szárhegy földtani és ércgenetikai adatai. (Données concernant la géologie et la genèse des minerais du Szárhegy de Szabadbattyán. En hongrois). — Földt. Közl. 81. R.: R, F.
- Kiss, J. (1966): Constitution minéralogique, propriétés et problèmes de genèse du gisement uranifère de la Montagne Mecsek (I). — Ann. Univ. Sci. Budapest, Sectio Geologica, IX.
- Kiss, J. — Grossz, Á. (1958): Konkrecióképződés és karbonátos fácies a mecsek-hegységi pszammitos összletben. (Formation of concretions and a new carbonatic facies in the Permian arenetic sequence of the Mecsek Mountains. En hongrois). — Földt. Közl. 88.
- Kiss, J. — Virágh, K. (1959): Urántartalmú foszfátos kőzetfácies a balatonfelvidéki (pécselei) triász összletben. (An uranium-bearing phosphatic rock in the Triassic of the Balaton Uplands around Pécsely. En hongrois). — Földt. Közl. 89. R.: A.
- Kotljár, V. N. (1961): Geologiya i genetičeskie tipy promislyennih mestoroždeniyi urana. — Gosgeolizdat, Moscow.
- Maksimović, Z. (1958): Geohimiya raspadanya ultrabazičnih stena u Srbiji. (Manuscript) Beograd.
- McKelvey, V. E. (1905—1955): Origin of uranium deposits. — Econ. Geol. Part I.
- McKelvey, V. E. (1955): Search for uranium in the United States. — Geol. Surv. Bull. 1030—X.
- Miholić, St. (1954): Genesis of the Witwatersrand golduranium deposits. — Econ. Geol. Vol. 49. No. 5.
- Miholić, St. (1958): Radioactive waters from sediments. — Geochimica et Cosm. Acta. Vol. 14. No. 3.
- Murray, E. B. — Adams, A. S. (1958): Thorium, uranium and potassium in some sandstones. — Geochim. et Cosm. Acta. Vol. 13. No. 4.
- Nininger, R. (1956): Minerals for the atomic energy. — New-York.
- Pabst, A. (1951): X-ray examination of uranothorite. — Amer. Min. Vol. 36. No. 7—8.
- Pavlović, S. — Savić, P. (1954): Contribution à l'étude du cycle minéralogique de l'uranium. — Comptes Rend. Ac. Sci. Paris.
- Ramdohr, P. (1954): Neue Beobachtungen an Erzen des Witwatersrands in Südafrika, und ihre genetische Bedeutung. — Abh. Dtsch. Ak. Wiss. Berlin, No. 5.
- Reed, G. W. — Hamaguchi, H. — Turkevich, A. (1958): The uranium contents of iron meteorites. — Geochim. et Cosm. Acta. Vol. 13. No. 4.
- Robinson, S. C. — Sabina, A. P. (1955): Uraninite and thorianite from Ontario and Quebec. — Amer. Min. Vol. 40. No. 7—8.

- Robinson, S. C.: Mineralogy of uranium deposits Goldfields, Saskatchewan. — Geol. Surv. Canada, Bull. 31. Paris.
- Roubault, M. (1955): Essai de classification des gisements d'uranium et de thorium. Comptes Rend. Ac. Sci.
- Roubault, M. (1958): G ologie de l'uranium. Masson et Cie. Paris.
- Š erbina, V. — Ignatova, I. J. (1956): Obrazovanie i rastvorenje otenita. Geohimiya — 2.
- Š erbina, V. (1957): Povedenie urana i toriya v usloviyah sulfatno — karbonatnoy i fosfatnoy sved zoni hipergeneza. Geohimiya, No. 6.
- Soboleva, M. V. — Pudovkina, J. I. (1957): Minerali urana. — Gosgeolizdat. Moscow.
- Starik, J. E. — Sac, M. M. (1952): Opredelenie uranov v kamenovih i  eleznh meteoritah. — Geohimiya, 2.
- Stieff, L. R. — Stern, T. V. etc.: Coffinite, a uranous silicate with hydroxyl substitution: a new mineral. — The Amer. Mineralogy.
- Schumacher, P. (1954):  ber Uranlagerst tten. — Gl ckauf 90.
- Szalay, S. (1948): Investigations into the thorium and uranium contents of the eruptive rocks in Hungary by means of Geiger-M ller counter tubes. — M FI  vi Jel. Besz mol  X.
- Sz deczky-Kardoss, E. (1956): A mecseki li sz k sz n sszlet komplex vizg lata. I. (Bildung und Haupteigenschaften der liassischen Steinkohlen der s dlichen H lfte des Mecsek-Gebirges im Lichte der neuen kollektiven Untersuchungen. En hongrois). — M FI  vk. XLV. 1, Res.: G.
- Sz deczky-Kardoss, E. — F ldv rin  Vogl, M. (1955): Geok miai vizg latok a magyarorsz gi k szeneken. (Geochemische Untersuchungen auf Aschen ungarischer Kohlen. En hongrois). — F ldt. K zl. 85, Res.: R, G.
- Sz deczky-Kardoss, E. (1955): Geok mia. (G ochimie. En hongrois.) — Akad. Kiad , Budapest.
- Szepesh zi, K. (1957): A Magyar medence aljzat nak krist lyos k zetei. (Les roches cristallines du socle du Bassin Pannonien. En hongrois). — Manuscrit, O.K.G.T.
- Tomor, J. (1958): A magyarorsz gi olajkutat s  j eredményei  s lehet s ge. (R sultats nouveaux et possibilit s de la prospection de gisements p troliers en Hongrie. En hongrois). — B ny. Lapok 10—11.
- Thompson, M. E. (1953): Distribution of uranium in rich phosphate beds of the Phosphoria Formation. — U.S. geol. Surv. Bull. 988. — D.
- Vad sz, E. (1909): A Mecsek-hegys g. — (La Montagne de Mecsek. En hongrois). — Magyar T jak F ldt. Leir sa, I.
- Vad sz, E. (1953): Magyarország f ldtana. (G ologie de la Hongrie. En hongrois). — Akad. Kiad , Budapest.
- Vendel, M. (1955): Die Substituierbarkeit der Ionen und Atomen von geochemischem Gesichtspunkte I. — Acta Geol. Tom. III. 1—3.
- Vendel, M. (1958): Die Substituierbarkeit der Ionen und Atomen von geochemischem Gesichtspunkte II. — Acta Geol. Tom. V. 3—4.
- Vickers, R. C. (1957): Alteration of sandstone as a guide to uranium deposits and their origin northern Black Hills, South Dakota. — Econ. Geol. Vol. 52, No. 6.
- Waldani, S. A. E. (1957): On the geochemistry of germanium. Geochim. et Cosm. Acta, Vol. 13, no. 1.
- Weir, D. B. (1952): Geologic guides to prospecting for carnotite deposits on Colorado Plateau. — U.S. Geol. Surv. Bull. 988.



INVESTIGATION OF MONTMORILLONITES TREATED BY UREA SOLUTIONS (II). THERMAL INVESTIGATION OF UREA-CONTAINING NA- AND H-MONTMORILLONITES

by

O. LIBOR, L. GRABER

(Institute of Chemical Technology, Eötvös University, Budapest)

and

É. P.-DONÁTH

(Institute of Petrography and Geochemistry, Eötvös University, Budapest)

(Received: 1st June, 1970)

РЕЗЮМЕ

Авторы настоящей работы изучили термическое поведение H- и Na-монтмориллонитов, обработанных водным раствором мочевины. При этом было установлено, что мочевины каждый из этих двух типов катионных монтмориллонитов связывает по-разному.

H-монтмориллонит привязывает значительную часть мочевины химическим путем к поверхности своей кристаллической решетки. Na-монтмориллонит часть мочевины привязывает к своей поверхности (по-видимому, не химической связью), другая же часть связывается внутри кристаллической решетки глинистого минерала. Такой вывод хорошо согласуется с результатами предварительных рентгенодиффрактометрических исследований, проведенных авторами настоящей работы.

The quality of cations bonded to montmorillonite will influence the characteristics of the clay mineral (1). Montmorillonites containing different cations are characterized by divergencies in both swelling (2, 3, 4, 5) and reacting capacities (6, 7, 8, 9, 10, 11).

The thermal behaviour of montmorillonites of different genesis from different localities (12, 13) and of various organo-montmorillonites was examined by several authors (14, 15, 16, 17, 18).

The thermal decomposition of urea melts containing kaolinite was examined by Weiss (19) and his collaborators (20). While testing kaolinite treated by aqueous urea solutions, Weiss and Rothenstein (21) observed that the urea was bonded with a hydrogen bridge to the oxygen of the $[\text{SiO}_4]^{4-}$ tetrahedrons of the kaolinite lattice.

As observed during the present authors' earlier investigations, the swelling of H-montmorillonite brought into contact with aqueous urea solutions was substantially lower than it was the case with Na-montmorillonite under similar conditions. Its rheological behaviour too was different from that of Na-montmorillonite (for instance, it did not show any tixotropy) (22). This different behaviour of the two types of montmorillonite allowed the authors to conclude that in an aqueous environment the interaction of H- and Na-montmorillonite with the urea is different. This is also indicated by the observation that in presence of water molecules urea also penetrated into the basal spaces of the lattice of the

pre-expanded clay mineral (22). To interpret the different behaviour of the two types of urea-treated montmorillonite, the authors have tested these montmorillonites for thermal behaviour. It was supposed that testing with a derivatograph would provide additional information to the knowledge of the properties of H- and Na-montmorillonite.

Experiments and their evaluation

Materials investigated with the derivatograph were urea, Na- and H-montmorillonite, respectively, and the afore-mentioned two types of montmorillonites were treated for respectively 12 and 18.5 months by 10% aqueous solution of urea (22).

The resulting Na- and H-montmorillonite gel was separated by centrifuging from the reacting solutions. Afterwards the wet gel was dried in a vacuum, above CaCl_2 at normal room temperature. The material prepared this way was then tested for thermal behaviour. The data concerning the wet gels are given in Table 1.

Table 1

Composition of cationic montmorillonite-urea gel

Sample name	Composition of wet gel				Weight % of water removed by drying the gel	Weight % of composition of dried gel		
	Weight of wet gel	Weight % of gel components				Urea	Clay min.	Water
		Urea	Water	Clay mineral				
(1)	(2)	(3)	(4)	(5)	(6)	(7)	(8)	(9)
Na-montmorillonite — urea	5.75	5.04	86.26	8.70	82.7	29.0	50.0	21.0
H-montmorillonite — urea	2.21	10.86	65.60	23.54	105.5	31.7	68.3	—

Air-dry H- and Na-montmorillonites were prepared as described in an earlier paper (22). The urea investigated was of the same quality as that described there.

The differential thermal analyses were performed with a derivatograph designed by Paulik and Erdey. The same heating gradient, $10^\circ\text{C}/\text{minute}$, was used for each sample.

The chemical reactions involved in the thermal changes of urea take place simultaneously in the particular temperature intervals. These reactions are influenced by both the rate of heating of the reacting mixture and the time for which the mixture is held at the particular temperature (23, 24). Therefore the changes observed during the recording of the derivatogram apply only to the case of the given temperature gradient ($10^\circ\text{C}/\text{minute}$).

Table 2

Weight loss of urea as shown by the derivatogram

Peak temperature °C	Weight loss %	Correspond- ing to given temperature °C	Weight loss %	Correspond- ing to given temperature range °C
(1)	(2)	(3)	(4)	(5)
150 endothermic	1.33	190	1.33	0 - 190
	10.66	220	9.33	190 - 220
240 endothermic	21.32	240	10.66	220 - 240
260 endothermic	46.66	260	25.34	240 - 260
300 endothermic	49.33	320	2.67	260 - 320
	50.66	380	1.33	320 - 380
420 endothermic	92.00	460	41.34	380 - 460
480 endothermic	96.00	500	4.00	460 - 500
520 endothermic	98.66	545	2.66	500 - 545
580 exothermic	100,00	600	1.34	545 - 600
600 exothermic				

For the interpretation of the thermal behaviour of urea-containing clay minerals, the derivatogram of the urea was also prepared at the same temperature gradient (Fig. 1, Table 2). The derivatogram of H- and Na-

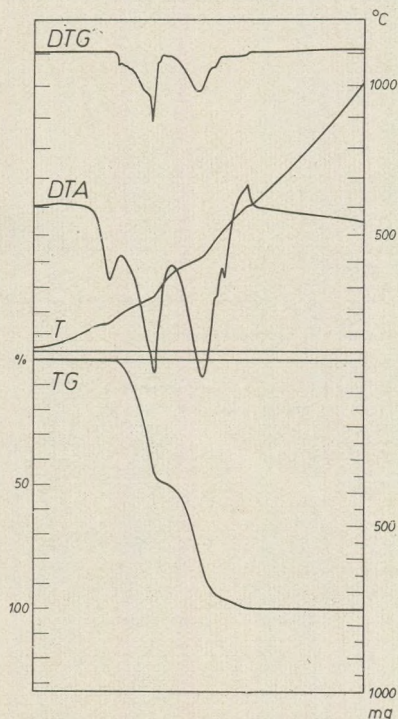


Fig. 1. Derivatogram of urea

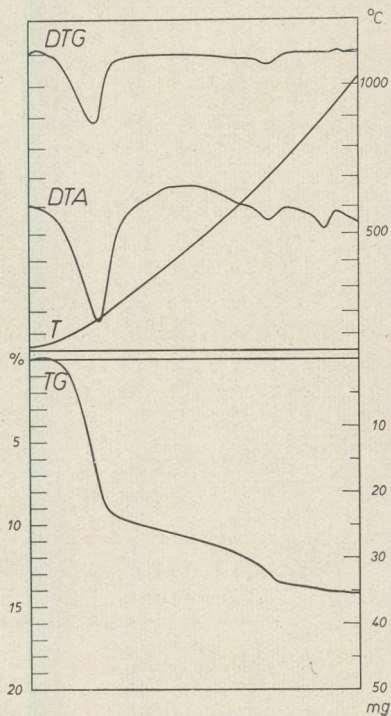


Fig. 2. Derivatogram of H-montmorillonite

montmorillonite (Fig. 2, 3 and Tables 3, 4) shows the known peaks agreeing well with literature data. However, on the derivatograms of urea-containing Na- and H-montmorillonite the present authors found characteristic features which had to be interpreted.

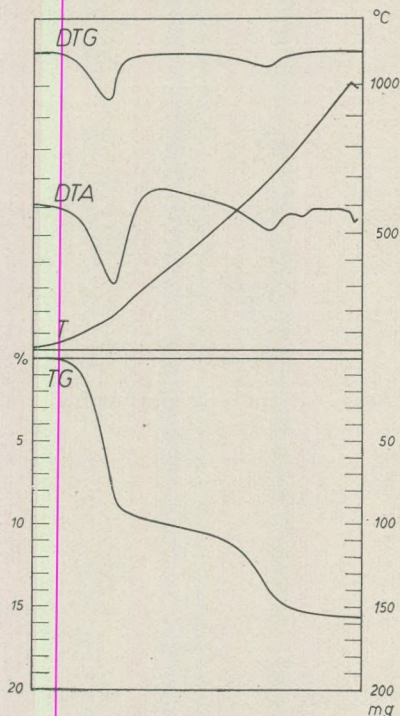


Fig. 3. Derivatogram of Na-montmorillonite

Table 3

Weight loss of H-montmorillonite as shown by its derivatogram

Peak temperature °C	Weight loss %	Correspond- ing to given temperature °C	Weight loss %	Correspond- ing to given temperature range °C
(1)	(2)	(3)	(4)	(5)
170 endothermic	4.21	130	4.21	0 — 130
340 endothermic				
400 endothermic	10.60	395	6.40	130 — 395
600 endothermic				
705 endothermic				
760 endothermic	13.65	760	3.40	395 — 760
905 endothermic				
950 endothermic	14.00	950		

Table 4
Weight loss of Na-montmorillonite as shown by its derivatogram

Peak temperature °C	Weight loss %	Corresponding to given temperature °C	Weight loss %	Corresponding to given temperature range °C
(1)	(2)	(3)	(4)	(5)
180 endothermic	1.8	120	1.8	0 - 120
	3.0	135	1.2	120 - 135
	8.9	200	5.9	135 - 200
340 endothermic	9.8	340	0.9	200 - 340
690 endothermic				
770 endothermic	15.0	770	5.2	340 - 770
810 endothermic				
880 endothermic	15.4*	880	0.4	770 - 880

* Weight loss calculated for soda-free Na-montmorillonite: 14.3%.

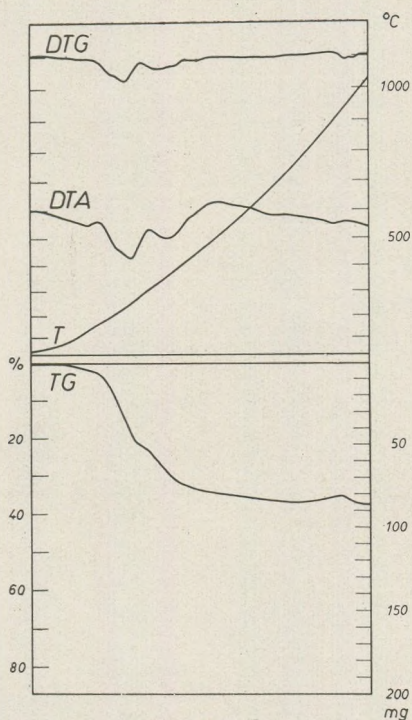


Fig. 4. Derivatogram of urea-containing Na-montmorillonite

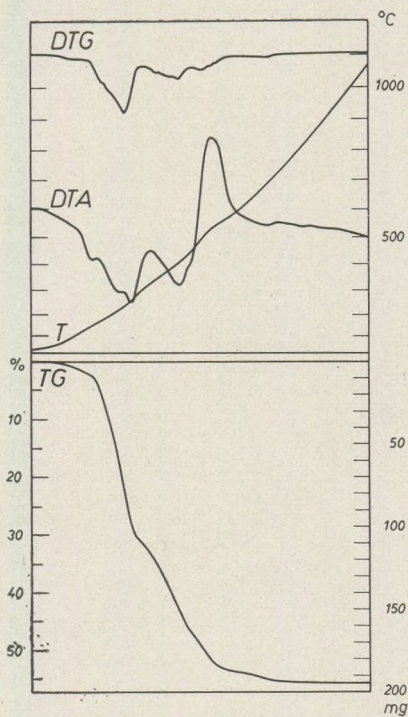


Fig. 5. Derivatogram of urea-containing H-montmorillonite

On the derivatogram of the urea-containing Na-montmorillonite (Fig. 4, Table 5) the peaks characteristic of the urea can be recorded one after another: at 140°, 250°, 410°, 450°, 540°C. In addition, the peaks of Na-montmorillonite also appear: at 690°, 820°C. Thus it is evident that the co-occurrence of the two substances does not influence essentially the thermal decomposition of either of the two.

However, the derivatogram of the urea-containing H-montmorillonite (Fig. 5, Table 6) differs fundamentally from both the curve of urea and from that of H-montmorillonite: the peak characteristic of the melting of urea has decreased to 115°C. Surprisingly enough, the endothermic peak of the thermal decomposition of urea at 420°C has disappeared and has been replaced by a slightly endothermic peak at 360°C — a peak probably due to various processes. The exothermic peak of the thermal decomposition of the urea at 520°C has also disappeared — a peak which can be recorded for instance in the case of urea-containing Na-montmorillonite.

Table 5

Weight loss of urea-containing Na-montmorillonite as shown by its derivatogram

Peak temperature °C	Weight loss %	Correspond- ing to given temperature °C	Weight loss %	Correspond- ing to given temperature range °C
(1)	(2)	(3)	(4)	(5)
140 endothermic	3.45	160	3.45	0 — 160
	14.42	195	10.97	160 — 195
	21.14	230	6.72	195 — 230
220 endothermic	31.43	300	10.29	230 — 300
250 endothermic	33.71	320	2.28	300 — 320
	36.57	360	2.86	320 — 360
410 endothermic				
450 endothermic	46.85	450	10.28	360 — 450
540 exothermic	51.71	530	4.86	450 — 530
			2.00	530 — 580
690 endothermic	53.71	580	1.72	580 — 740
820 endothermic	55.4	740	—	—

Conclusions

The different behaviour of H- and Na-montmorillonite-urea during their thermal decomposition (Fig. 6, 7) suggests that urea is differently bonded to either H- or Na-montmorillonite. Both cationic montmorillon-

Table 6

Weight loss of urea-containing H-montmorillonite as shown by its derivatogram

Peak temperature °C	Weight loss %	Corresponding to given temperature °C	Weight loss %	Corresponding to given temperature range °C
(1)	(2)	(3)	(4)	(5)
130 endothermic	1.15	120		
160 endothermic	1.34	160	1.34	0 - 160
			5.18	160 - 195
210 endothermic	12.04	220	10.56	220 - 300
250 endothermic	22.60	300		
310 endothermic				
360 endothermic	23.17	420	9.57	300 - 420
440 endothermic				
500 exothermic	34.34	495	2.17	420 - 495
610 exothermic				
670 endothermic	36.52	740	2.18	495 - 740
890 endothermic				

ites have bonded a part of the urea to their surfaces. This is confirmed by the low-temperature peaks on the differential thermal curves of the derivatograms, peaks indicating the beginning of the thermal decomposition of the urea bonded to the surface of clay minerals. The divergence of these peak temperatures relates to the fact that the two different types of cationic montmorillonite have differently bonded the urea to their surfaces.

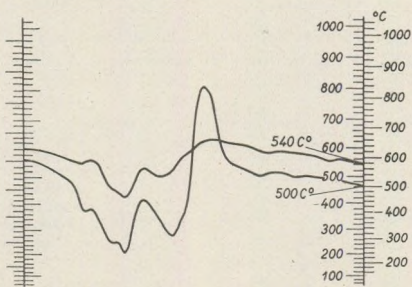


Fig. 6 Thermal decomposition of H- and Na-montmorillonite-urea DTA curves

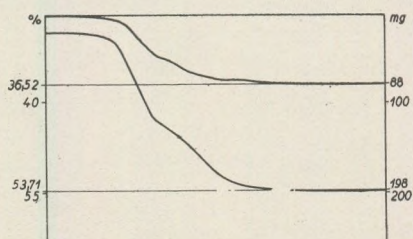


Fig. 7. Thermal decomposition of H- and Na-montmorillonite-urea TG curves

Nota-bene, H-montmorillonite, a mineral of acid nature (25, 26, 27), is likely to react with the urea, a slightly basic substance (28), in a way corresponding to the acid-base reaction. This assumption is supported by the investigations performed by Mortland (29) and Harter (30) using infrared techniques. The resulting complex H-montmorillonite-urea molecule (31) will certainly impede the penetrations of water- or urea molecules into the lattice of the clay mineral — a statement confirmed on the one hand by that no selectivity can be observed to occur during the thermal decomposition of H-montmorillonite-urea and that the two substances are interaction in this respect. On the other hand, the same is related to the fact that, upon treatment with an aqueous urea solution, H-montmorillonite was swollen very little (32).

Na-montmorillonite too bonded the urea in two different ways. In this case too, a part of the urea was bonded to the lattice surface of the clay mineral, but the type of this bonding was different from that described above. This is also indicated by the derivatogram on which the peaks characteristic of the thermal decomposition of the urea on the one hand and of Na-montmorillonite on the other are distinctly apart.

The rest of the urea bonded to Na-montmorillonite penetrated into the lattice of the clay mineral — a fact shown by the exothermic peak observable at 520°C on the differential thermal curve of Na-montmorillonite-urea. Within the temperature range of 420–600°C the weight losses corresponding to the total of the urea present in the system are the same for both urea and H-montmorillonite-urea, whereas in the case of Na-montmorillonite-urea their value is about threefold the former figure (Table 7, Columns 2, 4). It is also evident, that in the case of the urea and of urea-containing H-montmorillonite the weight loss observed at low temperatures (0–300°C) is essentially higher than it is in case of urea-containing Na-montmorillonite. Decompositions at medium temperatures (300–420°C) do not show so great divergence. These data also verify the different urea-bonding capacities of H- and Na-montmorillonite and

Table 7

Weight loss data of urea and urea-containing clay minerals on the basis of the thermogravimetric curves of the derivatogram and of the balance of substances

Temperature interval °C	420–600	300–420	0–300	
Analysed substances	weight loss in % of total urea present			moisture removed in % of the initial material
	(2)	(3)	(4)	(5)
Urea	8,0	42,7	49,3	—
H-montmorillonite-urea	9,6	30,2	60,4	3,5
Na-montmorillonite-urea	23,7	53,0	23,3	24,5

the fact that it is in its crystal structure that Na-montmorillonite has bonded a considerable part of the urea. The penetration of the urea into the lattice of Na-montmorillonite was also confirmed by the present authors' earlier X-ray diffraction studies (22).

REFERENCES

1. Kruglitzkij, N. N., Ovcsarenko, F. D., Niesiporenko, S. P. & Orobcsenko, V. I. (1966): Vlijanie obmennich ionov na razvitie koaguljacionnih sztruktur v vodnih diszperszijah glinisztih mineralov. Ukrainskij Himiceszkij Zsurnal 32 (5), 467-73.
2. Greenland, D. J., Quirk, J. P. & Theng, B. K. G. (1964): Influence of increasing proportions of exchangeable alkylammonium ions on the swelling of calcium montmorillonite in water. J. Colloid Sci. 19 (9), 837-40.
3. El-Swaify, S. A. (1965): Swelling pressures of clays with varying ionic composition. Dissertation Abstr. 26 (3), 1364-5.
4. Kerns, R. L. R., Jr. (1966): Structural charge site influence on the interlayer properties of expandable three layer clay minerals. Diss. Abstr. B 27, 1230.
5. El-Swaify, S. A. & Henderson, D. W. (1967): Water Retention by Osmotic Swelling of Certain Colloidal Clay with Varying Ionic Composition. Journal Science 78 (2), 223-32.
6. Glaeser, R. (1955): Organo-clay complexes and the role of exchangeable cations I. Exchange capacity and exchangeable cations. Mem. services chim. état (Paris) 39 (1), 19-58 (1954) Cit. CA. 49, 13735 a.
7. Glaeser, R. (1955): Organo-clay complexes and the role of the exchangeable cations II. Organo-clay complexes. Mém. services chim. état (Paris) 39, 81-108 (1954) cit. CA. 49, 13735 b.
8. Bodenheimer, W., Kirson, B. & Yariv, Sh. (1963): Organometallic Clay Complexes Part I. Israel J. Chem. 1, 69-78.
9. Farmer, V. C. & Mortland, M. M. (1966): An infrared study of the coordination of pyridine and water to exchangeable cations in montmorillonite and saponite. J. Chem. Soc. A. Inorg. Phys., Theoret. (3), 344-51.
10. Taraszevics, Ju. I., Rzaev, P. B., Taraszevics, V. B. & Sarkina, E. V. (1969): Adsorpcija piridina na kationzamescennom montmorillonite. Ukr. Him. Zsur. 35 (3), 273-7.
11. Mitra, N. K. & Sandilya, B. (1969): Flocculation characteristics of bentonite clay when substituted by different cations in exchangeable positions. Indian Ceram. 13 (11), 257-61.
12. Grim, R. E. & Kulbicki, G. (1961): Montmorillonite High Temperature Reactions and Classification. Am. Min. 46 1329-1369
13. Taraszevics, Ju. I., Kazarskii, V. M. & Valitskaja, V. M. (1968): Thermograms of isothermal drying of cation-substituted montmorillonite samples. Fiz. Khim. Mech. Liofil'nost Dispers, Sistem 158-62 cit. CA. 71, 14966 (1969).
14. Bodenheimer, W., Heller, L. & Yariv, S. (1966): Organometallic Clay Complexes VII. Thermal Analyses of Montmorillonite-Diamine and Glycol Complexes. Clay Minerals 6, 167-77.
15. Suito, E., Arakawa, M. & Yoshida, T. (1966): Adsorbed State of Organic Compounds in Organo-Bentonite II. Differential Thermal Analysis. Bull. of the Institute for Chem. Res., Kyoto Univ. 44 (4), 325-34.
16. Yariv, S., Birnie, A. C., Farmer, V. C. & Mitchell, B. D. (1967): Interactions between Organic Substances and Inorganic Diluents in Differential Thermal Analysis. Chemistry and Industry 1744-45.
17. Choei, S. & Yozo, O. (1966): Differential thermal analysis of the bentonite-poly (vinilalcohol) complex, Kogyo Kagaku Zasshi 69 (9), 1740-3 cit. CA. 68, 115093 (1968).

18. Diacsenko, N. S., Bondarenko, S. V., Kliger, A. B. & Vdovenko, N. V. (1968): Thermal study of organo-substituted clays. *Fiz. Khim. Mekh. Liofil'nost Dispers Sist.* 142–8. C.A. 71, 64471 (1969).
19. Weiss, A. (1961): Eine Schichteinschlussverbindung von Kaolinit mit Harnstoff. *Angewandte Chemie* 73, 736.
20. Weiss, A., Thielepape, W., Göring, G., Ritter, W. & Schäfer, H. (1963): Kaolinit-Einlagerungs-Verbindungen. *Intern. Clay Conf. Proc. Stockholm* 14, 287–305., Vol. 1.
21. Weiss, A. & Rothenstein, W. (1963): Über den Mechanismus der Entwässerung von Kaolinit und Kaolinitlagungsverbindungen. *Clays and Clay Minerals* 21, *Natl. Proc. Conf.* 1963. *Clays and Clay Minerals* Vol. 2., 101–4.
22. Libor, O. & K. Graber, L. (1969): Karbamiddal érintkező montmorillonitok vizsgálata I. Karbamid-oldatokkal érintkezésbe hozott montmorillonitok vizsgálata. *Agrokémia és Talajtan* 18 (3–4), 431–52.
23. Kazarnovszkij, Sz. N. & Malkina, N. I. (1957): K mehanizmu reakcij, protekajustih pri vzaimodejsztvii cianurovoj kisljoti sz amiakom. *Zsur. Prikl. Himii* 30, 490–3.
24. Malkina, N. I. & Kazarnovszkij, Sz. N. (1961): Szintez cianurovoj kisljoti iz mocsevinii. *Zsur. Prikl. Himii* 34, 1583–7.
25. Pommer, A. M. & Carroll, D. (1960): Interpretation of potentiometric titration of H-montmorillonite. *Nature* 185 (4705), 595–6.
26. Glaeser, R., Mantin, I. & Mering, J. (1960): The acidity of montmorillonite. *Intern. Geol. Congr. Rept. 21st, Copenhagen Pt. 24,* 28–34 (1961) cit. CA. 58, 360 b (1963).
27. Sawhney, B. L. & Frink, C. R. (1966): Potentiometric titration of Acid Montmorillonite. *Soil Sci. Soc. Amer. Proc.* 30 (2) 181–4.
28. Sabalitschka, Th. & Kubisch, G. (1924): Der Einfluß der Base auf den Grad der Umsetzung primärer Salze zweibasischer Säuren in wäßriger Lösung. *Z. Anorg. u. allg. Chem.* 134, 79–86.
29. Mortland, M. M. (1966): Urea Complexes with Montmorillonite: an Infrared Adsorption study. *Clay Minerals*, 6, 143–56.
30. Harter, R. D. (1967): Acidity dependent reactions between organic acids and amines and montmorillonitic clay surfaces. *Diss. Abstr. B* 27 (7), 2226.
31. Werner, E. A. (1923): *The Chemistry of urea.* Longmans, London.

A LINEAR FILTERING METHOD FOR DECOMPOSING RESIDUAL ANOMALIES

by

A. MESKÓ and I. VÉGES

(Department of Geophysics, L. Eötvös University, Budapest)

(Received: 6. September 1970)

SUMMARY

A linear filtering method for decomposing interfering residual anomalies is presented. The theoretical transfer function is shown and the accuracy of the approximations applied to a practical realization of the operation is investigated. The effectiveness of the method is illustrated by model computations.

Introduction

Zurflueh (1967), Urych (1968) and some other authors used the function

$$f(x) = a \cdot e^{-k(x-x_0)^2} \quad (1)$$

for describing the shape of geophysical anomalies. The parameter a gives the amplitude, x_0 denotes the center of the anomaly. The parameter k bears a relation to the width of the anomaly, viz. the distance between the points of inflection is given by

$$\Delta = \sqrt{\frac{2}{k}}.$$

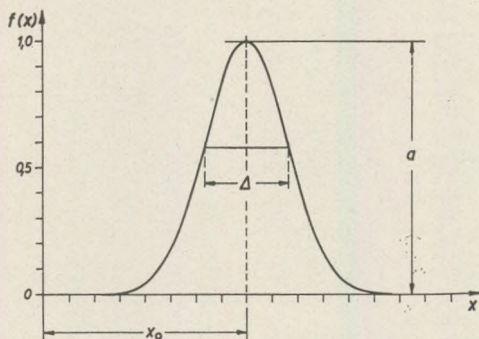


Fig. 1. The Gaussian function for describing the shape of a geophysical anomaly

(See Fig. 1. The composite field of several anomalies can be described by

$$g(x) = \sum_i a_i e^{-k_i (x-x_{0i})^2}. \quad (2)$$

If the centers of the anomalies are close to each other, the individual anomalies dissolve in a general picture and the parameters (amplitudes, centers, widths) cannot be determined. A filtering method will be given which enables us to separate the anomalies and offers, in certain cases, the possibility of determining their parameters.

The ideal filter

Let us consider at first a single anomaly. Suppose, for the sake of simplicity, that its Fourier transform is

$$A \cdot e^{-Ku^2} \quad (3)$$

where u denotes wave-number (or spatial frequency). The anomaly itself — as the inverse Fourier transform of (3) — is described by

$$F^{-1}\{Ae^{-Ku^2}\} = A \sqrt{\frac{\pi}{K}} e^{-\frac{\pi^2 x^2}{K}}. \quad (4)$$

Thus the parameters a and k can be expressed by the parameters of the spectrum as follows

$$a = A \sqrt{\frac{\pi}{K}} \quad \text{and} \quad k = \frac{\pi^2}{K}.$$

The width of the anomaly is given by

$$\Delta = \sqrt{\frac{2}{k}} = \frac{1}{\pi} \sqrt{2K}.$$

We propose the use of the transfer function

$$H(u) = e^{Pu^2}, \quad (P < K).$$

The spectrum of the filtered anomaly will be

$$Ae^{-Ku^2} \cdot e^{Pu^2} = Ae^{-(K-P)u^2}.$$

The corresponding inverse Fourier transform, i.e. the filtered anomaly, yields

$$A \sqrt{\frac{\pi}{K-P}} e^{-\frac{\pi^2 x^2}{K-P}}$$

The filtering results in an enhanced amplitude and a decreased width, viz.

$$a_{\text{filt}} = A \sqrt{\frac{\pi}{K-P}} = a \sqrt{\frac{K}{K-P}} = \lambda a \tag{5}$$

and

$$\Delta_{\text{filt}} = \frac{1}{\pi} \sqrt{2(K-P)} = \Delta \sqrt{\frac{K-P}{K}} = \frac{\Delta}{\lambda} \tag{6}$$

The schematic representation of the effect of the application of the "ideal" filter $H(u) = \exp(-Pu^2)$ is shown by Fig. 2. We wrote $0.75 \cdot K$ for P , and thus the factor

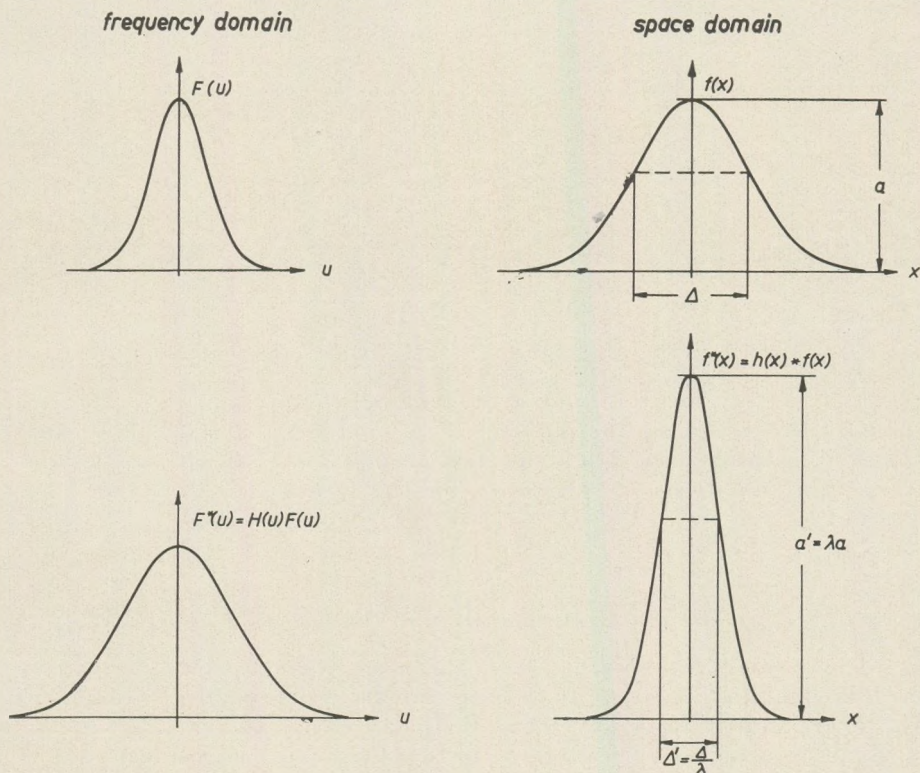


Fig. 2. The effect of the application of the "ideal" filter $H(u) = \exp(-Pu^2)$ to the anomaly $f(x)$

$$\lambda = \sqrt{\frac{K}{K-P}} = \sqrt{4} = 2,$$

i.e. the amplitude is doubled and the width is halved. The filter is obviously of zero phase, and on this account the center of the anomaly remains in its original place.

Applying the filter to the composite field (2) each individual anomaly will be somewhat "sharper", i.e. the amplitudes increased and the widths decreased. This effect facilitates the separation of the individual anomalies. In advantageous cases the parameters a and Δ can be determined by applying two different filters with parameters P_1 and P_2 , respectively. The amplitudes of an individual anomaly after the two filterings be denoted by a_1 and a_2 . It follows from Eq. (5) that

$$a_1 = a \sqrt{\frac{K}{K - P_1}},$$

$$a_2 = a \sqrt{\frac{K}{K - P_2}}.$$

From these two relations we obtain for the original amplitude a and width Δ

$$a = a_1 a_2 \sqrt{\frac{P_1 - P_2}{a_1^2 P_1 - a_2^2 P_2}} \quad (7)$$

and

$$\Delta = \frac{1}{\pi} \sqrt{2 \frac{a_1^2 P_1 - a_2^2 P_2}{a_1^2 - a_2^2}}. \quad (8)$$

Eqs. (7) and (8) are valid with some approximation only. The real anomaly is not exactly of Gaussian shape and the "tails" of other anomalies appearing in its neighbourhood also disturb the picture. Some other approximations are necessary for the practical realization of the filtering.

The practical realization of the operation

The operation to be achieved in the space domain can be derived by the following mathematical trick. The transfer function $H(u) = \exp(Pu^2)$ will be expanded into a Taylor series. Each component of the series corresponds to a known operation in the space domain. The series reads

$$\begin{aligned} H(u) &= e^{Pu^2} = 1 + Pu^2 + \frac{P^2}{2!} u^4 + \frac{P^3}{3!} u^6 + \dots \\ &= 1 - \frac{P}{(2\pi)^2} (i2\pi u)^2 + \frac{P^2}{2!(2\pi)^4} (i2\pi)^4 + \frac{P^3}{3!(2\pi)^6} (i2\pi u)^6 + \dots \end{aligned} \quad (9)$$

Dean (1958) has proved that the computation of the $2n$ -th derivative of a function corresponds to a filtering with the transfer function

$$S_{(2n)}(u) = (i2\pi u)^{2n}. \quad (10)$$

Thus the operation to be carried out on the original function can be obtained without making use of the inverse Fourier transform. Merely by comparing (9) and (10), one can establish that the operation is

$$1 - \frac{P}{(2\pi)^2} \frac{\partial^2}{\partial x^2} + \frac{P^2}{2!(2\pi)^4} \frac{\partial^4}{\partial x^4} - \frac{P^3}{3!(2\pi)^6} \frac{\partial^6}{\partial x^6} + \dots \quad (11)$$

Further approximations are necessary because the derivatives cannot be analytically determined. We have to manipulate on a set of values, i.e. on the results of the measurements at discrete points instead of on a continuous function. If the distances between the points of measurements are equal and the "sampling interval" is d , the values of the derivatives at the measurement points can be approximated by the quantities:

$$\begin{aligned} \frac{\partial^2 g_i}{\partial x^2} &\approx \frac{g_{i+1} - 2g_i + g_{i-1}}{d^2} \\ \frac{\partial^4 g_i}{\partial x^4} &\approx \frac{g_{i+2} - 4g_{i+1} + 6g_i - 4g_{i-1} + g_{i-2}}{d^4} \\ \frac{\partial^{2n} g_i}{\partial x^{2n}} &\approx \frac{1}{d^{2n}} \sum_{k=0}^{2n} \binom{2n}{k} (-1)^k g_{i+n-k}. \end{aligned}$$

Introducing a dimensionless parameter $P' = P/d^2$ and applying the approximations we get the formula

$$\begin{aligned} g_i^{\text{filt}} = g_i - \frac{P'}{(2\pi)^2} [g_{i+1} - 2g_i + g_{i-1}] + \frac{(P')^2}{2!(2\pi)^4} [g_{i+2} - 4g_{i+1} + 6g_i - 4g_{i-1} + \\ + g_{i-2}] - \frac{(P')^3}{3!(2\pi)^6} [g_{i+3} - 6g_{i+2} + 15g_{i+1} - 20g_i + 15g_{i-1} - 6g_{i-2} + \\ g_{i-3}] \pm \dots = \sum_{n=0}^N \frac{(-P')^n}{n!(2\pi)^{2n}} \sum_{k=0}^{2n} \binom{2n}{k} (-1)^k g_{i+n-k}. \quad (12) \end{aligned}$$

The method can be generalized for the two-dimensional case without difficulties but then the amount of the numerical computation necessarily increases.

The operation is carried out on a digitized function. In the course of the derivation we supposed that the sampling interval d was short enough to meet the requirement of Shannon's rule $d \leq 1/2f_h$, where f_h is the upper frequency limit. As a consequence the transfer function $H(u)$ has

to be investigated in the Nyquist interval: $u \in \left[-\frac{1}{2d}, +\frac{1}{2d} \right]$. If we introduce the dimensionless frequency variable $u' = u \cdot d$ the theoretical transfer function takes the following modified form:

$$H(u') = e^{P'(u')^2} \text{ for } -0,5 \leq u' \leq 0,5. \quad (13)$$

The transfer function of formula (12) deviates from the theoretical transfer function described by Eq. (13) because of the several approximations introduced in deriving the formula (12). Therefore it is necessary to investigate to what extent the accuracy of the operation as a whole has decreased.

Investigations of the accuracy

In order to estimate the approximation of formula (12) in an ideal case we have applied the filtering method to an anomaly described by

$$g(x) = e^{-\pi \left(\frac{x}{8} \right)^2}$$

The function has been digitized with a sampling interval $d = 1$, and then formula (12) has been repeatedly applied with various parameters ($N = 3$ in each case). The λ values obtained from the theoretical relation Eq. (6) and those computed from the filtered anomalies have been compared. The results are summarized in Table I. The deviation between the two sets of data is very small, in spite of the numerous approximations applied when deriving formula (12).

The foregoing analysis refers to a particular model, and thus a more general test of the accuracy has to be performed. The investigation of the transfer function of formula (12) offers the possibility of a check of general validity. After some manipulation the formula can be transformed into

$$g_i^{\text{filt}} = 1 + \sum_{k=1}^N a_k (g_{i-k} + g_{i+k}) \quad (14)$$

where the coefficients a_i contain various powers of P' and some constants.

The transfer function of operation (14) is given by

$$S_{\text{appr}}(u') = 1 + 2 \sum_{k=1}^N a_k \cos 2\pi k u' \quad (15)$$

where u' is the dimensionless frequency variable and the expression has to be computed over the Nyquist interval $-0.5 \leq u' \leq 0.5$.

The transfer function of the formula is compared with the theoretical transfer function (13). For practical reasons (both transfer functions are very rapidly increasing with increasing u') the ratio

$$R(u') = \frac{S_{\text{appr}}(u')}{H(u')} = \frac{S_{\text{appr}}(u')}{e^{P'(u')^2}} \quad (16)$$

has been computed and plotted. The ratio significantly deviates from unity if $u' > 0.25$. It involves that the deviation of the approximate formula from the theoretical operation becomes significant if the spectrum of the anomalies contains dimensionless frequencies higher than 0.25. This difficulty, however, can be easily overcome. If the sampling interval is chosen to be half of the necessary upper limit, given by the Shannon's rule, the spectral density expressed in terms of the dimensionless frequency becomes zero for $u' > 0.25$. Fig. 3 shows the ratio $R(u')$ for some values of the parameter P' . The approximation over this range and for the given parameters is acceptable.

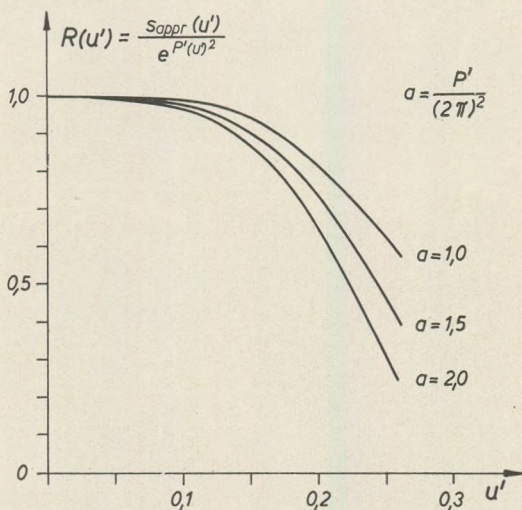


Fig. 3. The ratio of the actual and ideal transfer function against the dimensionless frequency u' for some filter parameters

Examples of application

The effectivity of the operation is clearly proved by Fig. 4. The filters were applied to a composite field shown on the upper part of Fig. 4. The two graphs in the lower parts of the figure show the results of the filtering with parameters $P' = \pi^2$ and $P' = 1.5\pi^2$. The filtering reveals that the composite field is an interference of three anomalies. The original amplitudes and widths of the individual anomalies are given in the first column of Table II. There is no doubt that they cannot be determined from the composite field. The results of the filtering and formulas (7) and (8), on the other hand, yield the possibility of estimation a and Δ . The computed values are given in the second column of Table II. The third column shows the relative errors (in %). The errors are comparatively small, and this proves that the method can be used to obtain fairly good

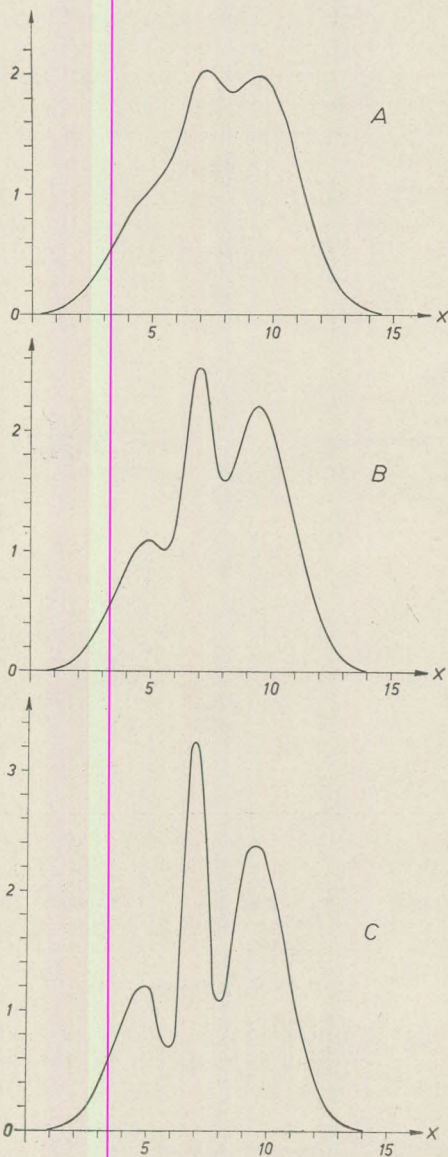


Fig. 4. The effect of the operation on Gaussian anomalies

A: The composite of three Gaussian anomalies

B: The Gaussian anomalies decomposed by a filter of parameter $P' = \Pi^2$

C: The Gaussian anomalies decomposed by a filter of parameter $P' = 1.5\Pi^2$

information on the parameters of the individual anomalies in so far as their shape is a Gaussian function.

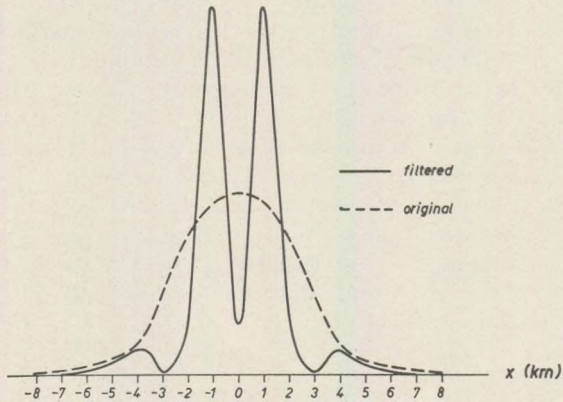


Fig. 5. The effect of the operation on the composite gravity field of two spheres. The dashed line is the original composite field, the continuous line represents the decomposed anomalies

A further example (Fig. 5) shows the effectivity of the method when the anomalies are described by other than Gaussian function. The dashed line shows the composite gravity field of two spheres along a profile which was taken through the maximum amplitudes of the individual anomalies. The x coordinates of the centers of the spheres are -1.0 and 1.0 (in kms) while the z coordinate (i.e. the depth) of both centers is 2 kms. The masses of the two spheres are identical. The gravity field along the profile (i.e. along the profile x -axis) is described by

$$g(x) = \frac{C}{[2^2 + (x-1)^2]^{3/2}} + \frac{C}{[2^2 + (x+1)^2]^{3/2}}. \quad (17)$$

Being a scaling factor and thus unaltered by the linear filter the constant C plays no role in the following and may be chosen arbitrarily.

The individual anomalies cannot be detected in the composite field. The function $g(x)$ has been digitized by a sampling interval of 1 km, and the linear filter (12) with parameter $P = (2\pi)^2$ has been applied. The output of the filter drawn by a continuous line clearly shows that the field is due to two separate sources.

Limitations

The purpose of the method is to decompose interfering anomalies, therefore it cannot be used either for eliminating the regional component or suppressing random noises. Before applying the proposed filter both the regional and random noises have to be eliminated. It can be easily understood that after the application of the filter the regional component remains almost the same. The regional described by a polynomial of the first degree remains unchanged: see Eq. (11). As the filter enhances

the amplitudes of the local anomalies they can be better detected against the background of regionals but this effect cannot be a substitute for the significant attenuation of the regional component.

The transfer function of the filter also shows that the operation is very sensitive to random noises, especially in the high-frequency range. Thus it might be necessary to pre-process the original data by an optimum smoothing filter before applying the decomposition. Clarke recently (1969) suggested the combination of second derivative (and downward continuation) filters with optimum smoothing filters. The method we need to apply is similar to that described by Clarke, only the decomposition filter has to be substituted for the second derivative (or downward continuation) filter.

Table I
Comparison of λ values

Parameter	λ	
	theoretical	with approximate formula (12)
P		
1.0	1.115	1.113
1.5	1.191	1.188
2.0	1.283	1.284
3.0	1.560	1.592

Table II
Results of the model computation

Anomaly No.	Parameter	Theoretical value	Estimated value	Difference in %
1	a	1.0	0.938	- 6.2
	Δ	3.12	2.71	- 13.1
2	a	2.0	1.891	- 5.3
	Δ	1.56	2.12	+ 26.4
3	a	2.00	1.992	- 0.4
	Δ	3.12	3.12	0.0

REFERENCES

- Clarke, G. K. C. (1969): Optimum second derivative and downward continuation filters, *Geophysics*, v. 34, no. 3, pp. 424-438
- Ulrych, T. J. (1968): Effect of wavelength filtering on the shape of the residual anomaly, *Geophysics*, v. 33, no. 6, pp. 1015-1019
- Zurflueh, E. G. (1967): Applications of two-dimensional linear wavelength filtering, *Geophysics*, v. 32, no. 6, pp. 1015-1035

SINGLE CHANNEL GHOST FILTER IN THE PRESENCE OF WHITE NOISE

by
A. MESKÓ

Geophysical Institute of L. Eötvös University, Budapest
(Received: 6 September 1970)

SUMMARY

In designing deghosting filters the presence of the random noise is often neglected (e.g. Lindsey, 1960). The paper should call attention to the fact that the presence of the random noise significantly influences the transfer function of the optimum filter and thus its taking into consideration is necessary.

Transfer function of the optimum filter is derived for the general case: extraction of signal (primaries) buried in coherent (ghosts) and random noises. The case of random white noise is dealt with in detail.

Introduction

The design of single-channel ghost rejecting filter has been discussed in the literature (e.g. Lindsey, 1960). If the random noise is neglected the deghosting operator can easily be determined and using an operator long enough the ghost reflections are effectively attenuated by the process. The aim of this short contribution is to call attention to the fact that in the presence of random noise the simple deghosting operator is far from the optimum. We should like to emphasize that it is of inevitable importance attenuating both types of noises i.e. both coherent and random noises. In the first part the transfer function of the optimum filter is derived. The second part deals with the special case when the spectrum of the random noise is white.

Transfer function of the optimum filter

The filter to be designed is a particular kind of the smoothing filters. The input to the filter consists of signal plus noises. The signal is the series of primary reflections denoted by $s(t)$. The noises are the series of ghost reflections, denoted by $g(t)$, (coherent noises component) and random noise, denoted by $z(t)$. We suppose that the ghost reflections have the same shape as the primaries but are delayed by a time T and attenuated relative to the corresponding primary events

$$g(t) = -ks(t-T),$$

where k is the reflection coefficient of the ghosting surface. The input to the filter can be written as

$$x(t) = s(t) - ks(t-T) + n(t).$$

We wish to minimize the difference between the output of the filter and the signal. It is well known that by using the least-mean-square-error criterion for judging how closely this objective has been achieved the transfer function of the optimum filter can be determined and it reads as follows

$$H(f) = \frac{\Phi_{sx}(f)}{\Phi_{xx}(f)}, \quad (1)$$

where $\Phi_{sx}(f)$ is the cross-spectrum between the signal and the input, $\Phi_{xx}(f)$ is the power spectrum of the input.

The spectra can be determined by Fourier transformation from the corresponding correlation functions

$$\Phi_{sx}(f) = \int \varphi_{sx}(\tau) e^{-j2\pi f\tau} d\tau, \quad (2)$$

$$\Phi_{xx}(f) = \int \varphi_{xx}(\tau) e^{-j2\pi f\tau} d\tau \quad (3)$$

where $\varphi_{sx}(\tau)$ is the crosscorrelation function for $s(t)$ and $x(t)$ and $\varphi_{xx}(\tau)$ is the autocorrelation function of the input.

These functions have to be determined from the structure of the input. We assume that the random noise is uncorrelated with the signal or the coherent noise. The crosscorrelation function by definition is

$$\begin{aligned} \varphi_{sx}(\tau) &= \lim_{T \rightarrow \infty} \frac{1}{2T} \int_{-T}^T s(t)x(t-\tau)dt = \lim_{T \rightarrow \infty} \frac{1}{2T} \int_{-T}^T s(t)[s(t-\tau) - \\ &\quad - ks(t-T-\tau) + z(t-\tau)]dt = \lim_{T \rightarrow \infty} \frac{1}{2T} \int_{-T}^T s(t)s(t-\tau)dt - \\ &\quad - k \lim_{T \rightarrow \infty} \frac{1}{2T} \int_{-T}^T s(t)s(t-T-\tau)dt = \varphi_{ss}(\tau) - k\varphi_{ss}(\tau+T). \end{aligned} \quad (4)$$

Similarly it can be shown that the autocorrelation function for the input is

$$\varphi_{xx}(\tau) = (1+k^2)\varphi_{ss}(\tau) - k\varphi_{ss}(\tau+T) - k\varphi_{ss}(\tau-T) + \varphi_{zz}(\tau) \quad (5)$$

In the equations (4) and (5) $\varphi_{ss}(\tau)$ and $\varphi_{zz}(\tau)$ denote the autocorrelation function of the signal and that of the random noise, respectively.

Putting the determined $\varphi_{sx}(\tau)$ into Eq. (2) and using the shift theorem of the Fourier transformation we obtain

$$\Phi_{sx}(f) = \Phi_{ss}(f)(1 - ke^{-j2\pi fT}) \quad (6)$$

where $\Phi_{ss}(f)$ is the power spectrum of the signal.

Similarly, by putting $\varphi_{xx}(\tau)$ into Equ. (3) we obtain

$$\begin{aligned}\Phi_{xx}(f) &= \Phi_{ss}(f)[1 + k^2 - k(e^{-j2\pi fT} + e^{j2\pi fT})] + \Phi_{zz}(f) = \\ &= \Phi_{ss}(f)[1 + k^2 - 2k \cos 2\pi fT] + \Phi_{zz}(f)\end{aligned}\quad (7)$$

where $\Phi_{zz}(f)$ denotes the power spectrum of the random noise.

By making use of the results (6) and (7) equation (1) yields the transfer function of the optimum filter for our particular model as follows

$$H(f) = \frac{\Phi_{ss}(f)(1 - ke^{j2\pi fT})}{\Phi_{ss}(f)(1 + k^2 - 2k \cos 2\pi fT) + \Phi_{zz}(f)}.\quad (8)$$

The filter rejects both the coherent and random noises at the same time.

Before embarking upon further specialization it is of worth investigating two particular cases.

Case A: No random noise is present

This case corresponds to that described by Lindsey. If the power of the random noise is equal nought, $\Phi_{zz}(f) = 0$ and the transfer function of the filter reduces to

$$\begin{aligned}H(f) &= \frac{\Phi_{ss}(f)(1 - ke^{j2\pi fT})}{\Phi_{ss}(f)(1 + k^2 - 2k \cos 2\pi fT)} = \frac{1 - ke^{j2\pi fT}}{(1 - ke^{j2\pi fT})(1 - ke^{-j2\pi fT})} = \\ &= \frac{1}{1 - ke^{-j2\pi fT}}.\end{aligned}\quad (9)$$

In the ordinary way the weighting function of a filter is determined by taking the inverse Fourier transform of the transfer function. In the present case inverse Fourier transformation cannot be applied. We are able, however, to use some known relations to avoid the emerging difficulties.

The transfer function is a sum of an infinite geometric series

$$\frac{1}{1 - ke^{-j2\pi fT}} = 1 + ke^{-j2\pi fT} + k^2e^{-j2\pi 2fT} + \dots\quad (10)$$

The Fourier transform of a Dirac-delta pulse displaced from the origin by nT is

$$F\{\delta(t - nT)\} = e^{-j2\pi n fT}$$

which corresponds to

$$\delta(t - nT) = F^{-1}\{e^{-j2\pi n fT}\}.$$

Thus the weighting function — as the inverse Fourier transform of the right-hand-side of Eq. (10) yields as

$$h(t) = F^{-1}\{H(f)\} = \delta(t) + k\delta(t - T) + k^2\delta(t - 2T) + \dots\quad (11)$$

The output of the filter is the convolution of the input and the weighting function (11) i.e.

$$\begin{aligned} y(t) &= x(t) * h(t) = \int_{-\infty}^{+\infty} h(\tau)x(t-\tau)d\tau = \\ &= \int_{-\infty}^{+\infty} [\delta(\tau) + k\delta(\tau-T) + k^2\delta(\tau-2T) + \dots]x(t-\tau)d\tau = \\ &= x(t) + kx(t-T) + k^2x(t-2T) + \dots \end{aligned} \quad (12)$$

Thus in the lack of random noises the effect of the filter is identical with the operation derived by Lindsey.

Case B: No ghost activity is present.

If the ghost reflections are negligibly small the reflection coefficient $k=0$ and the transfer function (8) simplifies into

$$H(f) = \frac{\Phi_{ss}(f)}{\Phi_{ss}(f) + \Phi_{zz}(f)} \quad (13)$$

i.e. the result is the well known optimum smoothing filter.

The special cases clearly show that the filter (8) simultaneously attenuates both the coherent and random noises.

Ghost filter in the presence of white noise

Before applying the filter the parameters k and T and functions $\Phi_{ss}(f)$ and $\Phi_{zz}(f)$ have to be determined. The determination of the power spectrum of the noise is most difficult. Therefore it became usual to assume white noise. Then the noise spectrum is constant.

The transfer function (8) in the special case becomes

$$H(f) = \frac{\Phi_{ss}(f)(1 - ke^{j2\pi fT})}{\Phi_{ss}(f)(1 + k^2 - 2k \cos 2\pi fT) + \lambda}, \quad (14)$$

where λ is in connection with the power of the white noise

$$\lambda = \nu \frac{1}{f_h} \int_0^{f_h} \Phi_{ss}(f)df \quad (15)$$

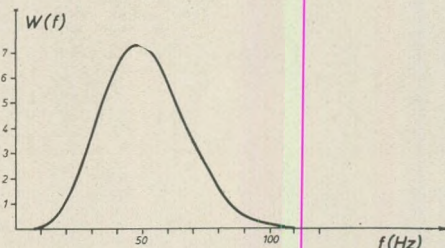


Fig. 1. The power spectrum of the signal

where f_h denotes the upper frequency limit of the signal. The power spectrum of the signal is shown in Fig. 1. The upper frequency limit was set equal to 125 cps. It involves that the noise spectra is white over the interval 0 cps – 125 cps. The scaling factor ν gives the ratio of the power

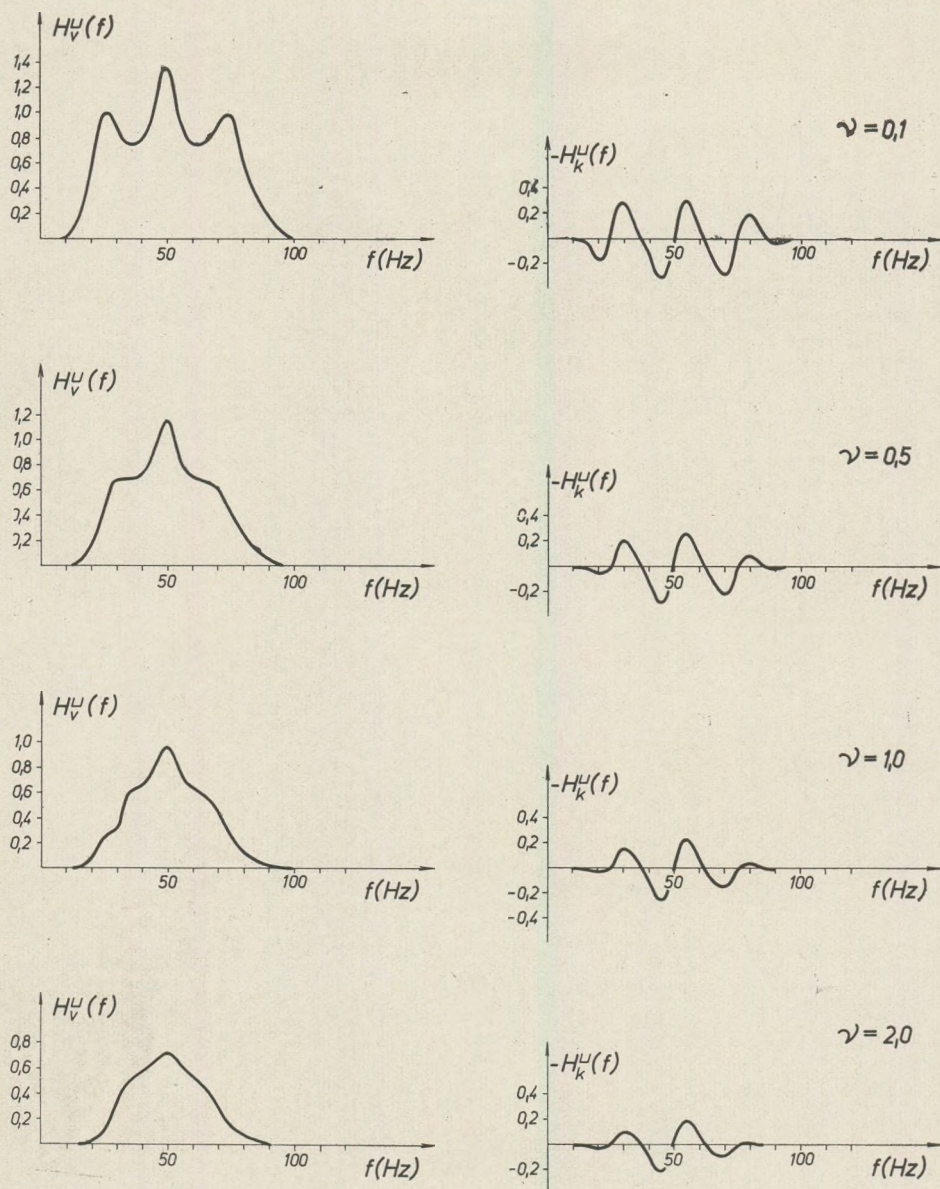


Fig. 2. Transfer functions of optimum smoothing filters which attenuate ghost reflections and random noises.

The reflection coefficient of the ghost is $k = 0.3$. The ratio of the powers of the random white noise to that of the signal is denoted by ν and varies from $\nu = 0.1$ to $\nu = 2.0$. The real and imaginary parts of the transfer functions are denoted by $S_r(f)$ and $S_i(f)$, respectively.

$$k=0,4$$

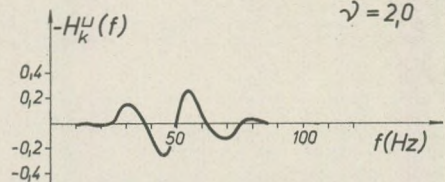
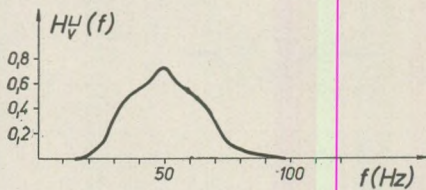
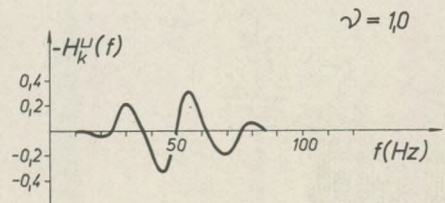
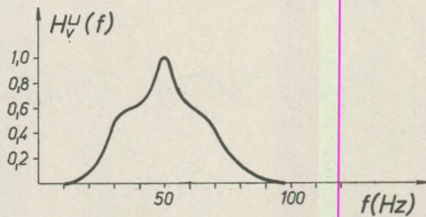
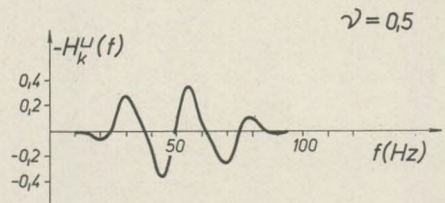
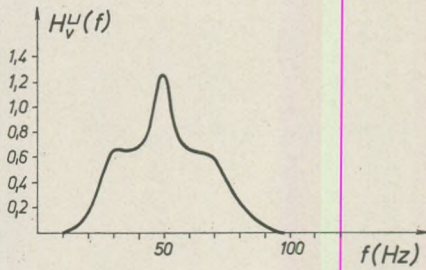
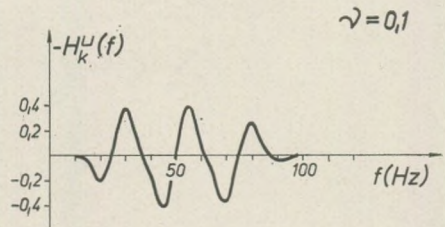
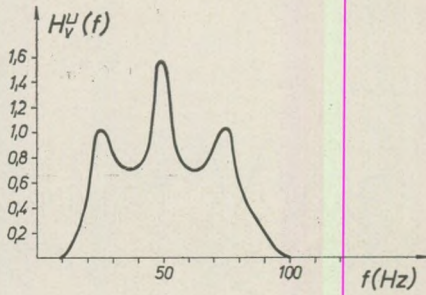


Fig. 3. Transfer functions of optimum smoothing filters which attenuate ghost reflections and random white noises. $k = 0.4$

$k = 0,5$

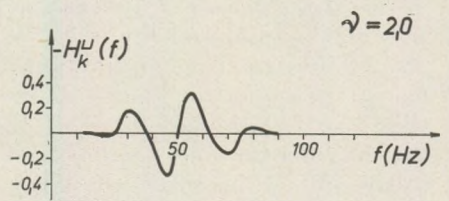
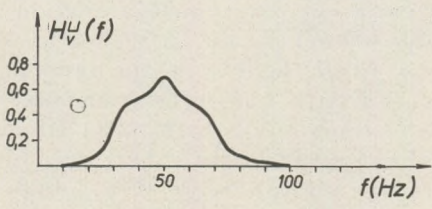
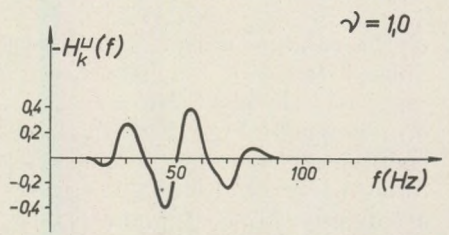
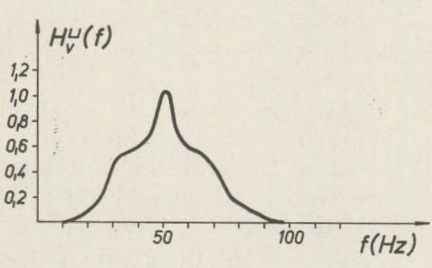
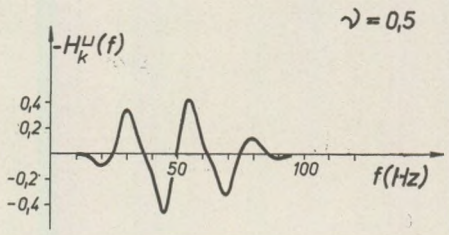
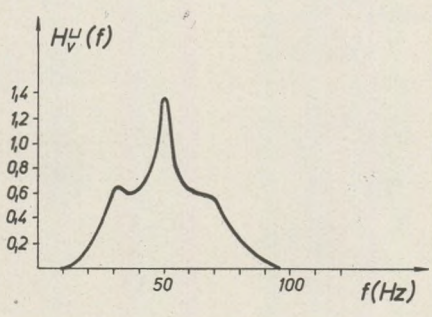
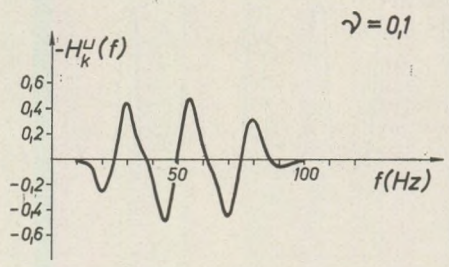
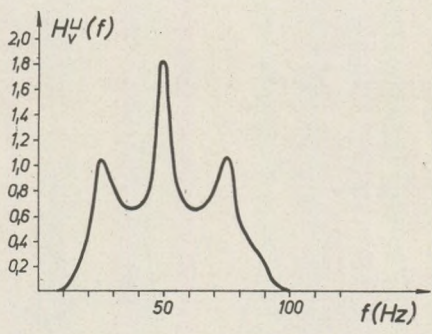


Fig. 4. Transfer functions of optimum smoothing filters which attenuate ghost reflections and random white noises. $k = 0.5$

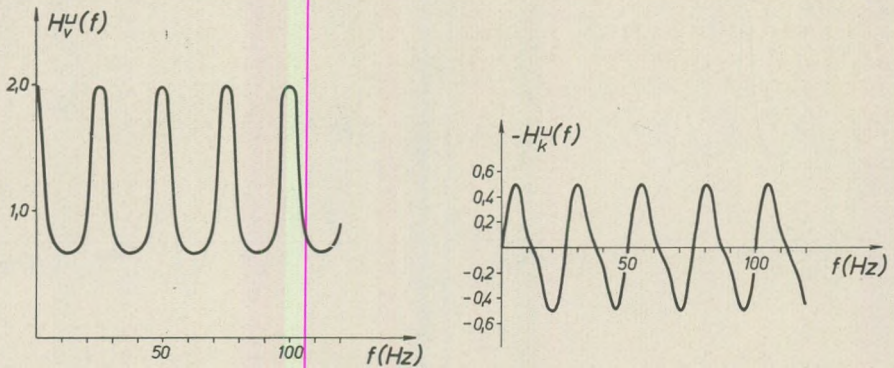


Fig. 5. Transfer function of the deghosting filter derived by Lindsey. No random noise is present $\nu = 0$. The reflection coefficient is 0.5

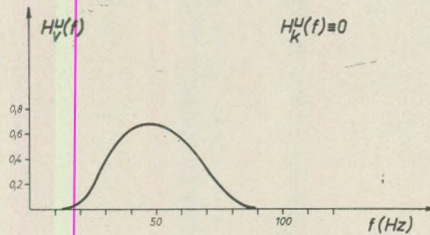


Fig. 6. Transfer function of the optimum smoothing filter when the power of the random white noise is double of the power of the signal. No ghosts are present.

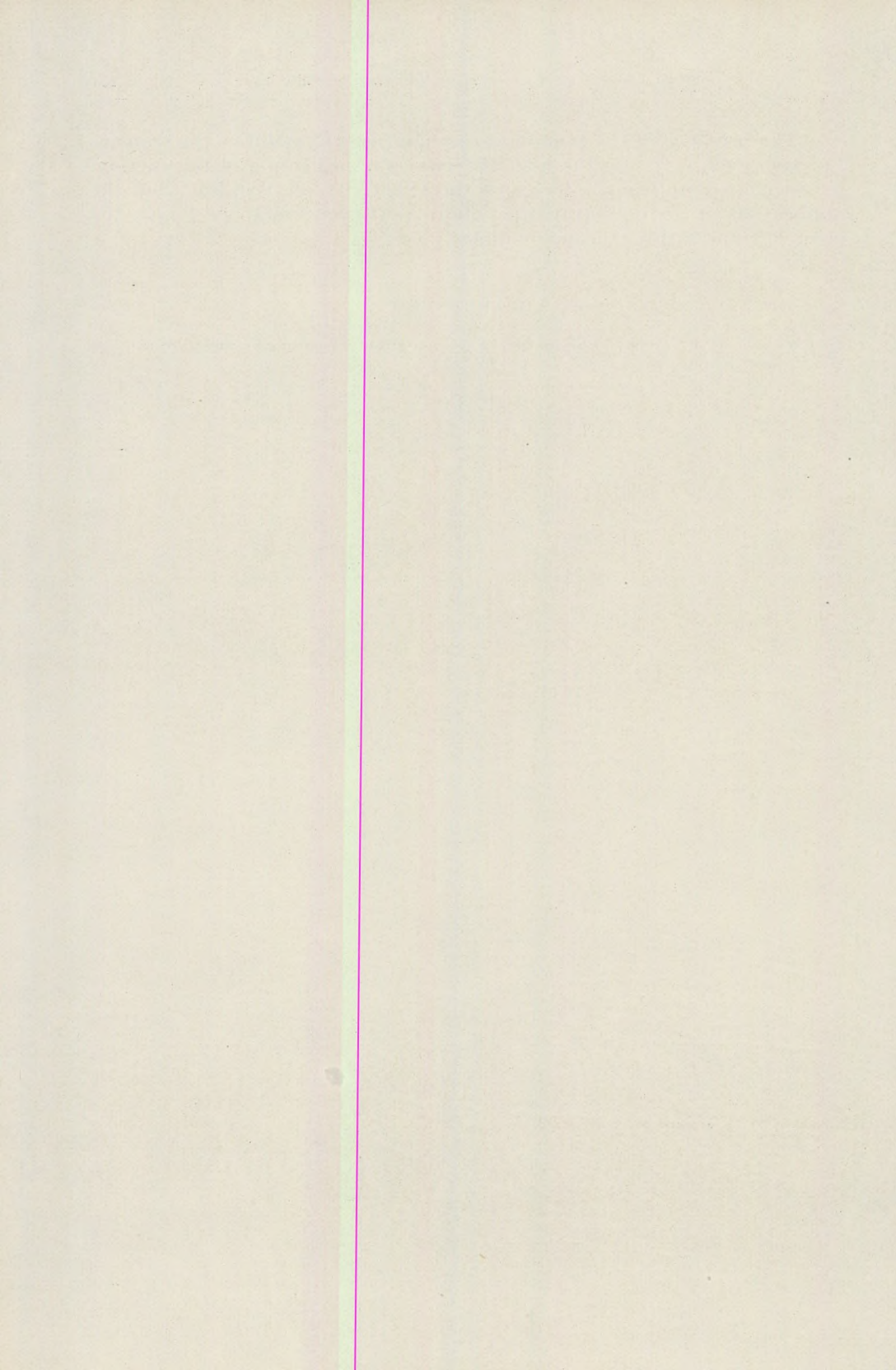
of the random noise to the power of the signal. The cases $\nu = 0.1$ (low noise level), $\nu = 0.5$ (significant noise) $\nu = 1.0$ and $\nu = 2.0$ (extremely high noise levels) were investigated. The series of the transfer functions are shown in Figs. 2 through 4. These were computed using reflection coefficients $k = 0.3$, $k = 0.4$ and $k = 0.5$, respectively. The transfer functions are complex quantities. The real parts and the imaginary parts are denoted by $S_r(f)$ and $S_i(f)$.

The regular variation with the increasing noise level is remarkable. To make easier the tracing of this variation the transfer functions of two special cases treated in the previous section are also given as Fig. 5 ($\nu = 0$, $k = 0.5$) and Fig. 6 ($\nu = 2.0$, $k = 0$). If the level of the random noise is low the transfer functions in Figs 2 through 4 have the same maxima at the same frequencies as the transfer function of the Lindsey filter (Fig. 5). When the level of the random noise increases the values of the maxima become smaller and at $\nu = 2.0$ the filters are very similar to the smoothing filter (the latter is shown in Fig. 6).

The presence of the random noise significantly modifies the transfer function even if its level is low. Therefore the neglect of the random noises more significantly decreases the effectivity of the filter than the application of an inaccurate reflection coefficient would (as far as the error remains within reasonable limits).

REFERENCE

- Lindsey, J. P. (1960): Elimination of seismic ghost reflections by means of a linear filter. *Geophysics*, vol. 25, No. 1. 130 – 141.



ГЛУБИННОЕ СТРОЕНИЕ И ГЕОТЕРМИЧЕСКИЕ УСЛОВИЯ В ВЕНГРИИ

by

L. STEGENA

(Geophysical Institute of Loránd Eötvös University)

(Received: 7. Sept. 1970)

SUMMARY

The Hungarian Basin is characterized by the following geological-geophysical features:

1. It is a young Tertiary sedimentary basin filled up by 5–10 mill. year old Pannonian-Pontian sediments with a thickness of 2,5 km in average.
2. Beneath it the earth's crust is thin, 25 km in average.
3. In this region the upper mantle has a lower than normal density.
4. It is characterized by an unusually high temperature in the depth (in 1 km e.g.: 70°C in average).
5. The high conductivity layer of the upper mantle is in an elevated position (~ 80 km).

The enumerated facts permit to draw the following conclusions:

1. The evolution of the basin is the consequence of a thinning of the earth's crust. The 8–10 km thinning of the crust resulted, as follows from isostatic calculations, in a subsidence as large as 1 km. The sedimentation lead to a further 1,5 km subsidence.
2. The thinning of the earth's crust did not originate from a phase-transition. By a higher geothermal heat not the eclogite but the gabbro phase is favoured, thus a phase-transition would cause not a thinning, but a thickening and an elevation of the crust.
3. It is difficult to connect the elevated position of the high conductivity layer in the upper mantle with the surface geothermal conditions. The Hungarian Basin developed during 3–10 mill. years; the heat transfer from a depth of 50–100 km up to the surface requires 30–100 mill. years.
4. It seems to be probable that the evolution of the basin is due to the warm convection currents immediately below the Mohorovicic discontinuity; these currents lead to the thinning of the crust and to the rising of the temperature in the upper mantle.

Венгерский бассейн представляет собой бассейн осадконакопления, заполненный молодыми третичными, в основном паннонско-понтическими отложениями (мио-плицен, 5–10 милл. лет). (Рис. 1.) Проведенные работы ГСЗ (Г а л ь ф и – Ш т е г е н а, 1957 М и т у х – П о ж г а и, 1965) показывают, что земная кора имеет здесь исключительно малую мощность, глубина залегания поверхности M равна в среднем 25 км (рис. 2.). По данным сейсмических исследований, проведенных в различных регионах мира, это явление имеет общее действие: под прогибами имеется тонкая кора (Ш т е г е н а, 1967). Этот факт позволяет судить о том, что утоньшение земной коры генетически связано с погружением; утоньшение коры вызывает погружение.

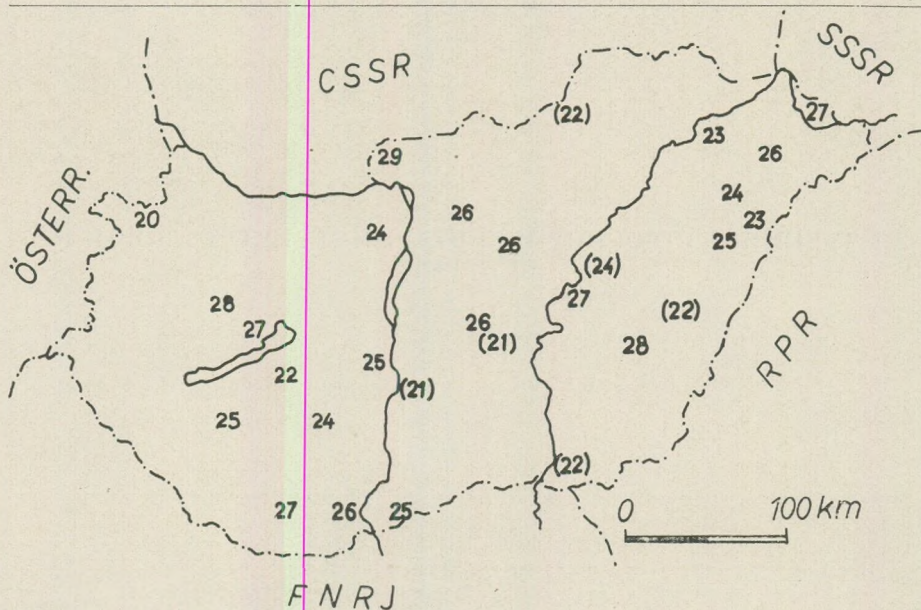


Рис. 1. Мощность третичных осадочных отложений в Венгрии, в км (Кёрёши, 1964)

Fig. 1. Thickness of the tertiary sediments in km in Hungary (after K ó r ö s s y, 1964)

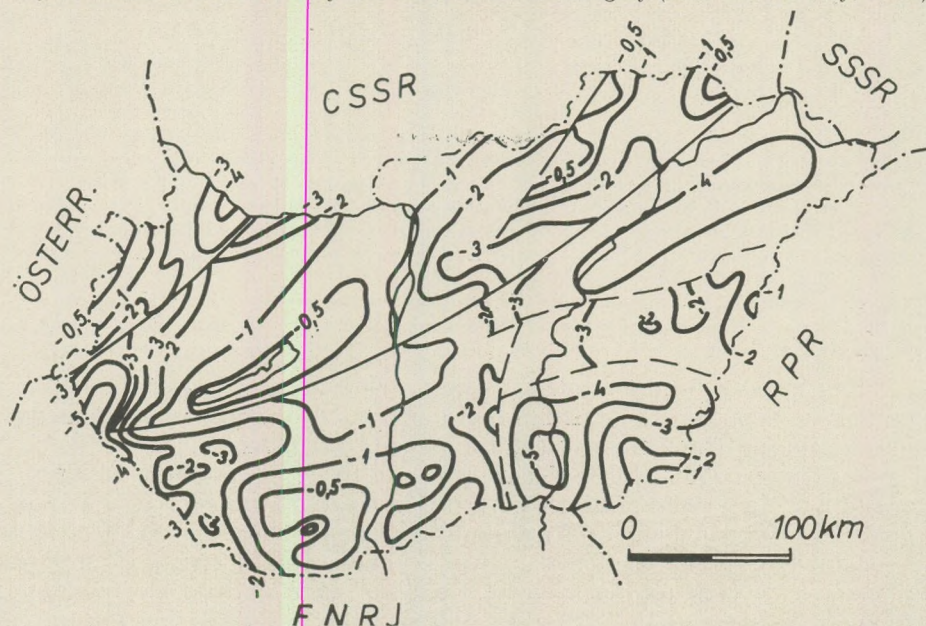


Рис. 2. Глубина залегания поверхности Мохоровичича в Венгрии в км, по данным исследований Гальфи, Митух, Пожгаи и Штегена

Fig. 2. The depth of the Moho-discontinuity in km in Hungary, based on measurements by G á l f i, M i t u c h, P o s g a y and S t e g e n a

Под Венгерским бассейном утоньшение земной коры в размере 8–10 км, вызвало, по данным изостатических вычислений, (Б а л к а и, Ш т е г е н а, 1968) погружение равное ок. 1 км. К этому добавилось погружение ~1,5 км, обусловленное осадконакоплением, достигшим мощности ок. 2,5 км (рис. 3).

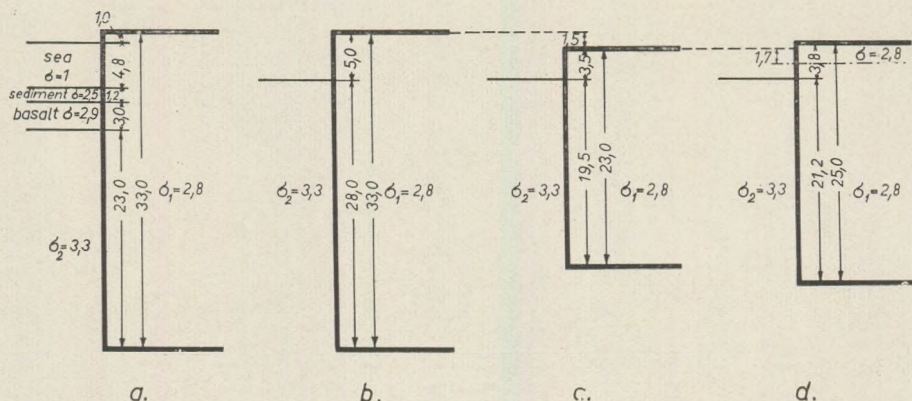


Рис. 3. Строение земной коры в условиях изостатического равновесия. Условное обозначение: а – средняя, „нормальная” кора; б – то же, морское строение в пересчете на вещество мантии; в – снизу кора утоньшилась на 10 км, причем поверхность погрузилась на 1,5 км; г – сверху на кору отложилось коровое вещество мощностью в 2 км, старая поверхность коры погрузилась на дополнительное 1,7 км

Fig. 3. Crustal structures in isostatic equilibrium

Legend: a) average “normal” crust; b) idem, marine structure converted into mantle material; c) crust thinning by 10 km in thickness at its base, surface subsided by 1,5 km; d) the thinned crust is overlain by 2 km of mantle material, the former surface has subsided by an additional 1,7 km

В осадочных отложениях Венгерского бассейна господствуют весьма высокие величины геотермической температуры (см. приложение); средняя температура, измеренная на глубине в 1 км (70°C) составляет в два раза большую величину по сравнению с восточно-европейским средним значением.

Сопоставление мощности земной коры с геотермическими условиями позволяет судить о том, что преобразование коры под бассейном обусловлено не фазовым переходом габбро-эклогит (К е п п е д ы 1959, W y l l i e 1963, S t i s h o v 1963, Y o d e r - T i l l e y 1961). Повышенные температуры способствуют габбровой фазе (рис. 4) и так повышение температуры привело бы к утолщению и подъему коры.

Данные магнитотеллурических исследований (А д а м, 1969) показывают, что под Венгерским бассейном хорошо проводящий горизонт находится в приподнятом положении; средняя глубина его

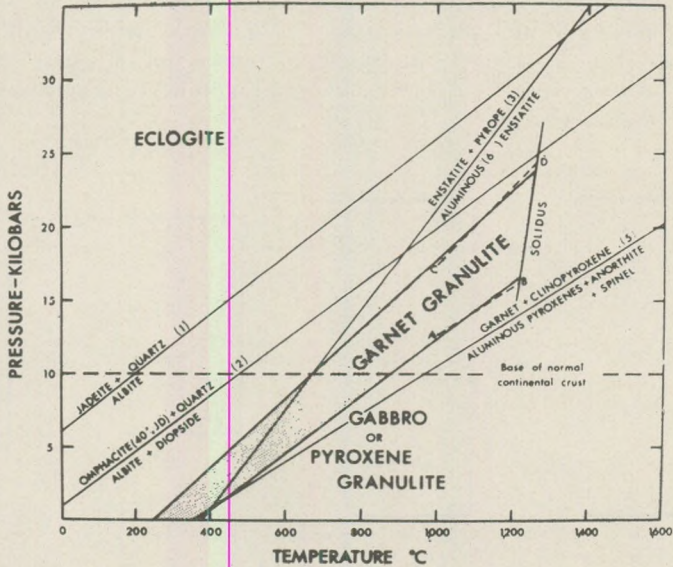


Рис. 4. Поля устойчивости габбро и эклогита, по Ringwood, Green, 1966
 Fig. 4. Stability fields of gabbro and eclogite, after Ringwood and Green 1966

залегания составляет 80 км. Кажется, что такая связь имеет общее действие: в регионах с повышенными величинами геотермического тепла хорошо проводящий слой имеет приподнятое положение.

При попытках связывать приподнятое положение хорошо проводящего слоя с высокими величинами геотермического тепла вблизи дневной поверхности и с образованием Венгерского бассейна возникают затруднения. Эти затруднения связаны с медленностью теплопроводности.

Скорость теплопроводности. Посмотрим однородный горизонтальный слой, температура которого до момента времени $t = 0$ равна $T = 0$. Пусть на его нижней поверхности $z = h$ в момент $t = 0$ возникает постоянная температурная аномалия с амплитудой T_0 , причем на верхней поверхности сохраняется постоянная температура $T = 0$. Такая модель (рис. 5) хорошо согласуется с фактическими геологическими условиями.

Как известно, температура T , действительная в момент t для глубины z , выражается в виде

$$T = T_0 \left(\frac{z}{h} + \frac{2}{\pi} \sum_{n=1}^{\infty} \frac{(-1)^n}{n} e^{-\frac{h^2 \pi^2 n^2 t}{h^2}} \sin n\pi \frac{z}{h} \right)$$

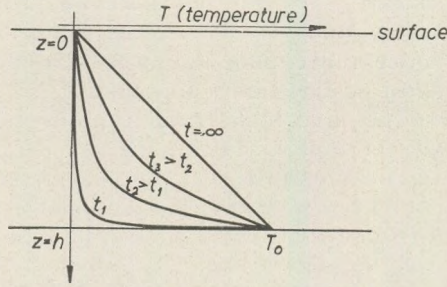


Рис. 5. Образование стационарного температурного поля в слое мощностью h
 Fig. 5. Formation of stationary temperature field in a layer of h thickness

а стационарная температура ($t = \infty$) —

$$T = T_0 \frac{z}{h}$$

Посмотрим, когда фактически образующееся температурное поле достигает α_1 ($\alpha \leq 1$) — кратной величины стационарной температуры ($T = \alpha T_0 \frac{z}{h}$). Вблизи дневной поверхности, при достаточно низких величинах $\frac{z}{h}$, $\sin n\pi \frac{z}{h} = n\pi \frac{z}{h}$, и так

$$\frac{\alpha - 1}{2} = \sum_{n=1}^{\infty} (-1)^n e^{-h^2 \pi^2 \frac{kt}{h^2}}$$

При решении уравнения получаются следующие принадлежащие друг к другу пары величин α и $\frac{kt}{h^2}$ (критерия Фурье):

α	0,5	0,9	0,99
$\frac{kt}{h^2}$	0,14	0,30	0,53

50% от приповерхностной температурной аномалии, происходящей из нижней температурной аномалии, возникает при величине параметра Фурье, равной $\frac{kt}{h^2} = 0,14$; если $k = 10^{-2} \text{ см}^2\text{s}^{-1}$ и $h = 100 \text{ км}$, то $t = 44$ милл. лет. 90% от температурной аномалии появляется вблизи дневной поверхности после истечения времени $t = 95$ милл. лет, а 99% — $t = 168$ милл. лет после появления нижней температурной аномалии.

В итоге можно сказать, что для достижения температурной аномалией, возникшей на глубине 50–100 км, дневной поверхности требуется значительно более длительное время по сравнению с временем, истекшим с образования Венгерского бассейна.

Температурные аномалии, появляющиеся на территории более молодых геологических регионов, как правило, всегда трудно связывать с аномальным положением хорошо проводящего слоя, залегающего на глубинах 50–100 км. Разности теплового потока, измеренные на территории США. (Ray, Blackwell и Birch, 1968) приурочиваются к глубинам 7–11 км.

Теплопередача. Теплопередача может быть более быстрым процессом, чем теплопроводность. Учитывая скорость растяжения дна океана (несколько см в год), для проходки пути в 100 км достаточно несколько миллионов лет.

Интересно отметить, что на территории Венгерского бассейна на больших глубинах наблюдается интенсивная геоэлектрическая анизотропия. Эту анизотропию легче всего объяснить наличием очень глубокого (50–100 км) разлома широтного простирания (Адам, 1969). Расплавленное вещество, проникшее вверх по этим разломам могло способствовать переносу тепла к поверхности.

Растяжение. Вероятно, что утоньшение земной коры под Венгерским бассейном вызвано теплыми конвекционными течениями ниже поверхности Мохоровичича. Они привели к утоньшению коры и к повышению температуры в верхней мантии. Конвекционные течения могут быть связаны с растяжением Тетисского моря (Syvester – Bradley, 1968).

LITERATURE

- Á d á m, A. (1969): Appearance of the electrical inhomogeneity and anisotropy in the result of the complex electrical exploration of the Carpathian Basin. *Acta Geodaet. Geophys. et Montanist. Acad. Sci. Hung.* 4. 1-2.
- B a l k a y, B., S t e g e n a, L. (1968): Some geophysical and geological aspects of crustal structure evolution in the Hungarian Basin. *Ann. Univ. Sci. Budapestiensis, Sec. Geol.* XI. 1967.
- М е С о n n e l l, R. (1968): Viscosity of the mantle from relaxation time spectra of isostatic adjustment. *Jour. Geophys. Res.* 73. 22.
- Y o d e r, H. S., T i l l e y, C. E. (1961): Origin of basalt magma: an experimental study of natural and synthetic rock systems. *Jour. Petrol.* 3.
- K e n n e d y, G. C. (1959): The origin of continents, mountain ranges and ocean basins. *Am. Scientist*, 47.
- K u t a s, R. I. (1968): О связи теплового потока с глубинными процессами. *Геофиз. Сборн.* 25. 1968.
- Л ю б и м о в а, Е. А. (1968): О связи распределения теплового потока с тектоническими структурами. 23 Международн. Геол. Конг. Прага, 1968. Доклады Советских Геологов Проб. 5. Издательство Наука, 1968.
- R i n g w o o d, A. E., G r e e n, D. H. (1966): An experimental investigation of the gabbro-eclogite transformation and some geophysical implications. *Tectonophysics* 3. 5.
- R a y, A. F., B l a c k w e l l, D. D., B i r c h, F. (1968): Heat generation of plutonic rocks and continental heat flow provinces. *Earth and Plan. Sci. Letters*, 5. 1.
- С т и ш о в, С. М. (1963): Природа границы Мохоровичича. Изд. АН СССР сер. геоф. 1.
- S y l v e s t e r, C., B r a d l e y, P. C. (1968): The last ocean. *Sci. Journ.* 4. 9.
- S t a c e y, F. D. (1968): Energy balance of mantle convection. *Tectonophysics* 5.4.
- S t e g e n a, L. (1967): Il principio dell' attualismo e la superficie Moho. *Boll. di Geofisica* VIII. 31.
- T u r c o t t e, D. L., O x b u r g h, E. R. (1969): Convection in a mantle with variable physical properties. *Jour. Geophys. Res.* 6.
- W i l l i e, P. I. (1963): The Nature of the Mohorovicic Discontinuity. A Compromise. *Jour. Geophys. Res.* 15.

DIE VORHERSAGE VON TEMPERATURMINIMA AN HEITEREN TAGEN AUF GRUND RELATIVER TOPOGRAPHIEN VON 850/1000 MB

RÁKÓCZI FERENC

(Lehrstuhl der Meteorologie, Eötvös Loránd Universität, Budapest)

(Eingegangen am 10. VI. 1970)

РЕЗЮМЕ

В работе даются формулы для предсказания минимальных величин температуры, действительные для городов Будапешт и Мюнхен. Описываются возможности применения этих формул.

Die Vorhersage von Temperaturminima ist aus wirtschaftlichem und synoptischem Standpunkte von Bedeutung. In der Alltagspraxis wird dies in den meisten Fällen im Wege von Abschätzung vorgenommen. Die Lösung des Problems wird von vielen Forschern auf theoretischem Wege oder mit Hilfe von empirischen Formeln versucht. Die theoretischen Formeln nehmen – wenn die Auswirkung aller das Temperaturminimum beeinflussenden Faktoren in Betracht gezogen wird – eine verwickelte Form an, die für die Praxis beinahe unverwendbar ist. Dies spornt die Forscher zur Ausarbeitung von Vereinfachungen an [Scherhag 1948, Reuter 1951].

Bei der Konstruktion von empirischen Formeln wird die Erfahrung und die Messungen zu Hilfe gerufen und man bemüht sich, anhand der in den Messungsergebnissen vorgefundenen Gesetzmässigkeiten eine Formel zur Vorhersage zu finden. Diese Formeln sind natürlicherweise mit den Eigenheiten des Beobachtungsortes belastet, so dass sie an anderen Beobachtungsorten nur mit Vorbehalt angewandt werden können.

Ein gemeinsamer Zug aller Formeln der Prognose der Temperaturminima besteht darin, dass sie die nächtliche Abkühlung auf die effektive Ausstrahlung zurückführen. Aus diesem Grunde wird eine besondere Aufmerksamkeit den Luft- und Bodenverhältnissen, dem Wasserdampfgehalt der Luft, dem Wind und der Bewölkung zugewendet. Dies ist auch evident, denn die günstigen Vorbedingungen der nächtlichen Abkühlung sind erfahrungsgemäss:

- a) klarer Himmel,
- b) Windstille,
- c) niedriger Wasserdampfdruck in der Atmosphäre.

Scherhag [1948] bewies, dass zwischen dem relativen Geopotential von 500/1000 mb, und dem Temperaturmaximum ein gut ausgedrückter, nahezu linearer Zusammenhang besteht. Ein ähnlicher Zusammenhang wurde auch von dem Verfasser des vorliegenden Aufsatzes hinsichtlich Budapest [Rákóczi, 1957] gefunden. Im Zusammenhang mit diesen Erwägungen tauchte der Gedanke auf, dass dieser Zusammenhang auch zwischen dem Temperaturminimum und dem am Nachmittag ausgeführten Aufstieg sich ergebenden relativen Geopotential von 500/1000 mb bestehen muss. Im Laufe des Beweises dieses Zusammenhanges wurde die Erfahrung gemacht, dass zwischen dem am Nachmittag registrierten relativen Geopotential von 500/1000 mb und dem Temperaturminimum kein so strenger Zusammenhang besteht, als zwischen dem bei Tagesanbruch registrierten relativen Geopotential von 500/1000 mb und dem Temperaturmaximum. Aero-logische Erfahrungen erwiesen, dass die Höhe der sich am Morgen bildenden Inversionen das Niveau von 850 mb erreicht [Béll, 1954]. Diese Tatsache führte auf den Gedanken, dass ein Zusammenhang zwischen dem am Nachmittag ausgeführten Aufstieg registrierten relativen Geopotential von 850/1000 mb und dem Temperaturminimum gesucht werden muss (Abb. 1).

Im Laufe der Bearbeitung des Materials wurde auf jene physikalischen Bedingungen besonderer Bedacht genommen, welche die Ausbildung der Temperaturminima begünstigen. Derart wurden aus dem zur Verfügung stehendem Material der Jahre 1953–1955 bezüglich München und Budapest jene Tage ausgewählt, an welchen:

- a) die Bewölkung im Laufe der ganzen Nacht 4/10 nicht überstieg,
- b) die Geschwindigkeit des Bodenwindes 3 m/sec nicht überstieg,
- c) kein Niederschlag registriert wurde.

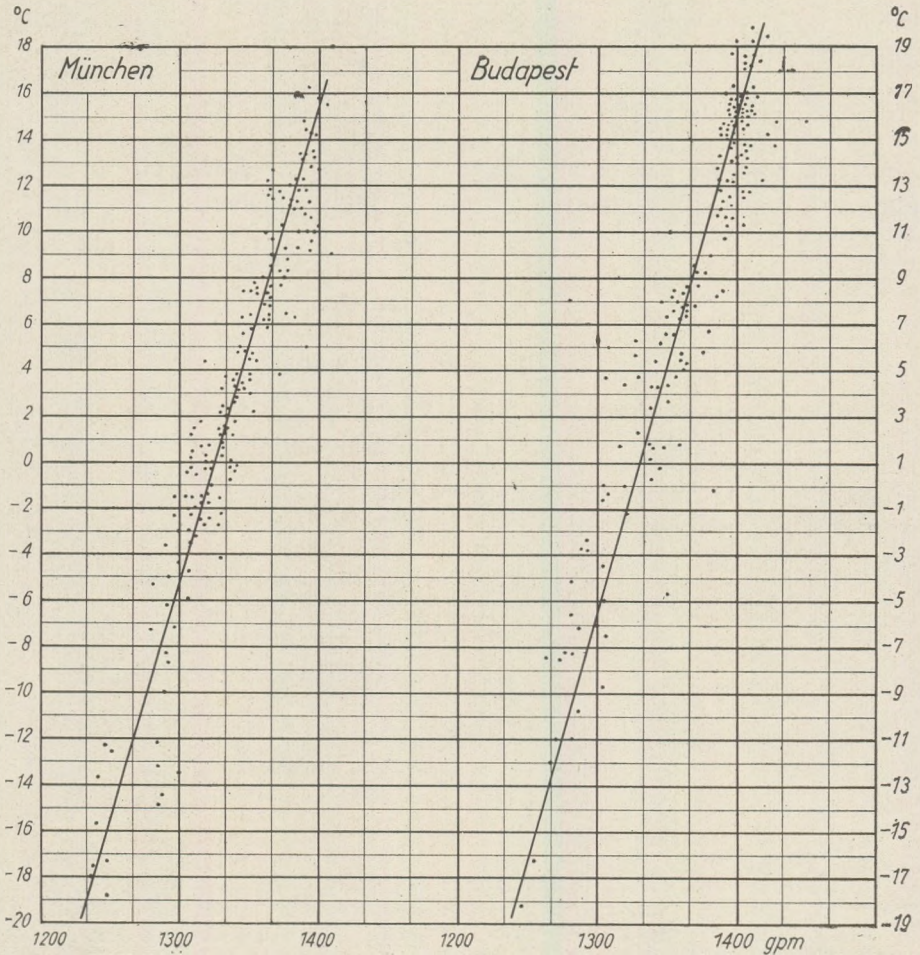
In der unterstehenden Tabelle 1 bringen wir die den obigen Bedingungen entsprechenden Tage aus den erwähnten drei Jahren:

Tabelle 1

Verteilung der zur Anwendung gelangten heiteren und nahezu windstillen Tage

		I	II	III	IV	V	VI	VII	VIII	IX	X	XI	XII	—
Budapest	1953	—	2	12	8	8	3	5	11	6	10	6	2	73
	1954	3	5	2	0	6	4	2	8	12	0	4	1	47
	1955	0	1	2	5	6	2	4	5	16	4	1	0	46
	Σ	3	8	16	13	20	9	11	24	34	14	11	3	166
München	1953	1	2	15	11	8	2	7	8	10	7	3	5	79
	1954	3	4	6	3	7	4	3	3	7	6	4	0	50
	1955	3	1	3	6	5	3	2	8	8	7	4	1	51
	Σ	7	7	24	20	20	9	12	19	25	20	11	6	180

Die Zusammenhängenden Werte der relativen Topographie und der Temperaturmaxima wurden auch graphisch dargestellt (Abb. 1). Auf der Abszissenachse wurden die an dem Nachmittage des vorhergegangenen Tages registrierten Geopotentialwerte, auf der Ordinate die Temperaturminima angebracht. Die Verteilung der zusammenhängenden Punkte sind auf der beiliegenden (Abb. 1) ersichtlich.



Aus der Abbildung geht klar hervor, dass zwischen dem Temperaturminimum und dem relativen Geopotential von 850/1000 mb ein stochastischer Zusammenhang besteht. Die Linearität dieses stochastischen Zusammenhanges steht ausser Zweifel. Die Streuung der Punkte um den — dem Mittelwert entsprechenden — Geraden ist so klein, dass es empfehlenswert erscheint, mit Hilfe der statistischen Methode einen Zusammenhang zwischen den in Rede stehenden Wertepaaren zu suchen.

Wie bekannt, kann der lineare Zusammenhang zwischen den um den Geraden mit einer kleinen Streuung liegenden Punkten in der Form einer Regressionsgleichung aufgeschrieben werden [Bogárdi, 1952]. Die Regressionsgleichung ermöglicht – in Kenntnis der unabhängigen Veränderlichen – die Bestimmung des wahrscheinlichsten Wertes der abhängigen Veränderlichen.

Zur Bestimmung des Regressionsgeraden wird laut der bekannten Theorie im Falle eines linearen Zusammenhanges die in der folgenden Form erscheinende Lösung gesucht:

$$(y - \bar{y}) = b(x - \bar{x}) \quad (1)$$

wo die Mittelwerte der beiden Wertepaare mit \bar{y} , bzw. \bar{x} bezeichnet und b den Tangens der gesuchten geraden Richtung bedeutet. Die Bestimmung der Richtungstangente kann mit Hilfe der folgenden Formel vorgenommen werden:

$$b = \frac{\sum \Delta x \cdot \Delta y}{\sum (\Delta x)^2} \quad (2)$$

wo $\Delta x = x - \bar{x}$, $\Delta y = y - \bar{y}$, $(\Delta x)^2 = (x - \bar{x})^2$ bedeuten.

Dem x entspricht im Laufe des Weiteren das relative Geopotential von 850/1000 mb, und dem y das Temperaturminimum. Das relative Geopotential von 850/1000 mb wird im weiteren mit RT_{1000}^{850} , das Temperaturminimum mit t_m bezeichnet. In Tabelle 2 werden Charakteristikenwerte der Regressionsgleichung auf München und Budapest angeführt.

Tabelle 2

Die Charakteristika der Regressionsgleichung bestimmenden Konstante

	\bar{t}_m	$\overline{RT}_{1000}^{850}$	$\Sigma \Delta RT_{1000}^{850} \Delta t_m$	$\Sigma (\Delta RT_{1000}^{850})^2$	$\Sigma (\Delta t_m)^2$	r
Budapest	8,95	13,72	550,63	31,64	11 117,38	0,93
München	3,08	13,39	502,11	25,48	10 349,07	0,97

In der obigen Tabelle bedeuten:

\bar{t}_m = Mittelwert des Temperaturminimums,

$\overline{RT}_{1000}^{850}$ = der in geopotentiellen Hektometer ausgedrückte Mittelwert des relativen Geopotentials,

$\Sigma \Delta RT_{1000}^{850} \Delta t_m$ = Summe der Produkte der Abweichungen vom Mittelwerte,

$\Sigma (\Delta RT_{1000}^{850})^2$ und $\Sigma (\Delta t_m)^2$ = Summe der Quadrate der Abweichungen,

r = Korrelationskoeffizient der in Rede stehenden Wertepaare.

An Hand der Tab. 2 können die gesuchten Regressionsgleichungen auf Budapest und München aufgeschrieben werden:

Budapest

$$t_m - 8,95 = 17,4(RT_{1000}^{850} - 13,72) \quad (3)$$

und

$$t_m = 17,4 RT_{1000}^{850} - 229,78 \quad (3a)$$

München

$$t_m = 19,7 RT_{1000}^{850} - 260,7 \quad (3b)$$

Der Korrelationskoeffizient ist der Ausdruck des Zusammenhanges zwischen den zwei Wahrscheinlichkeitsveränderlichen. Wie aus der letzten Spalte der Tab. 2 hervorgeht, ist dies ein sehr hoher Wert, nämlich 0,97 für München und 0,93 für Budapest.

Dies, sowie jene Tatsache, dass bei der Regressionsgleichung die Angaben der bei dem am Nachmittage ausgeführten Radiosondenaufstieg registrierten Topographien zu Grunde genommen wurden, ergibt — an Hand unserer Gleichungen — die Möglichkeit zur Vorhersage der Morgen-temperaturminima.

Unsere Vorhersageformeln behalten ihre Gültigkeit natürlich nur im Falle des Bestehens jener Bedingungen, bei welchen sie aufgestellt wurden. Auf dieser Weise muss im Laufe ihrer Anwendung Sorge dafür getragen werden, dass den obenerwähnten vier Postulaten nachgekommen wird.

Auf Grund von Budapester Angaben haben wir auf das Jahr 1956 den Versuch einer Prognose der Temperaturminima ausgeführt. Im Laufe des untersuchten Jahres wurden 65 solche Tage gefunden, an welchen die Wetterlage eine solche war, dass mit Hilfe unserer Formel 3a die Vorhersage der Temperaturminima versucht werden konnte. Es wurde festgestellt, dass diesem Jahre der Mittelwert des absoluten Wertes der Abweichungen zwischen den von uns vorhergesagten und tatsächlich registrierten Temperaturminima

$$\frac{\sum |\Delta t|}{m} = 1,5 \text{ } ^\circ\text{C}$$

war. In diesem Falle ist $\Delta t = t'_m - t_{msz}$, wo t'_m das beobachtete, und t_{msz} das berechnete Temperaturminimum bedeutet. Von besonderem Interesse ist auch das prozentuelle Vorkommen der einzelnen Abweichungen. Diese Werte sind in Tab. 3 angeführt.

In der obigen Tabelle sind die Vorkommenszahlen und das prozentuelle Vorkommen jener Fälle angegeben, welche sich auf die einzelnen Abweichungswerte beziehen. In die Abweichungskategorie $\cong |1,5| \text{ } ^\circ\text{C}$ gehören derart sämtliche, diesen Grad nicht erreichende Abweichungen, so auch die Abweichungen $\cong |0,5|$ und $\cong |1,0|$. Aus der Tabelle geht auch die Möglichkeit der synoptischen Verwendbarkeit der Methode hervor. Wenn nämlich erfordert wird, dass die Genauigkeit der Prognose im Intervall der in der Synoptik üblichen 3°C bleibt, so kann mit Hilfe der dargelegten Methode mit einer Wahrscheinlichkeit von 87% prognostiziert werden.

Tabelle 3

Vorkommenswahrscheinlichkeiten der Vorhersage

Abweichungen C°	Zahl der Fälle	%
0,5	14	21
1,0	29	44
1,5	38	58
2,0	48	74
2,5	52	80
3,0	57	87
3,5	58	89
4,0	62	95
7,6	65	100

An Mangel von Angaben konnten auf München keine ähnlichen Berechnungen ausgeführt werden. Der auf München bezügliche Korrelationskoeffizient von $r = 0,97$ lässt aber vermuten, dass auf dem Gebiete der Prognose ähnlich Resultate zu erwarten sind.

Der Grund des engen Zusammenhanges besteht unseres Erachtens darin, dass das Temperaturmittel der Atmosphärenschicht, welches eine Funktion auch des Temperaturgradienten ist, die Dicke jener Schicht bestimmt, welche durch die nächtliche Ausstrahlung in der Vorbereitung der Inversion teilnimmt. Hierauf lässt sich auch daraus zu schliessen, dass zwischen den aus den Morgenaufstiegen ermittelten Geopotentiale und den Temperaturmaxima des Nachmittags ein ähnlicher Zusammenhang besteht [Scherhag, 1948; Rákóczi, 1957].

Es muss von einer Überschätzung unserer Ergebnisse gewarnt werden, da die letzteren ihre Gültigkeit nur in einer beschränkten Anzahl der Fälle und bei dem Zutreffen der erwähnten Voraussetzungen behalten. Es kann aber festgestellt werden, dass an Hand unserer Prognoseformel die zu erwartenden Temperaturminima schnell und innerhalb der in der Synoptik erforderten Genauigkeitsgrenzen festgestellt werden können.

LITERATUR

- Scherhag, R. (1948): Wetteranalyse und Wetterprognose. Berlin.
- Reuter, H. (1949): Die Modifikation einer Luftmasse durch nächtliche Abkühlung der Erdoberfläche. Archiv für Meteorologie, S. A. B. T.
- Reuter, H. (1951): Forecasting Minimum Temperatures. Tellus.
- Dr. Béll B. (1954): A troposzféra éghajlata Magyarország fölött. (Klima der Troposphäre über Ungarn). Budapest.
- Bogárdi J. (1952): Korrelációs számítás és alkalmazása a hidrológiában. (Korrelationsrechnung und ihre Anwendung in der Hydrologie). Budapest.
- Dr. Rákóczi F. (1957): Az 500/1000 mb-os relatív geopotenciál kapcsolata a napi hőmérsékleti maximummal derült napokon. (Zusammenhang des relativen Geopotentials von 500/1000 mb mit dem Tagestemperaturmaximum an heiteren Tagen). Időjárás, 62.

THE LOWER AND MIDDLE JURASSIC BIVALVES OF THE VILLÁNY MOUNTAINS

by
A. VÖRÖS

(Chair of Palaeontology, Eötvös University, Budapest)

(Received: 28 May 1970)

РЕЗЮМЕ

Из юрских отложений гор Виллань описан 31 вид пластинчатожаберных моллюсков, из которых пять было найдено в плинсбахских отложениях, девятнадцать в батских и семь в келловейских. Два из этих видов являются новыми: *Proreamussium brevicostatum* n. sp. и *Pholadomya villanyensis* n. sp. Наряду с краткой палеоэкологической оценкой двусторок отдельных горизонтов можно было бы сделать вывод о том, что если фауна плинсбахских и батских отложений носит западноевропейский характер, то фауна аммонитовой пачки келловея однозначно не отражает такого же характера.

The investigated Bivalvia fauna derives from a discontinuous sequence of low thickness representing the Lower to Middle Jurassic in the eastern part of the Villány Mountains. The bivalves here are not too frequent. Nevertheless, a rather rich material has been accumulated in the museum of the Hungarian Geological Institute as a result of collecting for a hundred years or so. The present writer had the opportunity to study the fauna consisting of more than 200 specimens. In addition, Dr. A. Kaszap kindly gave the author his own collection for study.

The Villány fauna was first dealt with by Lóczy (1912, 1915). In both of his afore-mentioned papers he published the resulting faunal lists:

- Anisocardia campaniensis* (d'Orb) Cossm.
- Pholadomya escheri* Ag.
- Pleuromya* cf. *elongata* Ag.
- Pleuromya decurtata* Ag.
- Inoceramus obliquus* Morr., Lyc.
- Perna subtilis* Lahusen
- Lima* (*Plagiostoma*) *obscura* Sow.
- Pecten* (*Entolium*) *disciformis* Schübler Zieten
- Ostrea* (*Gryphaea*) n. sp.
- Pecten* (*Chlamys*) *Thierryi* Cossm.
- Pecten* (*Entolium*) *demissus* Phil.

Since Lóczy no publication has been devoted to this subject.

Stratigraphy

Exposed as it is at present, the Lower and Middle Jurassic of the Villány Mountains can be split up into four formations, each representing a more or less independent phase of sedimentation.

1. Pliensbachian carbonate sequence with varying percentage of terrigenous material,
2. Bathonian sandy limestones,
3. Lower Callovian oöid-patterned limestones,
4. Callovian ammonitic bed.

At the turn of the century a fifth formation too seems to have been exposed. This is suggested by the great number of such bivalves in the collection of the museum which are enclosed in a dark-brown rock sharply differing in lithology from all the above formations. Enclosed in the same extremely peculiar country rock are a very great number of brachiopods, a few ammonites and other faunal elements. The labels accompanying them in the museum indicate, in complete agreement, Villány as locality. However, no rock of this kind is presently available on the surface in the vicinity of Villány. Since a comparatively rich fauna is being considered, there is no question of eventual mixing of materials in the museum. Like the other formations in the vicinity of Villány, this one seems to have represented a lenticular body which totally disappeared during quarry operations.

A detailed discussion of the sedimentology and biostratigraphy of the rocks available in outcrop is the subject of a separate paper (V ö r ö s, 1971, in preparation).

The Pliensbachian carbonate sequence

This formation, attaining a maximum of 8 m or so near Villány and more than 12 m on the Harsány hill some 6 km farther west, was considered to be Bathonian since the earliest students of the area (L e n z, 1872; H o f m a n n, 1876; L ó c z y, 1912). During the excursions of the Colloquium on Mediterranean Jurassic Stratigraphy, Budapest 1969, a few well-preserved ammonites were found in special new diggings. On the basis of these Dr. J. C. Callomon and Dr. D. T. Donovan concluded to have here the Jamesoni Zone of the Pliensbachian. After studying brachiopods collected from this locality, Dr. D. V. Ager arrived at the same result (personal communication).

The basal levels of the formation are constituted by calcareous sandstones and conglomerates grading upwards into pure limestones which represent biomierite with organic matter and pyrite. As shown by lithological results, the formation was deposited in sublittoral, intermittently agitated waters.

The lower, sandstone, member is practically devoid of fauna, whereas the limestone member contains a comparatively rich micro- and macro-

fauna. Bivalves are represented by the following elements (in brackets: numbers of specimens):

- Isognomon* sp. (4)
- Entolium hehlii* (d'Orbigny) (13)
- Entolium* sp. indet. (7)
- Chlamys* (*Aequipecten* ?) cf. *prisca* (Schlotheim) (11)
- Chlamys* (*Aequipecten* ?) *humberti* (Dumortier) (3)
- Chlamys* sp. indet. (9)
- Anomia* sp. (1)
- Antiquilima succincta* (Schlotheim) (1)
- Plagiostoma* sp. (1)
- Gryphaea gigantea* J. de C. Sowerby (2)
- Gryphaea* sp. (3)
- Pleuromya* ? sp. (1)

The overwhelming majority of the fauna is constituted by epibenthonic Pectinacea, capable of swimming. These have been embedded in form of single valves. The burrowers are represented by a single, tiny *Pleuromya*. The lack of burrowing lamellibranchs, as a rule, is considered to be a feature suggestive of a hard ground. In the case under consideration, however, the rock shows distinct traces of bioturbation which can be considered to cancel a hypothesis of this kind. As evidenced by bioturbation phenomena, an anaerobic bottom environment cannot account for the absence of burrowing bivalves — a hypothesis suggested by Hudson and Palfyraman (1969) in a study of the Oxford Clay — either. (Such an explanation does not look plausible also because a burrowing bivalve obtains its oxygen and nutrients through a siphon exposed to the surface, thus being little disturbed by the anaerobic nature of the mud surrounding it.)

All of the five species determined of the fauna are widespread in Western Europe, being confined in the Alpine-Carpathian zone to isolated localities of the so-called "Gresten facies". Whereas the lamellibranch fauna of the Bakony Mountains Pliensbachian shows a definite South-Alpine (Mediterranean) feature, not a single species of Mediterranean character can be encountered among the lamellibranchs of the same age of the Villány Mountains in the south.

The Bathonian brown limestones

At present this formation is not exposed in the vicinity of Villány. On the basis of the few opeliid ammonites available in the museum, A. Galác referred its age to the Bathonian.

The lamellibranch fauna consists of the following elements:

- Cucullaea* (*Idonearca* ?) sp. (2)
- Inoperna sowerbyana* (d'Orbigny) (5)
- Modiolus anatinus* (Smith) (1)
- Modiolus* sp. (1)
- Stegoconcha* sp. aff. *granulata* (Sowerby) (1)
- Gervillella siliqua* (Deslongchamps) (3)
- Meleagrínella* sp. (1)

- Entolium corneolum* (Young et Bird) (5)
Chlamys sp. indet. (1)
Eopecten sp. (3)
Anomia sp. (1)
Ctenostreon sp. (2)
Plagiostoma subcardiiformis (Greppin) (1)
Plagiostoma sp. (4)
Myophorella (*Pseudomyophorella*) *polonica* (Lebküchner) (1)
Opis (*Trigonopsis*) sp. (1)
Anisocardia minima (Sowerby) (3)
Anisocardia tenera (Sowerby) (3)
Pholadomya lirata (Sowerby) (1)
Pholadomya ovalis (Sowerby) (3)
Pholadomya cf. *bucardium* Agassiz (1)
Pholadomya sp. indet. (1)
Pleuromya uniformis (Sowerby) (4)

The rich fauna includes a great number of in-faunal elements (40%), first of all deep-burrowing, passive *Pholadomya* and *Pleuromya*. This is an indication of stable soft bottom conditions. The comparatively slight agitation of water is also suggested by the fact that 45% of the lamelli-branches have been fossilized with double valves.

All the above species are common in Western Europe. In addition, most of them are known to occur in remote areas such as South Asia (Afghanistan, Kutch) and East Africa.

The Bathonian sandy limestones

This formation, representing a lens about 8 cm thick on Templom hill at Villány, was dated on the basis of its rich ammonite fauna as belonging to the Upper Bathonian by A. Galácz (personal communication)

The rock is a yellow limestone with a high percentage (30%) of quartz sands.

In the macrofauna, beside the ammonites, the bivalves are most frequent:

- Entolium* sp. (1)
Anomia sp. (4)
Ctenostreon proboscideum (Sowerby) (2)
Ctenostreon sp. (1)
Plagiostoma subcardiiformis (Greppin) (3)
Plagiostoma sp. (4)
Plagiostoma sp. indet. (5)
Astarte sp. aff. *ovata* (Smith) (2)
Opis (*Coelopsis*) cf. *leckenbyi* Lycett (1)
Opis sp. indet. (2)
Cardium sp. (1)
Pholadomya moeschi Rollier (2)
Pholadomya villanyensis n. sp.
Goniomya trapezicostata (Pusch) (1)

Much of the fauna is epibenthonic, though burrowing forms requiring a loose, unconsolidated bottom, are represented in a considerable number. The presence of passive, deep-burrowing *Pholadomya* is indicative of stable bottom conditions. Considering, however, that 97% of the lamellibranchs were enclosed as single valves and that the *Pholadomyas* themselves are represented by single valves, one can take it for sure that a considerable thickness of unconsolidated sediment was reworked from time to time. According to Mc Alester and Rhoads (1967), the forms burrowing vertically are at present frequent in the littoral and shallow-sublittoral zones, only. Accordingly, the lamellibranchs of the Bathonian sandy limestones can be shown to have had their habitat in the same zone.

All components of the fauna are of West European character. A few species (*C. proboscideum*, *P. subcardiiformis*, *G. trapezicostata*) show a very large geographic extension, being known to occur in several points of Africa and Eurasia.

The Lower Callovian oöid-patterned limestones

Like the former, this formation is only exposed on Templom hill at Villány, being represented there by a pinching-out lens attaining a maximum of 10 cm in thickness. According to the personal communication of Dr. B. Géczy, its age, based upon a few *Macrocephalites* sp., is Lower Callovian.

The rock is a brownish-yellow limestone containing plenty of limonite oöids and quartz sands. In its lower horizon limonite-coated Bathonian limestone debris, sometimes fossiliferous, of a few cm size, can be found.

The macrofauna is dominated by ammonites, lamellibranchs occur rather sporadically:

Plagiostoma sp. indet. (2)

Anisocardia sp. (2)

Pholadomya escheri Agassiz (1)

The low number of specimens and taxa does not allow to draw any far-going conclusion. Paleoecologically, however, with a view to the double-valved preservation of both the shallow- and deep-burrowing animals, a rather quiet water environment can be supposed to have served as their habitat.

The Callovian ammonitic bed

In spite of its low thickness (40 cm), this formation is rather widespread. Its Callovian age was proved long ago on the basis of its exuberant ammonite fauna (Till, 1906). For a long time it was believed to represent a very large span of time (Upper Bathonian + complete Callovian). This was due to its too broad lithostratigraphical interpretation as a unit including the two former formations combined (the Bathonian

sandy limestones + the Lower Callovian oöid-patterned limestones). According to Dr. B. Géczy's personal communication, the ammonitic bed, as interpreted today, seems to be limited in age to a single zone of the Middle Callovian.

The rock is a limestone, biomicrite, containing very little terrigenous detrital material. Very characteristic of the ammonitic bed are stromatolites, of which an excellent description was given by Radwanski and Sulczewski (1966).

In the macrofauna, beside the rock-forming ammonites, the representatives of belemnites and brachiopods can be encountered in great number. The lamellibranch fauna is rather poor:

- Inoceramus oosteri* Favre? (9)
- Inoceramus* sp. indet. (32)
- Entolium spathulatum* (Roemer) (15)
- Propeamussium brevicostatum* n. sp. (1)
- Chlamys* sp. aff. *luciensis* (d'Orbigny) (2)
- Eopecten* sp. aff. *aubryi* (Douvillé) (8)
- Placunopsis* sp. (1)
- Plagiostoma*? sp. (1)
- Astarte* cf. *subdepressa* Blake et Hudleston (1)

The fauna is predominated by *Inoceramus* whose ecological requirements cannot be estimated on the basis of now-living relatives. The lateral distribution of this genus in the Jurassic is not controlled by lithology, a fact hinting, *in se*, at the possibility of a pelagic mode of life. The specimens of *Inoceramus dubius* Sow. (Hauflf, 1953) found attached with their byssus to driftwood in the Aalenian shales of Holzmaden make a pseudoplanktonic way of life obvious, and this statement can be extended, with great probability, to the rest of the species of the same genus, at least as far the Jurassic is concerned. Burial together with driftwood cannot have been a general phenomenon. The specimens broken loose from the still floating driftwood, could settle on the bottom and were scattered over it. According to Kuffman (1969), *Propeamussium* and the smooth pectinids in general (*Entolium* in our case), are excellent swimmers occurring frequently in non-agitated deep-water environments, too. Consequently, on the basis of the predominant elements of the fauna no conclusion can be drawn either as to water depth, or to bottom conditions.

The same holds true of the character of the fauna. A few specimens occur in Western Europe, but the rest either show just an affinity or they are new forms. Hence, unlike in the case of the formations discussed previously, the fauna of the Callovian ammonitic bed does not show convincingly West European features.

Systematic descriptions

Classis Bivalvia

Subclassis Pteriomorphia

Ordo Mytiloidea

Superfamilia Mytilacae

Familia Mytilidae

Subfamilia Lithophaginae

Genus *Inoperna* Conrad in Kerr, 1875*Inoperna sowerbyana* (d'Orbigny, 1850)

Plate I, Fig. 1 a, b

1819. *Modiola plicata* Sow.; Sowerby: Min. Conch., p. 293, Pl. 248, Fig. 1,2 (In: Sowerby, 1837).
1850. *Mitylus Sowerbianus*, d'Orb.; d'Orbigny: Prodrôme . . . , p. 282.
1853. *Mytilus Sowerbyanus* d'Orb.; Morris et Lycett: Mon. Great Oolite Mollusca, p. 36, Pl. IV, Fig. 1.
1883. *Modiola Sowerbyana*, d'Orbigny; Loriol et Schardt: Couches a Mytilus. . . , p. 62, Pl. IX, Fig. 9-12.
1910. *Modiola plicata* Sow.; Daqué: Ostafrika, p. 30, Pl. V, Fig. 10.
1939. *Mytilus (Phaenomytilus) sowerbyanus* d'Orb.; Stefanini: Somalia, p. 217, Pl. XXIV Fig. 10.
1940. *Modiolus (Inoperna) plicatus* J. Sowerby; Cox: Jur. Lamellibr. Kachh, p. 71, Pl. V, Fig. 1.
1948. *Modiolus (Inoperna) plicatus* J. Sowerby; Cox et Arkell: Brit. Great Oolite Mollusca p. 4.
1949. *Modiolus (Inoperna) plicatus* Sow.; Venzo: Il batoniano à Trigonina, p. 126, Pl. I, Fig. 7 a, b.
1965. *Inoperna plicata* (Sowerby); Freneix: Bivalves Jur. Tunis., p. 47, Pl. V, Fig. 11.
1965. *Modiolus (Inoperna) sowerbianus* (d'Orbigny); Cox: Jur. Biv. Tanganyika, p. 38, Pl. III, Fig. 11.
- Number of specimens: 5

Description: Internal mould of medium size of well preservation, incomplete, partly shelled, lacking the umbonal part. Shape slender, sheath-like, elongated, rather convex near the umbo, flattening down backwards. Between the umbo and the posterior margin there is a rather distinct, diagonal carina running from the dorsal margin towards the ventral one. It divides the surface of valve into two parts. Ornamentations of the dorsal region is well developed. At the dorsal margin concentric, coarse plicae are visible, which show an oblique backward orientation. Their breadth is more or less equal to their intervals. The plicae number 13 in 4 cm. In the middle third of the dorsal region they flatten out and disappear. Close to the carina bordering the region, the surface is ornamented with finely concentric plicae numbering about thrice the former over the same distance. The ornamentation of the ventral region is constituted by growth lines running parallel to the margin.

Remarks: On the basis of the character of ornamentation the Villány specimens can be readily identified, for the plicae of the dorsal region

trifurcate while running towards the ventral margin – a feature distinguishing the species from *I. perplicata* (Étallon) in which the ratio of primary ribs to the secondary ones is always 1:2.

In 1791 Gmelin described a now-living species under the name *Mytilus plicatus* (Morris and Lycett, 1853). In 1816 it was reassigned to the genus *Modiola* (conf. Loriol and Scharadt, 1883). Thus the specific name *Modiola plicata*, Sowerby, 1819, was reserved for another taxon. Accordingly, d'Orbigny (1850) gave the species described by Sowerby a new name, *Sowerbianus*, whose validity was emphasized by Cox (1965), too.

Distribution: Upper Liassic to Lower Callovian of Great Britain, Bathonian, to Bathonian of France, Bathonian to Callovian of India, Callovian of Tunisia, Toarcian to Oxfordian of East Africa. The Villány specimens derive from the Bathonian brown limestones.

Subfamilia Modiolinae

Genus *Modiolus* Lamarck, 1799

Modiolus anatinus (Smith, 1817)

Plate I, Fig. 2

1818. *Modiola cuneata* Sow.; Sowerby: Min. Conch., p. 261, Pl. 211, Fig. 1–3 (In: Sowerby, 1837).
 1818. *Modiola gibbosa* Sow.; Sowerby: Min. Conch., p. 262, Pl. 211, Fig. 4,5 (In: Sowerby, 1837).
 1818. *Modiola reniformis* Sow.; Sowerby: Min. Conch., p. 262, Pl. 211, Fig. 6,7 (In: Sowerby, 1837).
 1863. *Modiola gibbosa*, Sow.; Lycett: Suppl. Monogr., p. 42, Pl. XXXIII, Fig. 11, 11a.
 1907. *Modiola gibbosa* Sow.; Cossmann: Callovien Haute-Marne, p. 52, Pl. III, Fig. 3.
 1915. *Modiola gibbosa* Sow.; Krenkel: Kelloway fauna Popilany, p. 304, Pl. XXVI, Fig. 32, 33.
 1918. *Modiola gibbosa* Sowerby; Couffon: Callovien du Chalet, p. 129, Pl. IV, Fig. 10, 10a.
 1948. *Modiolus anatinus* W. Smith; Cox et Arkell: Brit. Great Oolite Mollusca, p. 4.
 1957. *Modiola gibbosa* Sow.; Himsiasvili: Verhnejursk. fauna Gruzii, p. 94, Pl. XVII, Fig. 7; Pl. XVIII, Fig. 3.
 1965. *Modiolus anatinus* (Smith); Cox: Jur. Biv. Tanganyika, p. 37, Pl. III, Fig. 7.
 Number of specimens: 1

Description: Internal mould of small size, partly shelled, slightly incomplete. Valve oblique, elongated backwards, very markedly inflated. Anterior auricle (or antero-ventral part) inflated, well developed; posterior auricle flat, weaker, but distinct. Umbo bent markedly forward. Between the umbo and the point of intersection of the dorsal and ventral margins there is a diagonal carina. Between this and the anterior auricle there is a depression. The most prominent point of the posterior auricle is at about the half of valve length. The ornamentation is represented by growth lines extending gradually into the auricles. Close to the posterior margin, a fine radial striation is visible on the valve.

Remarks: Sowerby (1818) considered *M. anatina* Smith to be the synonym of *M. gibbosa*. This fact was underlined by Cox (1965) who

stated that *M. cuneata* Sow., *M. gibbosa* Sow. and *M. reniformis* Sow. were names given to one and the same species first described by Smith as *M. anatina*.

According to Cox (1965), this species is closely related to *M. imbricata* Sowerby 1918, but differs from it (among other features) by its greater convexity and more inflated anterior auricle (antero-ventral part) separated by a distinct furrow from the rest of the valve.

Distribution: Bajocian to Bathonian of Great Britain; Callovian of France the Russian Platform and Georgia, USSR; Bajocian of East Africa. The Villány specimen derives from the Bathonian brown limestones.

Superfamilia Pinnacea

Familia Pinnidae

Genus *Stegoconcha* Böhm, 1907

Stegoconcha sp. aff. *granulata* (Sowerby, 1824)

Plate I, Fig. 3

1824. *Pinna granulata* Sow.; Sowerby: Min. Coch., p. 380, Pl. 347 (In: Sowerby, 1837).

1933. *Trichites granulatus* (J. Sowerby); Arkell: Brit. Corall. Lamellibr., p. 228, Pl. XXIX,

Fig. 2,3.

Number of specimens: 1

Description: Internal mould large, of poor preservation, partly shelled, incomplete. Shell thick. The ornamentation on the mould, close to the umbo, consists of rather strong, concentric plicae and completely flat, radial ribs. Away from the umbo, the spacing of the ribs will increase and, at a distance of 8 cm or so, the surface will become smooth. From 9 to 12 cm, in the shelled part of the valve, small tubercles can be observed which are arranged according to the points of intersection of the widely spaced, radial ribs and the fine, closely spaced, concentric ones.

Remarks: The type specimen of *S. granulata*, of which Sowerby gave an undistinctive drawing, has been lost. The form from Villány agrees well, both in shape and ornamentation, with the specimen figured and identified with *S. granulata* by Arkell (1933), at least as far as the periumbilical zone is concerned. The postero-marginal part of the valve of *S. granulata* is ornamented with peculiar, ramifying furrows. On the Villány specimen this cannot be seen because of its incompleteness. Thus far *S. granulata* has been described from the Oxfordian and Kimmeridgian only, while the specimen from Villány is Bathonian. Thus, despite the great similarity in morphology, it is doubtful whether the form being described here belongs to the same species. Therefore it is just the affinity that can be supposed.

Distribution: Oxfordian and Kimmeridgian of Great Britain. The Villány specimen derives from the brown limestones of the Bathonian.

Ordo Pterioida
Subordo Pteriina
Superfamilia Pteriacea
Familia Bakewelliidae
 Genus *Gervillella* Waagen, 1907
Gervillella siliqua (Deslongchamps, 1824)
 Plate I, Fig 4

1824. *Gervillia siliqua* N.; Deslongchamps: Mém. Gervillie, p. 128, Pl. IV.
 1824. *Gervillia pernoides* N.; Deslongchamps: Mém. Gervillie, p. 126 (partim), Pl. II (non: Pl. I and III.)
 1915. *Gervilleia aviculoides* Sow.; Krenkel: Kellowayfauna Popilany, p. 293, Pl. XXVI, Fig. 4-7.
 1940. *Gervillella siliqua* (J. A. Eudes-Deslongchamps); Cox: Jur. Lamellibr. Kachh, p. 112, Pl. VII, Fig. 12-14.
 1965. *Gervillella siliqua* (Eudes-Deslongchamps); Cox; Jur. Biv. Tanganyika, p. 44, Pl. IV, Fig. 10.
 Number of specimens: 3

Description: Specimen of medium size, well preserved, slightly incomplete (with anterior auricle and part of umbo lacking), representing the left valve of the animal. Valve markedly oblique, greatly elongated backwards, very convex near the umbo, flattening down close to the margin. Ventral margin arched backwards, its anterior part forming an angle of about 30° with the upper margin of the elongated posterior auricle. The ornamentation of the valve is constituted by locally irregular growth lines passing gradually over the auricles.

Remarks: Deslongchamps (1824) considered the most essential difference between *G. siliqua* and *G. pernoides* to consist in the much greater size of the latter. According to Cox (1940), however, this difference alone is not enough for the separation of the two forms, so the specimen figured by Deslongchamps (1824, Plate II) belongs to the species *G. siliqua*. This species was several times mistaken for *G. aviculoides* (Sow., 1814) to which it is rather similar from various points of view. Excellent figures of the last-mentioned species were published by Arkell (1933, Pl. XXVI, Fig. 1-5), figures permitting to find out two essential divergences: 1. The hinge margin of *G. siliqua* (i. e. the upper margin of the posterior auricle) is shorter and thus the posterior auricle is less prominent, while the posterior and ventral margins are parallel, unlike it is the case with *G. aviculoides*, where these two lines converge backwards. 2. In lateral view *G. siliqua* has its whole valve arched, whereas in *G. aviculoides* it is only the ventral margin that shows a slight convexity. On the basis of these characteristics the specimens figured by Krenkel (1915) can be assigned to the species *G. siliqua*.

G. acuta (J. de C. Sowerby 1826), ranging from the Aalenian up to the Oxfordian, may belong to *G. siliqua* (Cox and Arkell, 1958, p. 9), or there must be at least a genetic connection between the two (Cox, 1950, p. 116). Accordingly, the assignment of the specimens from Villány

to *G. siliqua* is not impeded by the fact that their stratigraphic position (Bathonian) is different from the most frequent occurrence of *G. siliqua* (Oxfordian).

Distribution: Oxfordian of France, India and East Africa; Callovian of the Russian Platform. The specimens from Villány have come from the brown limestones of the Bathonian.

Familia Inoceramidae

Genus *Inoceramus* Sowerby, 1814

Inoceramus oosteri Favre, 1870?

Plate II, Fig. 1

1876. *Inoceramus Oosteri*, E. Favre; Favre: Description fossil. Fribourg, p. 64, Pl. VI, Fig. 2.

1967. *Inoceramus oosteri* Favre; Kunz: Fauna aus dem oberen Dogger, p. 269, Pl. II, Fig. 4, Pl. III, Fig. 1–2.

Number of specimens: 9

Dimensions: height:	87	breadth: 68	convexity: 34
	78	60	—
	72	55	—

Description: Internal mould of medium size, of medium preservation, partly shelled. Outline elliptical to subcircular, with a pointed umbo distinctly projecting from it. The lunula is recognizable, though difficult to study because of its poor preservation. The closure angle of valves is higher than 60° at the anterior margin, being as low as 15° or so at the posterior one. The greatest convexity is at the first one-third of valve length. The ornamentation consists of concentric growth lines, getting regularly spaced towards the margins.

Remarks: According to Kunz (1967), this species is close to *I. fuscus* Quenstedt 1958, the most important difference being that *I. oosteri* has a slightly elongated, oval outline. *I. inoceramoides* (Hudleston, 1877) (Arkell, 1933, p. 217, Plate XXVIII, Fig. 1.) looks also similar, but its outline is quite close to circular.

The specimens from Villány somewhat differ in the character of the umbo from the specimen figured by Favre (1876). As illustrated by Kunz's (1967) figures, the state of preservation of those specimens was rather poor. All these circumstances have made the identification of the specimens from Villány rather uncertain.

Distribution: Oxfordian of Switzerland, Bathonian to Callovian of Austria. The specimens of Villány derive from the Callovian ammonitic bed.

*Superfamilia Pectinacea**Familia Entoliidae*Genus *Entolium* Meek, 1865*Entolium* cf. *hehlii* (d'Orbigny, 1850)

Plate II, Fig. 2

1850. *Pecten Hehlii* d'Orb.; d'Orbigny: Prodrôme, p. 219.1867. *Pecten Hehlii* (d'Orbigny); Dumortier: Bassin du Rhône, p. 70, Pl. XII, Fig. 5, 6.1926. *Entolium Hehlii* d'Orbigny; Staesche: Pectiniden Schwäb. Jura, p. 59, Pl. II, Fig. 13–15.1936. *Entolium Hehlii* d'Orbigny; Dechaseaux: Pectinides jurassiques, p. 60, Pl. VIII, Fig. 10, 11.

Number of specimens: 13

<i>Dimensions:</i> height: 11	breadth: 10
20	18
27	27
28.5	27

Description: Small specimen of medium preservation, representing an incomplete valve. Outline slightly oval, subcircular. Apical angle of umbo 98° . Valve slightly convex, the highest convexity being observable at about one-third of height as calculated from the umbo. Surface almost completely smooth, being ornamented only by regular growth lines. In the periumbilical zone there are a few radial ornamenting elements which can be hardly distinguished.

Remarks: According to Staesche (1926), *E. hehlii* differs from the other *Entolium* species by its lower apical angle. Despite their incompleteness, the specimens from Villány greatly resemble the figures of Dechaseaux (1936) and thus can be assigned to *E. hehlii* (d'Orb.).

Distribution: According to Dechaseaux (1936), it is known to occur in France from the Hettangian up to the Pliensbachian; in Germany it was found in the Hettangian and Sinemurian. The Villány specimens derive from the Pliensbachian limestones.

Entolium corneolum (Young et Bird, 1828)

Plate II, Fig. 3

1829. *Pecten demissus*; Phillips: Geol. Yorkshire, Pl. VI, Fig. 5.1855. *Pecten demissus* Phill.; Morris et Lycett: Mon. Great Oolite Mollusca, p. 127, Pl. XIV, Fig. 7.1858. *Pecten demissus*; Quenstedt: Der Jura., p. 353, Pl. 48, Fig. 4.1888. *Pecten Rypheus* d'Orbigny; Schlippe: Bathon. Oberrhein. Tiefland., p. 126, Pl. II, Fig. 6.1917. *Pecten demissus* Goldf.; Borisjak and Ivanov: Pelecypoda jursk. otl. Evr. Rossii, p. 3, Pl. I, Fig. 5, 8, 10, 15, 18.1926. *Entolium demissum* Phil.; Staesche: Pectiniden Schwäb. Jura, p. 99, Pl. IV, Fig. 5.1930. *Entolium demissum* (Phillips); Arkell: Brit. Corall. Lamellibr., p. 91, Pl. VII, Fig. 4; Pl. IX, Fig. 8, text-figure 15–17.1948. *Entolium corneolum* (Young and Bird); Cox et Arkell: Brit. Great Oolite Mollusca, p. 15.

Entolium spathulatum (Roemer, 1839)

Plate II, Fig. 4

1839. *Pecten spathulatus* Nob.; Roemer: Verst. Nordd. Oolith., Nachtr., p. 26, Pl. XVII, Fig. 22.
 1858. *Pecten spathulatus*; Quenstedt: Der Jura, p. 433, Pl. 59, Fig. 13.
 1883. *Pecten demissus* Bean; Lahusen: Fauna Jur. Bild. Rjasan., p. 24 (partim), Pl. II, Fig. 4.
 1917. *Pecten spathulatus* Roem.; Borisjak and Ivanov: Pelecypoda jursk. otl. Evr. Rossii, p. 6, Pl. I, Fig. 13.
 ?1956. *Entolium spathulatum* (Roemer); Ksiazkiewicz: Jura i kreda Bachowic, p. 171, Pl. XIX, Fig. 1, 2.
 ?1966. *Entolium demissum* (Phillips); Andrejeva: Plastinchatozhab. jursk. otl. Pamira, p. 13 (partim), Pl. I, Fig. 4.
 1967. *Entolium spathulatum* (Roemer); Romanov and Sobeky: Jursk. Pektinid, p. 47, Pl. I, Fig. 6–8.

Number of specimens: 15

Dimensions: height: 18	breadth: 15.5
13	10.5
12	10

Description: Valve small, of good preservation, slightly incomplete. Outline slightly elongated, oval. Apical angle of umbo 94° . Upper margin of auricles slightly arched rather than straight. Valve slightly convex, the greatest convexity being a little above the half of valve height. Surface almost totally smooth, being ornamented with a few hardly distinguishable growth lines.

Remarks: Roemer (1839) described the species as having an elongated, oval outline. According to this, as calculated after the original figure, the apical angle attains 85° or so, height = 18.5 mm, breadth = 14 mm. An important feature, elongatedness was later emphasized by Quenstedt (1858) as well as by Borisjak and Ivanov (1917). The two latter authors pointed out the small size of the species, too. Staesche (1926) believed that *E. spathulatum* (Roemer) could be assigned to *E. demissum* (Phillips) [= *E. corneolum* (Young et Bird)] a species of extremely wide range of variability. Dechaseaux (1936), however, considered the species *E. spathulatum* (Roem.) to be discriminable on account of its more acute apical angle. While measuring a great number of *E. demissum* deriving from the Dogger of Dobrogea Barbulescu (1963) found the apical angle to vary from 70° to 120° as a function of size, thus being unsuitable for serving as a diagnostic feature. The representation of height-to-breadth ratios (*l. c.* Pl. II, Fig. 10), however, yielded a different result, for a group of more elongated forms is likely to be distinguishable on the diagramme. Accordingly, it is the elongated outline that appears to be the most important distinctive feature of *E. spathulatum*, but this could be proved convincingly only if a large population was examined statistically.

The apical angle of the specimens from Villány varies between 90° and 109° , their general characteristic feature being small size and elongated outline. On this basis their assignment to *E. spathulatum* (Roemer) is justified.

Distribution: Bajocian to Oxfordian of Germany, Bajocian of Poland, Bajocian to Oxfordian of the Russian Platform. The Villány specimens derive from the Callovian ammonitic bed.

Familia Pectinidae

Genus *Propeamussium* de Gregorio, 1884

Propeamussium brevicostatatum n. sp.

Plate II, Fig. 1a, b

Number of specimens: 1

Locus typicus: Villány, Somsich hill

Stratum typicum: Callovian ammonitic bed

Derivatio nominis: after the short inner ribs of the species

Dimensions: height: 8.4 mm breadth: 8.2 mm

Diagnosis: comparatively low number (9) of primary ribs ornamenting the inner surface of valve and ending a little after attaining the half of valve height as calculated from the umbo.

Description: Intact left valve of small size, in state of perfect preservation. Outline circular. Apical angle of the umbo about 105° . At the base of the anterior auricle a small concave curvature can be seen, the posterior margin of the posterior auricle being straight. The upper margins of the auricles form one straight line. The ornamentation of the outer surface of the valve is constituted by about 25 very fine, radial ribs which are irregularly broken in a few places. In addition, in the periumbonal zone concentric growth lines are visible, which cross the ribs, thus resulting in a net-like pattern. As observable through the very thin, transparent valve the inner surface is ornamented by 9 radial ribs which are joined towards the margin by 5 secondary ones. Growing gradually stronger, the ribs vanish soon after reaching the half of valve height as calculated from the umbo.

Remarks: The Jurassic representatives of *Propeamussium* were reviewed by Staesche (1926). According to him, *P. pumilum* (Lamarck, 1819) of the Lower Dogger, *P. penninicum* (Neumayr, 1871) of the Oxfordian and *P. nonarium* (Questedt, 1858) of the top of the Upper Jurassic would form a lineage characterized, beside slight changes in external ornamentation, in the first place by a decrease of the number of inner ribs. Whereas *P. penninicum* carries 11 ribs (Neumayr, 1871, p. 375, Pl. XXI, Fig. 4), the number of primary ribs of *P. nonarium* is as low as 9, though between these a few secondary ribs are included (Quenstedt, 1858, p. 795, Pl. XCVIII, Fig. 4). As regards its morphological features and external ornamentation, the specimen from Villány is closely related to the above group. On account of its Callovian age, it ought to resemble especially *P. penninicum*, but the number of its inner ribs corresponds to that of the Upper Jurassic *P. nonarium*. In addition, a substantial difference is that the inner ribs of all the aforementioned species reach up to the margin of the valve.

Genus *Chlamys* Röding, 1798
Chlamys sp. aff. *luciensis* (Thevenin ex d'Orbigny)
 Plate III, Fig. 1

Number of specimens: 1
 Dimensions: height: 50

breadth: 41 convexity: 10

Description: Internal mould of an incomplete left valve of medium size and preservation with some shell preserved. Outline elongated, slightly inaequilateral. Ornamentation constituted by 17 radial ribs. In the anterior and middle parts the ribs are straight, while in the posterior part they are arched backwards, becoming gradually more inflated. They are roof-shaped in cross-section, being slightly rounded at the top. Their intervals are U-shaped, being wider than the ribs themselves. The surface is covered by growth lines of irregular spacing, which become locally stronger, developing into plicae.

Remarks: The species *C. luciensis* has become known on the basis of the descriptions and excellent figures published by Thevenin (1913, p. 163, Pl. XXVIII, Fig. 28) and Fischer (1964, p. 17, Pl. I, Fig. 14–15). As far as its major features are concerned, the Villány specimen corresponds to these, but it differs from them by its lower number of ribs (19–20 in *C. luciensis*) and by the fact that 2 or 3 posterior ribs are arched backwards instead of being straight.

Distribution: *C. luciensis* is known to occur in the Bathonian of France; the specimen of Villány was found in the Callovian ammonitic bed.

Subgenus *Aequipecten* Fischer, 1886
Chlamys (*Aequipecten* ?) cf. *prisca* (Schlotheim, 1820)
 Plate II, Fig. 6

1858. *Pecten aequalis*; Quenstedt: Der Jura, p. 78, Pl. 9, Fig. 13.

1858. *Pecten prisca*; Quenstedt: Der Jura, p. 147, Pl. 18, Fig. 18–20.

1867. *Pecten prisca* (Schlotheim); Dumortier: Bassin du Rhône, (part: II), p. 216, Pl. XLVIII, Fig. 4.

1869. *Pecten prisca* (Schlotheim sp.); Dumortier: Bassin du Rhône (part: III), p. 138, Pl. XXII, Fig. 3.

1916. *Chlamys* (*Aequipecten*) *prisca* (Schloth.); Cossmann: Charmouthien Vendée, p. 137, Pl. V, Fig. 16.

1926. *Aequipecten prisca* Schlotheim; Staesche: Pectiniden Schwäb. Jura, p. 48.

Number of specimens: 11

Dimensions: height: 26

breadth: 24

Description: Right valve of medium size, of poor preservation, incomplete. Below the distinct anterior auricle a byssal notch is visible. Apical angle of umbo about 95°. Greatest convexity at the half of valve height. Ornamentation is constituted by 23 radial ribs of rounded cross-section, nearly as broad as the intervals between them.

The few left valves among the specimens from Villány show the following differences from the right valves: 1. at the base of the auricles no byssal notch can be observed, 2. the greatest convexity is at a quarter of valve height as calculated from the umbo, 3. the ribs are a little narrower than their intervals.

Remarks: As a difference between *P. aequalis* and *P. priscus*, Quenstedt (1858) mentioned the more widely spaced, narrower ribs of the latter. St a e s c h e (1926) showed the two forms to grade into each other. Thus it is justified to unite them. According to him (St a e s c h e, 1926), *P. bersaskensis* Tietze might be assigned to the same species, despite the lower number (16) of its ribs. As evident from T i e t z e ' s figure (1872, Pl. VI, Fig. 3), however, the intervals show almost twice the breadth of the ribs. Taken together with the low number of ribs, this does no longer justify the assignment to *C. prisca*.

Distribution: Hettangian to Pliensbachian of France (D e c h a s e a u x, 1936) and of Germany (S t a e s c h e, 1926). The specimens of Villány derive from the Pliensbachian limestones.

Chlamys (Aequipecten ?) humberti (Dumortier, 1869)

Plate II, Fig. 7

1869. *Pecten Humberti* (Nov. spec.); Dumortier: Bassin du Rhône, (part: III), p. 309, Pl. XL, Fig. 2.

1872. *Pecten Bersaskensis* nov. sp.; Tietze: Geol. Pal. Mitt. Banat. Gebirgs., p. 106, Pl. VI, Fig. 3.

1915. *Pecten* cfr. *Humberti* Dum.; Jekelius: A brassói hegyek . . . , p. 60, text-figure 3.

Number of specimens: 3

Dimensions: height: 17.3 breadth: 16.5

Description: Internal mould of small size, of medium preservation, with a little remnant of shell. Circular outline broken by the projecting umbo having an apical angle of about 90°. Valve strongly inflated, the greatest convexity being at about the half of valve height. Ornamentation consists of 14 ribs of rounded cross-section separated by flat intervals about twice the breadth of the ribs. The intervals are not concave, thus showing sharp contacts with the ribs.

Remarks: In spite of their poor preservation, the specimens from Villány can be readily indentified with the figures of D u m o r t i e r (1869) and J e k e l i u s (1915) on the basis of ornamentation characteristics. This species is characterized above all by a comparatively low number, 13 to 16, of ribs which are separated by flat intervals about twice their breadth. On account of this character *P. bersaskensis* Tietze can be assigned to the species. S t a e s c h e (1926) considered this species to be a synonym of *P. priscus* Schlotheim. The sharp contrast between the two is manifested in respect of both the number of ribs and the ratio of the breadth of the ribs to their intervals.

Distribution: Middle Lias of France; Lower to Middle Lias of the southern Carpathians. The Villány specimens derive from the Pliensbachian limestones of Mt. Harsány.

Genus *Eopecten* Douvillé, 1897*Eopecten* sp. aff. *aubryi* (Douvillé, 1886)

Plate III, Fig. 2

Number of specimens: 8

Dimensions: height: 41
29

breadth: 39

28

Description: Left valve of medium size and preservation, a little incomplete. Outline circular, slightly irregular. Anterior auricle not distinctly isolated. Valve more or less deformed, rather markedly convex, the greatest convexity being in the periumbonal zone. Ornamentation consisting of primary, secondary and tertiary ribs. Rather little prominent, the primary ribs number 18 or so. The secondary ribs are sometimes nearly so strong as the primary ones. The tertiary ribs are very fine, numbering 3 to 5 in the intervals of the primary ribs. The ribs run sometimes irregularly.

Remarks: Recently, Freneix (1965, p. 21, Pl. II, Fig. 15) published a nice figure of *E. aubryi* (Douvillé, 1886, p. 228, Pl. XII, Fig. 3). As far as the most important morphological and ornamentation features are concerned, the Villány species shows a great similarity to the aforementioned species. However, they differ from it by the higher number of their ribs and by their less prominent primary ribs.

Distribution: According to Cox (1965) and Freneix (1965), *E. aubryi* shows a wide geographic distribution in the Bathonian, Callovian and Oxfordian stages. Closely related to this species, the specimens from Villány derive from the Callovian ammonitic bed.

*Superfamilia Limacea**Familia Limidae*Genus *Antiquilima* Cox, 1943*Antiquilima succincta* (Schlotheim, 1813)

Plate III, Fig. 3

1867. *Lima succincta* (Schlotheim); Dumortier: Bassin du Rhône, (part: II), p. 66 and 212, Pl. XLVII, Fig. 6, 7; Pl. XLVIII, Fig. 1.

1869. *Lima succincta* (Schlotheim sp.); Dumortier: Bassin du Rhône, (part III), p. 286, Pl. XXXIV, Fig. 3, 4.

1916. *Lima succincta* (Schloth.); Cossmann: Charmouthien Vendée, p. 140, Pl. VIII, Fig. 16.
Number of specimens: 1

Description: Right valve of medium size, well-preserved, incomplete. Ornamentation constituted by radial, primary, secondary and tertiary ribs and by concentrical growth lines. The relative arrangement of ribs of different rank is rather irregular. The intersections of closely spaced, fine growth lines by the radial tertiary ribs produce a net-like ornamentation in the intervals of the ribs of higher rank. At a few irregularly spaced

growth plicae, the radial ribs are broken and, more or less preserving their orientation, they are shifted with regard to the first stretch.

Remarks: The umbonal part of the Villány specimen has been broken off together with the auricles, but its outline can be approximately reconstructed with the aid of ribs and growth plicae. On the basis of such features as the ribs of different intensity displaying a gradual shifting as well as the square-grid reticulation in the intervals of ribs the ornamentation can be readily identified with the excellent figures of Dumortier (1867, 1869) and Cossmann (1916).

Dumortier and Cossmann assigned *L. antiquata* Sowerby 1818 to this species. Judging by the figures, this does not seem to be firmly justified, for the ornamentation of *L. antiquata* consists of much denser and finer ribs.

Distribution: Different levels of the Sinemurian and Pliensbachian of France. The specimen from Villány derives from the Pliensbachian limestones.

Genus *Ctenostreon* Eichwald, 1862

Ctenostreon proboscideum (Sowerby, 1820)

Plate III, Fig. 4

1820. *Lima proboscidea* Sow.; Sowerby: Min. Conch., p. 304, Pl. 264, (In: Sowerby, 1837)
 1852. *Lima proboscidea*, Sowerby; Chapuis et Dewalque: Descr. foss. Sec. Luxemb., p. 202, Pl. XXXI, Fig. 1.
 1918. *Ctenostreon proboscideum* Sowerby; Couffon: Callovien du Chalet, p. 57, Pl. IV, Fig. 3.
 1924. *Ctenostreon proboscideum* (Sow.); Cossmann: Callovien de Montreuil-Bellay, p. 30, Pl. IV, Fig. 4, 5.
 1932. *Ctenostreon proboscideum* (Sowerby); Arkell: Brit. Corall. Lamellibr., p. 145,¹ Pl. XV, Fig. 3.
 1935. *Ctenostreon proboscideum* (J. Sowerby); Cox: Attock District, p. 16, Pl. I, Fig. 16.
 1957. *Ctenostreon proboscideum* Sow.; Himsiasvili: Verhnejurk. fauna Gruzii, p. 137, Pl. XXVII, Fig. 1, 2.
 1963. *Ctenostreon* cf. *pectiniforme* (Schlotheim); Azarjan: Jursk. otl. ASSR, p. 156, Pl. V, Fig. 1.
 1966. *Ctenostreon pectiniforme* (Schlotheim); Andrejeva: Jursk. otl. Pamira, p. 64, Pl. XX, Fig. 1-4.

Number of specimens: 2

Dimensions: height: 122 breadth: 118 convexity: 24

Description: Internal mould of great size, poorly preserved, partly shelled. Outline circular, slightly oblique backwards. Valves equal, slightly convex, showing the highest convexity near the umbo, at the one-third of valve height. Ornamentation consisting of 12 very strong, radial ribs separated by deep intervals, a little wider than the ribs themselves.

Remarks: In the Middle and Upper Jurassic three species of *Ctenostreon* are known, which were cited particularly frequently: *C. rugosum* (Smith, 1817), *C. proboscideum* (Sowerby, 1820) and *C. pectiniforme* (Schlotheim, 1820). Their separation was faced with great difficulties for a long time. Arkell (1932) demonstrated *C. rugosum* and *C. proboscideum* to have several diverging features of which the differ-

ence in the number of ribs seems to be most important: 9–10 in the former and 12 in the latter. According to Arkell, *C. pectiniforme* can be separated on the basis of its more rounded outline and the higher number of its ribs, a fact hinted at by Couffon already (Couffon, 1918). Later it was suggested (Cox, 1935; Cox and Arkell, 1948) that it would be advisable to examine a large population to be collected from one and the same horizon, in order to verify if the afore-mentioned species are independent. However, no substantial progress has been made ever since. The forms described by Azaryan (1963) and Andrejeva (1966) under the name *C. pectiniforme* carry 11 and 12–13 ribs, respectively. Therefore, accepting Arkell's (1932) opinion, we can assign these forms to *C. proboscideum*.

Distribution: Oxfordian of Great Britain, Bajocian to Callovian of Western Europe, Callovian to Tithonian of the Caucasus, Bajocian to Callovian of the Pamir and Oxfordian of India. The Villány specimens derive from the sandy limestones of the Bathonian.

Genus *Plagiostoma* Sowerby, 1814

Plagiostoma subcardiiformis (Greppin, 1867)

Plate III, Fig. 5

1853. *Lima cardiiformis*, Sow.; Morris et Lycett: Mon. Great Oolite Mollusca, p. 27, Pl. III, Fig. 2, 2a.
 1870. *Lima subcardiiformis*, Grepp.; Greppin: Jura Bernois, p. 44, 50.
 1888. *Lima (Radula) subcardiiformis* Greppin; Schlippe: Bathon. Oberrhein. Tieflande., p. 118, Pl. II, Fig. 7.
 1948. *Lima (Plagiostoma) subcardiiformis* Greppin; Cox et Arkell: Brit. Great Oolite Mollusca, p. 16.
 ?1959. *Lima subcardiiformis* Greppin; Mihajlovic: Srednejursk. fauna, p. 211, Pl. II, Fig. 4.
 1961. *Lima (Plagiostoma) subcardiiformis* Greppin; Rossi Ronchetti et Fantini Sestini: Fauna giur. Karkar, p. 125, Pl. X, Fig. 13.

Number of specimens: 4

Dimensions: length: 35

height: 33

convexity: 8

Description: Right valve of medium size, of good preservation, a little incomplete. Outline obliquely oval. Umbo relatively prominent. Convexity of valve mean. Ornamentation consists of a great number, about 50, of radial ribs interrupted locally by growth lines. Their tops are flat, therefore their cross-section is trapezoidal. The intervals are narrower than the ribs themselves. They are U-shaped in cross-section, showing a dense transversal reticulation.

Remarks: Cox and Arkell (1948) stated that Morris and Lycett had erroneously interpreted the species *P. cardiiformis* (Sow.) whose ornamentation consists of fewer and flatter ribs. The specimen figured by Morris and Lycett (1853) is the representative of the species *P. subcardiiformis* (Greppin). Greppin established it in 1867 (Cox and Arkell, 1948), using the name *subcardiiformis*. Although this name was later used with the same spelling, there must have been

a mistake, since in the same work Sowerby's species was quoted with the same error — under the name *cordiiformis*.

The specimens from Villány agree well, in morphology and ornamentation, with the figures quoted in the synonymy. The specimen figured by Mihajlovic (1959) is a little more elongated, oval, in outline.

Distribution: Bathonian of Great Britain, Germany and Switzerland; Middle Jurassic of Yugoslavia and Afganistan. Of the Villány specimens one has come from the brown limestones of the Bathonian, three derive from the Bathonian sandy limestones.

Subordo Ostreina

Superfamilia Ostreacea

Familia Gryphaeidae

Subfamilia Gryphaeinae

Genus *Gryphaea* Lamarck, 1801

Gryphaea gigantea J. de C. Sowerby, 1823

1823. *Gryphaea gigantea* Sow.; Sowerby: Min. Conch., p. 413, Pl. 391, (In: Sowerby, 1837).

1872. *Gryphaea fasciata* nov. sp.; Tietze: Geol. pal. Mitt. Banat. Gebirgs., p. 111, Pl. VI, Fig. 1.

1929. *Gryphaea gigantea* Sowerby, Schäfle: Lias- und Doggeraustern, p. 107, Pl. IV, Fig. 6, 7.

1968. *Gryphaea gigantea* J. de C. Sowerby; Hallam: The genus *Gryphaea* ..., p. 115, Pl. XII, Fig. 46–52.

Number of specimens: 2

Dimensions: height: 95 breadth: 95 convexity: 40

Description: Double valve of great size, of medium preservation, incomplete. Outline approximately circular. Umbo of left valve slightly coiled, valve strongly convex. Right valve concave. Because of the imperfect state of preservation and incompleteness neither growth lines, nor any other ornamentation are visible in either of the valves.

Remarks: The most important features of the species are truly illustrated by the figures of J. de C. Sowerby and of the other authors cited. On the basis of these the Villány specimens could be identified. As shown by Schäfle (1929), *Gryphaea fasciata* Tietze can be assigned to the species *G. gigantea*. The striking similarity was recognized by Tietze himself (1872) who established a new species because he knew *G. gigantea* to be an Upper Jurassic species.

Hallam (1968) suggested the possibility of separating the Lower Pliensbachian forms from the Upper Pliensbachian ones, as chronological subspecies. Morphologically, the Villány specimens are closely related to the Lower Pliensbachian forms, but their stratigraphic position is not known exactly.

Distribution: Pliensbachian of Great Britain, Germany and the southern Carpathians. The Villány specimens derive from the Pliensbachian limestones of Harsány hill.

*Subclassis Palaeoheterodonta**Ordo Trigonioida**Superfamilia Trigoniacea**Familia Trigoniidae*Genus *Myophorella* Bayle, 1878Subgenus *Pseudomyophorella* Nakano, 1961*Myophorella (Pseudomyophorella) polonica* (Lebküchner, 1932)

Plate IV, Fig. 1

1932. *Clavotrigonia polonica* Lebküchner; Lebküchner: Trigonien süddeutsch. Jura, p. 60, Pl. III, Fig. 8; Pl. IV, Fig. 5.

Number of specimens: 1

Dimensions: length: 59

height: 44

convexity: 12

Description: Left valve of good preservation, a little incomplete. Shape a slightly elongated, rounded rectangle. Umbo shifted forward to about one fifth of valve length, being backward-coiled. Anterior and lower margins arched evenly and continuously. Forming a broken arch, the posterior margin also describes an arch in passing over into the lower margin, but it forms an obtuse angle with the upper margin. The scutum is smooth, concave, attaining about the half of valve length. The area is separated from both the scutum and the lateral region by a carina, each dotted with tubercles for the whole length. The lower carina is slightly, the upper markedly, arched, concave. The ornamentation of the area is constituted, beside the growth lines extending throughout the valve, by fine, radial rows of tubercles, of which the middle is most distinct, dividing up the area into an upper, concave, sector and a lower, convex, one. Owing to intercalations, the rows of tubercles increase in number in both sectors towards the posterior margin. The lateral region is ornamented by 14 oblique and arched rows of marked tubercles. The longest row is constituted by 14 tubercles, decreasing in size from the centre of the region outwards in both directions. The rows of tubercles run normal to the anterior margin, reaching the lower margin without losing their curvature. In fact, while running towards the upper carina, they show a gradually increasing curvature and quasi flush with the carina. The first five ornamental elements close to the umbo are still fused into a continuous rib.

Remarks: As far as the ornamentation of its lateral region is concerned, *M. polonica* stands close to *M. signata* (Agassiz, 1840). Lebküchner (1932) too distinguished it within the specific description of *M. signata*, on the basis of the marked curvature of the area-bordering carina.

Of the Middle Jurassic *Myophorella* known so far, *M. polonica* is the only form to have distinct radial ornamental elements on the area. As believed by Cox et al. (1969) (Treatise), on account of this characteristic, this species should be assigned to the subgenus *Pseudomyophorella*. Since this subgenus has so far been described from the Upper Jurassic only, *M. polonica* can be regarded as its earliest representative.

The Villány specimen corresponds well to Lebküchner's figures (1932), the only difference consisting in the lower curvature of the area-limiting carina.

Distribution: Bathonian of Germany (Dogger ϵ). The specimen from Villány was found in the brown limestones of the Bathonian.

Subclassis Heterodonta

Ordo Veneroida

Superfamilia Crassatellacea

Familia Astartidae

Subfamilia Astartinae

Genus *Astarte* Sowerby, 1816

Astarte sp. aff. *ovata* Smith, 1817

Plate IV, Fig. 2

1829. *Crassina ovata* (Smith); Phillips: Geol. Yorkshire, Pl. III, Fig. 25.
 1839. *Astarte crassitesta* Nob.; Roemer: Verst. Nordd. Oolithengeb., Nachtr., p. 39, Pl. XIX, Fig. 18.
 1934. *Astarte ovata* Smith; Arkell: Brit. Corall. Lamellibr., p. 231, Pl. XXXII, Fig. 1-12; text-figures 55, 56.
 1952. *Astarte* (*Neocrassina*) *ovata*, W. Smith; Chavan: Pélécypodes Cordebugle, p. 55, Pl. III, Fig. 68, 69; text-figures 26, 27.
 1957. *Astarte ovata* Smith; Himsiasvili: Verhnejursk. fauna Gruzii, p. 148, Pl. XXIX, Fig. 5, 6.
 non 1965. *Astarte ovata* Fan (sp. nov.); Fan: Middle Jur. Lamellibr. Tibet, p. 255, Pl. I, Fig. 17.

Number of specimens: 2

Dimensions: length: 50 height: 44 convexity: 13

Description: Right valve of medium size and preservation, incomplete. Valve oval, slightly convex. Umbo shifted forward, lying at about one-third of valve length. Anterior margin relatively short, straight, the rest of valve margin being continuously rounded. Ornamentation consisting of fine, concentric ribs, which near the umbo (up to 10-15 mm distance) are regularly spaced. In the well-developed part of the valve this ornamentation is replaced by rather irregular growth plicae and lines.

Remarks: Arkell (1934) published a figure labelled "*Venus* sp." by Smith 1816, a figure which Smith referred to in his description of *A. ovata* in 1817. The other figures published by Arkell are also excellent. The Villány specimens show a good agreement with them. *A. ovata* was known to occur in the Oxfordian and Kimmeridgian only, whereas the Villány specimens are of Bathonian age. Despite the comparatively great difference in age, there seems to be at least a close relationship on account of the striking morphological resemblance.

Fan (1965) described a new species under the name *A. ovata*. The figured specimen does not correspond to *A. ovata* Smith, and the name has been reserved for a long time.

Distribution: Oxfordian to Lower Kimmeridgian of Great Britain, Kimmeridgian of France, Oxfordian and Kimmeridgian of Georgia. The specimens of Villány derive from the sandy limestones of the Bathonian.

Astarte cf. subdepressa Blake et Hudleston, 1877

Plate IV, Fig. 3

1934. *Astarte subdepressa* Blake and Hudleston; Arkell: Brit. Corall. Lamellibr., p. 235, Pl. XXXIII, Fig. 1-9.

Number of specimens: 1

Dimensions: length: 25

height: 22

convexity: 8

Description: Internal mould of small size, of poor preservation, partly shelled. Shape oval. Umbo slightly prominent, at one-third of valve length as calculated from the anterior margin. Valve of medium convexity. Ornamentation consists of fine, regular, concentric plicae. In the zone lying close to the lower margin of the valve, 13 ornamental elements occur over 7 mm distance.

Remarks: Arkell (1934) re-figured the holotype of the species. On this the concentric plicae number 44 in 20 mm, a figure varying between 40 and 45 within the species. Of the similar species, *A. hilpertensis* Lycett, 1863, has, as shown by Arkell, about 30 ornamental elements over the same distance, in spite of its usually very great size. The Villány specimen, occupying in age an intermediary position between the two afore-mentioned species, can be assigned to *A. subdepressa* on account of morphological resemblances.

Distribution: The holotype of the species was found in the Oxfordian of Great Britain. The Villány specimen derives from the ammonitic bed.

Subfamilia Opinae

Genus *Opis* De France, 1825

Subgenus *Coelopsis* Munier-Chalmas, 1885

Opis (Coelopsis) cf. leckenbyi Lycett, 1863

Plate IV, Fig. 4

1863. *Opis Leckenbyi*, Wright; Lycett: Supplement. Monogr., p. 61, Pl. XXXVII, Fig. 9, 9a.

1924. *Opis (Coelopsis) cf. Leckenbyi*, Wright; Cossmann: Callovien de Montreuil-Bellay, p. 43, Pl. V, Fig. 22, 23.

1948. *Opis (Coelopsis) leckenbyi* Lycett; Cox et Arkell: Brit. Great Oolite Mollusca, p. 29.

non 1867. *Opis Leckenbyi*, Wright; Laube: Biv. Braun. Jura, p. 42, Pl. IV, Fig. 3.

non 1888. *Opis Leckenbyi*, Whright; Greppin: Grande Oolithe de Bâle, p. 94, Pl. VII, Fig. 5, 6.

Number of specimens: 1

Dimensions: length: 23

height: 23

convexity: 10

Description: Right valve of medium size, a little incomplete. Umbo very prominent and bent forward. Lunula deep, readily delimitable.

Carina very strong, prominent, traceable radially throughout the valve. It borders a posterior region making up about a quarter of total surface. Scutum of medium size can be readily delimited from the posterior region. Ornamentation consists of regular growth plicae traceable over the entire surface.

Remarks: The first valid description of the species was given by Lycett. Earlier the name was *nomen nudum*, as pointed out by Cox and Arkell (1948). On the basis of Lycett's excellent figure (1863) the Villány specimen could be well identified and the only difference consisted in the slightly closer spacing of its growth plicae. The specimens figured by Laube (1867) and Greppin (1888) are much more elongated, their anterior part is pointed, i.e. the transition between the anterior and the lower margins is less rounded than it is the case with *O. leckenbyi*. These differences may be due to the much smaller size of the above-mentioned specimens.

Distribution: Callovian of Great Britain and France. The specimen from Villány derives from the sandy limestones of the Bathonian.

Superfamilia Arcticea

Familia Arcticideae

Genus *Anisocardia* Munier-Chalmas, 1863

Anisocardia minima (Sowerby, 1821)

Plate IV, Fig. 5a, 5b

1821. *Isocardia minima* Sow.; Sowerby: Min. Conch., p. 334, Pl. 295, Fig. 1–3. (In: Sowerby, 1837)
1829. *Isocardia tumida*; Phillips: Geol. Yorkshire, p. 134, Pl. IV, Fig. 25.
- ?1829. *Isocardia minima*; Phillips: Geol. Yorkshire, p. 144, Pl. VII, Fig. 6.
1853. *Isocardia tenera*, Sow.; Morris et Lycett: Mon. Great Oolite Mollusca, p. 66, Pl. (part.) VII, Fig. 1, 1a.
1863. *Isocardia tenera*; Lycett: Supplement. Monograph, p. 57, (part.) Pl. XXXVIII, Fig. 5, 5a, 5b.
1934. *Anisocardia minima* (J. Sowerby); Arkell: Brit. Corall. Lamellibr., p. 275, Pl. XXXVI, Fig. 8–11.
1948. *Anisocardia minima* (J. Sowerby); Cox et Arkell: Brit. Great Oolite Mollusca, p. 31.
1952. *Anisocardia tenera* (Sowerby); Makowski: Faune Callov. Lukow, p. 12, Pl. V, Fig. 7.
1957. *Anisocardia tenera* Sow.; Himsiasvili: Verhnejursk. fauna Gruzii, p. 150, Pl. XXX, Fig. 7.
- ?1960. *Anisocardia* cf. *minima* (Sowerby); Desio et Rossi Ronchetti: Giur. med. Garet el-Bellaa, p. 184, Pl. XVII, Fig. 7.
1965. *Anisocardia minima* (J. Sowerby); Cox: Jur. Biv. Tanganyika, p. 112, Pl. XVIII, Fig. 8.
- non 1863. *Isocardia minima*, Sow.; Lycett: Supplement. Monograph, p. 56, Pl. XXXVI, Fig. 1, 1a.
- Number of specimens: 3
- | | | |
|------------------------|------------|---------------|
| Dimensions: length: 27 | height: 28 | convexity: 25 |
| 24 | 24 | 23 |

Description: Internal mould of small size, of poor preservation with a little shell remnant. Umbo markedly prominent. Lower and posterior

margins rounded, slightly convex; anterior margin forming a strongly projecting peak. Convexity of double valve almost attaining the height. Lunula large, heart-shaped, bordered by carinae running between the umbo and the most prominent point of the anterior margin. On the shell remnant concentric growth lines and fine, radial striae are visible.

Remarks: Arkell (1934) represented, together with the holotype, several specimens of the species and pointed to the fact that *A. minima* was often mistaken for *A. tenera*, and viceversa. As found by Arkell during the examination of the holotypes, *A. tenera* showed the following divergences from *A. minima*: 1. lower convexity, 2. greater length compared to height, 3. more rounded anterior margin. On the basis of these considerations the specimens described as *A. tenera* by Makowski (1952) and Himsiasvili (1957) can be assigned to *A. minima*. Lycett's specimen (1863, Pl. XXXVI, Fig. 1, 1a) has a very slightly prominent umbo and its valve is less convex. Thus it can be stated for sure, that it does not belong to *A. minima*.

Distribution: Bathonian to Oxfordian of Great Britain, Callovian of Poland, Bathonian to Callovian of the Caucasus, Bathonian of North Africa, Callovian of East Africa. The Villány specimens derive from the brown limestones of the Bathonian.

Anisocardia tenera (Sowerby, 1821)

Plate IV, Fig. 6a, 6b

1821. *Isocardia tener* Sow.; Sowerby: Min. Conch., p. 334, Pl. 295, Fig. 4–6. (In: Sowerby, 1837)
1888. *Anisocardia tenera* Sowerby sp.; Schlippe: Fauna Bathon. Oberrhein. Tieflande, p. 166, Pl. III, Fig. 4.
- ?1915. *Anisocardia tenera* Sowerby; Krenkel: Kellowayfauna Popilany, p. 325, Pl. XXVI, Fig. 37.
- ?1934. *Anisocardia tenera* Sowerby sp.; Stoll: Pommerschen Doggergeschiebe, p. 13, Pl. I, Fig. 39.
- non 1853. *Isocardia tenera* Sow.; Morris et Lycett: Mon. Great Oolite Mollusca, p. 66, Pl. VII, Fig. 1, 1a.
- non 1863. *Isocardia tenera*; Lycett: Supplement. Monograph, p. 57, Pl. XXXVIII, Fig. 5, 5a, 5b.
- non 1952. *Anisocardia tenera* (Sowerby); Makowski: Faune Callov, Lukow, p. 12, Pl. V, Fig. 7.
- non 1957. *Isocardia tenera* Sow.; Himsiasvili: Verhnejursk. fauna Gruzii, p. 150, Pl. XXX, Fig. 7.

Number of specimens: 3

Dimensions: length: 33
33

height: 36
34

convexity: 31
31

Description: Double valve of medium size, of good preservation, incomplete. Shape a rounded triangle in lateral view. Umbo markedly prominent, slightly bent forward. Lower margin slightly, the upper a little more, convex, but not prominent. Valve intensively convex. Lunula wide, shallow, but not sharply delimited. Ornamentation consists of fine growth lines which are regular over much of the valve. In the

posterior part there is an inflated carina running from the umbo up to posterior margin.

Remarks: Arkell (1934) examined the holotypes of *A. tenera* and *A. minima*, species often mistaken for each other, and found *A. tenera* to show the following divergences: 1. lower convexity, 2. anterior margin more rounded, 3. length greater than height. It is especially on the basis of the first two features that the Villány specimens could be identified and assigned to *A. tenera*.

A. tenera is a species quoted rather frequently, and however great is the number of the specimens figured, there are among them very few which on the basis of Arkell's criteria could be identified unequivocally with this species.

Distribution: Callovian of Great Britain, Bathonian of Germany, Callovian of the Russian Platform. The Villány specimens derive from the brown limestones of the Bathonian.

Subclassis Anomalodesmata

Ordo Pholadomyoidea

Superfamilia Pholadomyacea

Familia Pholadomyidae

Genus *Pholadomya* G. B. Sowerby, 1823

Pholadomya lirata (Sowerby, 1818)

Plate IV, Fig. 7

1818. *Cardita* (?) *lirata* Sow.; Sowerby: Min. Conch., p. 246, Pl. 197, Fig. 3. (In: Sowerby 1837)
1826. *Pholadomya Murchisoni* Sow.; J. de C. Sowerby; Min. Conch., p. 570, Pl. 545. (In: Sowerby, 1837)
- ?1836. *Pholadomya Murchissonae* Sow.; Roemer: Versteinerungen Nordd. Oolithengeb., p. 128, Pl. XV, Fig. 7.
1845. *Pholadomya Murchisoni* Sow.; Agassiz: Études critiques . . . , p. 79, Pl. 4c, Fig. 5-7.
1852. *Pholadomya Murchisoni*; Chapuis et Dewalque: Descr. foss. sec., p. 122, Pl. XVII, Fig. 4.
1855. *Pholadomya Heraulti*, Ag.' Morris et Lycett: Mon. Great Oolite Mollusca, p. 124, Pl. XII, Fig. 1; Pl. XV, Fig. 4.
1863. *Pholadomya lyrata*, Sow.; Lycett: Supplement. Monograph, p. 87, Pl. XLIII, Fig. 3, 3a.
1869. *Pholadomya Murchisoni*, Sow.; Terquem et Jourdy: Mon. Étage Bathonien, p. 72 (partim), Pl. V, Fig. 2-6 (non: Fig. 1).
1874. *Pholadomya Murchisoni*, Sow.; Moesch: Mon. Pholadomyen, p. 44, Pl. XVII, Fig. 6-9; Pl. XVIII, Pl. XIX.
1893. *Pholadomya Murchisoni*, Sowerby; Choffat: Faune jur. Portugal, p. 22, Pl. VI, Fig. 2-6 and 8, 10.
1917. *Phol. Murchisoni*, Sow.; Regineck: Jurassische Pholadomyen, p. 36, Pl. I, Fig. 3.
1948. *Pholadomya lirata* (J. Sowerby); Cox et Arkell: Brit. Great Oolite Mollusca, p. 43.
1954. *Pholadomya murchisoni* Sow.; Ksiazkiewicz: Jura i Kreda Bachowic, p. 181, Pl. XVII, Fig. 11.
- ?1957. *Pholadomya murchisoni* Sow.; Himsiasvili: Verhnejursk. fauna Gruzii, p. 159, Pl. XX, Fig. 1.
- ?1961. *Pholadomya cf. lirata* (Sowerby); Rossi Ronchetti et Fantini Sestini: Fauna Giur. Karkar, p. 135, Pl. XII, Fig. 7-9.

?1963. *Pholadomya* cf. *murchisonia* Sowerby; Azarjan: Jursk. otl. ASSR, p. 149, Pl. II, Fig. 8.

1965. *Pholadomya lirata* (J. Sowerby); Cox: Jur. Biv. Tanganyika, p. 126, Pl. 20, Fig. 8.

1967. *Pholadomya lirata* Sowerby; Mongin: Mollusques Bathonien, p. 65, Pl. IV, Fig. 21.

Number of specimens: 2

Dimensions: length: 46

height: —

convexity: 30

Description. Double valve of medium size, of good preservation, incomplete. Umbonal part completely absent. The preserved part of valve is rounded in outline, the posterior margin being pointed. From the point of view of ornamentation the surface of the valve can be divided up into three parts. The anterior region is smooth with one very faint, radial rib. In the lateral region there are 7 radial ribs of which the most posterior is weaker, the rest being of equal strength. The ribs are roughly as wide as their intervals. Growth lines varying in intensity, inflated. They run over the entire surface and produce tubercles when crossing ribs. A little distance away from the lower margin, 5 tubercles can be observed over 1 cm length. At the lower margin both tubercles and ribs become indistinct, while the growth lines get gradually more pronounced. The posterior region is ornamented solely by concentrical growth plicae.

Remarks. S o w e r b y (1818) published a rather featureless drawing of *P. lirata*. This seems to have been responsible for the fact that later authors were unable to identify their specimens with this, but they could identify them with *P. murchisoni*, a species established and nicely documented by J. de C. Sowerby in 1826. Moesch (1874) considered the two species to be synonyms, but he used the name *murchisoni* rather than the senior synonym — *lirata*. Priority was first applied by Cox in 1935 (Cox and Arkell, 1948). He stated that the extreme forms of the variability range of a single species had been given different names, so that the name *P. lirata* was valid. During a study of the materials in the Paris museum, Mongin (1967) was able to distinguish four groups within the species, groups including transitions ranging from typical *P. lirata*, carinated, wedge-shaped with 9 ribs or so, up to typical *P. murchisoni*, oval, 7-ribbed. The Villány specimen resembles most the type specimen of *P. murchisoni*.

Distribution. Bajocian to Callovian of Western Europe at large, Bathonian to Callovian of Portugal, Bajocian of Poland, Bathonian to Tithonian of the Caucasus, Bathonian to Callovian of Afganistan, Bathonian of Morocco, Bajocian and Callovian of East Africa. The Villány specimens derive from the brown limestones of the Bathonian.

Pholadomya ovalis (Sowerby, 1819)

Plate IV, Fig. 8

1819. *Lutraria ovalis* Sow.; Sowerby: Min. Conch., p. 276, Pl. 226, Fig. 1 (non: Fig. 2). (In: Sowerby, 1837)

1845. *Pholadomya ovulum*, Ag.; Agassiz: Études critiques, p. 119, Pl. 3, Fig. 7–9; Pl. 3b, Fig. 1–6.

1855. *Pholadomya ovulum*, Ag.; Morris et Lycett: Mon. Great Oolite Mollusca, p. 122, Pl. XIII, Fig. 12.

Description: Internal mould of very poor preservation of a large right valve. Outline oval, with its smaller axis shifted a little forward. Umbo very little prominent, curved markedly inwards and slightly backwards. Very convex, the point of highest convexity being in the first quarter of valve length. Of the ornamentation, only 5 subradial ribs are visible. The first rib is still subvertical, the rest of the ribs, rather equally spaced, becoming backwards gradually more oblique. The first rib is entirely faint, the second is the strongest and sharpest of all, the next three showing a gradual weakening backwards.

Remarks: The ribs of subequal intensity figured by Agassiz (1845) number 7. As evident from the description, it is usually the second rib that is the strongest. On the basis of the illustrations the specimens figured by Moesch (1874) can be divided up into three groups: i. The specimens of Pl. XIV, Fig. 1 and 2, have a very prominent umbo; in addition, in Fig. 2 only four, very closely spaced ribs of equal intensity can be seen. ii. The specimens visible on Pl. XIII, Fig. 5–8, show a good agreement with Agassiz's species, the only difference seems to consist in the stronger curvature of the ribs. iii. Pl. XI, Fig. 4; Pl. XII, Fig. 1 and Pl. XIII, Fig. 3, 4 show specimens which differ a little from Agassiz's figures, since their ribs are a little arched forward and these ribs always include a strikingly intensive one. This feature is underlined in Moesch's description (1874), so that he seems to have considered this group to be the typical representative of *P. bucardium*. Consequently, his idea of the species may have been somewhat different from Agassiz's. The Villány specimen belongs to group iii, showing a particularly striking agreement with Pl. XIII, Fig. 4.

Without a study of the original specimens, it would not be advisable to split up Moesch's material into several species. Therefore, despite the divergences, the Villány specimen and the above three groups can be regarded as belonging to the species *P. bucardium* Agassiz.

Distribution: Bathonian of Switzerland. The Villány specimen derives from the brown limestones of the Bathonian.

Pholadomya escheri Agassiz, 1845

Plate V, Fig. 1

1845. *Pholadomya Escheri* Ag.; Agassiz: Études critiques . . . , p. 102, Pl. 7f, Fig. 16.

1874. *Pholadomya Escheri*, Ag.; Moesch: Mon. Pholadomyen, p. 50, Pl. XX, Fig. 12; Pl. XXI, Fig. 1–7.

1893. *Pholadomya Escheri*, Agassiz; Choffat: Faune jur. Portug., p. 14, Pl. V, Fig. 2–7.

Number of specimens: 1

Dimensions: length: 71

height: 54

convexity: 43

Description: Internal mould of medium size, of medium preservation. Shape a rounded triangle, elongated backwards. Umbo not strong, but pointed and prominent, in the first one-third of valve length. Very convex in the anterior part, the valve flattens down backwards. Between the umbo and the lower margin there are 12 relatively faint ribs. Their

line forming a more elongated ellipse, with its umbo less prominent and with its rib bordering the anterior region being oblique and a little backward-arched.

Distribution: Bathonian of Great Britain, Bathonian to Callovian of Switzerland. The Villány specimens derive from the sandy limestones of the Bathonian.

Pholadomya villanyensis n. sp.

Plate V, Fig. 3

Number of specimens: 1

Locus typicus: Villány, Templom hill

Stratum typicum: Bathonian sandy limestones

Derivatio nominis: after the name of the locality — Villány

Dimensions: length: 81 height: 74 convexity: 29

Diagnosis: Ribs few, (4), arched strikingly forward, traceable throughout even on the markedly forward-curved umbo.

Description: Right valve large, of good preservation, incomplete. Outline oblique, oval. Convexity very marked. Umbo strikingly prominent, curved and shifted extremely forward. Between the umbo and the lower margin there are four ribs arched markedly backwards, separated by roughly uniform intervals, much wider than the ribs themselves. The first rib, faint but sharp, is in the anterior region; the second rib bordering the anterior region is very strong and sharp; the third one is fainter and less sharp; the fourth being flat and very faint. Over the entire surface of the valve growth lines represented by irregular plicae can be observed. In their intersections with ribs there are faint, tubercle-like elevations.

Remarks: It is *P. moeschi* Rollier of all the Middle Jurassic *Pholadomya* that is most closely related to the new species being described. At Villány locality the two species occur in one and the same bed. Most important divergences: I. *P. villanyensis* shows a more elongated, more regular ellipse in outline; II. its umbo is more markedly shifted forward and strongly forward-curved; III. the strongest rib is oblique and not perpendicular to the longitudinal axis, unlike in the case of *P. moeschi*; IV. the ribs are forward-arched, while in *P. moeschi* they are straight; V. the anterior region bordered by the strongest rib is more convex. *P. villanyensis* shows some similarity to the specimen which Moesch presented as *P. crassa* Agassiz, 1874, Pl. XVI, Fig. 2, but which does not seem to belong to *P. crassa* (see in the description of *P. moeschi*). However, Moesch's specimen differs from *P. villanyensis* by its outline and by that its umbo is not curved forward and that its ribs are backward-arched in running towards the lower margin.

Genus *Goniomya* Agassiz, 1841*Goniomya trapezicostata* (Pusch, 1836)

Plate V, Fig. 4

1836. *Lutraria trapezicostata*; Pusch: Polens Paläontologie, p. 80, Pl. VIII, Fig. 10a-c.
- ?1867. *Goniomya trapezicostata* Pusch sp.; Laube: Biv. Braun. Jur. Balin, p. 52, Pl. V, Fig. 5.
1934. *Goniomya trapezicostata* Pusch; Peelinev: Faune mezoz. zap. Gruzii, p. 35, Pl. I, Fig. 9.
1965. *Goniomya trapezicostata* (Pusch); Cox: Jur. Biv. Tanganyika, p. 129 (partim), Pl. 21, Fig. 2 (non: Fig. 3).
- non 1924. *Goniomya trapezicostata* (Pusch); Cossmann: Callovien Montreuil-Bellay, p. 51, Pl. VII, Fig. 9, 10.
- Number of specimens: 1

Description: Right valve of small size, of good preservation, incomplete. Strikingly convex. Umbo small, pointed, forward-shifted. Running obliquely downwards in the posterior and anterior thirds of valve surface, the ribs in the middle third are intercalated by horizontal ones, giving rise to an ornamentation consisting of rows of trapezes. The ribs are convexe in cross-section, their much narrower intervals being groove-like.

Remarks: The Villány specimen agrees well with the figures published by Pusch (1836), Peelinev (1934) and Cox (1965). Beside the trapezoidal ornamentation their most important common features are the shield-like shape and the very small, pointed, prominent umbo. Most of the *Goniomya* species of trapezoidal ornamentation are characterized by elongated, cylindrical shape. The specimen figured by Laube (1867) approaches this shape. Cossmann's specimen (1924) can also be assigned to this group. Cox (1965) described a Bajocian and a Callovian specimen from Tanganyika, noting that the second form, standing closer to typical *G. trapezicostata*, carried in the middle one-third of its valvelonger horizontal ribs than the Bajocian specimen did. However, he did not find the difference to be sufficient for separating species. *G. hemicostata* Morris et Lycett, 1855, differs from *G. trapezicostata* by the replacing of the periumbonal trapezoidal ornamentation by arched growth plicae towards the margin.

Distribution: Middle Jurassic of Poland; Bathonian to Callovian of Georgia, USSR; Callovian of East Africa. The Villány specimen derives from the sandy limestones of the Bathonian.

Familia *Pleuromyidae*Genus *Pleuromya* Agassiz, 1845*Pleuromya uniformis* (Sowerby, 1813)

Plate V, Fig. 5

1813. *Unio uniformis* Sow.; Sowerby: Min. conch., p. 58, Pl. 33 Fig. 4. (In: Sowerby, 1837)
1845. *Pleuromya tellina* Ag.; Agassiz: Études critiques . . . , p. 250, Pl. 29, Fig. 1-10.

1855. *Myacites securiformis*, Phil. sp.; Morris et Lycett: Mon. Great Oolite Mollusca, p. 136, Pl. XIII, Fig. 15.
1855. *Myacites decurtatus*, Phil. sp.; Morris et Lycett: Mon. Great Oolite Mollusca, p. 137, Pl. XV, Fig. 10.
1915. *Pleuromya tellina* Ag.; Krenkel: Kellowayfauna Popilany, p. 329, Pl. XXVII, Fig. 7.
1924. *Pleuromya Elea* (d'Orb.); Cossmann: Callovien Montreuil-Bellay, p. 51, Pl. VII, Fig. 21, 22.
1932. *Pleuromya decurtata* d'Orbigny mutation *Elea* d'Orbigny; Corroy: Callovien du Bassin de Paris, p. 177, Pl. XXVII, Fig. 18.
1935. *Pleuromya uniformis* (J. Sowerby); Cox: Attock District, p. 15, Pl. II, Fig. 9, 10.
1935. *Pleuromya uniformis* (J. Sowerby); Arkell: Brit. Corall. Lamellibr., p. 325, Pl. XLV, Fig. 1-13.
1948. *Pleuromya uniformis* (J. Sowerby); Cox et Arkell: Brit. Great Oolite Mollusca, p. 40.
1957. *Pleuromya uniformis* Sow.; Himsiasvili: Verhnejurk. fauna Gruzii, p. 155, Pl. XIX, Fig. 5.
1961. *Pleuromya uniformis* (Sowerby); Rossi Ronchetti et Fantini Sestini: Fauna Giur. Karkar, p. 131, Pl. XI, Fig. 6-8.
1965. *Pleuromya uniformis* (J. Sowerby); Cox: Jur. Biv. Tanganyika, p. 131, Pl. 20, Fig. 6.

Number of specimens: 4

Dimensions: length: 86	height: 46 (?)	convexity: 33
43	25	19
33	18	14
32	19	14

Description: Internal mould of medium size, of poor preservation, with some shell remnant. Outline oval, elongated, with an umbo of medium prominence, situated at about one-third of valve length as calculated from the front. Convexity of medium size, the greatest convexity being a little behind the umbo, closer to the half of valve length. Between the umbo and the first one-sixth of the length of the lower margin there is a very faint depression breaking the arch of the lower margin. The ornamentation consists of concentric growth lines and plicae.

Remarks: S o w e r b y ' s original figure is rather featureless. Therefore later authors cited P h i l l i p s ' species (just as Agassiz's) frequently than those which are much better documented. As shown by A r k e l l (1935), one and the same species, extremely variable and persistent, was re-named several times, the earliest, valid, name being *P. uniformis* (Sowerby). According to C o x (1935) and A r k e l l (1935), *P. elea* (d'Orbigny, 1850) is also a synonym of *P. uniformis*. This is supported by the figures published by C o s s m a n n (1924), too.

Distribution: Bajocian to Portlandian of Great Britain, Callovian to Upper Jurassic of France, Upper Jurassic of Georgia, USSR, Callovian of the Russian Platform, Bathonian to Callovian of Afganistan, Oxfordian of India, Oxfordian to Kimmeridgian of East Africa. The Villány specimens derive from the brown limestones of the Bathonian.

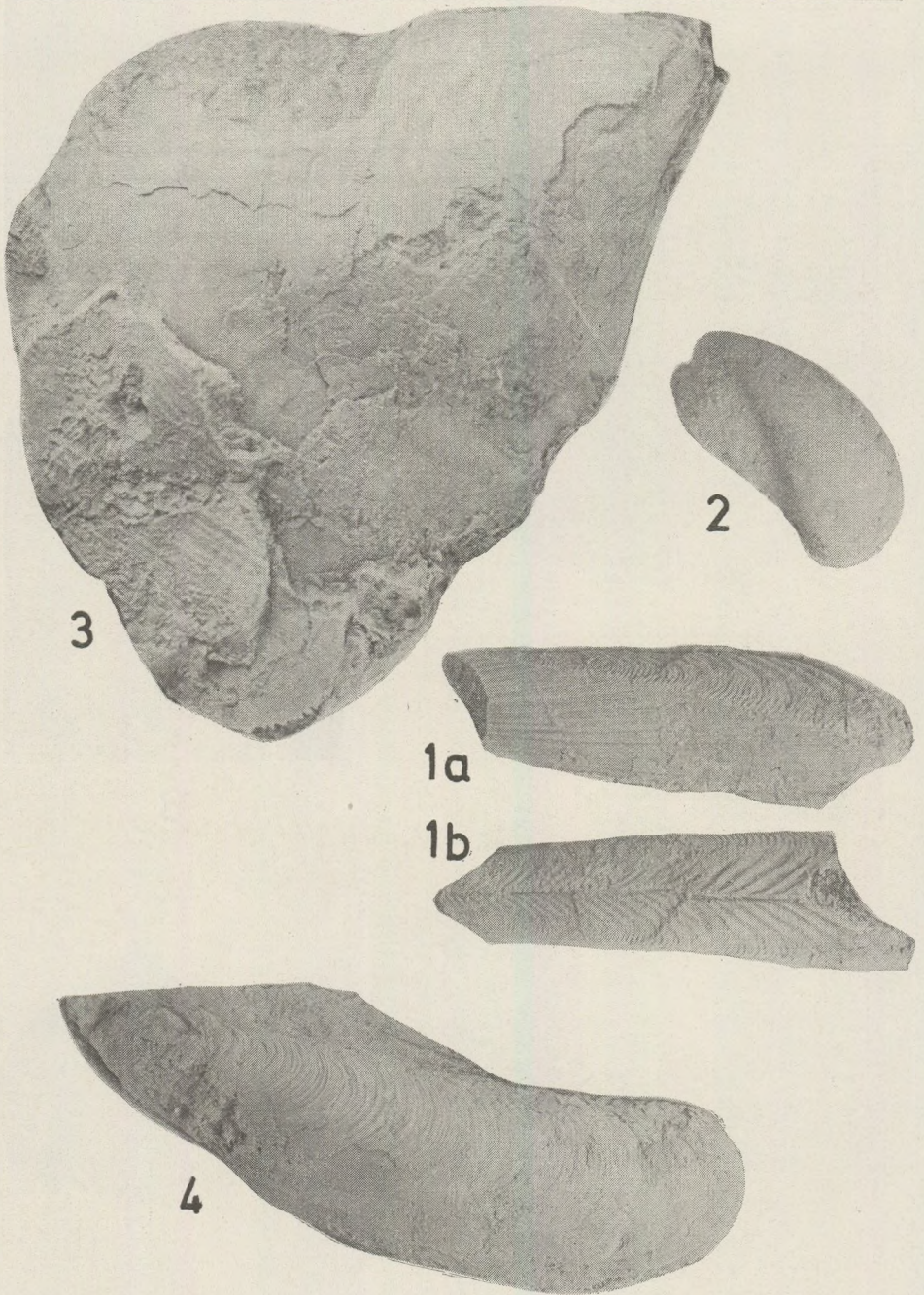
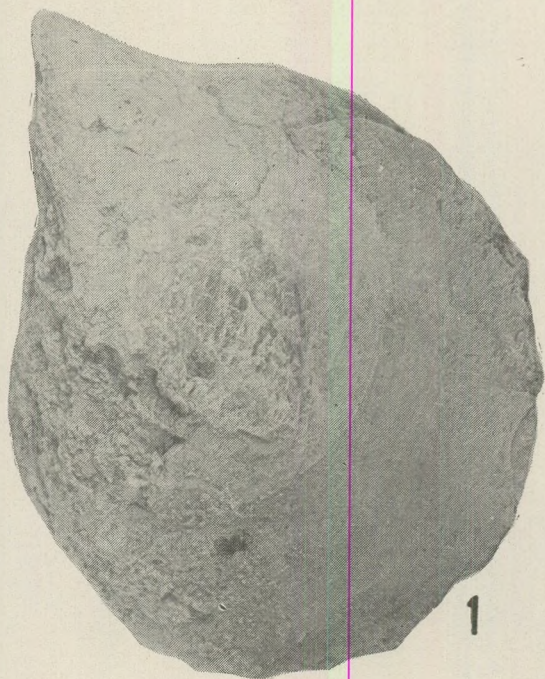
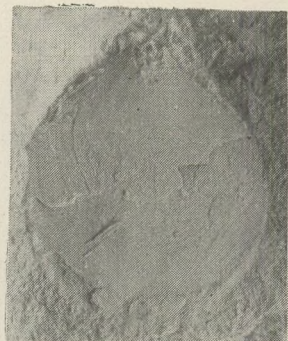


Plate I

Fig. 1. *Inoperna sowerbyana* (d'Orbigny) 1a: lateral view; 1b: top view (x 1) Fig. 2. *Modiolus anatinus* (Smith) (x 1) Fig. 3. *Stegoconcha* sp. aff. *granulata* (Sowerby) (x 1) Fig. 4. *Gervillella siliqua* (Deslongchamps) (x 1)



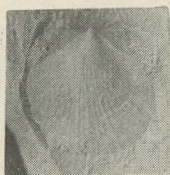
1



2



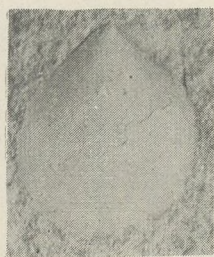
3



5a



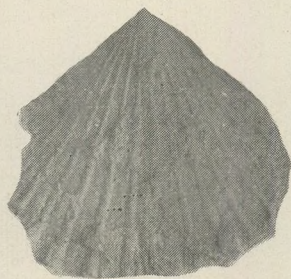
5b



4



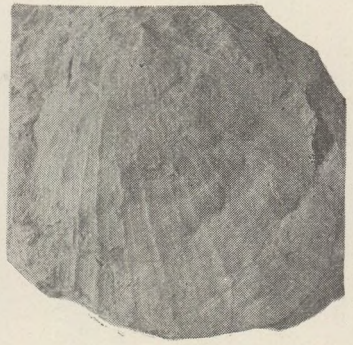
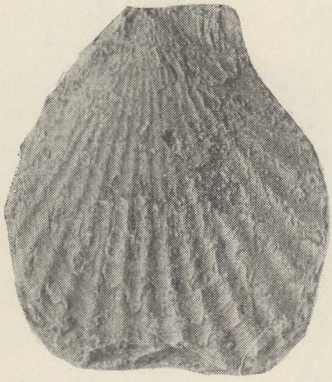
6



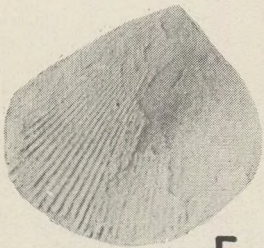
7

Plate II

Fig. 1. *Inoceramus oosteri* Favre? (x 1) Fig. 2. *Entolium* cf. *hehlii* (d'Orbigny) (x 2) Fig. 3. *Entolium corneolum* (Young et Bird) (x 1) Fig. 4. *Entolium spathulatum* (Roemer) (x 2) Fig. 5. *Propeamussium brevicostatum* n. sp. 5a: external ornamentation; 5b: internal ornamentation (x 2) Fig. 6. *Chlamys* (*Aequipecten*?) cf. *prisca* (Schlotheim) (x 1) Fig. 7. *Chlamys* (*Aequipecten*?) *humberti* (Dumortier) (x 2)



3



5



4

Plate III

Fig. 1. *Chlamys* sp. aff. *luciensis* (Thevenin ex d'Orbigny) (x 1) Fig. 2. *Eopecten* sp. aff. *aubryi* (Douvillé) (x 1) Fig. 3. *Antiquilima succincta* (Schlotheim) (x 1) Fig. 4. *Ctenostreon proboscideum* (Sowerby) (x 0,66) Fig. 5. *Plagiostoma subcardiiformis* (Greppin) (x 1)

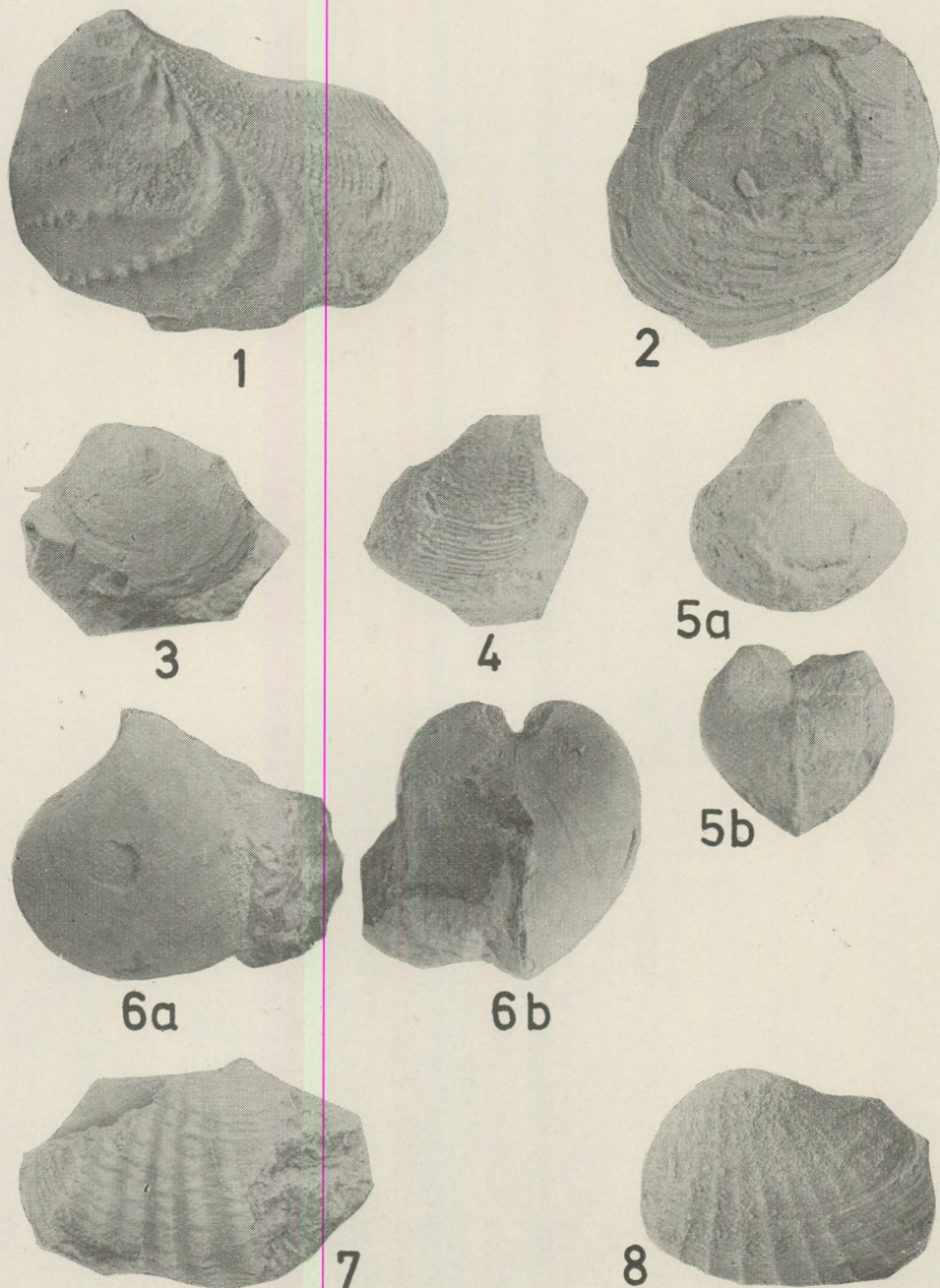


Plate IV

Fig. 1. *Myophorella* (*Pseudomyophorella*) *polonica* (Lebküchner) (x 1) Fig. 2. *Astarte* sp. aff. *ovata* Smith (x 1) Fig. 3. *Astarte* cf. *subdepressa* Blake et Hudleston (x 1) Fig. 4. *Opis* (*Coelopis*) cf. *leckenbyi* Lycett (x 1) Fig. 5. *Anisocardia minima* (Sowerby) 5a: lateral view; 5b: front view (x 1) Fig. 6. *Anisocardia tenera* (Sowerby) 6a: lateral view; 6b: front view (x 1) Fig. 7. *Pholadomya lirata* (Sowerby) (x 1) Fig. 8. *Pholadomya ovalis* (Sowerby) (x 1)

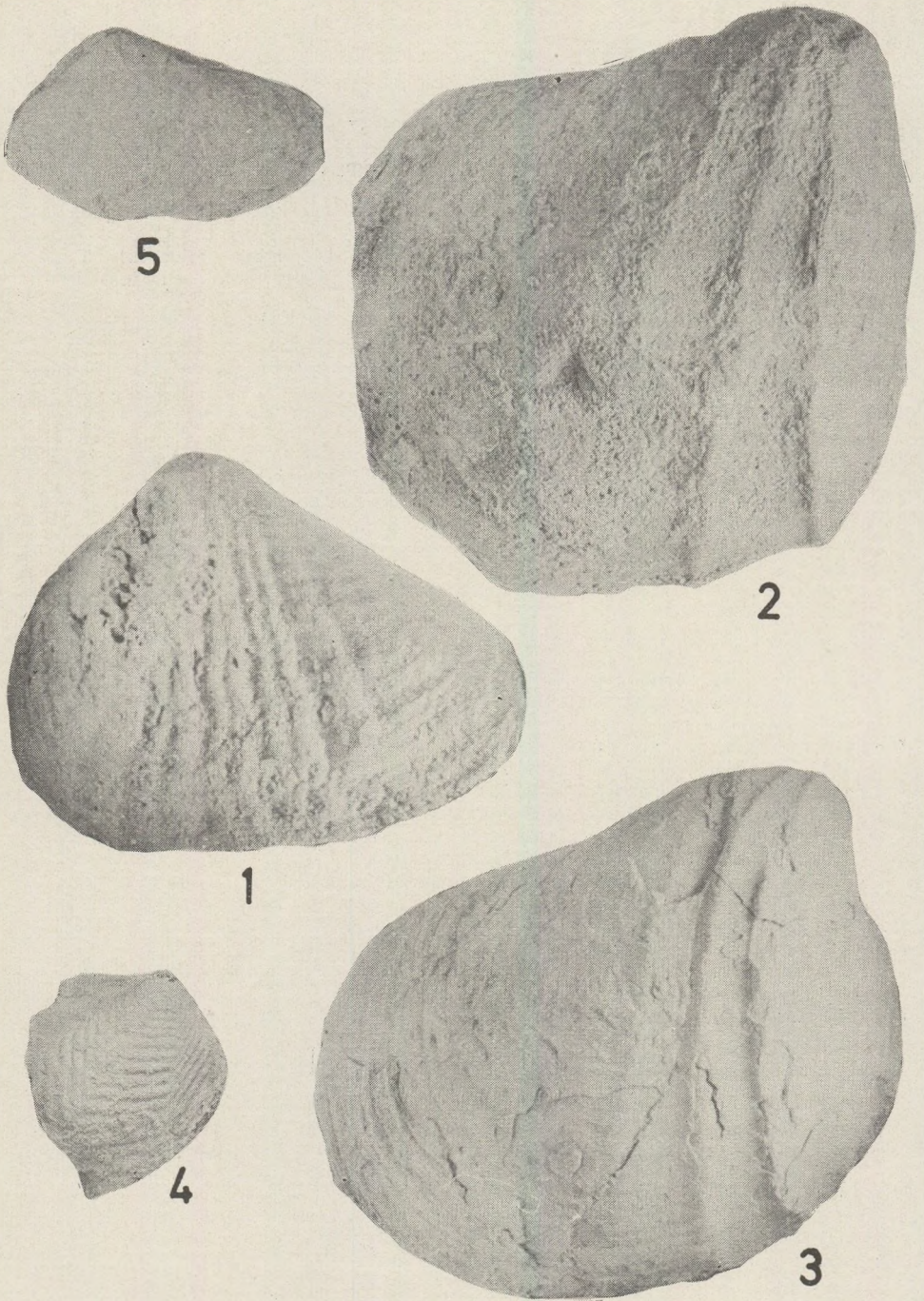


Plate V

Fig. 1. *Pholadomya escheri* Agassiz (x 1) Fig. 2. *Pholadomya moeschi* Rollier (x 1) Fig. 3. *Pholadomya villanyensis* n. sp. (x 1) Fig. 4. *Goniomya trapezicostata* (Pusch) (x 2) Fig. 5. *Pleuromya uniformis* (Sowerby) (x 1)

REFERENCES

- Agassiz, L. (1840): Études critiques sur les Mollusques fossiles. Mémoire sur les Trigonies. Neuchâtel.
- Agassiz, L. (1842-45): Études critiques sur les Mollusques fossiles. Monographie des Myes. Neuchâtel.
- Andreeva, T. F. (1966): Platinchatozhabernye iz jurskikh otlozheniy Yugo-Vostochnogo i Centralnogo Pamira. (semejstva: Pectinidae, Limidae i Ceratomyiidae). Trudy Upr. geol. Sov. Min. TSSR, 2.
- Arkell, W. J. (1929-1937): A Monograph of British Corallian Lamellibranchia., Palaeontogr. Soc. London.
- Azarian, N. R. (1963): Stratigrafia i fauna jurskikh otlozhenij Alaverdskogo rudnogo rayona Armianskoy SSR., Erevan.
- Barbulescu, A. (1963): Contributii la studiul faunei de Lamelibranchiate jurasice din Dobrogea. Studii cercet. geol., VIII., 1.
- Borissiak, A. A., Ivanov, E. (1917): Pelecypoda jurskikh otlozheniy Evropeyskoy Rossii. V.: Pectinidae. Trudy Geol. Kom., N.S., 143.
- Chapuis, F., Dewalque, G. (1853): Description des fossiles secondaires de la province de Luxembourg. Mém. Acad. Roy. Belg., XXV.
- Chavan, A. (1952): Les Pélécytopodes des sables astartiens de Cordebugle (Calvados). Mém. Soc. Pal. Suisse, LXIX.
- Choffat, P. (1893): Description de la faune jurassique du Portugal. Mollusques, Lamellibranches., I.: Siphonida.
- Corroy, G. (1932): Le Callovien de la Bordure orientale du Bassin de Paris. Mém. Carte géol. dét. France.
- Cossmann, M. (1907): Paléontologie. In: Thiéry, P., Cossmann, M.: Note sur le Callovien de la Haute-Marne et spécialement sur un gisement situé dans la commune de Bricon. Vesoul.
- Cossmann, M. (1916): Étude complémentaire sur le Charmouthien de la Vendée. Bull. Soc. géol. Normandie, XXXIII., (1913-15).
- Cossmann, M. (1924): Extension dans les Deux-Sèvres de la faune du Callovien de Montreuil-Bellay. Mém. Soc. géol. min. Bretagne., 1.
- Cox, L. R. (1935): The Triassic, Jurassic and Cretaceous Gastropoda and Lamellibranchia of the Attock District. Pal. Indica, N.S., XX. (5).
- Cox, L. R. (1940): The Jurassic lamellibranch fauna of Kuchh (Cutch). Pal. Indica, Ser. 9., III., 3.
- Cox, L. R. (1965): Jurassic Bivalvia and Gastropoda from Tanganyika and Kenya. Bull. Brit. Mus. (Nat. Hist.), Suppl., 1.
- Cox, L. R., Arkell, W. J. (1948-50): A survey of the Mollusca of the British Great Oolite Series, primarily a nomenclatorial revision of the monographs by Morris and Lycett (1851-1855), Lycett (1863), and Blake (1905-1907). Palaeontogr. Soc. London.
- Cox, L. R., Newell, N. D., Branson, C. C., Casey, R., Chavan, A., Coogan, A. H., Dechaseaux, C., Fleming, C. A., Haas, F., Hertlein, L. G., Keen, A. M., LaRocque, A., McAlester, A.: L., Perkins, B. F., Puri, H. S., Smith, L. A., Soot-Ryen, T., Stenzel, H. B., Turner, R. D., Weir, J. (1969): Systematic descriptions. In: Moore, R. C. (Ed.): Treatise on Invertebrate Paleontology. Part: N., Bivalvia. Kansas.
- Dacqué, E. (1910): Dogger und Malm aus Ostafrika. Beitr. Pal. Geol. Öst-Ung. XXIII.
- Dechaseaux, C. (1936): Pectinidés jurassiques de l'est du Bassin de Paris. Ann. Paléont., XXV.
- Desio, A., Rossi Ronchetti, C. (1960): Sul Giurassico medio di Garet el-Belláa (Tripolitania) e sulla posizione stratigrafica della formazione di Tacbal. Riv. Ital. Pal., LXVI., 2.
- Deslongchamps, E. (1824): Mémoire sur les coquilles du genre Gervillia. Mém. Soc. Linn. Calvados, I.

- Douvillé, H. (1886): Examen des fossiles rapportés des Choa par M. Aubry. Bull. Soc. géol. France, (3), 14.
- Dumortier, E. (1867): Études paléontologiques sur les dépôts jurassiques du bassin du Rhône. II.: Lias inférieur. Paris.
- Dumortier, E. (1869): Études paléontologiques sur les dépôts jurassiques du Bassin du Rhône. III.: Lias moyen. Paris.
- Fan Jia-Song, (1965): On some Middle Jurassic Lamellibranchiata from northern Tibet. Acta Pal. Sinica, 13., 2.
- Favre, E. (1876): Description des fossiles du terrain Oxfordien des Alpes Fribourgeoises. Mém. Soc. Pal. Suisse, III.
- Fischer, J.-C. (1964): Contribution à l'étude de la faune bathonienne dans la Vallée de la Greuse (Indre). Brachiopodes et Mollusques. Ann. Paléont. (Invert.), L., 1.
- Freneix, S. (1965): Les Bivalves du Jurassique moyen et supérieur du Sahara tunisien. (Arcacea, Pteriacea, Pectinacea, Ostreacea, Mytilacea). Ann. Paléont. Invert., LI., 1.
- Greppin, E. (1888): Description des fossiles de la Grande oolithe des environs de Bâle. Mém. Soc. Pal. Suisse, XV.
- Greppin, J. B. (1870): Description géologique du Jura Bernois et de quelques districts adjacents. Matér. Cart. Géol. Suisse, VIII.
- Hallam, A. (1968): Morphology, palaeoecology and evolution of the genus Gryphaea in the British Lias. Phil. Trans. Roy. Soc. London, (B), 254., 792.
- Hauff, B. (1953): Das Holzmadenbuch. Öhringen.
- Hofmann, K. (1876): Aufnahmsbericht. Verh. k. k. geol. Reichsanst., (1876), p. 22.
- Hudson, J. D., Palframan, F. B. (1969): The ecology and preservation of the Oxford Clay fauna at Woodham, Buckinghamshire. Quart. Journ. Geol. Soc. London, 124., 4.
- Jekelius E. (1915): A brassói hegyek mezozóós faunája. (The mesozoic fauna of the hills at Brassó.) Magy. k. Földt. Int. Évkönyve, XXIII., 2.
- Kauffman, E. G. (1969): Form, function and evolution. In: Moore, R. C. (Ed.): Treatise on Invertebrate Paleontology. Part: N Kansas.
- Khimshiasvili, N. G. (1957): Verkhneyurskaya fauna Gruzii. Tbilisi.
- Krenkel, E. (1915): Die Kelloway-Fauna von Popilany in Westrussland. Palaeontographica, 61.
- Ksiazkiewicz, M. (1954): Jura i Kreda Bachowic. Rocznik Pol. Tow. Geol., XXIV., 2-3.
- Kunz, B. W. L. (1967): Eine Fauna aus dem oberen Dogger der niederösterreichischen Kalkvorpalpen. Ann. Naturhist. Mus. Wien, 71.
- Lahusen, I. (1883): Die Fauna der Jurassischen Bildungen des Rjasanschen Gouvernements. (in russian, germ. abstr.) Trudy Geol. Kom., I., 1.
- Laube, G. (1867): Die Bivalven des Braunen Jura von Balin. Denkschr. Ak. Wiss., math.-nat. Kl., XXVII.
- Lebküchner, R. (1932): Die Trigonien des süddeutschen Jura. Palaeontographica 77.
- Lenz, O. (1872): Aus dem Baranyaer Komitate. Verh. k. k. geol. Reichsanst., (1872).
- Lóczy L., jun. (1912): A Villányi és Báni hegység geológiai viszonyai. (Geology of Villány and Bán Hills.) Földt. Közl., 42.
- Lóczy L., jun. (1915): Monographie der villányer Callovien-Ammoniten. Geol. Hung., I., 3-4.
- Loriol, P., Scharadt, H. (1883): Étude paléontologique et stratigraphique des couches à Mytilus des Alpes Vaudoises. Mém. Soc. Pal. Suisse, X.
- Lycett, J. (1863): A supplementary monograph of the Mollusca from the Stonesfield Slate, Great Oolite, Forest Marble and Cornbrash. Palaeontogr. Soc. London.
- Makowski, H. (1952): La faune Callovienne de Luków en Pologne. Palaeont. Polon., 4.
- McAlester, A. L., Rhoads, D. C. (1967): Bivalves as bathymetric indicators. Marine Geol., 5., 5-6.
- Mihajlovic, M. (1959): Srednje jurska fauna sa planine Budosa (Niksic). Bull. Mus. Hist. Nat. Pays Serbe, ser. A., 11.
- Moesch, C. (1874): Monographie der Pholadomyen. Mém. Soc. Pal. Suisse, I.

- Mongin, D. (1967): Les Mollusques du Bathonien saumâtre du Moyen Atlas. Notes et Mém. Serv. Géol. Maroc, 200.
- Morris, J., Lycett, J. (1853 | 55): A Monograph of the Mollusca from the Great Oolite. II.: Bivalves. Palaeontogr. Soc. London.
- Neumayr, M. (1871): Jurastudien. 4. Die Vertretung der Oxfordgruppe im östlichen Theile der mediterranean Provinz. Jb. k. k. geol. Reichsanst., XXI.
- d'Orbigny, A. (1850): Prodrome de Paléontologie stratigraphique universelle des animaux Mollusques et rayonnés. (I.) Paris.
- Peelincev, V. F. (1934): Nekotorye dannye o faune mezozoya Zapadnoy Gruzii. Trudy VGRO., 252.
- Phillips, J. (1829): Illustrations of the geology of Yorkshire. London.
- Pusch, G. G. (1836–37): Polens Paläontologie. Stuttgart.
- Qunstedt, F. A. (1858): Der Jura. Tübingen.
- Radwanski, A., Szulcowski, M. (1966): Jurassic stromatolites of the Villány Mountains (Southern Hungary). Ann. Univ. Sci. Budapest, Sec. Geol., IX.
- Regineck, H. (1917): Die Pelomorphen-Deformation bei den jurassischen Pholadomyen und ihr Einfluss auf die bisherige Unterscheidung der Arten. Mém. Soc. Pal. Suisse, XLII.
- Roemer, F. A. (1836): Die Versteinerungen des norddeutschen Oolithen-Gebirges. Hannover.
- Roemer, F. A. (1839): Die Versteinerungen des norddeutschen Oolithen-Gebirges. Nachtrag. Hannover.
- Romanov, L. F., Sobetski, V. A. (1967): K kharakteristike yurskikh pektinid Preddobrudzhskogo progiba. Bull. Akad. St. Mold. SSR., 4.
- Rossi Ronchetti, C., Fantini Sestini, N. (1961): La fauna Giurassica di Karkar (Afghanistan). Riv. Ital. Pal., LXVII., 2.
- Schäffle, L. (1929): Über Lias- und Doggeraustern. Geol. Pal. Abh., N. F., 17., 2.
- Schlippe, O. (1888): Die Fauna des Bathonien im Oberrheinische Tieflande. Abh. geol. Spez.-Karte Elsass-Lothr., 4., 4.
- Sowerby, J. (1837): Mineral Conchologie. (germ. edition) Neuchâtel.
- Staesche, K. (1926): Die Pectiniden des Schwäbischen Jura. Geol. Pal. Abh., N. F., 15., 1.
- Stefanini, G. (1939): Molluschi del Giurassico della Somalia. Gasteropodi e Lamellibranchi. Palaeontogr. Ital., XXXII., Suppl. 4.
- Stoll, E. (1934): Die Brachiopoden und Mollusken der pommerischen Doggergeschiebe. Abh. geol. pal. Inst. Greifswald, 13.
- Terquem, O., Jourdy, E. (1869): Monographie de l'étage Bathonien de la Moselle. Mém. Soc. Géol. France, (2), IX., 1.
- Thevenin, A. (1913): Types du Prodrome de paléontologie stratigraphique universelle de d'Orbigny. Ann. Paléont., VI.
- Tietze, E. (1872): Geologische und paläontologische Mittheilungen aus dem südlichen Theil des Banater Gebirgsstockes. Jb. k. k. geol. Reichsanst., XXII.
- Till, A. (1906): Der fossilführende Dogger von Villány (Südungarn). Verh. k. k. geol. Reichsanst., (1906).
- Venzo, S. (1949): Il Batoniano a Trigonina dell'Oltregiuba settentrionale e del Borana sud-orientale. (Africa orientale). Palaeontogr. Ital., 45.
- Vörös A. (1971): A Villányi hegység alsó és középső júra képződményeinek üledékföldtani vizsgálata. (Sedimentological study of the lower and middle Jurassic rocks of the Villány Hills.) Földt. Közl., 101. (in preparation).

INVESTIGATION OF PLATE TECTONICS BY MAGNETOTELLURIC ANISOTROPY

by

A. ÁDÁM, F. HORVÁTH and L. STEGENA

(Hungarian Academy of Sciences, Geodetical and Geophysical Research Institute; Geophysical Institute of L. Eötvös University)

РЕЗЮМЕ

В результате взаимодействия плит литосферы на их краях обычно возникают линейные структуры большой глубины. Магнитотеллурический метод является эффективным средством для исследования этих структур. Изучив материалы магнитотеллурического глубинного зондирования пяти районов, расположенных на предположенных краях плит литосферы (Венгерский бассейн, передовой прогиб Копет-Дага, Байкальская система разломов, Исландия и Камчатка), авторы настоящей работы узнали о том, что в каждом из этих районов проявляется ясно выраженная магнитотеллурическая анизотропия. Эти проявления анизотропии авторы связывают новой глобальной тектоникой.

1. Introduction

According to the new hypothesis on global tectonics, the Earth's surface consists of 6 main lithospheric plates covering the whole Globe (Le Pichon, 1968; Isacks et al., 1968). The lithospheric plates are in motion with respect to one another. The areas, where the plates move off one another (Mid-Oceanic Ridges, African and Baikal Rift Systems), are called accreting plate margins; those, where the plates approach one another, are termed consuming plate margins (oceanic trenches, orogenic belts).

The interaction of lithospheric plates is the most efficient morphogenetic agent. As shown by Le Pichon (1968), Dewey and Bird (1970), Dewey and Horsfield (1970), McKenzie (1970), Dickinson (1971) and others, the consuming margins of the lithospheric plates are areas of active tectonism and orogeny. In the last 60–120 million years the Pacific and the Tethys have played the role of consuming oceans (Illies, 1970); orogenic movements took place on the coasts of these. The convergent displacements of the Eurasian and African plates have resulted in the closure of the Tethys sea and in the folding (still going on) of the Alpine-Himalayan Mountain System.

The structures produced by the interaction of the lithospheric plates are characterized by the common feature of being *linear structures extending for a long distance in one direction*, structures usually reaching from the surface down to great depths. The most efficient method for studying deep subsurface structures is provided by seismology; however, any other techniques confirming or supplementing seismological information may prove extremely useful. The magnetotelluric method has, inter alia, two characteristics that can enable it to serve as a tool in investigating global tectonics. Let us quote them:

a) sensitive detecting of linear structures by the aid of the so-called magnetotelluric anisotropy;

b) ability of obtaining geophysical information from great depths should these be as large as 100 or 200 km.

The following discussion is devoted to a review of the results of the MTS performed on the supposed margins of the lithospheric plates. In these areas a definite magnetotelluric anisotropy can be observed to occur. Let us try to interpret magnetotelluric anisotropies in the light of the new global tectonics.

2. Magnetotelluric anisotropy

According to the theory of magnetotelluric soundings, the curves of apparent specific resistivity (ρ) versus time of period (T) determined in any direction above an infinite half-space consisting of horizontally stratified isotopic layers are identical. In platform areas the sounding curve $\rho_x(T)$ corresponding to the N-S direction and that corresponding to the E-W direction, $\rho_y(T)$, are identical or at least very similar to each other. A pattern like this is shown by the MTS curves measured on the Russian Platform (Y a n o v s k y et al., 1966) and in Western Canada (C a n e r et al., 1969). If the afore-mentioned structural conditions are not fulfilled, the connection between the electric (\vec{E}) and magnetic fields (\vec{H}) is expressed by the relation $\vec{E} = \{Z\} \vec{H}$, where $\{Z\}$ is the impedance tensor. In this case the apparent specific resistivity curves defined by the expressions $\rho_x = 0,2 T (E_x/H_y)^2$ and $\rho_y = 0,2 T (E_y/H_x)^2$ differ from one another in dependence on the field-distorting effect of the geological structures. Thus magnetotelluric anisotropy is brought about. The observed anisotropy has its highest value in the case when the measurements are parallel to the strike and dip of the geological structure or to the direction of the highest and lowest specific resistivities. The effects producing magnetotelluric anisotropy may be either regional or local. On the basis of magnetotelluric anisotropy, definite conclusions concerning a regional structure can be deduced only in the case when the sounding curves obtained for several points of a large area show similar characteristics.

3. Results of measuring and their interpretation

Magnetotelluric soundings are known from five areas lying on the supposed margins of lithospheric plates: the Hungarian Basin, the foreland of the Kopet-Dag Mountains, the Baikal Rift System, Kamchatka and Iceland (Fig. 1.). In the first three of these areas of measurement both the

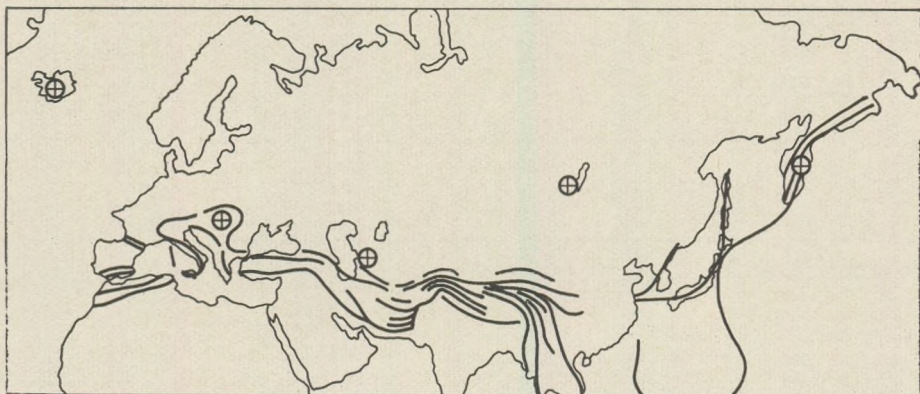


Fig. 1. The locii of the MTS measurements on the boundaries of the lithospheric plates.

quantity and quality of magnetotelluric information are so advantageous that they allow one to draw definite conclusions as to regional structure.

A) Magnetotelluric soundings on supposed consuming plate margins

The MTS curves obtained for the Hungarian Basin show a considerable regional anisotropy (Fig. 2. and 3.). In general, if $T > 60$ sec, $\rho_x > \rho_y$, and the major axes of the anisotropy ellipses will gradually turn to meridional direction with increasing period. This can be explained by two effects (Ádám, 1969; Ádám, 1970). On the one hand, under the influence of a compression of $N-S$ trend the rocks of the basement have been metamorphosed and have become anisotropic; the direction of high resistivity has been approximately $N-S$, that of low resistivity

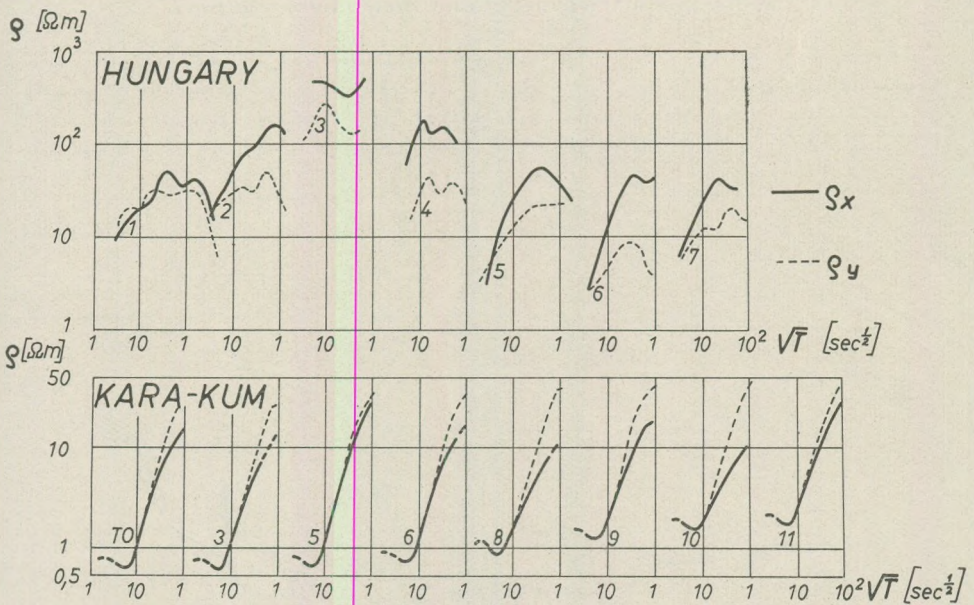


Fig. 2. MTS curves measured in the Hungarian Basin and on the foreland of the Kopet-Dag (Kara-Kum). The appropriate numbers refer to Fig. 3. (after Ádám; Avagimov et al.).

$E-W$ (Fig. 4.). On the other hand, this basement seems to include steeply dipping interlayers of nearly $E-W$ strike and of good conductivity. This structure appears to be consistent with plate tectonics. The Hungarian Basin is integral part of the Alpine orogen. Just recently, $E-W$ striking, regional lines of overthrusting could be detected in its Cretaceous-Paleogene basement (Dank and Bodzay, 1970) (Fig 3.). The Alpine orogen, however, is the result of the consumption of the African and Eurasian plates upon each other, generally with underthrustings of nearly $E-W$ strike (Le Pichon, 1968; Dewey and Bird, 1970; McKenzie, 1970).

The Kopet-Dag Mountains are also a member of the Alpine orogen. According to McKenzie (1970), the relative movement of the Eurasian and African plates is of $N-S$ trend and there are nearly $E-W$ striking underthrustings in a broad belt within this territory. The soundings carried out (by Avagimov et al., 1969) in the Kara-Kum Desert, the foreland of the Kopet-Dag, also yielded different MTS curves in two directions (Fig. 2. and 3.). As a rule, if $T > 100$ sec, $\rho_y > \rho_x$. The specific resistivity curves, determined by the aid of polar diagrams of impedance parallel to the $NW-SE$ strike of the structure and perpendi-

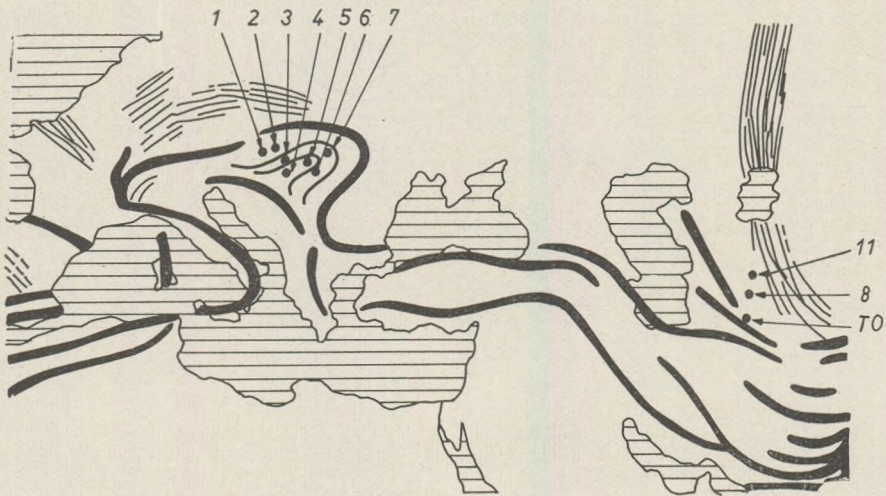


Fig. 3. The loci of MTS measurements carried out in the Hungarian Basin and on the foreland of Kopet-Dag. (The strikelines of the Paleozoic orogen and those of the Alp-Himalayan system are indicated by thin and heavy lines, respectively. In the Hungarian Basin the thrusting lines in Cretaceous-Paleogene basement are also shown, according to Dank and Bodzay).

cularly to it, differ even more markedly from one another. In terms of the Krajev effect the electric component normal to the highly resistive mountain mass is distorted and thus all *MTS* curves do show anisotropy.

From Kamchatka, the vicinity of Kliuch village, a single pair of *MTS* curves are known (Kopytenko et al., 1967). These show a marked magnetotelluric anisotropy (Fig. 5.). On the basis of one pair of curves, however, no statement of the regional distribution of anisotropy can be made. Therefore, no definite conclusions can be deduced with regard to the regional structure either. However, $\rho_x > \rho_y$ may indicate an *E-W* strike of the underthrusting Pacific plate, which may occur, since Kliuch is situated close to the point of intersection of the Aleutian and Kuril trenches.

Generally, the *MTS* measurements at island arcs may give informations about the thermal conditions connected with underthrusting of lithospheric slab (Fig. 6.).

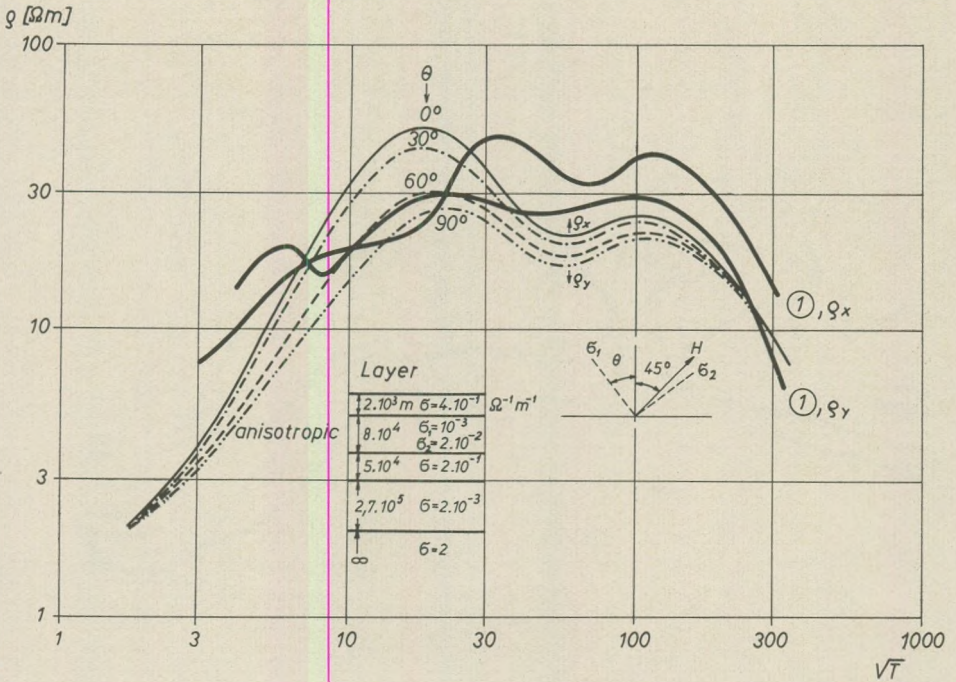


Fig. 4. A tentative comparison of the observed and calculated MTS curves for the Hungarian Basin indicates that thickness of the metamorphosed layers amounts to several tens of kilometres.

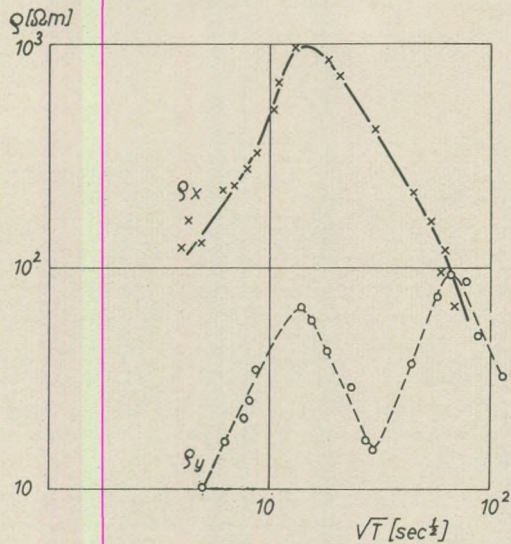


Fig. 5. MTS curves measured in Kamchatka (after Kopytenko et al.).

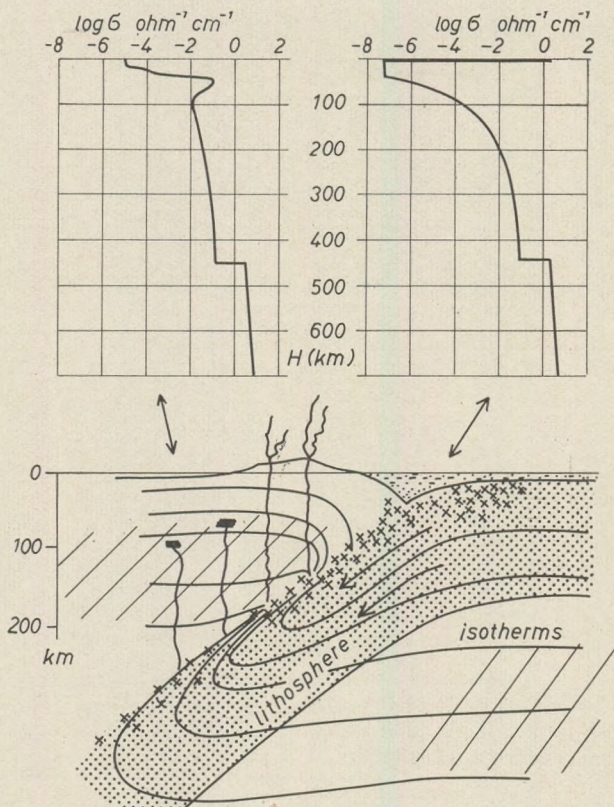


Fig. 6. Resistivity curves referring to different regions of island-arc model proposed by Hasebe et al., Lubimova and Feldman.

B) Magnetotelluric measurements on accreting plate margins

The Baikal Rift System is part of the global fracture system (Florensov, 1969; Lubimova, 1969). The magnetotelluric soundings performed in this region have shown a marked regional magnetotelluric anisotropy. The directions of the major axes of the anisotropy ellipses are perpendicular to the strike of the rift zone (Pospëev, 1971), (Fig. 7.). Electric inhomogeneity is so heavy as to define the character of anisotropy as far as 400 km away from Lake Baikal. In the rift zone the horizon of good electric conductivity is considerably elevated (Gornostayev et al., 1960), (Fig. 8.). This is in good agreement with the heat flux values varying between 1.6 and 3.4 *HFU* in the Baikal Rift Zone (Lubimova, 1969).

The *MTS* curves measured in Iceland also show some anisotropy, moreover a high conductivity layer in the crust and upper mantle (Hermann and Grillot, 1970). The data obtained, however, are not sufficient.

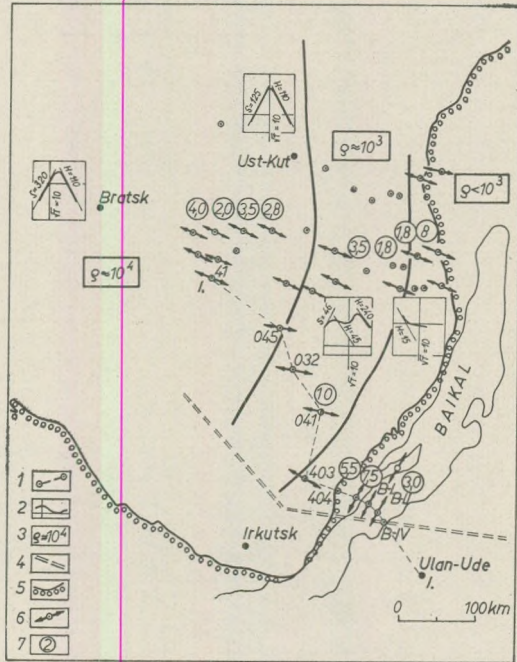


Fig. 7. Results of the MTS in the Baikal rift zone (after Pospeev).

Key: 1. locii of MTS; 2. the MTS curve characteristic to the given region; 3. The specific resistivity of the basement; 4. DSS profile; 5. Pre-Cambrian rocks on the surface; 6. The direction of major axis of MTS anisotropy ellipse; 7. value of ρ_{\max}/ρ_{\min} at $T=100$ sec.

4. Conclusions

In the above discussion the results of a few magnetotelluric soundings performed on the supposed margin of lithosphere plates have been analysed. These results have provided valuable contributions to the geometry and physics of plate tectonics. Regional magnetotelluric anisotropy can be used for tracing the margin of the plate, since this margin, with its electric pattern differing from its environment, induces considerable distortions of the electromagnetic field. In addition to this, the interpretation of MTS curves may provide information as to the extension of metamorphism connected with spreading tectonics, to the direction of the stresses responsible for metamorphism and to the distribution of temperatures in the deep subsurface zones.

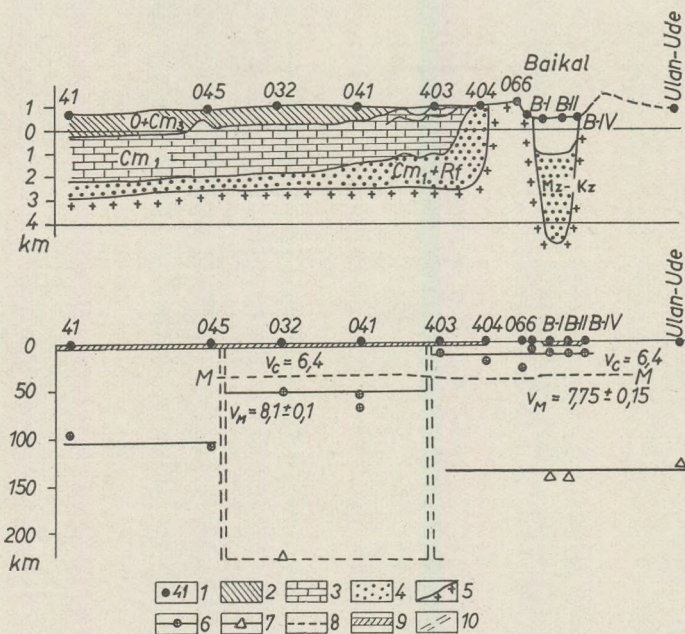


Fig. 8. Cross section in the Baikal rift zone along the profile I. of Fig. 7. (after Gornostaev et al.).

Key: 1. Locif of MTS and their identity numbers; 2. The upper highly conducting complex, $\rho=20-100 \Omega \text{ m}$; 3. Precambrian complex, $\rho=150-200 \Omega \text{ m}$; 4. The lower highly conducting complex, $\rho=20-100 \Omega \text{ m}$ (under the Lake of Baikal $\rho=5-7 \Omega \text{ m}$); 5. The surface of the basement; 6. The surface of the first highly conducting layer in the crust and upper mantle; 7. The surface of the second highly conducting layer in the upper mantle; 8. M discontinuity on the base of DSS; 9. sedimentary complex; 10. Supposed boundary between different blocks.

REFERENCES

- Á d á m, A. (1969): Über die gutleitende Schicht des oberen Erdmantels. Acta Geodaet. Geophys. et Mountainist. Vol. 5. No. 1-2.
- Á d á m, A. (1970): Problems of the electric upper mantle research in the Hungarian Basin. Bull. of Geodet. Geophys. Res. Lab. Sopron, Vol. 1.
- A v a g i m o v, A. A., D u b r o v s k y, V. G., L a g u t i n s k a y a, L. P., N i k o l a y e v a, L. S., S o l o h o v, V. V., F e i n b e r g, E. B. and S i h a m o v i c, E. L. (1969): Main results of the application of the MTS in Turkmenia. (in Russian). Results of Int. Geophys. Res. Projects.
- C a n e r, B., C a m f i e l d, P. A., A n d e r s e n, F. and N i b l e t t, E. R. (1969): A large-scale magnetotelluric survey in Western Canada. Can. Journ. Earth Sci., Vol. 6. No. 5.
- D a n k, V. and B o d z a y, J. (1970): A magyarországi potenciális szénhidrogén készletek fejlődéstörténeti háttere. OKGT spec. publ.
- D e w e y, J. F. and B i r d, J. M. (1970): Mountain belts and the new global tectonics. Journ. Geophys. Res., Vol. 75., No. 14.
- D e w e y, J. F. and H o r s f i e l d, B. (1970): Plate tectonics, orogeny and continental growth. Nature, Vol. 225., No. 5232.

- Dickinson, W. R. (1971): Plate tectonic models of geosynclines. *Earth and Planet. Sci. Letters*, Vol. 10., No. 2.
- Florensov, N. A. (1969): Rifts of the Baikal mountain region. *Tectonophysics*, Vol. 8. No. 4-6.
- Gornostaev, V. P., Mihalevsky, V. I. and Pospseev, V. I. (1970): Magnetotelluric deep soundings on the southern Siberian platform and in the region of the Baikal rift. (in Russian). *Geologia i Geofizika*, No. 4.
- Hasebe, K., Fujii, N. and Uyeda, S. (1970): Thermal processes under island arcs. *Tectonophysics*, Vol. 10., No. 1-3.
- Hernance, J. F. and Grillo, L. R. (1970): Correlation of magnetotelluric, seismic and temperature data from southwest Iceland. *Journ. Geoph. Res.*, Vol. 75., No. 32.
- Illies, J. H. (1969): An intercontinental belt of the world rift system. *Tectonophysics*, Vol. 8., No. 1.
- Isacks, B., Oliver, J. and Sykes, L. R. (1968): Seismology and the new global tectonics. *Jour. Geophys. Res.* Vol. 73., No. 18.
- Kopytenko, Y. A., Gorsnkov, E. S., Gorsnkova I. A., Feldman, I. S. and Feldman, T. A. (1967): Magnetotelluric sounding in the village Kliuchi of the Kamchatka region (in Russian). *Izv. Akad. Nauk. Ser. Fiz. Zemli*, No. 9.
- Le Pichon, X. (1968): Sea-floor spreading and continental drift. *Jour. Geophys. Res.* Vol. 73., No. 12.
- Lubimova, E. A. (1969): Heat flow in Baikal and other rift zones. *Tectonophysics*. Vol. 8., No. 4-6.
- Lubimova, E. A. and Feldman, I. S. (1970): Heat flow, temperature and electrical conductivity of the crust and upper mantle in the USSR. *Tectonophysics*, Vol. 10., No. 1-3.
- McKenzie, D. P. (1970): Plate tectonics of the Mediterranean region. *Nature*, Vol. 226., No. 5242.
- Moore, E. (1970): Ultramafics and Orogeny, with models of the US Cordillera and the Tethys. *Nature*, Vol. 228., No. 5274.
- Pospseev, V. I. (1971): personal communication.
- Yanovsky, B. M., Kovtun, A. A., Raspopov, O. M. and Chicherina, N. D. (1966): Deep structure of Central Russian Basin based on magnetotelluric deep sounding data (in Russian). *Vop. Geofiz.*, Vol. 16. (Izdat. Leningradskovo Univ.).

INDEX

Professor László Egyed	3
Ager, D. V. — Callomon, J. H.: On the Liassic age of the "Bathonian" of Villány (Baranya)	5
Bognár, L.: Mineralogical and geochemical study of zircons in the granitoids of Hungary	17
Géczy, B.: The Pliensbachian of Kericser hill, Bakony Mountains, Hungary ..	29
Grossz, Á.: Kohlengeologische Untersuchungen der Lagerstätte Hidas im Mecsek Gebirge	53
Kiss, J.: Constitution mineralogique et g�n�se du gisement uranif�re de la treated by urea Montagne Mecsek (II)	79
Libor, O.—Graber, L.—Don�th �. P.: Investigation of montmorillonites solutions (II)	123
Mesk�, A. — V�ges, I.: A linear filtering method for decomposing residual anomalies	133
Mesk�, A.: Single channel ghost filter in the presence of white noise	143
Штегена, Л. Глубинное строение и геотермические условия в Венгрии ..	153
R�k�czi, F.: Die Vorhersage von Temperaturminima an heiteren Tagen auf Grund relativer Topographien von 850/1000 mb	161
V�r�s, A.: The Lower and Middle Jurassic bivalves of the Vill�ny Mountains ..	167
�d�m, A. — Horv�th, F. — Stegena, L.: Investigation of plate tectonics by magnetotelluric anisotropy	209

A kiadásért felelős: az Eötvös Loránd Tudományegyetem rektora
A kézirat nyomdába érkezett: 1970. október — Megjelent: 1971. július
Terjedelem: 18,75 (A/5) ív +3 db. színes mell. — Példányszám: 800
Készült monó szedéssel, íves magasnyomással, az MSZ 5061–59 és az 5602–55 szabvány szerint
71.1716. Állami Nyomda, Budapest